Universidade Nova de Lisboa
Instituto de Tecnologia Química e Biológica

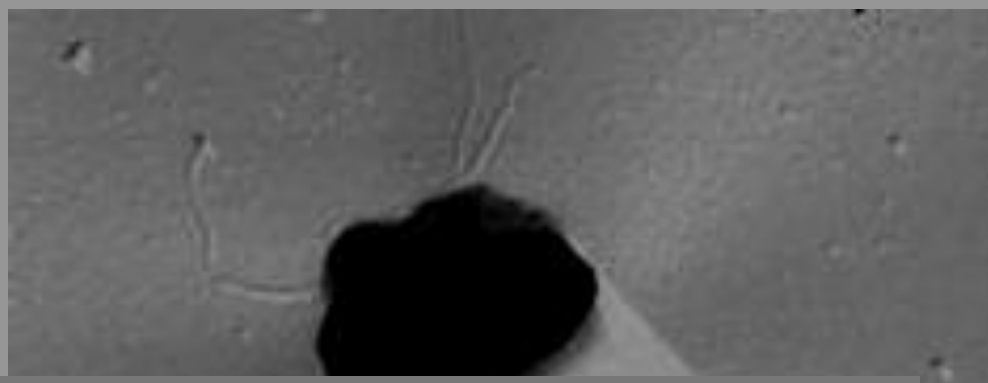

Osmo- and thermo-adaptation in hyperthermophilic *Archaea*:

identification of compatible solutes, accumulation profiles, and biosynthetic routes in *Archaeoglobus* spp.

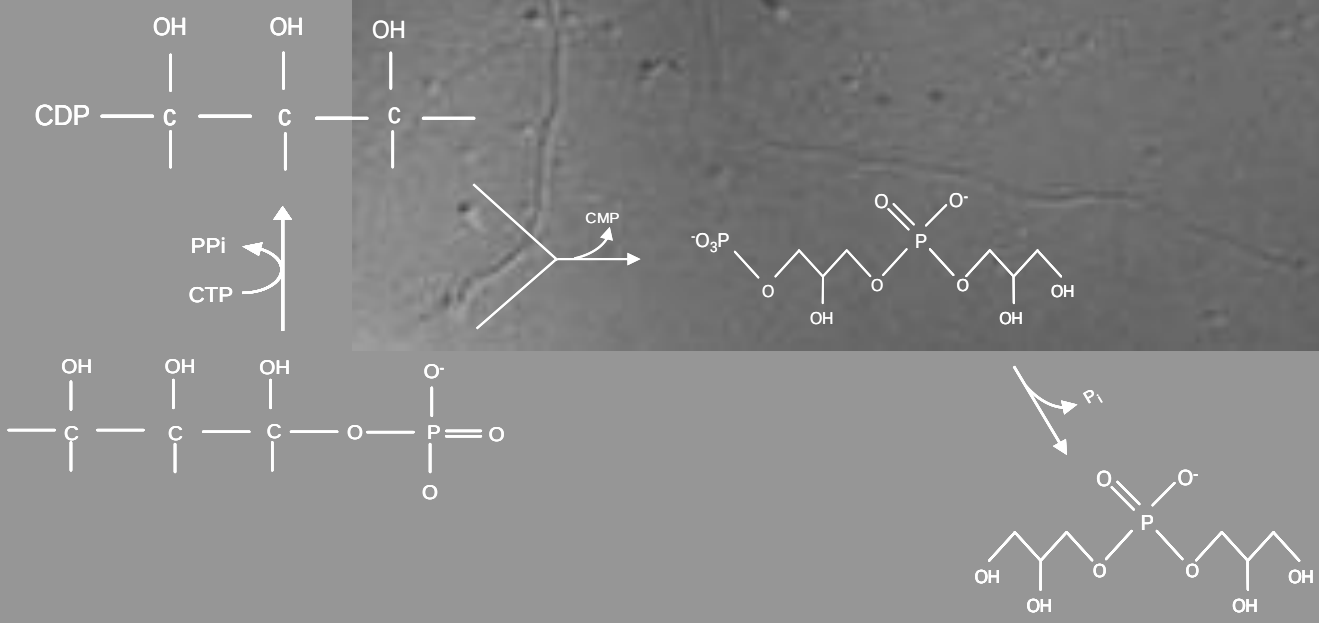

Luís Pedro Gafeira Gonçalves

2008

Universidade Nova de Lisboa

Instituto de Tecnologia Química e Biológica

Osmo- and thermo-adaptation in hyperthermophilic *Archaea*: identification of compatible solutes, accumulation profiles, and biosynthetic routes in *Archaeoglobus* spp.

This dissertation was presented to obtain a Ph. D. degree in Biochemistry at the Instituto de Tecnologia Química e Biológica, Universidade Nova de Lisboa.

By **Luís Pedro Gafeira Gonçalves**

Supervised by **Prof. Dr. Helena Santos**

Oeiras, January, 2008

Apoio financeiro da Fundação para a Ciência e Tecnologia (POCI 2010 – Formação Avançada para a Ciência – Medida IV.3) e FSE no âmbito do Quadro Comunitário de apoio, Bolsa de Doutoramento com a referência SFRH / BD / 5076 / 2001.

ACKNOWNLEDGMENTS

The work presented in this thesis, would not have been possible without the help, in terms of time and knowledge, of many people, to whom I am extremely grateful.

Firstly and mostly, I need to thank my supervisor, Prof. Helena Santos, for her way of thinking science, her knowledge, her rigorous criticism, and her commitment to science. Her attitude as a scientist taught me what a scientist should be. Her investment, with time and knowledge, together with her ability of providing financial support, allowed the fulfilment of this work.

To Dr. Paula Fareleira, who was always available with an enthusiastic word to say, for her deep knowledge about the tricky *Archaea* and her priceless metabolic maps, and above all for her friendship, which was absolutely essential for the completion of this thesis.

To Prof. R. Huber of Regensburg University, who provided us with some of the organisms studied in the present work, I thank his scientific interest in my work.

To Prof. Milton da Costa, I thank his interest in my work and our stimulating and useful scientific discussions.

To Dr. Nuno Borges, for his availability to help, his concern with the evolution of the work and his critic spirit; his support was essential for this thesis.

To Dr. Pedro Lamosa, for his NMR knowledge and his availability to teach and help; his fluent way of thinking was extremely important for this work.

To Isabel Pacheco e Ana Mingote, I thank their technical support in purification procedures and for teaching me some of their expertise.

To Marta Rodrigues, for her youth, working capability and her continuous search for new challenges, that was of great help in this work.

To all my colleages in Cell Physiology & NMR group, specially Dr. Rute Neves, Dr. Tiago Faria, Dr. Luís Fonseca, Dr. Mané Sampaio, Dr. Melinda Noronha, Dr Claudia Sanchez, Dr. Clélia Neves, Tiago Pais, Paula Gaspar, Carla Jorge, Rute Castro, Ana Lúcia Carvalho, Susana Gonçalves and Carla Patrícia, whose friendship contributed to make me a "richer" person. A special thanks to Filipa Cardoso, who started with me the long PhD way and to whom I have a lot to thank.

To Cristina Amaral, Isabel Bahia, and especially to Anabela Bernardo (the little pony) for all the logistic and informatics support, and their friendship and joy.

To Fundação para Ciência e Tecnologia for the financial support provided by the PhD grant, and to the Instituto de Tecnologia Química e Biólogica, for providing conditions to pursue scientific excellence. I wish it can continue as dreamt by his relentless creator, Prof. António Xavier.

Ao Nuno, Pedro, Tiago e Paula, pois algumas das minhas mais gratas recordações neste longo caminho foram no Beer Hunter ou num jantar de quarta-feira.

Aos meus amigos pois sem eles a vida não tinha o mesmo significado, temos de nos encontrar nem que seja no Biotretas. Em especial ao Vítor, pelos quase vinte anos de amizade; ao João, que me acompanhou nos primórdios desta jornada; e as meninas do IGC, Sofia e Patrícia, por tornarem os dias mais alegres.

À minha família, obrigado por todo o amor. Joana, apesar da distância e ausência de telefonemas estás sempre no meu coração. Mãe e Pai, obrigado.

À minha família em construção. O amor incondicional do Freud. Inês, o teu sorriso vale uma vida inteira. Jacinta, pelo teu amor e pela nossa vida junta, que me faz uma melhor pessoa.

Ao futuro, pois é ele que me faz andar para a frente.

ABSTRACT

Hyperthermophilic organisms have optimum growth temperatures above 80°C and belong to genera that are placed near the root of the Tree of Life, in short phylogenetic branches within the domains *Bacteria* or *Archaea*. Although hyperthermophiles have been isolated from a variety of hot environments, most species originate from marine geothermal areas, hence they are slightly halophilic. The accumulation of low-molecular mass organic solutes, i. e., compatible solutes, is one of the most common strategies developed by cells to cope with fluctuations of the salinity of the medium. Interestingly, in marine hyperthermophiles, compatible solute accumulation occurs not only in response to an increase in the external salt concentration, but also in response to supraoptimal growth temperatures. Moreover, microorganisms adapted to grow optimally at elevated temperatures tend to use negatively charged solutes that are not present or rarely encountered in mesophilic organisms.

In this work, the organic solute pool of several members of the genus *Archaeoglobus* as well as of the extreme hyperthermophile *Pyrolobus fumarii* was investigated by Nuclear Magnetic Resonance (NMR). The profiles of solute accumulation as a function of the growth temperature and the NaCl concentration were determined; moreover, the pathways for the synthesis of two major compatible solutes, diglycerol phosphate and mannosylglycerate, were elucidated.

Pyrolobus fumarii belongs to the crenarchaeote branch of the domain Archaea. It is one of the most hyperthermophilic organisms known, being able to grow at temperatures up to 113°C. *P. fumarii* accumulates di-*myo*-inositol phosphate as the major solute (0.21 μmol/mg protein), a finding that reinforces the correlation between di-*myo*-inositol phosphate accumulation and hyperthermophily. The ethanol extracts of *P. fumarii* cells also contain several UDP-sugars (total concentration 0.11 μmol/mg protein). The structures of the two major UDP-sugars were identified as UDP-α-GlcNAc3NAc and UDP-α-GlcNAc3NAc-(4←1)-β-GlcpNAc3NAc. Interestingly, the latter compound appears to be derived from the first one by addition of a 2,3-*N*-diacetylglucoronic acid unit, suggesting that these UDP-sugars are intermediates of an *N*-linked glycosylation pathway.

Representatives of three species of the genus *Archaeoglobus* were studied: *Archaeoglobus profundus*, *Archaeoglobus veneficus* and three strains of *Archaeoglobus fulgidus* (7324, VC-16 and VC-16S). *A. fulgidus* VC-16S is a variant of the type strain, *A. fulgidus* VC-16, isolated from cultures obtained after a stepwise transfer from media containing 1.8% to 6.3% (w/v) NaCl. The variant strain showed an increased salt tolerance when compared to the

parental strain, displaying higher growth rates throughout the entire NaCl concentration range, and shifting the higher limit for growth from 4.5% to 6.3% NaCl. The optimal NaCl concentration was, however, the same for both strains, around 1.8% NaCl. Surprisingly, the total pool of compatible solutes was lower than in the parental strain, but increased notably at salinities above 4.5% NaCl, reaching a value of 3.34 μmol/mg protein at 6.0% NaCl. In response to salt stress, *A. fulgidus* VC-16S accumulated mainly diglycerol phosphate, an osmolyte thus far confined to the *Archaeoglobales*. Furthermore, the level of diglycerol phosphate increased approximately 28-fold in cells grown in medium containing 6.0% NaCl, when compared with cells grown at low salinity (0.9% NaCl). At supra-optimal growth temperatures, di-*myo*-inositol phosphate was the predominant solute, increasing 11-fold from the optimal to the maximal growth temperature (83°C to 89°C). At the highest temperature examined, di-*myo*-inositol phosphate and diglycerol phosphate represented 75% (molar percentage) of the total solute pool.

An unknown solute, initially designated as "unknown di-*myo*-inositol phosphate isomer" was present in low amounts in extracts of strains *A. fulgidus* VC-16 and VC-16S. The structure of this compound was firmly identified as glycero-phospho-*myo*-inositol by using a combination of NMR and Mass Spectrometry. Thus far, this newly discovered solute has been found only in *A. fulgidus* (strains VC-16, VC-16S and 7324) and in two hyperthermophilic bacteria of the genus *Aquifex* (*Aquifex aeolicus* and *Aquifex pyrophilus*). The level of glycerol-phospho-*myo*-inositol responded primarily to the combination of supra-optimal temperature and supra-optimal NaCl concentration. The remarkable structural relationship between diglycerol phosphate, di-*myo*-inositol phosphate, and the newly identified solute is disclosed in this work. The unit glycero-phospho-*myo*-inositol is part of the polar head in phosphatidylinositol, an important constituent of lipid membranes, but this is the first report on the occurrence of glycero-phospho-*myo*-inositol as a cell metabolite.

Like *A. fulgidus* VC-16, a different strain of *A. fulgidus* (strain 7324) accumulated the polyolphosphodiesters, diglycerol phosphate, di-*myo*-inositol phosphate, and glycero-phospho-*myo*-inositol, when grown on lactate, but the nature of the intracellular osmolytes was remarkably different when starch was used as the carbon source. Under these growth conditions, mannosylglycerate was a major solute. Growth in medium containing 4.5% NaCl, a concentration well above the optimal value (1.8% NaCl), led to a 5-fold increase in the intracellular content of mannosylglycerate, which was the sole solute detected at this salinity. Interestingly, mannosylglycerate was also detected in members of two other *Archaeoglobus* spp., *i. e.*, *A. veneficus* and *A. profundus,* which use acetate as the preferred carbon source.

The solute pool of *A. veneficus* was composed by diglycerol phosphate, di-*myo*-inositol phosphate, mannosylglycerate and α-glutamate, and a similar set of solutes was observed in extracts of *A. profundus*, except that diglycerol phosphate was absent.

In summary, the major solutes found in members of the genus *Archaeoglobus* are di-*myo*-inositol phosphate, diglycerol phosphate and mannosylglycerate. Di-*myo*-inositol phosphate was found in all the strains examined; diglycerol phosphate was also a common solute being present in all strains except for *A. profundus*; mannosylglycerate accumulated in *A. profundus*, *A. veneficus* and *A. fulgidus* 7324, but was not detected in *A. fulgidus* VC-16 and VC-16S. The newly identified compound, glycero-phospho-*myo*-inositol, has only been found in the strains of the species *A. fulgidus*.

The pathways for the synthesis of mannosylglycerate and diglycerol phosphate were established based on the detection of relevant enzymatic activities in cell extracts. The synthesis of mannosylglycerate involved the condensation of GDP-mannose with D-3-phosphoglycerate by the action of mannosyl-3-phosphoglycerate synthase (MPGS) to form a phosphorylated intermediate, mannosyl-3-phosphoglycerate (MPG), which was subsequently dephosphorylated by a specific phosphatase, mannosyl-3-phosphoglycerate phosphatase (MPGP). Using degenerated PCR and inverse PCR, it was possible to identify two contiguous open reading frames homologous to *mpgS* (encoding MPGS) and *mpgP* (encoding MPGP) in *A. profundus* and *A. veneficus.* Downstream of these genes, an open reading frame coding for a putative mannosidase was found. This organization of the mannosylglycerate gene cluster, comprising a putative mannosidase, has not been observed elsewhere. The *mpgS* and *mpgP* genes of *A. fulgidus* 7324 have been partially sequenced.

The synthesis of diglycerol phosphate in *A. fulgidus* strains VC-16 and 7324 was also elucidated: the enzymatic activities were detected in cell extracts and the intermediate metabolite was characterized by NMR. Addition of glycerol 3-phosphate and CTP to cell-free extracts led to the formation of diglycerol phosphate; a transient accumulation of CDP-glycerol was also observed. Maximum diglycerol phosphate production was obtained when glycerol 3-phosphate and CDP-glycerol were used as substrates. It was verified that glycerol and other nucleotides (ATP, UTP and GTP) were not precursors for the synthesis of CDP-glycerol and diglycerol phosphate.

Firm evidence for the presence of a phosphorylated intermediate in the synthesis of diglycerol phosphate was obtained when CDP-glycerol and glycerol 3-phosphate were supplied to cell extracts treated with sodium fluoride, a known inhibitor of phosphatases. A new resonance appeared in the phosphodiester region of the ^{31}P-NMR spectrum of the reaction

mixture. Upon subsequent treatment with alkaline phosphatase, this resonance disappeared and the intensity of the diglycerol phosphate resonance increased by the corresponding amount. After purification using column chromatography this new metabolite was identified as diglycerol phosphate phosphate by 2D-NMR techniques.

It is concluded that the biosynthesis of diglycerol phosphate proceeds from glycerol 3-phosphate via three steps: (1) glycerol 3-phosphate activation to CDP-glycerol at the expense of CTP; (2) CDP-glycerol condensation with glycerol 3-phosphate yielding the phosphorylated intermediate, diglycerol phosphate phosphate; (3) finally, dephosphorylation of diglycerol phosphate phosphate into diglycerol phosphate by the action of a yet unknown phosphatase. Interestingly, a similar reaction scheme has been established for the synthesis of di-*myo*-inositol phosphate and glycero-phospho-*myo*-inositol, the two other polyol-phosphodiester solutes present in *A. fulgidus*.

Resumo

Os organismos hipertermófilos apresentam temperaturas óptimas de crescimento acima dos 80°C e pertencem a géneros dos domínios *Bacteria* e *Archaea*, que estão dispostos em ramos curtos, próximo da origem da Árvore da Vida. Apesar destes organismos terem sido isolados a partir de uma grande variedade de biótopos quentes, a maioria das espécies hipertermofílicas conhecidas foi isolada de áreas geotermais marinhas, apresentando portanto, halotolerância ou halofilia moderada. A acumulação de solutos orgânicos de baixa massa molecular, *i. e.*, solutos compatíveis, é uma das estratégias celulares mais comuns para fazer face a variações da salinidade do meio. Curiosamente, nos hipertermófilos marinhos a acumulação de solutos compatíveis ocorre não só em resposta a um aumento da salinidade, mas também em resposta a condições de agressão térmica. Além disso, estes microrganismos que proliferam optimamente a temperaturas elevadas, tendem a acumular solutos carregados negativamente, nunca, ou raramente, encontrados em organismos mesofílicos.

Neste trabalho, investigou-se por Ressonância Magnética Nuclear (NMR) a acumulação de solutos orgânicos em vários membros do género *Archaeoglobus* e no hipertermófilo extremo *Pyrolobus fumarii*. Foram determinados os perfis de acumulação de solutos em função da temperatura de crescimento e da concentração de NaCl presente no meio de cultura; para além disso, elucidou-se a biossíntese de dois solutos compatíveis em *Archaeoglobus*: o fosfato de diglicerol e o manosilglicerato.

O arqueão *Pyrolobus fumarii* pertence ao reino *Crenarchaeota* e é um dos organismos conhecidos que apresenta maior grau de termofilia, sendo capaz de crescer até 113°C. *P. fumarii* acumula como soluto maioritário o fosfato de di-*myo*-inositol (0,21 μmol/mg proteína), um facto que reforça a correlação entre hipertermofilia e acumulação deste composto. Os extractos etanólicos realizados a partir de massa celular de *P. fumarii* também revelaram a presença de vários derivados glicosilados de UDP (concentração total de 0,11 μmol/mg proteína). Utilizando técnicas de NMR bidimensional, foi possível identificar a estrutura de dois destes compostos como sendo: UDP-α-GlcNAc3NAc e UDP-α-GlcNAc3NAc-(4←1)-β-GlcpNAc3NAc. O segundo destes compostos aparenta ser derivado do primeiro através da adição de uma unidade de ácido 2,3-*N*-diacetilglucorónico, sugerindo a possibilidade destes compostos fazerem parte de uma via de *N*-glicosilação.

Foram estudadas três espécies representativas do género *Archaeoglobus*: *Archaeoglobus profundus*, *Archaeoglobus veneficus* e três estirpes de *Archaeoglobus fulgidus* (7324, VC-16 e VC-16S). A estirpe VC-16S é uma variante da estirpe tipo (*A. fulgidus* VC-16),

isolada a partir de culturas submetidas a um aumento brusco da salinidade do meio de 1,8% para 6,3% (p/v) de NaCl. Quando comparada com a estirpe parental, a nova estirpe demonstrou possuir uma maior tolerância salina, apresentando taxas de crescimento mais elevadas em toda a gama de salinidades testada e desviando o limite superior de salinidade que ainda permite o crescimento de 4,5% para 6,3% de NaCl. No entanto, a concentração de NaCl a que corresponde crescimento óptimo não se alterou, sendo cerca de 1,8% para ambas as estirpes. Surpreendentemente, a quantidade total de solutos compatíveis acumulada pela estirpe variante era inferior à da estirpe parental, aumentando notavelmente apenas a concentrações de NaCl superiores a 4,5%, e atingindo um valor de 3,34 μmol/mg proteína a 6,0% de NaCl. Como resposta a agressão salina, *A. fulgidus* VC-16S acumulou principalmente fosfato de diglicerol, um osmólito cuja ocorrência parece confinada à ordem *Archaeoglobales*. Comparando com células cultivadas em meio de baixa salinidade (0,9% NaCl), a presença de 6,0% NaCl no meio causou um aumento de cerca de 28 vezes na concentração intracelular de fosfato de diglicerol. A valores de temperatura acima da óptima, o soluto predominantemente acumulado foi o fosfato de di-*myo*-inositol, cujos níveis aumentaram 11 vezes em resposta a um aumento de 6°C (da temperatura óptima de crescimento de 83°C para 89°C). À mais elevada temperatura estudada, os fosfatos de di-*myo*-inositol e de diglycerol constituíram 75% (em percentagem molar) da quantidade total de solutos presente.

Em extractos das estirpes de *A. fulgidus* VC-16 e VC-16S encontraram-se quantidades relativamente baixas de um soluto desconhecido, designado previamente como "um isómero desconhecido de fosfato de di-*myo*-inositol". Usando uma combinação de técnicas de NMR bidimensional e Espectrometria de Massa foi possível elucidar a estrutura deste composto, tratando-se de gliceril-fosfo-*myo*-inositol. Este composto apenas foi observado em *A. fulgidus* (estirpes VC-16, VC-16S e 7324) e em duas bactérias hipertermofílicas classificadas no género *Aquifex*, nomeadamente, *Aquifex aeolicus* e *Aquifex pyrophilus*. Os níveis de gliceril-fosfo-*myo*-inositol responderam principalmente a uma combinação de agressões térmica e salina. Este é um facto curioso tendo em conta as relações estruturais do composto agora identificado com os fosfatos de diglicerol e de di-*myo*-inositol, que respondem primariamente à salinidade e à temperatura, respectivamente. A unidade gliceril-fosfo-*myo*-inositol está presente na constituição da cabeça polar do fosfatidilinositol, um constituinte importante das membranas lipídicas; no entanto, esta foi a primeira vez que a ocorrência do gliceril-fosfo-*myo*-inositol como metabolito celular foi relatada.

Quando cultivada usando ácido láctico como fonte de carbono, a estirpe de *A. fulgidus* 7324 também acumula os poliol-fosfodiésteres fosfato de diglycerol, fosfato de di-*myo*-inositol e

gliceril-fosfo-*myo*-inositol. No entanto, a natureza dos composto acumulados muda radicalmente quando o ácido láctico é substituido por amido, sendo manosilglicerato o soluto maioritariamente acumulado nestas condições de crescimento. Na presença de amido, o crescimento desta estirpe em meio contendo 4,5% de NaCl, uma concentração bem acima do valor óptimo para o crescimento (1,8% NaCl), conduziu a um aumento dos níveis intracelulares de manosilglicerato em cerca de 5 vezes, tornando-se este soluto o único detectável nestas condições. O manosilglicerato também foi detectado nas outras duas espécies estudadas de *Archaeoglobus*, nomeadamente, *A. veneficus* e *A. profundus,* que utilizam acetato como fonte de carbono preferencial. O conjunto dos solutos acumulados por *A. veneficus* compreende fosfato de diglycerol, fosfato de di-*myo*-inositol, manosilglicerato e α-glutamato. Um conjunto semelhante de solutos foi também observado em extractos de *A. profundus*, com a única excepção da ausência de fosfato de diglycerol.

Em resumo, os solutos maioritários encontrados em membros do género *Archaeoglobus* são fosfato de di-*myo*-inositol, fosfato de diglicerol e manosilglicerato. Encontrou-se fosfato de di-*myo*-inositol em todas as estirpes examinadas; o fosfato de diglicerol era também um soluto comum, estando presente em todas as estirpes à excepção de *A. profundus*; observou-se acumulação de manosilglicerato em *A. profundus*, *A. veneficus* e *A. fulgidus* 7324, mas não em *A. fulgidus* VC-16 e VC-16S. O composto identificado neste trabalho, gliceril-fosfo-*myo*-inositol, apenas foi detectado em estirpes da espécie de *A. fulgidus*.

As vias de síntese de manosilglicerato e de fosfato de diglicerol foram determinadas com base na detecção das actividades enzimáticas relevantes em extractos celulares. A síntese de manosilglicerato envolveu a condensação de GDP-manose com D-3-fosfoglicerato através da actividade da sintase de manosil-3-fosfoglicerato (MPGS), produzindo um intermediário fosforilado, manosil-3-fosfoglicerato (MPG), que foi subsequentemente desfosforilado por uma fosfatase específica, a fosfatase de manosil-3-fosfoglicerato (MPGP). Usando técnicas de PCR degenerado e PCR inverso, foi possível identificar dois genes contíguos com homologia a *mpgS* (que codifica para MPGS) e a *mpgP* (que codifica para MPGP) em *A. profundus* e *A. veneficus.* A jusante destes genes, encontrou-se um gene putativamente atribuído a uma manosidase. Esta organização do conjunto de genes que codifica para a síntese do manosilglicerato, incluindo o gene codificante da manosidase, nunca tinha sido observada. Os genes *mpgS* e *mpgP* de *A. fulgidus* 7324 foram sequenciados parcialmente neste trabalho de tese.

A síntese de fosfato de diglicerol nas estirpes VC-16 e 7324 de *A. fulgidus* também foi elucidada: as actividades enzimáticas foram detectadas em extractos celulares e o metabolito intermediário foi caracterizado por NMR. A adição de 3-fosfoglicerol e CTP a extractos celulares

levou à formação de fosfato de diglicerol com a acumulação transiente de CDP-glicerol. Obteve-se uma produção maximizada de fosfato de diglicerol quando se utilizaram 3-fosfoglicerol e CDP-glicerol como substratos. Verificou-se que a síntese de CDP-glicerol e fosfato de diglicerol não ocorria quando glicerol ou outros nucleótidos (ATP, UTP e GTP) foram usados como substratos.

Ao incubar um extracto celular com 3-fosfoglicerol e CDP-glicerol na presença de fluoreto de sódio, um conhecido inibidor de fosfatases, obteve-se evidência sólida para a existência de um intermediário fosforilado na síntese de fosfato de diglicerol. Nestas condições, foi detectada uma nova ressonância na região dos fosfodiésteres no espectro de ^{31}P-NMR da mistura reaccional. Ao tratar esta preparação com fosfatase alcalina, a nova ressonância desapareceu, com aumento concomitante de intensidade do sinal correspondente ao fosfato de diglicerol. Após a purificação por cromatografia em coluna, este novo metabolito foi identificado como fosfato de diglicerol fosfato por técnicas de NMR bidimensional.

Concluiu-se que a biossintese do fosfato de diglicerol se processa a partir de 3-fosfoglicerol em três passos: (1) a activação de 3-fosfoglicerol a CDP-glicerol com consumo de CTP; (2) a condensação de CDP-glicerol com 3-fosfoglicerol resultando num intermediário fosforilado, fosfato de diglicerol fosfato; (3) finalmente, a desfosforilação de fosfato de diglicerol fosfato a fosfato de diglicerol através da acção de uma fosfatase ainda desconhecia. Curiosamente, vias de síntese semelhantes a esta foram descritas recentemente para o fosfato de di-*myo*-inositol e e para o gliceril-fosfo-*myo*-inositol, os dois outros poliol-fosfodiésteres presentes em *A. fulgidus*.

CONTENTS

THESIS OUTLINE

(Hyper)thermophilic organisms living in aqueous environments are periodically confronted with fluctuations in osmolarity and/or temperature, to which they must adapt to survive and proliferate. The knowledge of the mechanisms developed by these organisms to cope with osmotic and/or heat stress is an important scientific issue with high biotechnological potential.

The work presented in this thesis was planned to determine the organic solute pool of several members of the genus *Archaeoglobus* as well as of the extreme hyperthermophile *Pyrolobus fumarii*. The three species of the genus *Archaeoglobus* were chosen as targets for the determination of the profile of solute accumulation as a function of the growth temperature and NaCl concentration in the growth medium. In addition, the pathways for the synthesis of two major compatible solutes, diglycerol phosphate and mannosylglycerate, were elucidated.

Chapter 1, starts with an overview of the domain *Archaea* and the extremophilic organisms, highlighting the adaptive mechanisms developed by these organisms to cope with high temperature and salinity. This is followed by a general overview on distribution, accumulation and roles of compatible solutes in osmoadaptation and thermoadaptation, specially in (hyper)thermophiles. The pathway for the synthesis of mannosylglycerate, one of the most common compatible solutes in (hyper)thermophiles, is explained as model case. Finally, the genus *Archaeoglobus* is introduced with special attention given to the metabolic features of *Archaeoglobus fulgidus*.

The organic solute pool of the extreme hyperthermophile *Pyrolobus fumarii*, that is able to grow up to 113°C, is depicted in Chapter 2. *P. fumarii* accumulates di-*myo*-inositol phosphate as the major solute along with several UDP-sugars that probably do not serve as compatible solutes. The structures of the two major UDP-sugars were identified as UDP-α-GlcNAc3NAc and UDP-α-GlcNAc3NAc-(4←1)-β-GlcpNAc3NAc. Interestingly, the latter compound appears to derive from the first one by addition of a 2,3-*N*-diacetylglucoronic acid unit, suggesting that these UDP-sugars are intermediates of an *N*-linked glycosylation pathway.

In Chapter 3, the accumulation pattern of compatible solute is shown for different species of the genus *Archaeoglobus*: *Archaeoglobus profundus*, *Archaeoglobus veneficus* and

two strains of *Archaeoglobus fulgidus* (7324 and VC-16). A new variant of *A. fulgidus* VC-16, *A. fulgidus* VC-16S, that was isolated from cultures adapted to high salinity was also studied. Moreover, an unknown compatible solute accumulating to minor amounts in *A. fulgidus* strains was firmly identified as glycero-phospho-*myo*-inositol. The occurrence of this compound as a cell metabolite is described here for the first time. The major solutes found in members of the genus *Archaeoglobus* are di-*myo*-inositol phosphate, mainly accumulating at supra-optimal temperatures, and diglycerol phosphate and mannosylglycerate, two solutes preferentially accumulating in response to high salinity. Di-*myo*-inositol phosphate was found in all the strains examined; diglycerol phosphate was also a common solute being present in all strains except for *A. profundus*; mannosylglycerate accumulated in *A. profundus*, *A. veneficus* and *A. fulgidus* 7324, but was not detected in *A. fulgidus* VC-16 or VC-16S. The novel compound, glycero-phospho-*myo*-inositol, has only been found in the strains of the species *A. fulgidus*. The effect of the carbon source used for growth in the pattern of solute accumulation was studied in *A. fulgidus* 7324; when lactate was utilised, mannosylglycerate was absent; growth on starch, however, led to the accumulation of mannosylglycerate, which became the major solute in the response to salt stress.

In Chapter 4, the activity of mannosyl-3-phosphoglycerate synthase (MPGS), the synthase of the two-step pathway for mannosylglycerate synthesis, was detected in cell extracts of *A. profundus* and *A. fulgidus* 7324. Based on degenerated and inverse PCR, two contiguous genes, *mpgS* (encoding MPGS) and *mpgP* (encoding mannosyl-3-phosphoglycerate phosphatase), were identified in *A. profundus* and *A. veneficus.* Downstream of *mpgP*, a gene coding for a putative mannosidase was found. This organization of the mannosylglycerate gene cluster, including a putative mannosidase, was observed here for the first time.

The biosynthetic pathway of diglycerol phosphate (DGP) in *A. fulgidus* strains VC-16 and 7324 is proposed in Chapter 5. The synthesis of DGP proceeds from glycerol 3-phosphate via three steps: (1) glycerol 3-phosphate activation to CDP-glycerol at the expense of CTP; (2) CDP-glycerol condensation with glycerol 3-phosphate yielding the phosphorylated intermediate, diglycerol phosphate phosphate; (3) finally, dephosphorylation of the intermediate into diglycerol phosphate by the action of a yet unknown phosphatase.

Finally, an overall discussion of the work described in this thesis is presented in Chapter 6.

ABBREVIATIONS

cBPG	Cyclic-2,3-bisphosphoglycerate
COSY	Homonuclear shift COrrelation SpectroscopY
DGP	Diglycerol phosphate
DGPP	Diglycerol phosphate phosphate
DGPPS	Diglycerol phosphate phosphate synthase
DIP	Di-*myo*-inositol phosphate
DIPP	Di-*myo*-inositol phosphate phosphate
DIPPS	Di-*myo*-inositol phosphate phosphate synthase
FPLC	Fast protein liquid chromatography
GCT	CTP:L-glycerol-3-phosphate cytidylyltransferase
GDH	Glutamate dehydrogenase
GPI	Glycero-phospho-*myo*-inositol
GPIP	Glycero-phospho-*myo*-inositol phosphate
GPIPS	Glycero-phospho-*myo*-inositol phosphate synthase
Glu	Glutamate
Gly 3-P	Glycerol 3-phosphate
HMBC	Heteronuclear Multiple Bond Connectivity by 2D multiple quantum NMR
HMQC	^{1}H detected Heteronuclear Multiple Quantum Coherence via direct coupling
Ino 1-P	*myo*-inositol 1-phosphate
IPTG	Isopropyl-1-thio-β-D-galactopyranoside
MG	Mannosylglycerate
MGS	Mannosylglycerate synthase
M1P-GT	Mannose 1-phosphate guanylyl transferase
MPG	Mannosyl-3-phosphoglycerate
MPGP	Mannosyl-3-phosphoglycerate phosphatase
MPGS	Mannosyl-3-phosphoglycerate synthase
NAD^+	Nicotinamide adenine dinucleotide, oxidised form
NADH	Nicotinamide adenine dinucleotide, reduced form
NADPH	Nicotinamide adenine dinucleotide phosphate, reduced form
NMR	Nuclear magnetic resonance
NOESY	Nuclear Overhauser Effect SpectroscopY
PAGE	Polyacrylamide gel electrophoresis
3PGA	3-phosphoglycerate
ORF	Open reading frame
Pi	Inorganic phosphate
PMI	Phosphomannose isomerase
PMM	Phosphomannose mutase
PPi	Pyrophosphate
PMSF	Phenylmethane-sulphonyl fluoride
TOCSY	Homonuclear TOtal-Correlation SpectroscopY

UDP-α-GlcNAc3NAc (UGNN)	UDP-N-2,3-diacetamino-2,3-dideoxy-D-α-glucopyranose
UGNN-(4←1)β-Glc*p*NAc3NAc	UDP-*N*-2,3-diacetamino-2,3-dideoxy-D-glucopyranose-(4←1)-β-2,3-diacetamido-2,3-dideoxy-*β*-glucoronic acid
TLC	Thin layer chromatography
WALTZ	Wideband Alternating-phase Low-power Technique for Zero-residue splitting

CHAPTER 1

General Introduction

Chapter | 1| Contents

Archaea

In 1977, the research group of Carl Woese at NASA (*National Aeronautics and Space Administration*) disclosed the view that the simplistic division of the natural world into *Prokaria* and *Eukaria* no longer made sense, given the profound differences encountered among the prokaryotes (Woese and Fox 1977). This meant that "prokaryote" was not a valid taxonomic class as it had been defined in opposition to *Eukaria* rather than based on a solid set of biological characteristics. This finding led eventually to the currently accepted proposal that

considers the division of the natural world into three domains, *Bacteria*, *Archaea* and *Eukarya*, based on the comparison of 16S rRNA sequences (Woese et al. 1990; Kates 1993). The differences between these three domains run very deep at different levels of cell organisation. The most representative, distinctive, characteristics are summarised in Table I.1.

Table I.1 Some representative characteristics of the three natural domains (adapted from Woese et al. 1990).

	Bacteria	***Archaea***	***Eukarya***
Nucleus	-	-	+
Membrane lipids	Ester	Ether	Ester
Cell wall with muranic acid	+	-	-
Ribosome	70S	70S	80S
tRNA	Formylmethionine	Methionine	Methionine
Operons	+	+	-

(+) presence and (-) absence

Archaea means "ancient", and the reason for this term is that the organisms initially described as belonging to the domain *Archaea* inhabited extreme environments resembling those thought to be present in the primordial earth, and accordingly were described as ancestral forms of life. Today, however, an increasing number of isolates showed that archaea are in fact present in almost all Earth environments, either terrestrial or aquatic (Rothschild and Mancinelli 2001). At the molecular systems level, archaea are more complex than bacteria (Keeling and Doolittle 1995; Langer et al. 1995). An illustrative example is the DNA replication apparatus: primases, helicases and replicative polymerases present in archaea and eukarya are very similar and completely different from their bacterial counterparts (Olsen and Woese 1996). In other aspects *Archaea* are more similar to *Bacteria*, like the size and organisation of the chromosome or the presence of polycistronic transcription units (Gribaldo and Brochier-Armanet 2006). Archaeal duality is eloquently expressed by the following phrase "*Archaea* look like organisms that use eukaryotic-like proteins in a bacterial-like context" (Gribaldo and Brochier-Armanet 2006). Aside from the common traits with bacteria or eukaryons, archaeons also have unique characteristics that distinguish them from members of the two other domains. For example, in all archaeons the membrane phospholipids are isoprenoid ethers in a glycerol 1-phosphate backbone, in contrast to the fatty acid esters linked to glycerol 3-phosphate present in *Bacteria* and *Eukarya*. Moreover, the position of the domain *Archaea* in the Tree of

Life is no longer near the root of the tree, but is now located as a phylogenetic arm at the same level of *Bacteria* and *Eukarya* (Figure I.1).

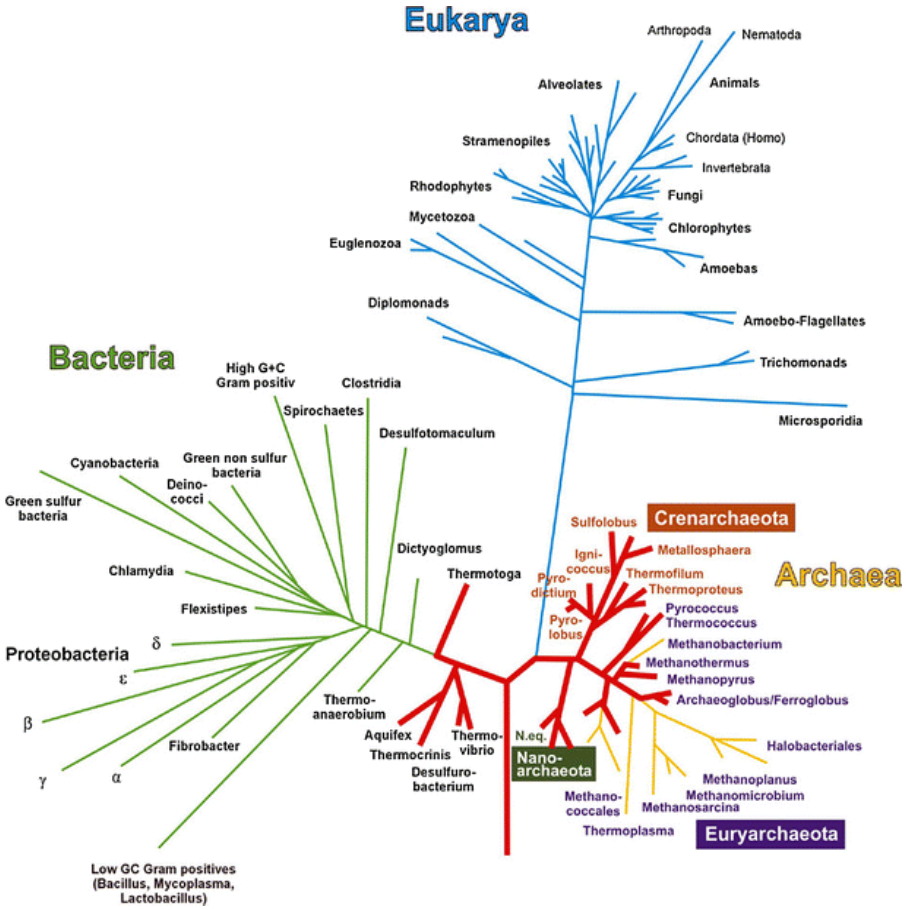

Figure I.1 Universal phylogenetic tree based on 16S rRNA. Red branches indicate hyperthermophilic lineages (Reproduced from Stetter (2006), History of discovery of the first hyperthermophiles, *Extremophiles* vol. 10, with permission of the publisher. License number: 1863710404742).

Together with the proposal of the domain *Archaea*, Woese *et al.* (1990) suggested the creation of two kingdoms within this domain: the *Euryarchaeota* and the *Crenarchaeota. Euryarchaeota* is a phenotypically heterogeneous group, comprising sulfate reducing hyperthermophiles (the class *Archaeoglobi*), other hyperthermophiles (the classes *Thermococci* and *Thermoplasmata*), extreme halophiles (the class *Halobacteria*) and most lineages of methanogens (the classes *Methanomicrobia, Methanococci*, *Methanobacteria* and *Methanopyri*). Despite this diversity of phenotypes, *Euryarchaeota* is a consistent group, and independently of

the method and the protein chosen as model, the resulting phylogenetic tree is very similar (Gribaldo and Brochier-Armanet 2006). *Crenarchaeota* was formerly a more homogeneous group, constituted entirely by thermoacidophilic organisms belonging to the class *Thermoprotei*, which comprises five orders (*Caldisphaerales, Thermoproteales, Cenarchaeales*, *Sulfolobales* and *Desulfurococcales*). However, DNA sequences obtained recently from marine plankton, freshwater samples, deep sub-surfaces, and soil environments revealed the existence of *Crenarchaeota* in these habitats (Schleper et al. 2005), hence extending the representatives of this kingdom beyond hyperthermophiles.

Nanoarchaeum equitans, an obligate hyperthermophilic symbiont of the crenarchaeon *Ignicoccus hospitalis*, is the smallest organism known to date and has the shortest genome sequenced thus far (490 Mb) (Huber et al. 2002; Huber et al. 2003; Waters et al. 2003). This remarkable discovery led to the proposal of a third phylum in *Archaea*, the *Nanoarchaeota* (Huber et al. 2002). However, this view is not consensual, with some authors considering that *Nanoarchaeum* represents an euryarchaeal fast-evolving lineage, distantly related to the *Thermococcales* (Brochier et al. 2005). Genomic sequences from two other groups of archaeons, *Korarchaeota* (Barns et al. 1996) and the Ancient Archaeal Group (Takai and Horikoshi 1999), were found in environmental hyperthermophilic samples (uncultivated organisms).

Although members of the domain *Archaea* are found in almost all biotopes, their presence is more frequent in environments with conditions that are inhospitable for animals and many other organisms.

Extremophiles

By definition, extremophiles are organisms requiring, or able to endure, extreme environmental conditions. Obviously, the term "extreme" has different meanings for different subjects. A pool of boiling water is an extreme environment for humans, but quite comfortable for *Pyrolobus fumarii*, an organism unable to grow at 30^{o}C, which is a moderate temperature for humans. So, how can we define an extreme environment? From an anthropocentric point of view, an extremophile can be considered as an organism that has optimal growth conditions outside the normal human standards (Kristjánsson and Hreggvidsson 1995). This definition, however, fails in objectivity, since it considers *Homo sapiens* as the environmental standard for all forms of life. Another way around this question is looking at the ranges of physico-chemical parameters (temperature, pH, water activity, or pressure) of the environments able to support life. For example, if life is possible between pH 0 and 12, then environments with pH values

below 2 or above 10 are approaching the limits for life, as far as this parameter is concerned. Naturally, this concept can be extended to other parameters to include high or low temperature, high salinity, elevated levels of gamma radiation or high hydrostatic pressure, among others (da Costa *et al.*, 1998). Table I.2 presents some environmental conditions that can be considered extreme and in which life can be found.

Table I.2 Extremophiles and growth conditions (adapted from Rothschild and Mancinelli 2001).

Enviromental condition	Type	Growth conditions	Examples
Temperature	Extreme hyperthermophiles	T_{op} >90°C	*Pyrolobus fumarii*
	Hyperthermophiles	T_{op} > 80°C	*Pyrococcus furiosus*
	Thermophiles	60< T_{op} <80°C	*Rhodothermus marinus*
	Psychrophiles	T_{op}<15°C	*Psychrobacter* spp.
Salinity	Halophiles	2-5 M NaCl	*Haloferax volcanii*
pH	Acidophiles	pH<4	*Sulfolobus solfataricus*
	Alkaliphiles	pH>9	*Natronobacterium* spp.
Pressure	Barophiles	>30 MPa	*Shewanella benthica*
Radiation	Radiation resistant		*Deinococcus radiodurans*

It is not unusual to find organisms living in environments characterised by more than one extreme condition. This is the case for many hyperthermophiles isolated from hydrothermal submarine areas with high salinity or sulfurous hot springs, with pH in the range of 1 to 5 (Stetter et al. 1990).

Hyperthermophilic and thermophilic organisms

Pyrolobus fumarii is an extreme hyperthermophile, able to grow up to 113°C, that was described in Stetter´s lab nearly a decade ago (Blöchl et al. 1997). More recently, an isolate capable of growing up to 121°C has been reported (Kashefi and Lovley 2003), extending the upper temperature limit for life beyond the "sterilisation" temperature. These remarkable organisms belong to the domain *Archaea* like all the extreme (hyper)thermophiles known to date. (Hyper)thermophilic representatives can be found in the domains *Archaea* and *Bacteria*, but no hyperthermophilic eukaryote was ever found and the upper temperature limit for eukaryotic life is believed to be around 60°C (Rothschild and Mancinelli 2001). A notable example of a thermophilic eukaryote is *Alvinella pompejana*, an alvinelli worm that lives in marine hydrothermal vents (Cary et al. 1998).

The placement of hyperthermophiles near the root of the Tree of Life in short phylogenetics branches within the *Bacteria* and *Archaea* (Fig. I.1) indicates an early separation and a slow rate of evolution of these organisms. This has been interpreted as evidence for a hyperthermophilic origin of life (Stetter 2006). However, this is a very controversial topic and this view has been often challenged (Lazcano and Miller 1996).

Hyperthermophiles have been isolated from different biotopes: terrestrial (hot springs, solfataric fields, and geothermally heated oil stratifications) and submarine (hydrothermal systems situated at shallow to abyssal depths). With this variety of biotopes, hyperthermophiles are adapted to distinct environmental factors, like different pH, redox potential, salinity and temperature. For example, the salt tolerance of hyperthermophiles isolated from terrestrial hot springs is quite different from that of isolates from marine hydrothermal vents. Within the genus *Thermococcus*, species thriving in freshwater hot springs, such as *Thermococcus zilligii* and *Thermococcus waiotapuensis*, grow optimally in medium containing less than 0.6% NaCl and tolerate a maximum of 1.4% NaCl; in contrast, species isolated from marine environments, like *Thermococcus marinus, Thermococcus profundus* and *Thermococcus hydrothermalis*, grow optimally in salt concentrations between 2 and 4% NaCl, with a maximum of 8% for some species (Gonzalez et al. 1999; Kobayashi 2001; Jolivet et al. 2004).

The physiology of hyperthermophiles is diverse. Most species are chemolithoautotrophic, using inorganic redox reactions for energy production (chemolithotrophy) and CO_2 as the only carbon source for growth (autotrophy). The most common electron donor is molecular hydrogen, but some species can use sulfide, sulfur and ferrous iron. Diverse types of respiration can be found in hyperthermophiles, both anaerobic (*e.g.*, nitrate, sulfate, and sulfur respiration) and aerobic; in the latter case, hyperthermophiles are generally microaerophilic, requiring low concentrations of oxygen for optimal growth. Several chemolithoautotrophic hyperthermophiles also show heterotrophic growth and some are obligate heterotrophs, requiring organic substrates as carbon and energy sources (Stetter 2006).

Adaptation to high temperature

Whenever possible, microorganisms try to keep adverse conditions away from the cytoplasm. This is the case of acidophilic organisms, in which the cytoplasmic pH is maintained neutral by very efficient ATP-driven proton pumps (Sekler et al. 1991; Weiss and Pick 1996; Pick 1999). A similar strategy is used by metal tolerant bacteria, which remove copper or cobalt from the cytoplasm using very efficient efflux pumps (Nies 2003). However, some types of

aggression can not be transferred to the extracellular space. This is certainly the case of temperature, since it is impossible for any microorganism to have an internal temperature different from that of the environment. Therefore, (hyper)thermophiles had to develop mechanisms to protect all their cellular components against the damaging effects of high temperature. These mechanisms are not fully understood yet, but several features related to the stabilisation of cellular structures in these organisms have been identified (Ladenstein and Antranikian 1998; Daniel and Cowan 2000).

Another difficulty that hyperthermophiles have to overcome is the low thermal stability of some commonly used metabolites, such as ATP and NAD^+. To circumvent this problem, hyperthermophiles developed different strategies, which include microenvironmental protection, metabolite channelling, high catalytic efficiency, and substitution by other metabolites that are more stable at high temperature (Daniel and Cowan 2000). An example of metabolite substitution is the utilisation of pyrophosphate or ADP instead of ATP, a more thermolabile phosphate donor, in the catabolic reactions catalysed by hexokinase and phosphofructokinase (Selig et al. 1997; Siebers et al. 1998; Tuininga et al. 1999; Koga et al. 2000; Xavier et al. 2000; Labes and Schönheit 2001; Sakuraba et al. 2002; Dorr et al. 2003; Hansen and Schönheit 2004; Sakuraba et al. 2004). Additionally, some redox reactions are catalysed by ferredoxin-linked oxidoreductases instead of NAD(P) dependent enzymes (Mescher et al. 1976).

The tRNAs of (hyper)thermophiles have a higher GC content and an increased number of post-transcriptional modifications that seem to confer extra thermostability (Sundaran 1986). However, the same trend is not observed at the DNA level. Some hyperthermophiles, such as *Methanococcus igneus* and *Pyrococcus furiosus*, have a GC content between 30 and 40 %, which is near the lower limit allowing for preservation of information (Stetter 1998). A unique reverse gyrase, present in all hyperthermophiles studied so far and absent in mesophiles, has been associated to DNA stabilisation (Kikuchi and Asai 1984; Bouthier de la Tour et al. 1990). The enzyme introduces positive supercoils in DNA, which becomes more compact, and therefore more resistant to thermal denaturation. Reverse gyrase has been considered a marker of hyperthermophilia (Bouthier de la Tour et al. 1990). However, this view was contested by a study involving the genetic manipulation of the hyperthermophile *Thermococcus kodakaraensis*, showing that mutants with disruption of the gene coding for reverse gyrase were able to grow up to 90°C (Atomi et al. 2004).

Interestingly, archaeal hyperthermophiles produce chaperones, histones, and other histone-like proteins similar to eukaryotic core histones (Drlica and Rouviere-Yaniv 1987; Pettijohn 1988) that are able to enhance DNA thermostability (Sandman et al. 1990). Another

mechanism likely to be involved in thermoadaptation of hyperthermophiles is the preferential usage of some codons in detriment of others that are more frequent in mesophiles; this approach would lead to error minimisation at the translation level by preventing mutations that could harm protein thermostability (De Farias and Bonato 2002; van der Linden and Farias 2006).

(Hyper)thermophilic *Archaea* have also developed strategies to increase the thermal resistance of the cytoplasmic membranes. Some members of the thermoacidophiles have bipolar phytanyl chain lipids fused in C_{40-44} tetraether core, forming a monolayer, instead of the bilayer commonly found in mesophilic *Bacteria* (Kates 1993; Daniel and Cowan 2000). Also, the ether bond of the lipidic chain to the glycerol unit contributes to a higher membrane stability, since it is more resistant to hydrolysis than the ester bond (Daniel and Cowan 2000). In some cases, cyclopentane rings are present in the biphytanyl chains, a feature that enhances membrane packing and reduces membrane fluidity (Daniel and Cowan 2000). Among (hyper)thermophilic bacteria, diether lipids are present only in *Thermotoga maritima*, as components of the cytoplasmic membrane (Huber et al. 1986). In the others cases, the thermostability of the membrane is achieved by an increase in the length and degree of saturation of the acyl chain and the ratio iso/anteiso branching (Tolner et al. 1998).

Surprisingly, there are no striking differences between proteins from (hyper)thermophilic organisms and those from mesophiles. The amino acid sequences of homologous (hyper)thermophilic and mesophilic proteins present an identity of 40 to 80%; they have overlapping three-dimensional structures and share the same catalytic mechanisms (Vieille et al. 1996; Vieille and Zeikus 2001). No new amino acids, covalent modifications or structural motifs were found in proteins from (hyper)thermophiles that could explain their ability to function at higher temperatures (Li et al. 2005). Nevertheless, it was observed that enzymes from (hyper)thermophilic organisms are usually more thermostable (exhibit a higher intrinsic stability) and thermophilic (with higher optimal temperature) than their mesophilic counterparts (Li et al. 2005). This increased stability may be the result of the combination of small structural modifications that are achieved with exchange of amino acids and modulation of the canonical forces (e.g. hydrogen bonds, ion-pair interactions, hydrophobic interactions) (Li et al. 2005).

With the rapidly increasing number of characterised hyperthermophilic proteins, several features have been associated to the high stability of these proteins. The preferential use of longer α-helix and β-sheet structures by hyperthermophilic proteins, allowing the establishment of more ion interactions and the formation of a higher number of ionic pair networks has been observed in (hyper)thermophilic proteins (Perutz and Raidt 1975; Walker et

al. 1980). The ionic pair networks between several amino acid residues are uncommon in typical proteins of mesophiles, though they are frequently found in hyperthermophilic proteins. The increased packing density in the hydrophobic cores of thermophilic proteins has also been related to their higher thermostability. An optimised packing reduces the protein/water contacts, increasing the intermolecular van der Waals forces, and consequently increasing the compactness of the protein (Jaenicke 1991; 1996). Other features are a decrease in the degree of cavity formation (Yamagata et al. 2001), an increase in the number of disulfide bonds (Littlechild et al. 2004), of hydrophobic interactions at subunit interfaces (Roitel et al. 2002), and a higher number of subunits when compared with mesophilic homologues (Thoma et al. 2000). In respect to amino acid composition, hyperthermophilic proteins have a lower number of residues that are susceptible to undergo covalent modifications induced by heat, namely cysteine, asparagine and glutamine (Hensel 1993), and show a preference for charged over neutral amino acids, specially glutamate and lysine over glutamine and histidine (De Farias and Bonato 2002; Farias and Bonato 2003). However, a universal strategy for protein stabilisation has not been identified, because individual proteins, with particular sequence and structural characteristics, utilise differently the palette of mechanisms available.

Surprisingly, some proteins from hyperthermophilic organisms exhibit a thermostability that is lower than expected from its optimal growth temperature (Hensel and König 1988), indicating that protein stability is not exclusively derived from factors intrinsic to the protein structure. A higher protein turnover is one of the mechanisms suggested to be used by hyperthermophiles to overcome the problem of protein denaturation at high temperatures. Another possible mechanism involves the presence of extrinsic stabilising factors. In fact, several hyperthermophiles possess high levels of chaperones, whose concentration increases in response to heat shock. For example, 80% of the soluble protein content in cells of *Pyrodictium occultum*, grown at the supra-optimal temperature of 108°C, is composed of thermosome, a heat inducible molecular chaperone (Phipps et al. 1991). *In vitro* assays demonstrated the protein thermostabilising effect of a recombinant chaperonin derived from *Pyrococcus* sp. strain KOD1 (later designated *Thermococcus kodakaraensis*) (Yan et al. 1997). Natural substrates or co-factors are also described as enzyme stabilisers, specifically by stabilising their active site structure (Takai et al. 1997). Additionally, the presence of compatible solutes, also designated chemical chaperones, could play an important role in protein stability.

A correlation between intracellular accumulation of compatible solutes and growth at supra-optimal temperatures has been observed in halotolerant or slightly halophilic (hyper)thermophiles, indicating that these solutes could have a thermostabilising function

(Hensel and König 1988; Martins and Santos 1995). *In vitro* studies designed to evaluate the ability of compatible solutes to protect proteins against several stresses confirmed a positive effect, not only on proteins isolated from thermophiles and hyperthermophiles, but also from mesophiles (Ramos et al. 1997; Lamosa et al. 2000; Borges et al. 2002; Lamosa et al. 2003; Pais et al. 2005)

Osmoadaptation

All microorganisms must adapt to fluctuations in the water activity of the environment to maintain cell turgor. When the osmotic pressure of the external medium is lower than that of the intracellular space (<0.15 M), water enters the cell, leading to turgidity. If the net internal osmotic pressure exceeds the limits of the cell wall resistance, the cell will lyse. In contrast, when the osmotic pressure is higher in the external medium, water leaves the cell, leading to plasmolysis (da Costa et al. 1998). For these reasons, organisms must develop mechanisms of adaptation that enable them to avoid cell damage induced by fluctuations in water activity of the external medium. The strategies to maintain the osmotic equilibrium through the cell membrane can be categorised in two groups and involve: i) influx of high amounts of inorganic ions (K^+, Na^+, Cl^-) to the cytoplasm; or ii) intracellular accumulation of organic solutes (Brown 1976; da Costa et al. 1998) (Fig I.2).

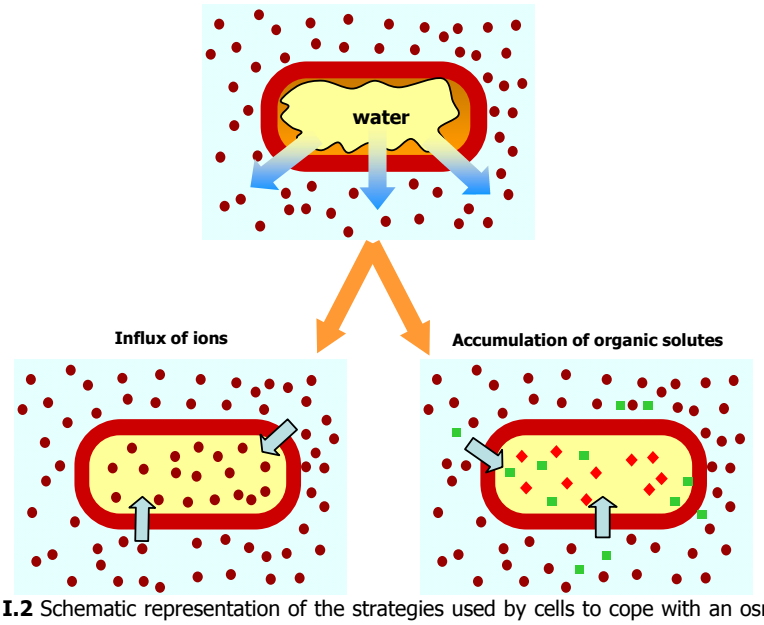

Figure I.2 Schematic representation of the strategies used by cells to cope with an osmotic up-shock: influx of inorganic ions from the medium to the cytoplasm (•); and the accumulation of small organic solutes via *de novo* synthesis (♦) and/or uptake from the external medium (■).

The osmoadaptation strategy using solely the influx of inorganic ions is confined to halophiles, such as those belonging to the archaeal extreme halophilic family *Halobacteriaceae,* the moderate halophilic anaerobic bacteria of the order *Haloanaerobiales*, and the extreme halophilic bacterium *Salinibacter ruber* (Rainey et al. 1995; Kamekura 1998; Anton et al. 2002). The influx of ions leads to increased ionic strength in the cytoplasm, implying that the whole cellular machinery has to be adapted to high salinity. In fact, these organisms exhibit a predominance of proteins with a negative, global charge, thought to support the protein hydratation layer by attracting water to the protein surface in the form of hydrated potassium and sodium cations. Also, the stability and activation of most enzymes from these organisms are dependent on salt (da Costa et al. 1998). This strategy allows the colonisation of highly saline environments (near NaCl saturation) where biological diversity is relatively low and competition for available resources less demanding; however, it also restricts these organisms to such type of environments.

The accumulation of low molecular mass organic compounds in the cytoplasm is the most common strategy of osmoadaptation. The organic compounds that serve as osmolytes can accumulate to high levels without interfering with cell metabolism, hence the term "compatible solutes" coined by Brown in the 70's (Brown 1976). When the water activity in the environment decreases the microorganism responds by accumulating compatibles solutes in the cytoplasm, thus preventing water efflux and maintaining cell turgor. This strategy allows the ionic strength of the cytoplasm to be kept approximately constant, while adapting to changes in the environmental salinity. Also, no drastic alterations in the cellular machinery are required, since the intracellular conditions are roughly the same throughout the colonisable salinity range (Galinski 1995; da Costa et al. 1998). Nevertheless, the flexibility allowed by this strategy comes with an energetic cost. Accumulation of compatible solutes in the intracellular space is accomplished either by *de novo* synthesis, or uptake from the medium. When suitable solutes are available in the medium, the second way is preferred, since the energetic cost of uptake is significantly lower than *de novo* synthesis (Pfluger and Muller 2004). Therefore, mesophilic, halophilic *Bacteria* and *Archaea* generally have active transport systems for compatible solutes (Lai et al. 1991; Horlacher et al. 1998; Lai et al. 2000; Robert et al. 2000; Grammann et al. 2002; Tetsch and Kunte 2002; Pfluger and Muller 2004; Vermeulen and Kunte 2004; Silva et al. 2005). These uptake systems must be efficient scavengers because the concentration of compatible solutes in the external medium is usually low. Therefore, they have high affinity for the substrates (K_M values in the μM range) and are osmotically regulated (Lai et al. 2000; Grammann et al. 2002; Tetsch and Kunte 2002). Within hyperthermophiles, however, it seems

that *de novo* synthesis is favoured since uptake systems for solutes typically associated with thermophily, such as mannosylglycerate and di-myo-inositol-phosphate, have not been found (unpublished results obtained in our team).

The chemical diversity of compatible solutes is not high and these compounds generally belong to the following categories: amino acids and derivatives, polyols and derivatives, sugars, betaines and ectoines (da Costa et al. 1998). Classically, the concept of compatible solute was restricted to molecules with low molecular mass, with polar functional groups (therefore, highly soluble in water), without global charge at physiological pH, and that accumulate in response to salt stress. More recently, with the isolation of new Extremophiles, the concept of compatible solute was extended to contemplate compounds that accumulate in response to stress types other than osmotic, namely high temperature and desiccation (da Costa et al. 1998). Here, the term "compatible solute" will be used to designate any small organic molecule that accumulates in response to heat or salt stress.

Compatible solutes of (hyper)thermophiles

In many halophilic or halotolerant (hyper)thermophiles, accumulation of compatible solutes occurs not only in response to an increased salinity, but also in response to supraoptimal growth temperatures. Interestingly, besides solutes that are frequently found in non-thermophilic organisms, (hyper)thermophiles accumulate solutes that have not been or are rarely encountered in mesophilic organisms (Table I.4). Trehalose, α-glutamate, aspartate, proline, and glycine betaine are some of the compatible solutes that can be found both in (hyper)thermophiles and mesophiles. On the other hand, di-*myo*-inositol phosphate and diglycerol phosphate have never been found outside the (hyper)thermophilic world; mannosylglycerate is widely distributed among (hyper)thermophiles and rarely occurs in mesophiles. Solutes whose accumulation is restricted to (hyper)thermophiles or rarely encountered in mesophiles have been denominated "thermolytes" (Santos et al.). Here, this term will be used for the convenience of a short designation. One of the characteristics common to most thermolytes studied thus far is the negative charge at physiological pH, mannosylglyceramide being the only exception (Fig. I.3).

Thermolytes belong mainly to two categories: hexose derivatives with the hydroxyl group at carbon 1 blocked in the α-configuration, and polyol-phosphodiesters. Mannosylglycerate is the most representative compound in the first category, being widespread among (hyper)thermophiles, either bacteria or archaea (Table I.3). despite having been initially identified in red algae of the order *Ceramiales* (Bouveng et al. 1955), mannosylglycerate is one

of the most widespread thermolyte. Among (hyper)thermophiles, mannosylglycerate was firstly reported in the thermophilic bacterium *Rhodothermus marinus* (Nunes et al. 1995). Since then it has been found in diverse organisms: the thermophilic bacteria *Thermus thermophilus* and *Rubrobacter xylanophilus*, the crenarchaeota *Aeropyrum pernix* and *Stetteria hydrogenophila*, the euryarchaeota *Methanothermus fervidus,* and in the three genera of the order *Thermococcales*: *Thermococcus*, *Pyrococcus*, and *Palaeococcus* (Table I.3) (Martins and Santos 1995; Martins et al. 1996; Martins et al. 1997; Lamosa et al. 1998; Silva et al. 1999; Neves et al. 2005). In these organisms, mannosylglycerate accumulation occurs primarily in response to osmotic stress; an exception to this behaviour was found in *Rhodothermus marinus*, an organism that accumulates mannosylglycerate also at supraoptimal growth temperatures (Silva et al. 1999).

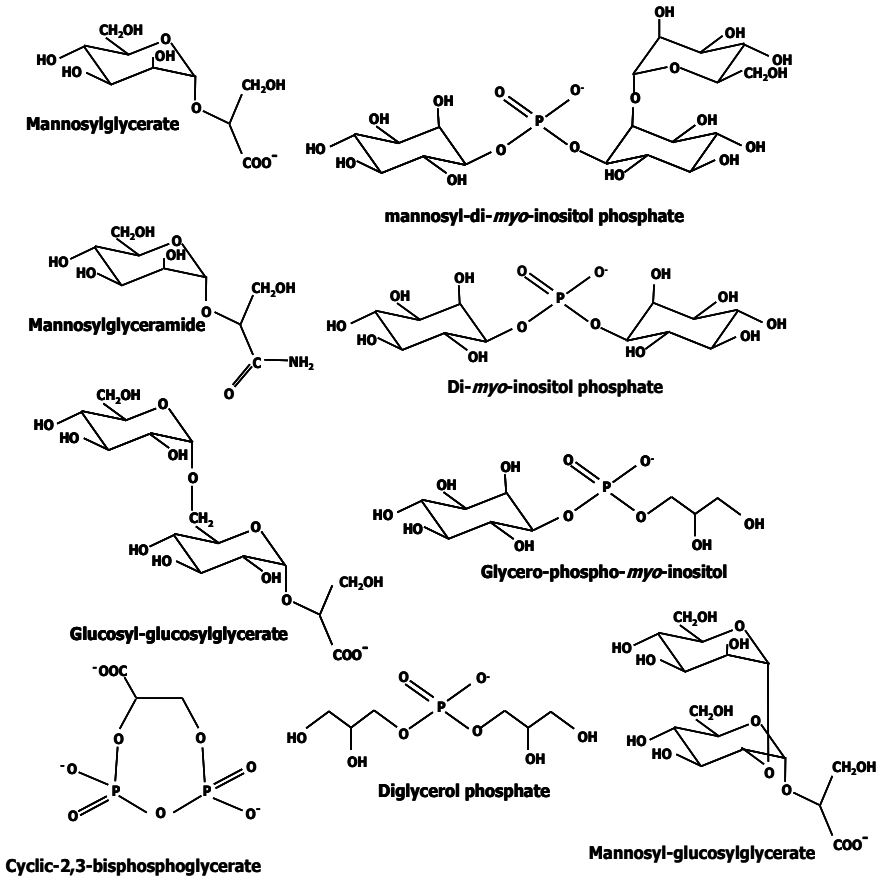

Figure I.3. Compatibles solutes primarily restricted to (hyper)thermophiles

Tabela I.3 Distribution of thermolytes among (hyper)thermophiles (adapted from Santos et al. 2007).

Organisms	$T_{Opt.}$ (ºC)	Solutes								
		cBPG	**Tre**	**MG**	**DIP**	**α-Glu**	**β-Glu**	**Asp**	**Other**	**Ref**
Archaea										
Pyrodictium occultum	105				+	+				1
Pyrobaculum aerophilum	100		+							1
Pyrobaculum islandicum	100									1
Pyrococcus furiosus	100			↑(S)	↑(T)	+				2
Pyrococcus horikoshii	98		+	↑(S)	+	+				3
Methanopyrus kandleri	98	+				+				1
Stetteria hydrogenophila	95		+	+	+					4
Aeropyrum pernix	90			+	+					5
Methanotorris igneus	88				↑(T)	↑(S)	↑(S)			6, 7
Thermoproteus tenax	88		+							1
Thermococcus stetteri	87			↑(S)	↑(T) ↑(S)	+		↑(S)		8
Thermococcus celer	87			↑(S)	↑(T)	+		↑(T)		8
Thermococcus litoralis	85		↑(S)	↑(S)	↑(T)	+		↑(S)	GalHl	8
Thermococcus kodakaraensis	85				+	+		+		9
Methanocaldococcus jannaschii	85						↑(S)			7
Palaeococcus ferrophilus	83			↑(T); ↑(S)		↑(T)		+		4
Methanothermus fervidus	83	+				+				1
Archaeoglobus fulgidus VC-16	83				↑(T)	+			DGP ↑(S), GPI ↑(T, S)	1
Acidianus ambivalens	80		+							2
Thermococcus zilligii	75									8
Sulfolobus sulfataricus	75		+							2
Metallosphaera sedula	75		+							2
Methanothermobacter Thermoautotrophicus	70	+				+			TCH	10
Methanothermococcus okinawensis	70					+		+		9
Methanococcus thermolithotrophicus	65					+	+	+	NAL	7, 11
Bacteria										
Aquifex pyrophilus	80				↑(T)				GPI ↑(T, S) mDIP ↑(S)	17
Thermotoga maritima	80				↑(S)				mDIP ↑ (T)	12
Thermotoga neapolitana	80				↑(S)	+	+		mDIP ↑(T)	12
Thermosipho africanus	75					+			Pro	12
Thermotoga thermarum	70									12
Marinitoga piezophila	70					+			Pro	9
Fervidobacterium islandicum	70									12
Persephonella marina	70				+		+		GG,GGG	9
Thermus thermophilus	70		↑(S)	↑(S)		+			GB	13
Rhodothermus marinus	65		+	↑(S) ↑(T)		+			MGA ↑(S)	14, 15
Petrotoga miotherma	55					+			MGG, Pro	16

Abbreviations: **cBPG**, cyclic 2,3-bisphosphoglycerate; **Tre**, trehalose; **MG**, α-mannosylglycerate; **MGA**, α-mannosylglyceramide; **DIP**, di-*myo*-inositol-1,3′-phosphate; **mDIP**, mannosyl-di-*myo*-inositol-phosphate; **DGP**, di-glycerol phosphate; **GPI**, glycerol-1,3-inositol phosphate **TCH**, 1,3,4,6-tetracarboxyhexane; **α-Glu**, α-glutamate; **β-Glu**, β-glutamate; **Asp**, aspartate; **GalHl**, β-galactopyranosyl-5-hydroxylysine; **GB**, glycine betaine; **Pro**, proline; **NAL**, N^{ε}-acetyl-β-lysine; **GG**, glucosylglycerate; **GGG**, glucosylglucosylglycerate; **MGG**, mannosylglucosylglycerate.

Symbols: The **plus sign** indicates the presence of the solute in cases for which the response to environmental conditions was not reported. ↑(S) and ↑(T) indicate that the intracellular level of the solute increases in response to osmotic and heat stress, respectively.

References: 1- Martins et al. 1997; 2- Martins and Santos 1995; 3- Empadinhas et al. 2001 4- Neves et al 2005; 5- Santos and da Costa 2001; 6- Ciulla et al. 1994; 7- Robertson et al. 1990 8- Lamosa et al. 1998; 9-our unpublished results; 10- Gorkovenko et al. 1993 1- Martins et al. 1999; 13- Martins et al. 1996; 14- Nunes et al. 1995; 15- Silva et al. 1999; 16- Jorge et al. 2007; 17- Lamosa et al. 2006.

In contrast to the frequent occurrence of mannosylglycerate, the other hexose derivatives are less common. Mannosylglyceramide, which resembles mannosylglycerate but has the carboxylic group of glycerate replaced by an amide group, was found only in a few strains of *R. marinus*, where it accumulates in response to salt stress and is absent at supra-optimal growth temperatures (Silva et al. 1999). The patterns of mannosylglycerate and mannosylglyceramide accumulation during *R. marinus* osmo-adaptation are different, the first solute being accumulated immediately after salt up-shock, whereas mannosylglyceramide accumulation presents a lag time (Borges 2004). Other compounds chemically related to mannosylglycerate were found in (hyper)thermophiles: *Persephonella marina* accumulates glucosylglucosylglycerate and glucosylglycerate (Santos et al. 2007). While the first was never found in any other organism, the latter is relatively common in halotolerant mesophilic bacteria (Robertson et al. 1992; Goude et al. 2004). In the thermophilic bacterium *Petrotoga miotherma*, mannosylglucosylglycerate was found to play a role during low-level osmotic adaptation (Jorge et al. 2007).

Di-*myo*-inositol phosphate is the principal representative of the polyol-phosphodiesters found in hyperthermophiles. This solute is widespread among marine (hyper)thermophiles, and has never been found in organisms with optimal growth temperature below 50ºC. It is present both in (hyper)thermophilic bacteria (*Thermotoga*, *Persephonella* and *Aquifex* spp.) and archaea (members of the genera *Pyrodictium, Pyrococcus, Thermococcus, Methanotorris, Aeropyrum* and *Archaeoglobus*); moreover, in all organisms studied to date, it accumulates in response to supraoptimal growth temperatures (Scholz et al. 1992; Ciulla et al. 1994; Martins and Santos 1995; Martins et al. 1996; Martins et al. 1997; Ramakrishnan et al. 1997; Lamosa et al. 2006; Empadinhas et al. 2007; Santos et al. 2007). All hyperthermophilic bacteria (*Thermotoga* and *Aquifex* spp.) that accumulate di-*myo*-inositol phosphate also accumulate a derivative, mannosyl-di-*myo*-inositol phosphate (the early identification as di-mannosyl-di-*myo*-inositol phosphate was revised recently, unpublished results of our group) ((Martins et al. 1996; Lamosa et al. 2006), which plays different roles. In *Thermotoga* spp. this compound accumulates primarily in response to heat stress, while in *Aquifex* spp. it accumulates primarily under conditions of high salinity (Martins et al. 1996; Lamosa et al. 2006). Other polyol-phosphodiesters occurring in hyperthermophiles are diglycerol phosphate, only found in

members of the genus *Archaeoglobus*, and glycerophospho-inositol, a structural chimera of di-*myo*-inositol phosphate and di-glycerol phosphate that was found only in *Archaeoglobus fulgidus* and *Aquifex* spp. (Martins et al. 1997; Lamosa et al. 2006).

Other organic solutes have been found in hyperthermophiles and do not fall into either of these two categories. These include cyclic-2,3-bisphosphoglycerate, which is restricted to methanogens; β-galactosylhydroxylysine, found in *Thermococcus litoralis* (Lamosa et al. 1998); 1,3,4,6-tetracarboxyhexane, found in *Methanothermobacter thermoautotrophicus* (Ciulla et al. 1994), and N^{ε}-acetyl-β-lysine, present in *Methanococcus thermolithotrophicus* (Ciulla and Roberts 1999).

An interesting feature of (hyper)thermophiles is the differential pattern of solute accumulation in response to different stress factors. Mannosylglycerate, di-glycerol phosphate and amino acids accumulate preferentially in response to salt stress, while the accumulation of di-*myo*-inositol phosphate and derivatives occurs mainly in response to heat stress. This behaviour is particularly evident in *Pyrococcus furiosus*, in which the pool of mannosylglycerate increases 10-fold when the salinity of the growth medium is increased from 2.8 to 5% NaCl, while di-*myo*-inositol phosphate levels increase 20-fold for a temperature up-shift of 6°C, being the only solute present at supra-optimal growth temperatures (Martins and Santos 1995).

This tendency of solute specialisation, however, is not always observed. In fact, organisms that do not accumulate di-*myo*-inositol phosphate tend to use mannosylglycerate during both thermo and osmo adaptation, as is the cases of *Rhodothermus marinus* and *Palaeococcus ferrophilus*e (Silva et al. 1999; Neves et al. 2005). Conversely, *Thermococcus kodakaraensis* and *Thermotoga* spp., that do not synthesise mannosylglycerate, accumulate di-*myo*-inositol phosphate in response to both types of stress (Martins et al. 1996; Santos et al. 2007). So, it seems that mannosylglycerate and di-*myo*-inositol phosphate can replace each other's typical function in osmo- and thermo-adaptation.

Uptake of compatible solutes in (hyper)thermophiles

For energetic reasons it is conceivable that (hyper)thermophiles also favour active transport of solutes from the medium over *de novo* synthesis. This preference is well illustrated in *Thermococcus litoralis*, in which aspartate is the major solute accumulating when peptone is present in the growth medium, being absent when tryptone is used. The accumulation of other amino acid derivatives such as galactosylhydroxylysine and hydroxyproline also depend on the presence of peptone in the growth medium (Lamosa et al. 1998). Likewise, *Thermococcus litoralis* accumulates trehalose only if this solute is present in the growth medium (Lamosa et al.

1998). A binding protein dependent ABC transporter with a high affinity for trehalose (K_m 17 nM) was found in *Thermococcus litoralis*. This transport system is induced by trehalose and probably is the responsible system for trehalose uptake and accumulation in *Thermococcus litoralis* (Xavier et al. 1996).

The low availability of suitable compatible solutes in (hyper)thermophilic biotopes and/or the unique nature of some of them, can imply the need for *de novo* synthesis instead of uptake. In the last years, the knowledge of the biosynthetic pathways of compatible solutes in (hyper)thermophiles increased significantly. Besides the compatible solutes commonly found in mesophiles, such as trehalose and glucosylglycerate, the biosynthetic pathways of some typical thermolytes, like mannosylglycerate and di-*myo*-inositol phosphate, have been elucidated.

Mannosylglycerate synthesis and regulation

The biosynthesis of mannosylglycerate has been characterised in depth in a variety of (hyper)thermophiles. Two distinct pathways were identified: a single-step and a two-step pathway. In the single-step pathway the direct condensation of GDP-mannose with D-glycerate occurs to yield mannosylglycerate through the action of the mannosylglycerate synthase (MGS). This pathway was found only in the thermophilic bacterium *Rhodothermus marinus* (Martins et al. 1999) and in the mesophilic red alga *Caloglossa leprieurii* (Santos et al. 2007) (Fig I.4). In the second pathway, GDP-mannose is condensed with D-3-phosphoglycerate to form a phosphorylated intermediate, mannosyl-3-phosphoglycerate (MPG), in a reaction catalysed by mannosyl-3-phosphoglycerate synthase (MPGS); this intermediate is subsequently dephosphorylated by a specific phosphatase, mannosyl-3-phosphoglycerate phosphatase (MPGP). This pathway is present in all (hyper)thermophiles known to accumulate mannosylglycerate.

Rhodothermus marinus mannosylglycerate synthase was the first studied enzyme involved in mannosylglycerate biosynthesis. The native protein was purified and characterised and the encoding gene identified. The *E. coli* recombinant protein was also characterised (Martins et al. 1999) and, recently, its three-dimensional structure solved (Flint et al. 2005). In terms of catalytic characteristics, MGS has maximal activity at 85 °C and pH 6.5 and the presence of divalent metal ions is essential for activity (Martins et al. 1999). MGS presents low specificity for both the sugar donor and the 3-carbon acceptor. Although GDP-mannose and D-glycerate are the preferred substrates, GDP-glucose, GDP-fucose, UDP-mannose, and UDP-glucose can also be used as sugar donors, and either D-lactate or glycolate, can function as 3-carbon acceptors, the substrate specificity being clearly dependent on temperature (Flint

et al. 2005). GDP-glucose, UDP-mannose, and UDP-glucose are used as substrates at 37°C but not at 90°C; at this temperature, GDP-mannose and D-glycerate are specific substrates for the reaction (Flint et al. 2005).

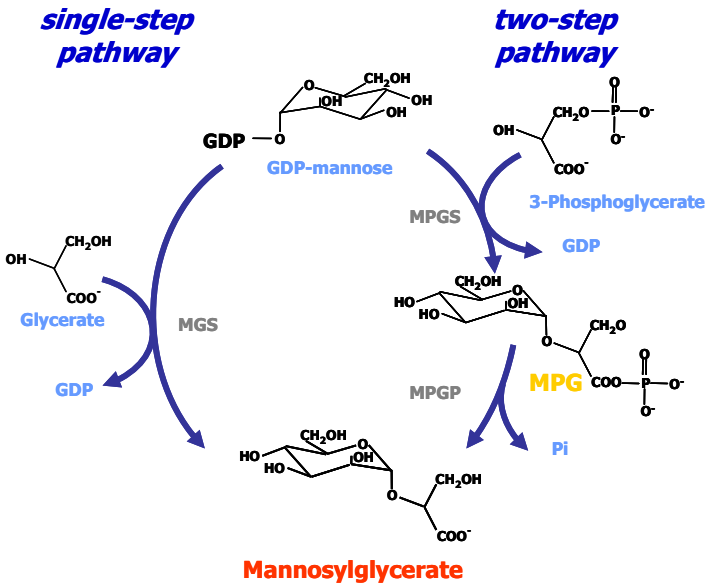

Figure I.4. The two pathways for the synthesis of mannosylglycerate. The single-step pathway is catalysed by mannosylglycerate synthase (MGS), while the two-step pathway involves the actions of mannosyl-3-phosphoglycerate synthase (MPGS) and mannosyl-3-phosphoglycerate phosphatase (MPGP).

Unlike the single-step pathway, the two-step pathway is widespread among (hyper)thermophiles. It was firstly identified in *Rhodothermus marinus* (Martins et al. 1999) and subsequently detected in *Pyrococcus horikoshii* (Empadinhas et al. 2001), *Thermus thermophilus* (Empadinhas et al. 2003), *Palaeococcus ferrophilus* and *Thermococcus litoralis* (Neves et al. 2005). All MPGSs present similar biochemical properties and kinetic parameters (Table I.4): high specificity for GDP-mannose and 3-phosphoglycerate at the temperature examined (83°C), an elevated optimal temperature (80-100°C) and an optimum pH around 7.3. The K_M values for both substrates are similar in all MPGSs, but the V_{max} of the MPGS from *Rhodothermus marinus* is 10 times lower than that observed for the other MPGSs. Interestingly, the *R. marinus* MPGS has 30 additional amino-acids in the C-terminus region; when this extension was deleted, the V_{max} of the enzyme became similar to that of other MPGSs. Moreover, when the complete MPGS was incubated with *R. marinus* cell extracts the activity was enhanced. This activation could not be observed in the presence of protease inhibitors

(Borges et al. 2004), indicating that, *in vivo*, the enzyme can be activated by proteolytic cleavage, as occurs with other enzymes involved in the synthesis of sugar derivative compatible solutes (Köhle and Kauss 1984; Londesborough and Vuorio 1991; Vicente-Soler et al. 1991).

MPGPs present similar catalytic characteristics; an interesting feature is the capacity of the enzymes from *Thermus thermophilus* and *Pyrococcus horikoshii* to dephosphorylate both mannosyl-3-phosphoglycerate and glucosyl-3-phosphoglycerate, although not being able to desphosphorylate other compounds (Empadinhas et al. 2001; Empadinhas et al. 2003; Borges et al. 2004; Costa et al. 2006). Probably, MPGPs recognise the glyceryl-phosphate moiety of those molecules.

Table I.4. Biochemical and kinetic properties of recombinant MPGS, MPGP and bifunctional MPGS/MPGP from bacteria and archaea.

Property		MPGS				MPGP				MPGS/MPGP
		Archaea		*Bacteria*		*Archaea*		*Bacteria*		*Bacteria*
		Pa. fer	*Py. hor*	*R. mar*	*T. the*	*Pa. fer*	*Py. hor*	*R. mar*	*T. the*	*D. eth*
Amino acid res.		393	394	427	391	210	243	277	259	694
T_{op} (°C)		90	90-100	80	80-90	90	95-100	70-80	95	50
pH optimum		~7.0	~7.6	~7.6	~7.0	~6.5	~6	~6	~6	~7
Mg^{2+} [a]		0	46	0	0	90	58	90	0	0
Substrate specificity [b]		GDPman 3PGA	GDPman 3PGA	GDPman 3PGA	GDPman 3PGA	MGP Nd	MGP GPG	MGP nd	MGP GPG	GDPman 3PGA MGP GPG
K_M (mM)	GDPman	nd	0.50	0.30	nd					0.70
	3PGA	nd	0.60	0.13	nd					2.18
	MPG					Nd	0.134	0.2	0.520	0.63
V_{max} (U/mg)	GDPman + 3PGA	331	186	~15	122					3.2
	MPG					101	111	200	172	6.1

[a] Values refer to the activity in the absence of Mg^{2+} as a percentage of the maximum activity obtained with 15 mM Mg^{2+}. [b] Measured at the optimum temperature. *Pa. fer, Palaeococcus ferrophilus; Py. hor, Pyrococcus horikoshii; R. mar, Rhodothermus marinus; T. the, Thermus thermophilus; D. eth, Dehalococcoides ethenogenes;* GDPman, guanosine-diphospho-D-mannose; 3PGA, 3-phosphoglycerate; MGP, mannosyl-phosphoglycerate; GPG, glucosyl-phosphoglyceratye; nd, not determined

A bifunctional mannosyl-3-phosphoglycerate synthase/phosphatase (MGSD) was characterised in the mesophilic bacterium *Dehalococcoides ethenogenes*. This protein contains N-terminal and C-terminal sequences with high homology to MPGSs and MPGPs, respectively (Empadinhas et al. 2004). This mesophilic enzyme presents an optimal activity at 50°C and exhibits some activity, approximately 10%, at low temperatures (10°C), presenting lower affinity and lower activity than the monofunctional homologues (Table I.4).

Homologues of the genes (*mpgS*) encoding the synthase of the two-step pathway have been found in diverse organisms. Besides other hyperthermophiles, also mesophiles, such as the fungi *Magnaporthe grisea* and *Neurospora crassa*, and uncultured archaea from moderate environments possess *mpgS* homologs (Empadinhas et al. 2004). In most cases, *mpgS* and the phosphatase encoding gene, *mpgP*, are positioned consecutively in the genome. In all *Thermococcales* examined thus far, *mpgS* and *mpgP* are organised in an operon-like structure that includes the genes encoding the enzymes that catalyse the reactions that convert fructose 6-phosphate to GDP-mannose (bifunctional phosphomannose isomerase/mannose-1-phosphate guanylyl transferase, *m1p-gt*/*pmi*, and phosphomannose mutase, *pmm*) (Empadinhas et al. 2001; Neves et al. 2005) (Fig. I.5). In *Thermus thermophilus* and *Rhodothermus marinus*, the *mpgS* gene overlaps the *mpgP* gene, while in *Aeropyrum pernix* the two genes are separated by 21-base pairs. These three organisms do not have the genes coding for M1P-GT/PMI and PMM in an adjacent location (Empadinhas et al. 2001; Empadinhas et al. 2003; Borges et al. 2004).

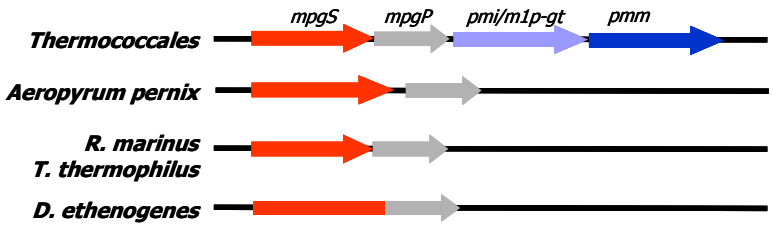

Figure I.5. Genomic organisation of mannosylglycerate biosynthesis via the two-step pathway. Abbreviations: *mpgS*, mannosyl-3-phosphoglycerate synthase; *mpgP*, mannosyl-3-phosphoglycerate phosphatase; *pmi/m1p-gt*, bifunctional phosphomannose isomerase/mannose 1-phosphate guanylyl transferase; *pmm*, phosphomannose mutase.

The presence of two different pathways for mannosylglycerate synthesis in *Rhodothermus marinus* was initially an intriguing feature. However, the physiological relevance of this pathway multiplicity was explained in a recent work (Borges et al. 2004). Using the Western blotting technique to assess the level of the two synthases, the authors demonstrated

that the two pathways have specific roles in the stress adaptation of this organism: while the level of MGS (the synthase of the single-step pathway) is selectively enhanced in response to heat stress, the amount of the synthase involved in the two-step pathway is increased under osmotic stress. The differential regulation of the biosynthetic pathways for mannosylglycerate in *Rhodothermus marinus* reinforces the view that this compound plays an important role in the adaptation of the organism to stressful conditions.

Overview on the physiology of *Archaeoglobus* spp.

The genus *Archaeoglobus*

The first identified representative of the genus *Archaeoglobus* was isolated from the Volcano hydrothermal system off the coast of Napoli (Italy) (Achenbach-Richter et al. 1987; Stetter 1988). This strain was designated *A. fulgidus* VC-16 and was considered as the type strain of the genus *Archaeoglobus*. Later on, two other strains of *A. fulgidus*, named Z and 7324, were isolated, respectively from marine hydrothermal sediments in Volcano (Italy) (Zellner et al. 1989) and from hot oil field waters in the North Sea (Norway) (Beeder et al. 1994). Two other species, *A. profundus* and *A. veneficus,* have also been isolated from a deep-sea hydrothermal system in the hydrocarbon-rich Guaymas Basin off the coast of Mexico and abyssal black smokers in the mid-Atlantic ridge, respectively (Burggraf et al. 1990; Huber et al. 1997). An additional species of the genus was isolated from fluids of oil fields in North sea and designated *A. lithotrophicus* (Stetter et al. 1993). Together with the genera *Ferroglobus* and *Geoglobus*, the genus *Archaeoglobus* is included in the order *Archaeoglobales* of the archaeal phylum *Euryarchaeota*. Transverse analysis of 16S and 23S rRNA sequences led to the assignment of *Archaeoglobus* to the *Methanomicrobiales-Methanosarcinales-Halobacteriales* phylogenetic cluster (Woese et al. 1991), instead of in a deeper branch near the base of the euryarchaeotal cluster, between the *Methanococcales* and *Thermococcales* lineages, as suggested by former studies (Achenbach-Richter et al. 1987).

A. fulgidus, A. profundus and *A. lithotrophicus* are the only archaeal sulfate reducers known so far, both being able to use sulfate, tiosulfate and sulfite as electron acceptors (Stetter et al. 1987; Burggraf et al. 1990). *A. veneficus* is unable to use sulfate, but it can reduce sulfite into sulfide (Huber et al. 1997). Nitrate, nitrite and sulfur can not be used as electron acceptors by any *Archaeoglobus* species. While *A. fulgidus* and *A. veneficus* can grow chemolithoautotrophically and chemoorganotrophically, *A. profundus* is an obligate chemolithoheterotroph, requiring H_2 and an organic compound, *e. g.*, acetate, as electron

donor. A summary of the growth characteristics of the different members of the genus *Archaeoglobus* is presented in Table I.5.

Table I.5. Growth characteristics of different members of the genus *Archaeoglobus*

Species	Temperature range (ºC)	Electron donors	Electron acceptors
***A. fulgidus* VC-16**	60-94	Lactate, cell extracts, H_2/CO_2	$S_2O_3^{2-}$, SO_4^{2-}, SO_3^{2-}
***A. fulgidus* 7324**	60-85	Lactate, pyruvate, valerate, starch	$S_2O_3^{2-}$, SO_4^{2-}, SO_3^{2-}
***A. fulgidus* Z**	60-94	Lactate, cell extracts, H_2/CO_2	$S_2O_3^{2-}$, SO_4^{2-}, SO_3^{2-}
A. profundus	65-90	H_2/CO_2+acetate, H_2/CO_2+ cell extracts	$S_2O_3^{2-}$, SO_4^{2-}, SO_3^{2-}
A. veneficus	65-85	H_2/CO_2, acetate, formate, cell extracts	$S_2O_3^{2-}$, SO_3^{2-}
A. lithotrophicus	55-87	H_2/CO_2	$S_2O_3^{2-}$, SO_4^{2-}, SO_3^{2-}

Archaeoglobus fulgidus

A. fulgidus cells are Gram-negative irregular cocci, sometimes similar to triangular plate-shaped lobes, with 0.4 to 1 μm in width (Fig. I.15) (Stetter 1988). They possess monopolar polytrichous flagella and the cell envelope is constituted by a surface layer (*S*-layer) of hexagonally arranged monomeric peptide units. The cellular membrane is constituted by phytanyl ether-linked lipids arranged as a bilayer, rather than the more stable monolayer membrane found in the majority of hyperthermophilic *Archaea* (Kessel et al. 1990).

Like all *Archaeoglobus* spp., *A. fulgidus* presents a blue-green fluorescence at 420 nm that is originated by the presence of coenzyme F_{420}, a 5-deazaflavin derivative, also found in methanogens (Stetter et al. 1987). Besides this methanogenic related feature, *A. fulgidus* has other components that were thought to be confined to methanogenic microorganisms, such as methanofuran (White 1988), tetrahydromethanopterin (Stetter et al. 1987), and acetyl-CoA decarbonylase/synthase (Dai et al. 1998). However, *Archaeoglobus* spp. are unable to perform methanogenesis, since they are devoid of coenzyme M, coenzyme F_{430} and methyl-coenzyme M reductase, which are required for the terminal step of methane synthesis (Klenk et al. 1997).

Genetics

In 1997, the entire genome of *A. fulgidus* strain VC-16 was sequenced and annotated. This was the first sequenced genome of a sulfate-reducing organism (Klenk et al. 1997). The genome of *A. fulgidus* consists of a 2.178 Mbp single circular chromosome, with an average of 48.5% G+C content and 2,436 predicted open reading frames (ORFs), covering about 92.2% of

the genome (Klenk et al. 1997). The analysis of *A. fulgidus* genome showed extensive gene duplication, having, for example, 10 copies of 3-hydroxyacyl-CoA dehydrogenase and twelve copies of acyl-CoA dehydrogenase. Although the duplicated proteins are not identical, gene redundancy in *A. fulgidus* is largely superior to that found in other non-eukaryotes. These observations, together with the large number of paralogous gene families, led to the suggestion that gene duplication could play an important role in an evolutionary mechanism for improving physiological diversity in the *Archaeoglobales* (Klenk et al. 1997). A comparative analysis of *Methanococcus jannaschii* and *A. fulgidus* genomes showed that 80% of the genes involved in replication, transcription, translation and biosynthetic pathways in *A. fulgidus* have homologous genes in *Methanococcus jannaschii*, whereas only 35% of the genes implicated in the intermediary central metabolism have homologues in the two archaeons (Klenk et al. 1997).

A. fulgidus possesses two B DNA polymerases that are related to the eukaryal Δ DNA polymerase, as well as the only known archaeal homologue of the ε subunit of *E. coli* PolIII, which is involved in proofreading. This organism also contains a variety of DNA repair enzymes, including a eukaryotic-like Rad25, exodeoxynuclease III, topoisomerase VI and, as all hyperthermophiles, a reverse gyrase (Klenk et al. 1997). New types of repair enzymes were characterised in *A. fulgidus*, such as a uracil-DNA glycosylase (Sandigursky and Franklin 2000), endonuclease III (Shekhtman et al. 1999), and a novel N^1-methyladenine and N^3-methylcytosine repair glycosylase, A*f*ALkA (Leiros et al. 2007).

Genes encoding different homologues of bacterial-like transcription activators, like Lrp, PhoU, TetR and MerR, and sensor-kinase response regulators, are present in the *A. fulgidus* genome, while homologues of bacterial transcription factors have not been found (Klenk et al. 1997). Like other archaeons, *A. fulgidus* contains the eukaryotic-like initiation factors TFIIB, TFIID, and TFIIEα, small subunits of RNA polymerase (RPB5, RPB6, RPB8, RPB10, and RPB12), the large universal RNA polymerase subunits, and archaeal histones (Klenk et al. 1997). However, genetic tools for *A. fulgidus* are not available yet, and no plasmid or phage could be found in this organism; nevertheless, a 2.8 kb plasmid negatively supercoiled (pGS5) was isolated from *A. profundus* (Lopez-Garcia et al. 2000).

Metabolism

The main source of metabolic energy in *A. fulgidus* is the oxidation of L-lactate to CO_2 through the carbon monoxide dehydrogenase pathway (Stetter et al. 1987; Stetter 1988; Müller-Zinkhan et al. 1989). Besides lactate, *A. fulgidus* can use pyruvate, oxaloacetate, formate, or CO_2/H_2 as electron and carbon donors (Stetter et al. 1987; Stetter 1988). In early

studies, *A. fulgidus* strain VC-16 was reported to utilise other substrates for growth, such as glucose, formamide, casamino acids, peptone, casein, meat extract, yeast extract, cell homogenates, methanol, ethanol, formate, starch and gelatine, though very low growth rates were reported (Stetter et al. 1987; Stetter 1988). Although *A. fulgidus* VC-16 is unable to use glucose or starch for growth, recent studies showed that strain 7324 can use starch as sole carbon source (Labes and Schönheit 2001). Also, contrarily to all other species of *Archaeoglobus*, *A. fulgidus* is not able to use acetate as a substrate for growth, despite the presence in its genome of the genes involved in acetate utilisation (Burggraf et al. 1990; Huber et al. 1997; Klenk et al. 1997).

A. fulgidus VC-16 performs the complete oxidation of lactate to CO_2, with release of protons and molecular hydrogen (Möller-Zinkhan et al. 1989). Both L- and D-lactate can be used by this organism, and both are converted to pyruvate by membrane-associated enzymes (Möller-Zinkhan et al. 1989; Reed and Hartzell 1999). *In vitro* assays showed that L-lactate is oxidized to pyruvate by L-lactate dehydrogenase using dimethylnaphthoquinone as electron acceptor, suggesting that, *in vivo*, the acceptor could be a menaquinone (Möller-Zinkhan et al. 1989). A menaquinone (2-methyl-3-I,II,III,IV,V,VI,VII-tetradecahydro-heptaprenyl-1,4-naphthoquinone), composed by seven isoprenyl units and fully saturated side chains, was isolated from *A. fulgidus* cell membranes, and is the major respiratory lipoquinone found in this organism (Tindall et al. 1989). D-lactate dehydrogenase activity is dependent on FAD and Zn^{2+}, and seems to be coupled to a membrane-associated 16-kDa cytochrome *c* (Reed and Hartzell 1999; Pagala et al. 2002).

The pyruvate resulting from oxidation of lactate is oxidized by a pyruvate:ferredoxin oxidoreductase (Kunow et al. 1995), forming acetyl-CoA which, in turn, is converted to CO_2 and H^+ through a modified acetyl-CoA/carbon monoxide dehydrogenase pathway (Möller-Zinkhan et al. 1989). The cleavage of the acetyl-CoA carbon-carbon bond is accomplished by the acetyl-CoA decarbonylase/synthase complex, leading to the formation of both enzyme-bound CO and CH_4 (Dai et al. 1998). The same enzyme complex oxidizes the enzyme-bound CO to CO_2 and H^+ (Dai et al. 1998). The oxidation of enzyme-bound CH_4 in *A. fulgidus* VC-16 involves three methanogenic coenzymes: tetrahydromethanopterin (H_4MPT), methanofuran and coenzyme F_{420} (Möller-Zinkhan et al. 1989).

Sulfate is the preferred electron acceptor for the reducing power produced during lactate oxidation in *A. fulgidus*. This organism contains the complete bacterial pathway for the dissimilatory reduction of sulfate (Dahl et al. 1994; Speich et al. 1994; Sperling et al. 1998; Larsen et al. 1999; Sperling et al. 2001). Sulfate reduction is performed by cytoplasmic

enzymes and is strictly coupled to membrane-associated electron carriers. The first step is the activation of sulfate to adenosine 5'-phosphosulfate (APS) by ATP sulfurylase, at the expense of ATP. APS is then reduced to AMP and sulfite by adenylylsulfate reductase. Finally, sulfite is reduced to sulfide through the action of a sulfite reductase (Sperling et al. 1998; Sperling et al. 2001).

The global balance of the complete oxidation of lactate and reduction of sulfate in *A. fulgidus* VC-16 is the following:

$$CH_3CHCOHCOO^- + 1.5\ SO_4^{2-} + H^+ \rightarrow 3\ CO_2 + 1.5\ H_2S + 3H_2O$$

$$\Delta G^{0\prime} = -150.7\ kJ/mol\ de\ lactate$$

A. fulgidus strain Z is not able to perform the complete oxidation of lactate; instead, lactate is converted to formate, acetate and CO_2 (Zellner et al. 1989; Habicht et al. 2005). In the presence of high concentrations of sulfate in the growth medium (>600 mM), this strain reduces 1 mol of sulfate during the consumption of 1 mol of lactate, and CO_2 is the major carbon product. On the other hand, at low sulfate concentrations (<300 mM), only 0.6 mol of sulfate are consumed per mol of lactate oxidized, acetate being the main carbon product (Habicht et al. 2005).

A. fulgidus 7324 is the only sulfate-reducing organism able to use starch as carbon and energy source for growth (Hartzell and Reed 2006), performing its incomplete oxidation: in the presence of sulfate, starch (1 mol of glucose-equivalent) is oxidized to 2 moles of acetate and 2 moles of CO_2, concomitantly with the production of 1 mole of H_2S (Labes and Schönheit 2001). This organism possesses a modified Embden-Meyerhoff pathway, involving an ADP-dependent hexokinase, phosphoglucose isomerase, ADP-dependent 6-phosphofructokinase, fructose-1,6-phosphate aldolase, glyceraldehyde-3-phosphate:ferredoxin oxidoreductase, phosphoglycerate mutase, enolase, and pyruvate kinase (Labes and Schönheit 2001). Both hexokinase and 6-phosphofructokinase acting in this pathway are ADP-dependent, ATP not serving as a phosphoryl donor for these reactions (Labes and Schönheit 2001; Johnsen et al. 2003; Labes and Schönheit 2003; Hansen and Schönheit 2004), similarly to what occurs in other hyperthermophiles, *e. g.*, *Pyrocccus furiosus* (Kengen et al. 1994). When this modified pathway is active, acetyl-CoA formed by pyruvate:ferredoxin oxidoreductase is subsequently converted to acetate by an ADP-forming acetyl-CoA synthetase (Labes and Schönheit 2001). Despite the presence of an acetyl-CoA/carbon monoxide dehydrogenase that converts acetyl-CoA to CO_2 via CO, acetate is the final product of starch metabolism in this organism. When *A. fulgidus* 7324 is grown in starch, the intracellular levels of coenzyme F_{420} are very low (<0.03 nmol/mg protein); since the acetyl-CoA/carbon monoxide dehydrogenase pathway is linked to F_{420}-dependent

enzymes, it has been suggested that the production of F_{420} could be regulated by the substrate used for growth, indirectly limiting the operation of the acetyl CoA/carbon monoxide dehydrogenase pathway (Labes and Schönheit 2001; Hartzell and Reed 2006).

The initial steps involved in starch degradation in *A. fulgidus* 7324 were recently elucidated (Labes and Schönheit 2007). The common starch degradation enzymes, α-amylase and amylopullulanase, were not detected in cell extracts of this organism. Instead, an extracellular cyclodextrin glucanotransferase converts starch to cyclodextrins, which are then transported to the cytoplasm and converted to glucose 6-phosphate via cyclodextrinase, maltodextrin phosphorylase, and phosphoglucomutase (Labes and Schönheit 2007).

A. fulgidus can also grow chemolithoautotrophically, using CO_2/H_2 as carbon and energy source (Stetter et al. 1987). In this case, CO_2 fixation occurs via the reductive carbon monoxide dehydrogenase pathway, through which CO_2 is reduced to acetyl-CoA (Dai et al. 1998), using the methanogenic components also involved in the final steps of lactate oxidation.

A. fulgidus is able to synthesise the different amino acids, vitamins, cofactors, purines and pyrimidines that are needed for growth. However, it lacks several metabolic pathways normally found in other microorganisms and, in some cases, atypical enzymes are used to catalyse unusual reactions. This is the case of fructose 1,6-bisphosphatase activity: although genes encoding fructose 1,6-bisphosphatase are absent in the *A. fulgidus* genome, the corresponding enzymatic activity can be accomplished by an inositol monophosphatase (Chen and Roberts 2000). Similarly to other *Archaea*, *A. fulgidus* lacks a complete citric acid cycle, using a partial cycle to synthesise key metabolic intermediates and to obtain reducing power in the form of NADPH. Examples of such cases are the reductive formation of succinate from oxaloacetate and the oxidative formation of 2-oxoglutarate from oxaloacetate and acetyl-CoA (Steen et al. 2001). Two enzymes involved in other steps of the citric acid cycle, a $NADP^+$-dependent isocitrate dehydrogenase and malate dehydrogenase, have been identified and characterised in this organism (Langelandsvik et al. 1997; Steen et al. 1997).

CHAPTER 2

Di-*myo*-inositol phosphate and novel UDP-sugars accumulate in the extreme hyperthermophile *Pyrolobus fumarii*

Part of this chapter has been accepted for publication in:

Gonçalves, L.G.; Lamosa, P.; Huber, R and Santos, H. 2007. Di-*myo*-inositol phosphate and novel UDP-sugars accumulate in the extreme hyperthermophile *Pyrolobus fumarii. Extremophiles,* in press.

Chapter | 2| Contents

Abstract

The archaeon *Pyrolobus fumarii*, one of the most extreme members of hyperthermophiles known thus far, is able to grow at temperatures up to 113 °C. Despite over a decade has passed since the description of this organism, our knowledge about the structures and strategies underlying this remarkable thermal resistance remains very poor. The accumulation of a restricted number of negatively charged organic solutes is a common response to heat stress in hyperthermophilic organisms and accordingly their role in thermoprotection has been often suggested. In this work, the organic solute pool of *P. fumarii* was characterised using ^{1}H-, ^{13}C-, and ^{31}P-NMR. Di-*myo*-inositol phosphate was the major solute (0.21 μl/mg protein), reinforcing the correlation between the occurrence of this solute and hyperthermophily; in addition, several UDP-sugars (total concentration 0.11 μmol/mg protein) were present. The structures of the two major UDP-sugars were identified as UDP-α-GlcNAc3NAc and UDP-α-GlcNAc3NAc-(4←1)-β-Glc*p*NAc3NAc. Interestingly, the latter compound appears to be derived from the first one by addition of a 2,3-N-acetylglucoronic acid unit, suggesting that these UDP-sugars are intermediates of an *N*-linked glycosylation pathway in *P. fumarii*. The physiological roles of these organic solutes are discussed.

INTRODUCTION

Nearly a decade ago the scientific community was amazed with the discovery of *Pyrolobus fumarii*, a crenarchaeon able to grow up to 113 °C (Blöchl et al. 1997). This extreme hyperthermophile, isolated from the walls of a black smoker at the Mid Atlantic Ridge, is adapted to grow optimally at temperatures of superheated water (T_{op} 106°C) and the lower temperature limit for growth is 90°C. The position of *P. fumarii* as the most extreme hyperthermophile known was contested by a short report about an archaeon able to grow up to 121°C (Kashefi and Lovley 2003). Nevertheless, *P. fumarii* remains as the archetypal hyperthermophile growing at the upper temperature and pressure limits for life.

P. fumarii is well adapted to deep-sea vent environments, presenting an elevated resistance to high pressure (up to 250 atm), a salt requirement between 1 and 4% NaCl, and a high growth temperature. Moreover, *P. fumarii* is a facultative aerobic obligate chemolithoautotroph using H_2-oxidation as energy source and CO_2 as single carbon source. As electron acceptors NO^-_3, $S_2O_3^{2-}$, and low concentrations of O_2 (up to 0.3% v/v) can be used, yielding NH^+_4, H_2S, and H_2O as end products, respectively. Except for the presence of oxygen, all these conditions and compounds are usually found in deep sea hydrothermal vents (Blöchl et al. 1997).

The structural and metabolic features that allow this organism, and other extreme hyperthermophiles, to thrive under such hostile conditions are not satisfactorily understood. There is no doubt that the large majority of proteins from hyperthermophiles have enhanced intrinsic stability when compared to their mesophilic counterparts (Vieille et al. 1996; Vieille and Zeikus 2001). However, a growing body of evidence supports the role of extrinsic factors in the stabilisation of cellular components (Phipps et al. 1991; Ladenstein and Antranikian 1998; Takai et al. 1997, Daniel and Cowan 2000; Santos et al. 2007a). In particular, it has been shown that marine hyperthermophiles accumulate organic solutes that are believed to be part of their adaptation strategies to hot environments. Moreover, it appears that organic solutes of hyperthermophiles have specialised roles, *i. e.*, while solutes like mannosylglycerate and diglycerol phosphate are primarily involved in osmoprotection, di-*myo*-inositol phosphate and derivatives are consistently associated with the heat stress response, and therefore, their involvement in thermoprotection has been often speculated.

Driven by the curiosity of discovering the chemical diversity and physiological roles of compatible solutes of organisms adapted to high temperature, we examined the solute pool of several thermophiles and hyperthermophiles (Martins and Santos 1995; Nunes et al. 1995;

Martins et al. 1996; Martins et al. 1997; Lamosa et al. 1998; Silva et al. 1999; Empadinhas et al. 2003; Gonçalves et al. 2003; Neves et al. 2005; Lamosa et al. 2006; Empadinhas et al. 2007; Jorge et al. 2007; Santos et al. 2007) However, progress is often limited by the poor growth yields of many hyperthermophiles and the demand for peculiar culture conditions. Given that *P. fumarii* is one of the most extreme hyperthermophiles known we were particularly interested in determining the nature of the organic solutes potentially present in this remarkable member of the archaea.

MATERIAL AND METHODS

Culture conditions, extraction and quantification of intracellular solutes

Pyrolobus fumarii cells were grown at 106°C in medium containing 1.7% NaCl, as described by (Blöchl et al. 1997). Cells were recovered at late exponential phase and harvested by centrifugation (10000 × g, 4°C, 15 min), and washed twice with the growth medium without carbon sources. The cell pellet was freeze-dried. Cell mass was extracted twice with boiling 80% ethanol by the method of Reed *et al.* (1984) (Reed et al. 1984), modified as previously described by Martins and Santos (1995) (Martins and Santos 1995). The freeze-dried extracts were dissolved in D_2O for NMR analysis. The protein content of the cells was determined by the Bradford assay (Bradford 1976).

Partial purification of the NDP-sugar compounds

The NDP sugars were purified from *P. fumarii* cell extracts by anion exchange chromatography. The sample was loaded onto a 5 ml QAE-Sephadex column (Pharmacia, Uppsala, Sweden) equilibrated with 5 mM potassium carbonate (pH 8.2) and eluted with a linear gradient of ammonium carbonate (5 mM to 1 M). The target compounds were detected by UV absorption at 280 nm taking advantage of the absorption band displayed by the NDP moieties (with maxima around 260 nm). Fractions displaying UV absorption were analysed by TLC, using silica plates and a mixture of chloroform: methanol: acetic acid: water (7.5: 12.5: 2: 16) for sample elution. Three NDP-sugar containing fractions were identified; these were desalted in an activated Dowex 50W-X8 column, freeze-dried, and dissolved in D_2O for later NMR analysis.

NMR spectroscopy

All spectra were acquired on a Bruker DRX500 spectrometer. ^{1}H-NMR spectra were acquired with water presaturation, 6 μs pulse width corresponding to a 60^{o} flip angle, and a repetition delay of 5 s. Chemical shifts were relative to 3-(trimethylsilyl)propanesulfonic acid (sodium salt). For quantification purposes formate was added as an internal concentration standard and a repetition delay of 60 s was used for spectra acquisition. The resonance of proton 6 in the uracyl moiety was used for quantification of UDP-sugars and that of proton 5 in the inositol units was used for di-*myo*-inositol phosphate quantification. The results were confirmed by ^{31}P NMR using methylphosphonate contained in a capillary tube as concentration standard.

^{13}C-NMR spectra were recorded at 125.77 MHz using a 5 mm carbon selective probe head. Typically, spectra were acquired with a repetition delay of 1 s and a pulse width of 7 μs corresponding to a 75^{o} flip angle. ^{31}P-NMR spectra were recorded at 202.45 MHz on the same spectrometer using a 5 mm phosphorous selective probe head. Proton decoupling was applied in both cases during the acquisition time only, using the Wideband Alternating-phase Low-power Technique for Zero-residue splitting sequence (WALTZ). Chemical shifts were referenced with respect to (trimethylsilyl)propanesulfonic acid for ^{13}C and external 85% H_3PO_4 for ^{31}P.

Two dimensional spectra were performed using standard Bruker pulse programs. Phase-sensitive nuclear Overhauser effect spectroscopy (NOESY), proton-homonuclear shift correlation spectroscopy (COSY) and total-correlation spectroscopy (TOCSY) were acquired collecting 4096(t_2) x 512(t_1) data points; in ^{1}H-^{13}C heteronuclear spectra, 4096(t_2) x 256(t_1) data points were collected. In the heteronuclear multiple quantum coherence spectra (HMQC), a delay of 3.5 ms was used for the evolution of $^{1}J_{CH}$, and in the heteronuclear multiple bond connectivity spectrum (HMBC) a delay of 73.5 ms was used for the evolution of long range couplings.

Mass Spectrometry

Mass spectra were acquired on a LCQ advantage ion trap mass spectrometer from ThermoFinnigan (San Jose, CA, USA) equipped with an electrospray ionisation interface operated in the negative mode. Samples were injected at 300^{o}C and –33 V in 50% methanol/0.1% formic acid.

RESULTS

Identification of organic solutes in *Pyrolobus fumarii*

^{1}H-, ^{13}C- and ^{31}P-NMR spectral analysis of *P. fumarii* extracts revealed strong resonances immediately assigned to di-*myo*-inositol phosphate by comparison with the spectra of di-*myo*-inositol phosphate extracted from other sources. Besides di-*myo*-inositol phosphate, NMR spectra also revealed the presence of several unidentified compounds that displayed NMR features consistent with NDP-sugars: a set of resonances on ^{1}H-NMR spectra consistent with a urydine group (a resonance at 8 and two near 6 ppm) and resonances in the region characteristic of sugar anomeric groups; and, in the ^{31}P-NMR spectra, two resonances near 11.5 ppm, characteristic of nucleosideo-diphospho-sugars (Fig. II.1). Quantification of organic solutes in cell extracts showed that di-*myo*-inositol phosphate was the major solute (0.210 μmol/mg protein), while the total amount of NDP-sugars was 0.106 μmol/mg protein. It was not possible to identify the unknown NDP-sugars by spiking the sample with common NDP-sugars or by resorting to NMR databases. Therefore, the sample was subjected to chromatographic steps to facilitate the structural characterisation of the compounds.

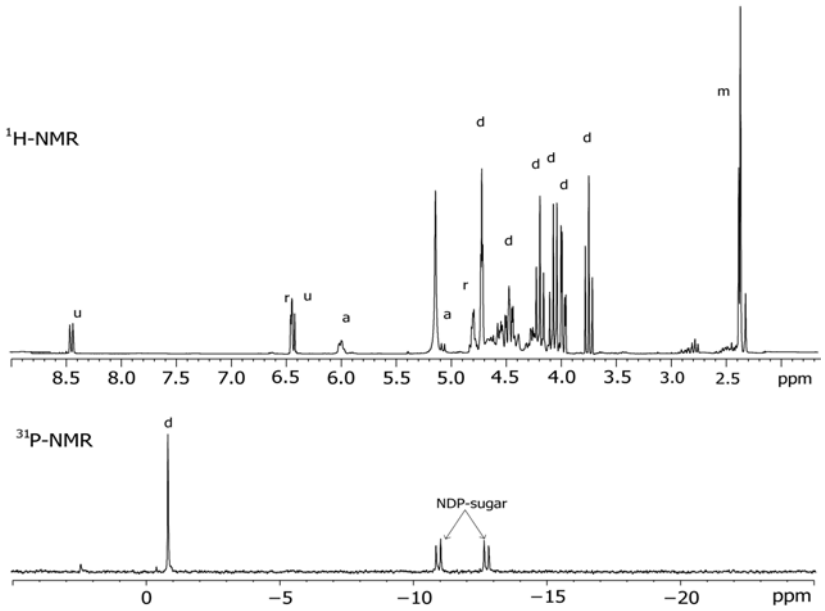

Figure II.1: ^{1}H and ^{31}P-NMR spectra of a *P. fumarii* ethanolic extract in 100% D_2O. The resonances assigned to di-myo-inositol phosphate are labelled with **d**, and resonances from UDP-sugar are labelled with: **u**- uracil moiety, **r**- ribosyl moiety, **a**- anomeric group of glucosyl moiety and **m**- methyl group.

Purification of NDP-sugars

The two fractions derived from ion-exchange chromatography displayed identical ^{31}P-NMR spectra, with two doublet resonances centred at -10.9 and -12.7 ppm ($^{2}J_{P}$= 19 Hz) characteristic of diphosphodiesters. However, ^{1}H-NMR showed that the chromatographic steps enabled the separation of two major compounds, both containing uridyl moieties. In addition to all the NMR spectral features typical of UDP-sugars, the compounds originated extra resonances consistent with the presence of *N*-acetyl groups linked to the sugar unit. To prove the occurrence of these groups and establish their position, the solvent in the NMR samples was exchanged to 90% H_2O / 10% D_2O; this led to the appearance of two extra doublet resonances in the amide region of the spectrum (7.95 and 8.15 ppm) obtained with the fraction eluted at the lowest ionic strength (compound A) and four extra similar resonances in the spectrum of the other fraction (compound B) (Fig. II.2).

After the purification of NDP-sugars, it was possible to calculate the ratio of the two compounds in the cell extract. Peak intensities of the methyl groups in the spectra of the cell extract led to the conclusion that compounds A and B appear in a relative proportion of 1.75: 1.

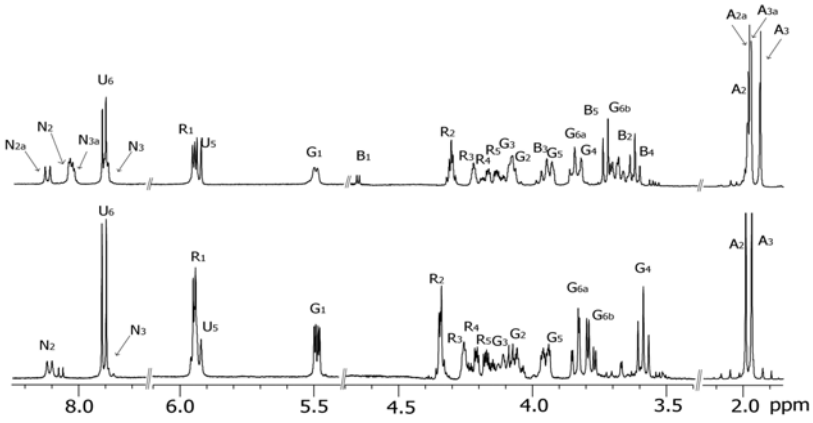

Figure II.2. ^{1}H-NMR spectra of compound A (bottom) and compound B (upper) after the last purification step in 90% H2O / 10% D_2O. Peaks due to α-glucosyl, β-glucosyl, ribosyl, uridyl, amide and acetyl moieties are labelled with G, R, B, U, N and A, respectively. The subscripts represent proton numbering (see also Fig II.6).

Identification of UDP-GlcNAc3NAc

The structure of the molecule was established from sets of 2D-NMR spectra (COSY, TOCSY, ^{13}C-^{1}H HMQC, NOESY and ^{13}C-^{1}H HMBC). The spectra of compound A showed that the

anomeric carbon at 94.9 ppm belonged to a hexose (resonances at 94.9; 52.4; 65.4; 67.9; 73.7 and 60.8 ppm), while the anomeric carbon at 89 ppm belonged to the ribosyl moiety (Fig. II.3 and II.4).

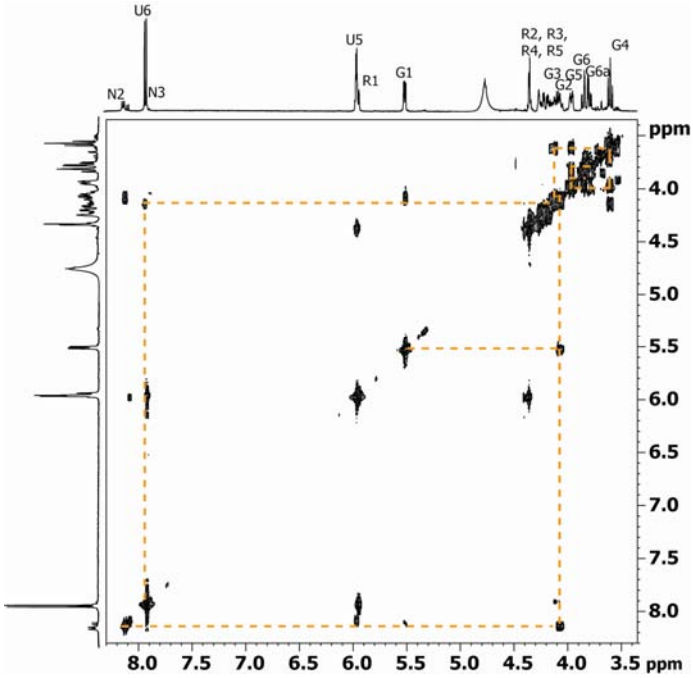

Figure II.4. COSY spectrum of UDP-GlcNAc3NAc dissolved in 90% H_2O / 10% D_2O. The peaks due to glucosyl, ribosyl, amide and uridyl moieties are labelled with G, R, N and U, respectively. The subscripts represent proton numbering. The orange line indicates the spin system of the glucosyl moiety. Cross peaks correspond to connectivities between vicinal protons.

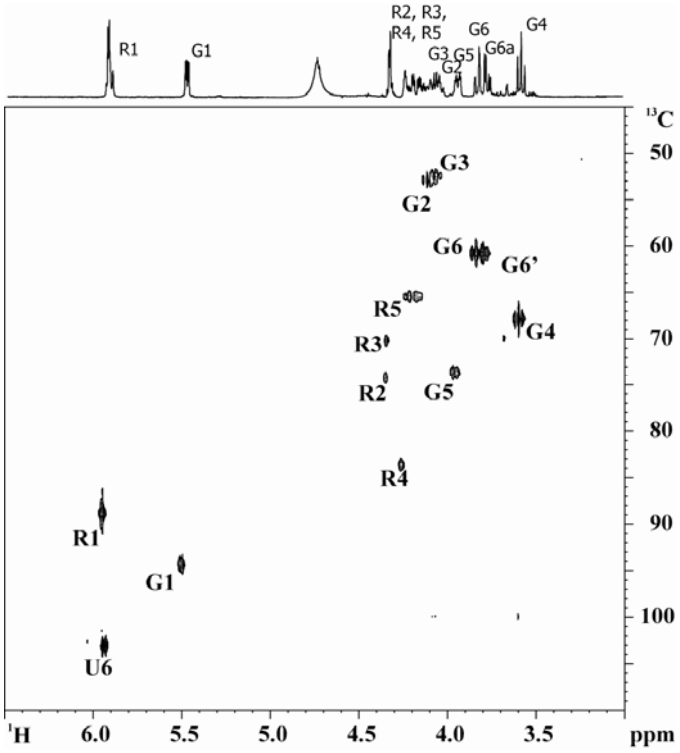

Figure II.5. ^{13}C-^{1}H HMQC of UDP-α-GlcNAc3NAc dissolved in 90% H_2O / 10% D_2O. Peaks due to glucosyl, ribosyl and uridyl moieties are labelled with G, R and U, respectively. The subscripts represent proton numbering. Cross peaks correspond to connectivities between proton and carbon atoms covalently bonded.

Analysis of the phosphorus-proton coupling pattern showed that carbon 5 of ribose and carbon 1 of the hexose were bound to the phosphate groups of the diphosphodiester bridge. The COSY, NOESY and ^{13}C-^{1}H HMBC experiments allowed identifying the positions of the two N-acetyl groups that are linked to C_2 and C_3 of the hexose moiety. Furthermore, the pattern of coupling constants ($J_{H\text{-}H}$) and ($J_{C\text{-}H}$) of the glycosyl moiety was characteristic of an α-glucopyranose configuration. Putting together all the NMR evidence, compound A was identified as UDP-N-2,3-diacetamino-2,3-dideoxy-D-α-glucopyranose, from now on abbreviated as UDP-α-GlcNAc3NAc (Fig. II.6).

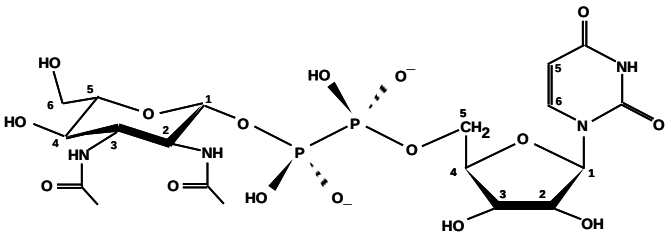

UDP-α- GlcNAc3NAc

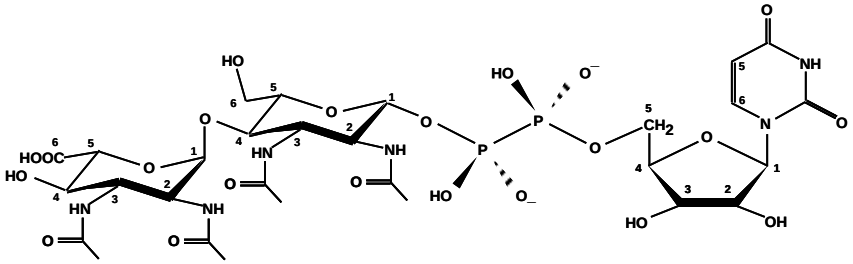

UDP-α- GlcNAc3NAc-(4←1)-β-Glc*p*NAc3NAc

Figure II.6. Structures of the UDP-sugars identified in ethanolic extracts of *P. fumarii*.

Identification of UDP GlcNAc3NAc-(4←1)-β-Glc*p*NAc3NAc

A similar strategy was followed to identify compound B. Besides the anomeric ribosyl resonance (at 6.04 ppm) two other resonances were apparent in the region characteristic of anomeric protons (5.56 and 4.67 ppm). Moreover, the intensity of each of these three anomeric resonances was identical to that of the uracil resonances, indicating that the activated sugar moiety in compound B was a disaccharide. The resonance at 5.56 ppm belonged to a spin system very similar to that observed for compound A (assigned to a glucosyl residue with two N-acetyl groups). The resonance at 4.67 ppm belonged to a spin system with five resonances in the aliphatic region (Fig. II.7).

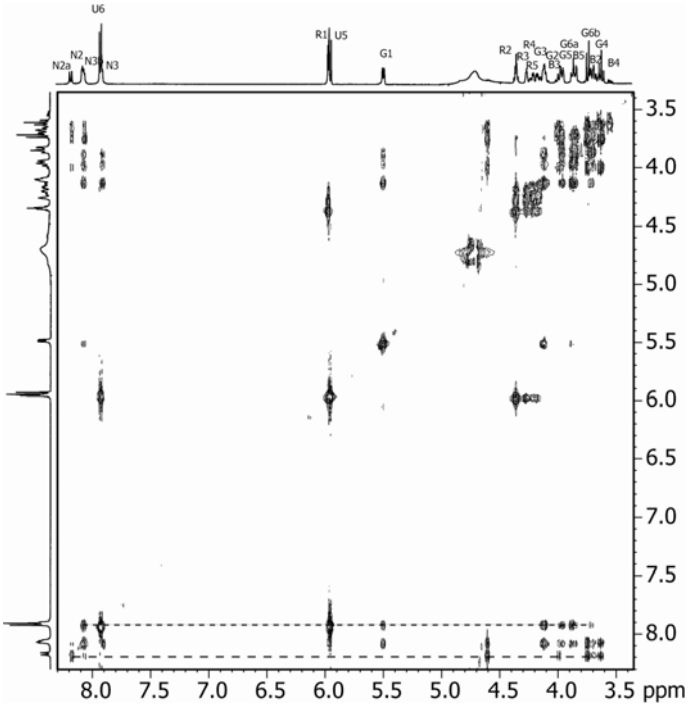

Figure II.7. TCOSY spectrum of the UDP-α-GlcNAc3NAc-(4←1)-β-Glc*p*NAc3NAc dissolved in 90% H_2O/10% D_2O. The two glucosyl spin systems are indicated by the dashed lines. Cross peaks correspond to connectivities between protons present in the same spin system.

^{13}C-^{1}H HMQC and HMBC experiments showed that the second sugar is a hexose with a carboxyl group at position 6, e.g. a glucoronyl residue with two N-acetyl groups at positions 2 and 3. The HMBC spectrum also showed that the anomeric carbon of the glucoronyl moiety is linked to carbon 4 of the glucosyl moiety (Fig. II.8).

The analysis of the coupling constants led to the conclusion that both sugars are glucopyranoses, the hexose directly linked to UDP having an α-pyranose conformation, and the other having a β-pyranose conformation. Combining all the data retrieved from NMR spectral analysis, it was depicted that the compound is UDP-*N*-2,3-diacetamino-2,3-dideoxy-D-glucopyranose-(4←1)-β-2,3-diacetamido-2,3-dideoxy-*β*-glucoronic acid (UDP GlcNAc3NAc-(4←1)-β-Glc*p*NAc3NAc). NMR parameters of the two NDP-sugars are summarised in Table II.1.

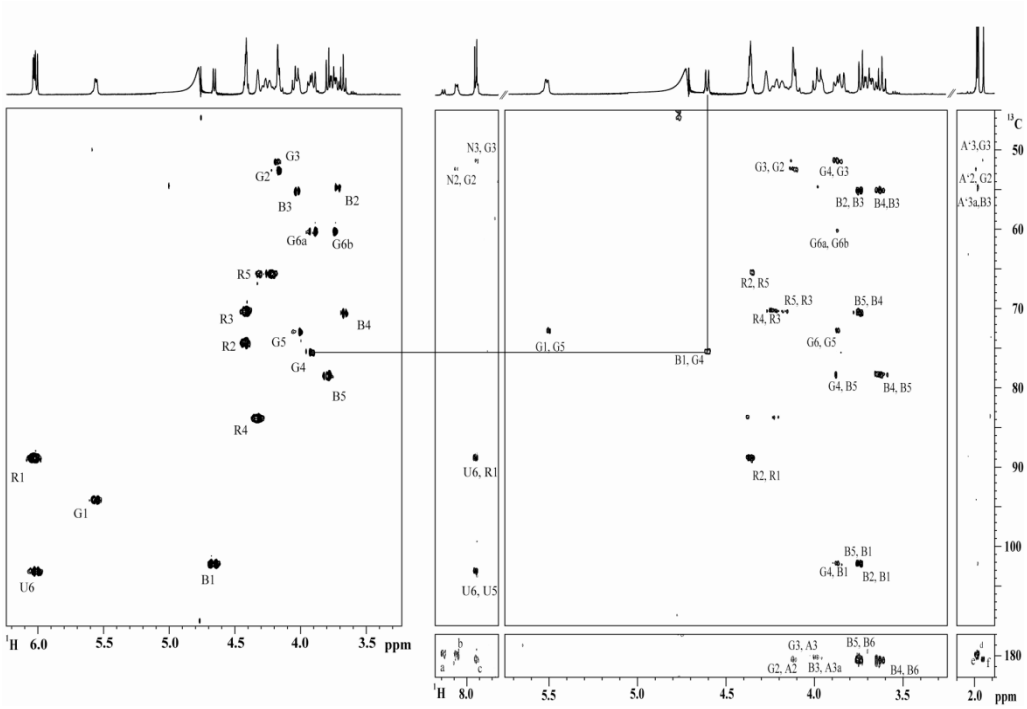

Figure II.8. ^{13}C-^{1}H HMBC (A) and a highlight of the ^{13}C-^{1}H HMQC (B) of UDP GlcNAc3NAc-(4←1)-β-Glc*p*NAc3NAc dissolved in 90% H_2O / 10% D_2O. Peaks due to the α-glucosyl, β-glucoronyl, ribosyl, uridyl, amide and acetyl moieties are labelled with G, R, B, U, N, and A (carbonyl A and methyl A'), respectively. The numbers represent proton numbering. Cross peaks correspond to connectivity between proton and carbon atoms. a- N2a, A2a; b- N2, A2; c- N3, A3; d- A'2a, A2a; e- A'2, A2; f- A'3, A3; g- A'3, G3; h- A'2, G2 and i- A'3a, B3

Table II.1. NMR parameters of the UDP sugars present in ethanolic extracts of *P. fumarii.*

Moiety	UDP-α-GlcNAc3NAc			UDP-α-GlcNAc3Nac-(4←1)-β-Glc*p*NAc3NAc		
	^{13}C-NMR	^{1}H-NMR		^{13}C-NMR	^{1}H-NMR	
	δ (ppm)	**δ (ppm)**	**$^{n}J_{HH}$ (Hz)**	**δ (ppm)**	**δ (ppm)**	**$^{n}J_{HH}$ (Hz)**
U_5	103.06	5.93	$^{3}J_{5,6}$= 8.0	103.06	6.02	$^{3}J_{5,6}$= 8.0
U_6	142.15	7.92		142.15	7.92	
R_1	88.98	5.95	n.d.	88.75	6.04	n.d.
R_2	74.30	4.39	n.d.	74.05	4.42	n.d.
R_3	70.11	4.35	n.d.	70.23	4.42	n.d.
R_4	83.62	4.26	n.d.	83.67	4.33	n.d.
R_5	65.9	4.2, 4.18	n.d.	65.5	4.31, 4.2	n.d.
G_1	94.952	5.50	$^{3}J_{1,2}$= 3.08	94.04	5.56	$^{3}J_{1,2}$= 2.46
G_2	52.39	4.09	$^{3}J_{2,3}$= 11.84	52.22	4.17	$^{3}J_{2,3}$= 9.87
G_3	53.01	4.18	$^{3}J_{3,4}$= 9.31	51.15	4.18	$^{3}J_{3,4}$= 9.18
G_4	67.87	3.59	$^{3}J_{4,5}$= 9.84	75.27	3.92	$^{3}J_{4,5}$=10.92
G_5	73.70	3.95	$^{3}J_{5,6a}$= 2.46	72.83	4.01	$^{3}J_{5,6a}$= 2.46
G_{6a}	60.88	3.85	$^{2}J_{6a,6b}$= 12.46	60.01	3.89	$^{2}J_{6a,6b}$= 14.00
G_{6b}		3.79	$^{3}J_{6b,5}$= 4.31		3.74	$^{3}J_{6b,5}$= 4.11
CH_3 -2	22.20	1.98		22.20	1.98	
CH_3 -3	22.54	1.96		22.54	1.96	
NH -2		8.16	$^{3}J_{N2,2}$= 9.84		8.07	$^{3}J_{N2,2}$= 9.11
NH -3		7.95	$^{3}J_{N2,3}$= 9.84		7.90	$^{3}J_{N2,3}$= 8.83
B_1				102.15	4.67	$^{3}J_{1,2}$= 8.18
B_2				54.43	3.72	$^{3}J_{2,3}$= 2.31
B_3				55.04	4.03	$^{3}J_{3,4}$= 9.73
B_4				70.39	3.66	$^{3}J_{4,5}$= 9.73
B_5				78.33	3.79	
B_6				175.33		
CH_3 -2				22.20	2.06	
CH_3 -3				22.54	2.03	
NH -2					8.17	$^{3}J_{N2,2}$= 9.74
NH -3					7.95	$^{3}J_{N2,3}$= 9.11

G, B, R and U represent the α-glucosyl, β-glucoronyl, ribosyl and uridyl moieties, respectively. The numbers represent proton numbering

The molecular masses of compounds A and B were determined by mass spectrometry. Each sample originated only a major signal with an m/z value of 647.2 and 905.2, respectively, which are in excellent agreement with the structures proposed: the expected mass of UDP-GlcNAc3NAc is 647 g.mol^{-1} and the one of UDP GlcNAc3NAc-(4←1)-β-Glc*p*NAc3NAc is 905 g.mol^{-1}.

Discussion

Di-*myo*-inositol-phosphate is the major organic solute found in *P. fumarii*, the most extreme hyperthermophilic organism known thus far. The strong correlation between

di-*myo*-inositol phosphate and hyperthermophiles has been widely illustrated (Santos and da Costa 2002; Santos et al. 2007). In fact, di-*myo*-inositol phosphate is present in the large majority of marine hyperthermophiles, whether bacteria (Martins et al. 1996; Ramakrishnan et al. 1997b; Lamosa et al. 2006; Santos et al. 2007) or archaea (Scholz et al. 1992; Ciulla et al. 1994; Martins and Santos 1995; Martins et al. 1997; Ramakrishnan et al. 1997a; Gonçalves et al. 2003; Santos et al. 2007); on the other hand, it has never been found in organisms with optimal growth temperature below 60°C.

Hyperthermophiles appear to accumulate different solutes in response to different stresses: while mannosylglycerate, diglycerol phosphate and amino acids are preferentially accumulated in salt stress conditions, the level of di-*myo*-inositol phosphate and its derivatives responds to supra-optimal growth temperatures (Santos et al. 2007). Moreover, in all organisms known to accumulate di-*myo*-inositol phosphate, the level of this solute increases consistently and strongly in response to heat stress. Therefore, the presence of di-*myo*-inositol phosphate as the major solute in *P. fumarii*, one of the most extreme hyperthermophiles described, further reinforces the view that di-*myo*-inositol phosphate may play an important role in the adaptation of organisms to hot environments. At least *in vitro*, the ability of di-*myo*-inositol phosphate to protect proteins against heat denaturation has been confirmed in several examples ((Shima et al. 1998); our unpublished results); in addition, the potential of di-*myo*-inositol phosphate to prevent protein aggregation and fibril formation was demonstrated recently (Santos et al. 2007).

Unexpectedly, relatively high amounts of UDP-sugars were also found in cell extracts of *P. fumarii*, but it is unlikely that these compounds play a role in osmo or thermo adaptation. Other hyperthermophilic *Archaea*, i.e., *Pyrococcus furiosus* (Ramakrishnan et al. 1997a), *Methanothermus fervidus* (Hartmann and Konig 1989) and *Methanobacterium thermoautotrophicum* (Hartmann et al. 1990) accumulate substantial amounts of UDP-sugars, which are the precursors in the synthesis of different glycosylated structures, namely peptidoglycan (Hartmann and König 1990), surface layer (S-layer) proteins (König et al. 1994) and exopolysaccharides (Parolis et al. 1999).

N-glycosylation is one of the glycosylation pathways present in *Archaea*. This pathway starts with the activation of a monosaccharide by UTP. To the resulting UDP-sugar, new units are sequentially added to form a nucleotide activated oligosaccharide. The final oligosaccharide (that can comprise a varying number of monosaccharides) is transferred to a lipid carrier, dolicholphosphate or dolicholpyrophospahte, and finally to the NH group of an amino acid acceptor (Hartmann and König 1990; Eichler and Adams 2005). With this in mind, the

simultaneous presence of an activated monosaccharide, UDP-α-GlcNAc3NAc, and the derivative, UDP-α-GlcNAc3NAc-(4←1)-β-GlcpNAc3NAc, strongly suggests that these are intermediates of an *N*-glycosylation pathway in *P. fumarii*. The cell wall of *P. fumarii* is composed of a S-layer of tretameric protein complexes (Blöchl et al. 1997), a common target for *N*-glycosylation in *Archaea* (Claus et al. 2002; Claus et al. 2005). Therefore, it is tempting to speculate that the S-layer is the final target of this hypothetical pathway.

A curious feature of the two NDP-sugars characterised in this study is the presence of two acetamido groups, instead of the single one commonly found in living systems. To our knowledge, the activated disaccharide UDP-α-GlcNAc3NAc-(4←1)-β-GlcpNAc3NAc has not been reported elsewhere. The hexose unit in UDP-α-GlcNAc3NAc is also very unusual, having been observed only in the hyperthermophilic bacterium *Aquifex pyrophilus* as a constituent of Lipid A (Plotz et al. 2000). The second hexose moiety, β-GlcpNAc3NAc, although rare is more common, having been found in lipopolysaccharides of a few bacterial species (Shashkov et al. 1995; Cory et al. 2005), in an exopolysaccharide of *Haloferax denitrificans* (Parolis et al. 1999) and in a trisaccharide of *Methanococcus voltae* flagellin (Voisin et al. 2005).

In conclusion, this work shows that di-*myo*-inositol phosphate is the major solute accumulating in *P. fumarii*, the most hyperthermophilic organism described thus far; moreover the structures of two unusual NDP-sugars, probably involved in *N*-glycosylation pathways of this organism were characterised. Regrettably, the knowledge on this amazing extremophile has barely progressed after it was isolated about a decade ago (Blöchl et al. 1997)

Acknowledgements

I thank Dr. Pedro Lamosa for help in the identification of the NDP-sugars by NMR. I also thank Ana Mingote for technical support in the purification of the NDP-sugars. I wish to acknowledge Dr. Ana Coelho from the mass spectrometry service at ITQB for performing the mass spectra. This work was supported by the European Commission, 5th and 6th Framework Programme contracts QLK3-2000-00640 and COOP-CT-2003-508644, FEDER, and POCTI, Portugal (Project A004/2005 Action V.5.1).

CHAPTER 3

Compatible Solutes of *Archaeoglobus* spp.

Parts of this chapter are published in:

Gonçalves, L.G., Huber, R., da Costa, M.S., and Santos, H. 2003. A variant of the hyperthermophile *Archaeoglobus fulgidus* adapted to grow at high salinity. *FEMS Microbiol Lett* **218:** 239-244.

Lamosa, P., **Gonçalves, L.G.**, Rodrigues, M.V., Martins, L.O., Raven, N.D., and Santos, H. 2006. Occurrence of 1-glyceryl-1-*myo*-inosityl phosphate in hyperthermophiles. *Appl Environ Microbiol* **72:** 6169-6173.

Chapter | 3 | Contents

Abstract

The accumulation of solutes was studied in different species of the genus *Archaeoglobus*: *Archaeoglobus profundus*, *Archaeoglobus veneficus* and two different strains of *Archaeoglobus fulgidus* (7324 and VC-16). A new variant of *A. fulgidus* VC-16 was also examined. This organism was isolated from cultures obtained after a stepwise transfer from media containing 1.8% to 6.3% NaCl by a plating-independent, selected-cell cultivation technique, using a laser microscope. This variant, *A. fulgidus* VC-16S, had a higher growth rate throughout the salt range of the parental strain; moreover, it was able to grow in media containing NaCl up to 6.3%, whereas the parental strain could not grow above 4.5% NaCl.

Diglycerol phosphate, a solute thus far encountered only in the *Archaeoglobales*, was the major solute accumulating in this new variant under supra-optimal salinities; di-*myo*-inositol phosphate was the predominant solute during growth at supra-optimal temperatures. The level of compatible solutes in the variant VC-16S was lower than in the parental strain within 1.8 to 4.5% NaCl, but increased sharply in the variant at higher salinity (5.5 and 6.0% NaCl). This variant represents, at this time, one of the most halophilic hyperthermophiles known, and its ability to grow at high salinity appears to be associated with the massive accumulation of diglycerol phosphate.

An unknown solute, initially designated as "unknown di-*myo*-inositol phosphate isomer" was present in low amounts in extracts of strains VC-16 and VC-16S. The structure of this compound was firmly identified as glycero-phospho-*myo*-inositol by using a combination of NMR and Mass Spectrometry. Thus far, this newly discovered solute has been found only in

A. fulgidus (strains VC-16, VC-16S and 7324) and in two hyperthermophilic bacteria of the genus *Aquifex* (*Aquifex aeolicus* and *Aquifex pyrophilus*). The level of glycerol-phospho-*myo*-inositol responded primarily to the combination of supra-optimal temperature and supra-optimal NaCl concentration. The remarkable structural relationship between diglycerol phosphate, di-*myo*-inositol phosphate, and the newly identified solute is disclosed in this work. The unit glycero-phospho-*myo*-inositol is part of the polar head in phosphatidylinositol, an important constituent of lipid membranes, but this is the first report on the occurrence of glycero-phospho-*myo*-inositol as a cell metabolite.

The polyolphosphodiesters, diglycerol phosphate, di-*myo*-inositol phosphate, and glycero-phospho-*myo*-inositol accumulated in *A. fulgidus* VC-16 as well as in a different strain of *A. fulgidus* (7324) when cells were cultivated on lactate, but the nature of the intracellular osmolytes was remarkably different when starch was used as the carbon source. Under these growth conditions, mannosylglycerate was a major solute. Growth in medium containing 4.5% NaCl, a concentration well above the optimal value (1.8% NaCl), led to a 5-fold increase in the intracellular content of mannosylglycerate, which was the sole solute detected at this salinity. Interestingly, mannosylglycerate was also detected in members of two other *Archaeoglobus* spp., *i. e.*, *A. veneficus* and *A. profundus,* which use acetate as the preferred carbon source. The solute pool of *A. veneficus* comprised diglycerol phosphate, di-*myo*-inositol phosphate, mannosylglycerate and α-glutamate, and a similar set of solutes was observed in extracts of *A. profundus*, except that diglycerol phosphate was absent.

INTRODUCTION

Many hyperthermophilic microorganisms have been isolated from low water activity environments, and therefore they have developed strategies to balance the osmotic pressure exerted by the external salinity. The most common strategy among these organisms is the accumulation of organic compatible solutes (Santos and da Costa 2002). Compatible solutes, by definition, accumulate intracellularly to high levels without major interference with cellular processes (Brown 1976). These substances are small, soluble molecules that usually belong to one of the following groups of compounds: amino acids, sugars, polyols, betaines, and ectoines (da Costa et al. 1998). In halophilic or halotolerant hyperthermophiles, compatible solute accumulation occurs not only in response to increased salinity, but also in response to supra optimal growth temperatures. The latter observation seems rather intriguing, especially if we

consider that the external water activity remains practically unaltered when the temperature is raised.

Interestingly, hyperthermophiles accumulate solutes that have not been found, or have been rarely encountered, in mesophilic organisms, such as diglycerol phosphate, mannosylglycerate, di-*myo*-inositol phosphate and derivatives. In contrast to the solutes typical of mesophiles, the solutes of hyperthermophiles, herein designated as "thermolytes", are usually negatively charged (Santos and da Costa 2002). On the other hand, the superior protective effect of thermolytes upon cellular structures is well documented (Hensel and König 1988; Ramos et al. 1997; Lamosa et al. 2000; Borges et al. 2002; Pais et al. 2005).

Archaeoglobus fulgidus is an anaerobic hyperthermophilic archaeon that utilises sulfate as terminal electron acceptor (Stetter et al. 1987; Stetter 1988). The type strain, designated VC-16, was isolated from marine hydrothermal vents in the Island of Vulcano, Italy. Other strains of *A. fulgidus* were isolated from samples collected in diverse environments: strain Z, from hot marine sediments (Zellner et al. 1989) and strain 7324, from oil field water in the North Sea (Beeder et al. 1994). Two other species of the genus *Archaeoglobus*, *A. profundus* and *A. veneficus*, have been isolated from abyssal geothermal areas and they are also slightly halophilic hyperthermophiles (Burggraf et al. 1990; Huber et al. 1997).

Like most halophilic organisms *A. fulgidus* VC-16 accumulates organic compounds in response to salt stress (Martins et al. 1997). However, this organism accumulates diglycerol phosphate as a major organic solute during osmoadaptation, an exquisite osmolyte thus far encountered only in members of the genus *Archaeoglobus*. Diglycerol phosphate has a high protective effect on several proteins isolated from different sources, even at relatively low concentration (100 mM) (Lamosa et al. 2001; Lamosa et al. 2003; Pais et al. 2005; Lentzen and Schwarz 2006). *A. fulgidus* VC-16 also produces a second polyolphosphodiester, di-*myo*-inositol-phosphate, but primarily in response to elevated growth temperatures (Martins et al. 1997).

In this work, we studied the pattern of solute accumulation in different organisms belonging to the genus *Archaeoglobus*: *A. profundus, A. veneficus*, *A. fulgidus* 7324 and a new variant of *A. fulgidus* VC-16. This new variant was isolated from an *A. fulgidus* VC-16 culture that was adapted to high salt concentrations by a stepwise transfer in medium with increasing NaCl concentrations. The strain was isolated from a medium containing 6.3% NaCl, by a plating-independent, selected-cell cultivation technique, based on the use of laser microscope "optical tweezers" (Huber et al. 1995; Huber et al. 2000). This variant, being able to grow at higher salinity, was considered as a better candidate for the production of high levels of diglycerol phosphate than the wild type strain; therefore, we decided to examine in detail the

pattern of solute accumulation in the new variant VC-16S as a function of growth temperature, medium salinity, and growth phase.

MATERIAL AND METHODS

Strains and culture conditions

Archaeoglobus fulgidus strain VC-16 (DSM 4304^T) and the variant VC-16S were routinely maintained in the medium described by Stetter et al (1987), except that Na_2SO_4 was replaced by the same concentration of $Na_2S_2O_3$ and sodium hydrogen carbonate was replaced by 20 mM PIPES (di-sodium salt). The total sodium ion concentration of the medium, prior to addition of NaCl, was 80 mM and the total chloride ion concentration was 39.4 mM,. In this study the medium was supplemented with NaCl to achieve the required salinity levels.

The organisms were cultured in 2-liter or 5-liter fermentation vessels with continuous gassing, using a gas phase composed of N_2 and CO_2 (80:20 by vol.), and with stirring at 80 rpm. Cell growth was monitored by counting with a Neubauer counting chamber (Weber, England). Unless otherwise stated, cultures were grown until the late exponential phase. Cells were harvested by centrifugation (10000 $\times$ g, 4°C, 15 min), and washed twice with the growth medium without carbon sources, PIPES, or resazurin. The cell pellet was resuspended in water to a final concentration of approximately 10 mg protein/ml.

The effect of salinity on the accumulation of organic solutes by *A. fulgidus* strains VC-16S and VC-16 was investigated in cultures grown in medium containing NaCl to a maximum of 6.0%. The effect of the growth temperature on the accumulation of solutes by *A. fulgidus* was examined between 65 and 89°C. The effect of the growth phase on the accumulation of solutes was investigated in medium containing 1.8 and 4.5% NaCl. For these investigations, strain VC-16S was cultured in a 5-liter fermentation vessel and, at appropriate time intervals, samples (500 ml) were collected and cells were harvested as described above.

A. fulgidus 7324 was routinely maintained in the medium described by Labes & Schönheit (Labes and Schönheit 2001), using lactate as the major carbon source. To study the effect of the carbon source in the solute accumulation profile, lactate was replaced by 0.5 g/l starch. The organism was cultured in 2-liter static vessels with a gas phase composed of N_2 and CO_2 (80:20 by vol.) until late exponential phase. Cell growth was monitored by optical density at 600 nm. Cell recovery was performed as described above.

A. profundus and *A. veneficus* were obtained from the DSMZ collection. *A. profundus* was grown in the medium described by Lopez-Garcia *et al.* (Lopez-Garcia et al. 2000), and

A. veneficus was cultured in the DSMZ medium 796, both using acetate as carbon source and thiosulfate as electron acceptor. The organisms were cultured statically in serum bottles under an atmosphere of H_2 and CO_2 (80:20 by vol., 200 kPa) at 85 °C until the late exponential phase. Cell recovery was done as described above.

Extraction of intracellular solutes

The intracellular solutes were extracted with boiling 80% ethanol as previously described by Martins and Santos (Martins and Santos 1995). Freeze-dried extracts were dissolved in D_2O and analysed by NMR. Intracellular solutes were quantified by ^{31}P-NMR and ^{1}H-NMR, using potassium phosphate and formate, respectively, as internal concentration standards. Glutamate levels were determined with an enzymatic assay (Lund 1987). The protein cell content in the samples used for solute analysis was determined by the Bradford assay (Bradford 1976) after cell lysis by sonication (B. Braun-Biotech SA).

Purification of glycero-phospho-*myo*-inositol from *A. fulgidus* extracts

A. fulgidus VC-16 biomass was obtained from a 300 L fermentation performed at 83^{o}C and with 1.8% NaCl in the culture medium. Cells were lysed in a French pressure cell at 3.3 MPa; the resulting cell mass was dialysed against 50 mM Tris-HCl buffer pH 7.5, containing 10 mM $MgCl_2$, 200 µM PMSF, and 1 mM EDTA. The dialysis buffer containing the intracellular organic solutes was freeze-dried. The resulting powder was treated four times with boiling 100% ethanol, after which the insoluble fraction was extracted twice with boiling 80% ethanol. ^{1}H-NMR analysis revealed that glycero-phospho-*myo*-inositol was only present in the 80% ethanol extraction, which also contained diglycerol phosphate, di-*myo*-inositol phosphate and Tris-HCl. This preparation was applied to an anionic exchange resin (QAE-Sephadex A-25, Pharmacia, Uppsala, Sweden), developed with a linear gradient of sodium carbonate buffer (5 mM to 1 M, pH 9.8). Fractions containing the new compound, as observed by NMR, were pooled, freeze-dried, desalted in an activated cation exchange resin (Dowex 50W-X8, Bio-Rad), and eluted with distilled water, after which samples were degassed under vacuum, and the pH adjusted to 5 with 1 M KOH. Glycero-phospho-*myo*-inositol was further purified by gel filtration (Sephadex-G10, Pharmacia, Uppsala, Sweden). Two partially purified samples containing glycero-phospho-*myo*-inositol as the major compound were obtained; one was contaminated with di-*myo*-inositol phosphate, while the other was contaminated with diglycerol phosphate. At this stage these fractions were judged to be pure enough for NMR analysis.

Determination of K^+ and Cl^- intracellular contents

To determine the intracellular content of K^+ and Cl^- in *A. fulgidus* VC-16S, the organism was grown as described above, in medium containing 4.5 and 5.5% NaCl. Cells were harvested by centrifugation (10000 × g, 4°C, 15 min), and washed twice with a Na_2SO_4 solution with the same osmotic strength of the growth medium. The pellet was ressuspended in deonised water. Potassium and chloride determinations were performed by ion chromatography in Analytical Chemistry Laboratory of Instituto Superior Técnico da Universidade Técnica de Lisboa.

NMR spectroscopy

Routine mono-dimensional ^1H and ^{31}P-NMR spectra were acquired in a Bruker AMX300 spectrometer using a 5-mm inverse detection probe head at 30°C. ^1H-NMR spectra were obtained with presaturation of the water signal, a 60° flip angle and a repetition delay of 40 s. Chemical shifts were referenced with respect to sodium 3-trimethylsilyl[2,2,3,3-^2H]propionate. ^{31}P-NMR spectra were recorded at 121.50 MHz, with proton broad-band decoupling using a repetition delay of 30 s and a 90° flip angle. The intensity of the resonances was compared with that of the signal due to a known amount of potassium phosphate added to the sample. Chemical shifts were referenced to external 85% H_3PO_4.

Two dimensional spectra were acquired in a Bruker DRX500 spectometer, using standard Bruker pulse programs. Phase-sensitive nuclear Overhauser effect spectroscopy (NOESY), proton-homonuclear shift correlation spectroscopy (COSY) and total-correlation spectroscopy (TOCSY) were acquired collecting 4096(t2) x 512(t1) data points, while in the heteronuclear spectra 4096(t2) x 256(t1) data points were acquired. In the ^1H-^{13}C heteronuclear multiple quantum coherence spectra (HMQC) (Bax and Summers, 1986), a delay of 3.5 ms was used for evolution of $^1J_{CH}$ and in the heteronuclear multiple bond connectivity spectrum (HMBC) a delay of 73.5 ms was used for evolution of long range couplings. The ^1H-^{31}P HMQC was acquired using a delay of 41.6 ms for the evolution of J_{PH} constants.

Mass Spectrometry

Mass spectra were acquired on a LCQ advantage ion trap mass spectrometer from ThermoFinnigan (San Jose, CA, USA) equipped with an electrospray ionisation interface operated in the negative mode. Samples were injected at 300°C and –33 V in 50% methanol/0.1% formic acid.

RESULTS

Isolation of *A. fulgidus* strain VC-16S

A stepwise transfer of *A. fulgidus* VC-16 in medium with increasing NaCl concentrations led to appearance of populations with different cell volumes. The diameter of single cells increased significantly with the NaCl concentration: in medium containing 1.8% NaCl the diameter was about 1 µm, in 4.5% NaCl medium it was about 2 µm, and in medium with 6.3% NaCl it was up to 4 µm. The latter cell dimension corresponds to an increase in cell volume of about 70 fold in the NaCl range examined. A single, enlarged cell was selected and isolated from this last medium containing 6.3% NaCl, and further cultivated. This high-salt adapted culture of *A. fulgidus* VC-16 was designated *Archaeoglobus fulgidus* strain VC-16S. This work was performed by Dr. R. Huber at Regensburg University.

Growth profile of *A. fulgidus* strain VC-16S

Strain VC-16S grew in media containing NaCl up to about 6% (0.8 to 6.8% total salts in the medium), with optimum growth at approximately 1.8% NaCl (Fig. III.1). Growth at 6.5 and 7.0% NaCl was not observed within 48 h incubation . At the optimum growth temperature, the doubling times of strain VC-16S were similar in medium containing between 0.9 to 4.5% NaCl, but at lower (0.0% NaCl) or higher salinities (5.5 and 6.0% NaCl) the doubling times increased sharply. The doubling times of *A. fulgidus* VC-16 were approximately 2-fold higher than those obtained for *A. fulgidus* VC-16S in media with the same concentration of NaCl, and reached lower cell densities at optimum conditions than strain VC-16S. Moreover, strain VC-16 did not grow in media containing 5.5 or 6.0% NaCl within 48 h, while variant VC-16S reached the stationary phase within the same period of time in medium containing 6.0% NaCl (Fig. III.1). Lag phases were not observed in any of the conditions examined. Strain VC-16 and variant VC-16S grew between 65 and 89°C, with optimal temperature for growth in the vicinity of 83°C. The highest cell density attained during growth under optimum conditions of temperature and salinity, was around 2×10^8 cells per ml; strain VC-16 normally reached slightly lower cell densities than the variant.

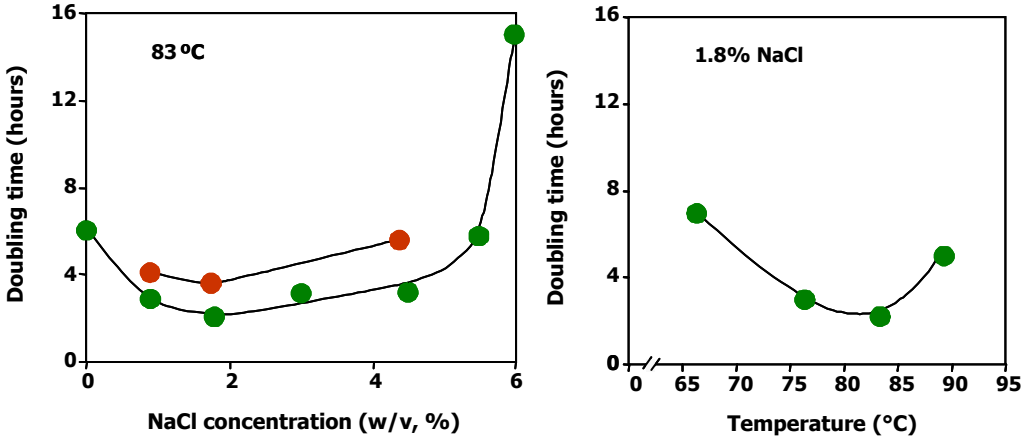

Figure III.1. Doubling times for growth of *A. fulgidus* VC-16 and *A. fulgidus* VC-16S as a function of the NaCl concentration in the growth medium (left panel) and the growth temperature (right panel). Green symbols refer to *A. fulgidus* VC-16S and red symbols refer to *A. fulgidus* VC-16.

Growth profile of *A. fulgidus* strain 7324

It has been reported that *A. fulgidus* can utilise starch, instead of lactate, as carbon source for growth (Stetter 1988; Beeder et al. 1994). In our hands, however, when lactate was replaced by starch in the culture medium of *A. fulgidus* VC-16, no growth could be observed. In contrast, *A. fulgidus* 7324 was able to grow using starch as the major carbon source, though reaching lower values of final biomass (maximum OD_{600} = 0.35) than with lactate (maximum OD_{600}=0.5) at optimum salinity, 1.8% NaCl.

Identification of major intracellular solutes in *Archaeoglobus* species

^{1}H-NMR spectra of ethanol extracts of *A. fulgidus* strain VC-16S revealed the presence of α-glutamate and vestigial amounts of acetate, as well as diglycerol phosphate and di-*myo*-inositol phosphate. The presence of these compounds was confirmed by ^{31}P-NMR: the spectra showed three resonances in the phosphodiester region, at 1.57, 0.4 and -0.57 ppm; the first and the last resonances were assigned to diglycerol phosphate and di-*myo*-inositol phosphate, respectively. The resonance at 0.4 ppm was previously observed in *A. fulgidus* VC-16 cell-free extracts and referred to as an "unidentified isomer of di-*myo*-inositol phosphate" (Martins et al. 1997).

This new compound was partially purified from *A. fulgidus* VC-16 extracts. After an anion exchange chromatography and a gel filtration steps, two partially purified samples,

containing the new solute as the major compound, were obtained; one was contaminated with di-*myo*-inositol phosphate, while the other was contaminated with diglycerol phosphate. At this stage these fractions were judged to be pure enough for NMR and mass spectrometry analyses. The two samples presented a signal with a m/z of 332.88, together with signals at m/z 244.9 and 420.8 corresponding to diglycerol phosphate and di-*myo*-inositol phosphate, respectively. However, the low amounts of the new compound in these samples precluded its NMR characterisation.

In parallel, ethanolic extracts of *Aquifex pyrophilus* were also analysed in our laboratory and found to contain a compound with very similar ^{1}H and ^{31}P-NMR spectral characteristics to the unknown compound of *A. fulgidus* and with the same m/z. In that organism, the compound was present in higher amounts than in *A. fulgidus,* representing more than 50 % of the total pool of solutes. NMR analysis (^{1}H-NMR, ^{31}P-NMR, ^{13}C-NMR, COSY, TOCSY, NOESY, ^{1}H-^{13}C HMQC and ^{1}H-^{13}P HMQC) of *Aq. pyrophilus* extracts revealed that the phosphorous signal correlated with two partially overlapping signals in the proton spectrum. This correlation was further confirmed by the carbon-phosphorous splitting that could be observed in the carbon signals directly bonded to these two proton resonances (Fig. III.2). The TOCSY spectrum showed that these two signals belong to two different spin-systems of three and six members. According to the ^{13}C-^{1}H HMQC, all carbon signals of this compound appeared in the spectral region of primary alcohols. The coupling patterns and chemical shift values in carbon and proton spectra clearly indicate that these moieties are glycerol and *myo*-inositol.

The combined analysis of the ^{1}H-COSY and ^{13}C-^{1}H HMQC spectra allowed the complete assignment of all the proton and carbon resonances (Table III.1). The compound present in cell extracts of *Aquifex pyrophilus* was therefore identified as glycero-phospho-*myo*-inositol (Fig. III.3).

The partially purified preparations of *A. fulgidus* containing the "unidentified isomer of di-*myo*-inositol phosphate" were spiked with extract from *Aq. pyrophilus* cells grown at 88^{o}C and 4% NaCl. A complete identity between the several signals was observed thus establishing that glycero-phospho-*myo*-inositol is the previously unidentified compound, and that it occurs both in *Aq. pyrophilus* and in *A. fulgidus.*

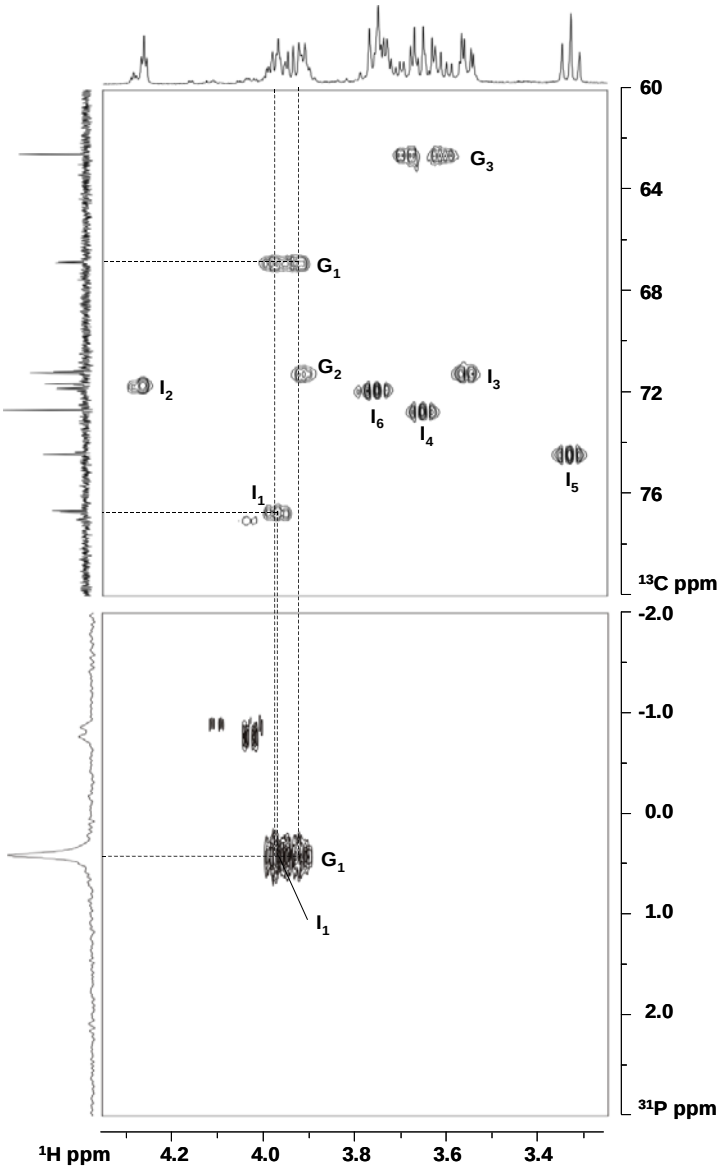

Figure III.2. ^{1}H-^{13}C HMQC (top) and ^{1}H-^{31}P HMQC (bottom) correlation spectra of glycero-phospho-*myo*-inositol in an ethanolic extract of *Aquifex pyrophilus* grown at 88ºC and 4% NaCl. The assignments are indicated next to each signal: G- glycerol moiety, I- inositol moiety.

TABLE III.1. NMR parameters of glycero-phospho-*myo*-inositol.

Moiety	^{13}C-NMR	^{1}H-NMR		^{31}P-NMR	
	δ (ppm)	δ (ppm)	$^{n}J_{HH}$ (Hz)	δ (ppm)	$^{n}J_{PX}$ (Hz)
Inositol					
C_1	77.0	3.97	$^{3}J_{1,2}$= 2.75		$^{2}J_{P,C}$= 6.24
C_2	71.9	4.27	$^{3}J_{2,3}$= 2.75		
C_3	71.4	3.56	$^{3}J_{3,4}$= 9.92		
C_4	72.9	3.66	$^{3}J_{4,5}$= 9.60		
C_5	74.6	3.34	$^{3}J_{5,6}$= 9.31		
C_6	72.1	3.76	$^{3}J_{6,1}$= 10.0		
Glycerol					
C_1	67.1	3.98 / 3.94	n.d.		$^{2}J_{P,C}$= 5.76
C_2	71.5	3.92	$^{3}J_{2,3a}$= 4.13 $^{3}J_{2,3b}$= 6.20		$^{3}J_{P,C}$= 6.72
C_3	62.8	3.69 / 3.61	$^{2}J_{3a,3b}$= 12.40		
Phosphate					
P				0.4	

n.d. – not determined.

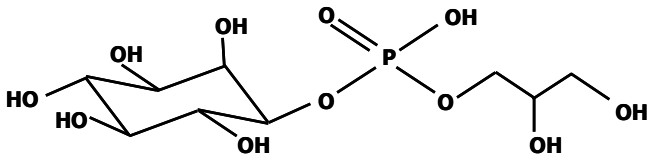

Figure III.3. Molecular representation of the newly identified compound glycero-phospho-*myo*-inositol. The stereochemistry has not been established.

^{1}H- and ^{31}P-NMR ethanolic extracts of *A. fulgidus* 7324 grown with lactate as carbon source presented the same pattern of compounds found in *A. fulgidus* VC-16 and VC-16S: diglycerol phosphate, di-*myo*-inositol phosphate, glycero-phospho-*myo*-inositol and α-glutamate. However, when starch, instead of lactate, was used as carbon source, besides the ^{1}H-NMR resonances due to the previous solutes, we also found mannosylglycerate, whose presence was confirmed by spiking the sample with the pure compound.

In the case of *A. veneficus*, ^{1}H and ^{31}P-NMR spectra showed the presence of mannosylglycerate, diglycerol phosphate, di-*myo*-inositol phosphate and α-glutamate. A similar

solute pool was observed in extracts of *A. profundus*, but diglycerol phosphate was absent in this organism (Table III.2).

Table III.2: Compatible solutes accumulated by the *Archaeoglobus* strains studied at optimum growth conditions.

	MG	DGP	DIP	GPI	Glut
***Archaeoglobus fulgidus* VC-16**	–	+++	+	++	+
***Archaeoglobus fulgidus* VC-16S**	–	+++	+	++	+
***Archaeoglobus fulgidus* 7324**	+++	+++	+	++	+
***Archaeoglobus veneficus* SNP6**	+++	+	+	–	++
Archaeoglobus profundus	+++	–	+	–	++

The + sign is a qualitative indication of the relative amounts of the different compounds.

Optimum growth conditions: 83°C and 1.8% NaCl for *Archaeoglobus fulgidus* strains and 85°C and 1.8% NaCL for *Archaeoglobus profundus* and *Archaeoglobus veneficus*.

MG- mannosylglycerate; DGP- diglycerol phosphate DIP- di-*myo*-inositol phosphate; GPI- glycero-phospho-*myo*-inositol; Glut- α-glutamat.

Effect of salinity and temperature on the accumulation of compatible solutes in *A. fulgidus* VC-16S

Diglycerol phosphate was the major solute accumulated by *A. fulgidus* VC-16S under all growth conditions examined, except when the medium was not supplemented with NaCl, where α-glutamate was the only solute detected in vestigial levels (0.01 μmol/mg protein) (Table III.3). The total pool of solutes increased concomitantly with higher levels of NaCl in the medium, this increase being attributed primarily to higher levels of diglycerol phosphate. At the highest NaCl concentration examined (6.0%), the total amount of solutes reached 3.3 μmol/mg protein, and diglycerol phosphate corresponded to about 85% of the total organic solute pool (Table III.3, Fig. III.4). The level of diglycerol phosphate increased 17-fold between the optimum and the maximum NaCl concentration for growth. The level of glutamate peaked to 0.71 μmol/mg protein in cells derived from growth in medium with 5.5% NaCl, which corresponded to 39% of the total organic solute pool, thereafter decreasing to only 9% of the total compatible solute pool at the highest salinity for growth. At the optimum temperature, di-*myo*-inositol phosphate was only detected in vestigial concentrations within the salinity range examined, whereas the levels of glycero-phospho-*myo*-inositol varied between 4% and 8% of the total pool in response to an increase in the salinity.

Table III.3. Quantification of organic solutes in the parental strain and the variant using ^{31}P-NMR[a]

A. fulgidus	Conditions		Solutes (μmol/mg protein)				
	Temp (°C)	NaCl (%)	DGP	DIP	GPI	Glut[b]	Total pool
VC-16	83	1.8	0.19	0.02	0.03	0.02	0.26
	83	4.5	0.68	ND	0.05	0.08	0.81
VC-16S	66*	1.8	0.07	0.01	ND	0.05	0.13
	76*	1.8	0.09	0.01	0.01	0.02	0.12
	83	0.0	ND	ND	ND	0.01	0.01
	83	0.9	0.10	0.02	0.01	0.03	0.16
	83	1.8	0.17	0.02	0.02	0.04	0.25
	83	3.0	0.31	0.01	0.02	0.08	0.41
	83	4.5	0.37	ND	0.02	0.11	0.50
	83	5.5	1.02	ND	0.07	0.71	1.81
	83	6.0	2.81	ND	0.23	0.29	3.34
	89	1.8	0.14	0.22	0.06	0.06	0.48
	89	4.5	0.45	0.05	0.09	0.06	0.64

[a] Values are the mean of two to four replicates, but in the cases labelled with an asterisk, the determination was performed only once. Replicate determinations varied less than 20%.

[b] Glutamate concentrations were determined by an enzymatic assay.

ND: below the detection limit.

DGP- diglycerol phosphate; DIP- di-*myo*-inositol phosphate; GPI- glycero-phospho-*myo*-inositol; Glut.- α-glutamate

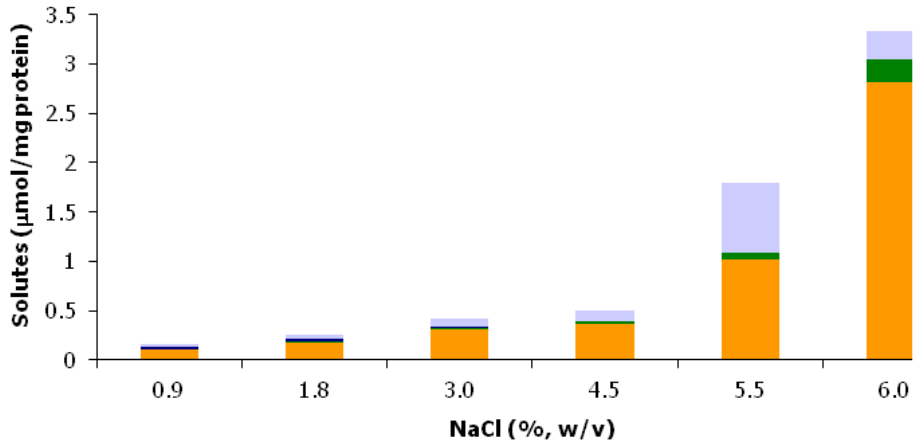

Figure III.4. Effect of NaCl concentration on the solute pool of *A. fulgidus* VC-16S. Samples were collected during the late exponential phase of growth. Bar code: diglycerol phosphate (■), glycero-phospho-*myo*-inositol (■), di-*myo*-inositol-phosphate (■) and α-glutamate (■).

An increase in the growth temperature from 66 to 89°C, at the optimum salinity, resulted in a 4-fold increase in the total pool of compatible solutes (Fig. III.5). At supra-optimal

temperatures di-*myo*-inositol phosphate became the major solute, constituting 46% of the total organic solute pool at 89°C.

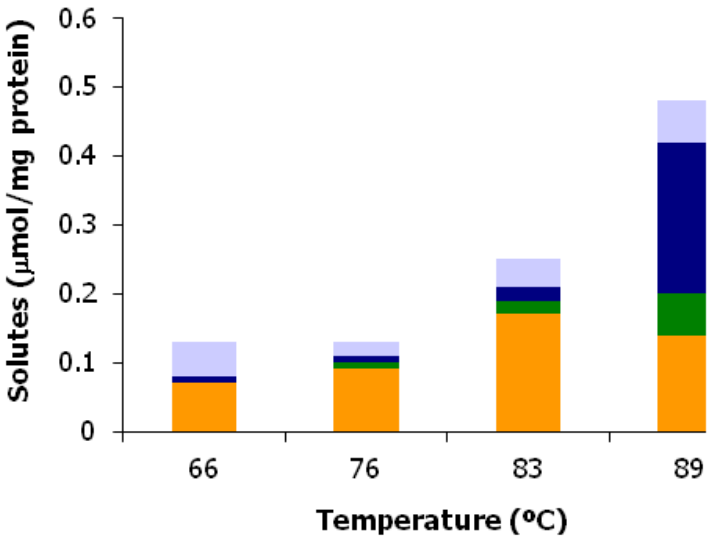

Figure III.5. Effect of growth temperature on the accumulation of solutes by *A. fulgidus* VC-16S. Samples were collected during the late exponential phase of growth**.** Bar code: diglycerol phosphate (■), glycero-phospho-*myo*-inositol (■), di-*myo*-inositol-phosphate (■), and α-glutamate (■).

The combination of a moderate osmotic stress (4.5% NaCl) with heat stress (89°C) resulted in an increase of 30% in the total level of solutes. Under these conditions, the proportion of diglycerol phosphate and di-*myo*-inositol phosphate was drastically altered as compared with growth at 89°C and optimal salinity. The pool of diglycerol phosphate was 9-fold higher than that of di-*myo*-inositol phosphate when the two stresses were combined. Conversely, the pool of di-*myo*-inositol phosphate was 1.6-fold higher than that of diglycerol phosphate when the organism was grown under heat stress (89°C) at the optimum salinity (Fig. III.6). The pool of glycero-phospho-inositol increased when the two stresses were combined, reaching a maximum relative value of 14% of the total solute pool.

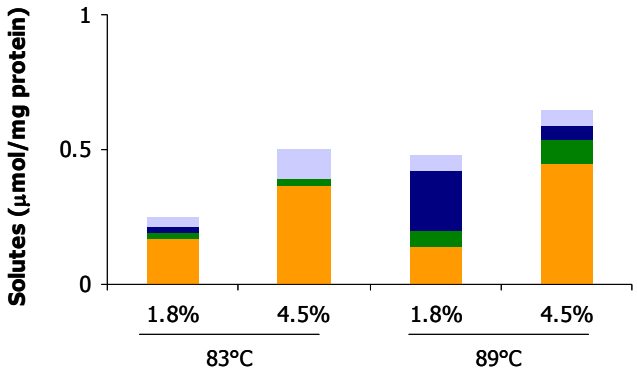

Figure III.6. Effect of combined high salinity and supraoptimal growth temperature on the accumulation of solutes by *A. fulgidus* VC-16S. Samples were collected in the late exponential phase of growth. Bar code: diglycerol phosphate (■), glycero-phospho-*myo*-inositol (■), di-*myo*-inositol-phosphate (■), and α-glutamate (■).

The same compatible solutes were used during osmoadaptation by the parental strain and the variant; however, strain VC-16 accumulated higher amounts of compatible solutes in response to salt stress within the range of salt concentration tolerated by both organisms (up to 4.5% NaCl). For example, the total organic solutes in strain VC-16 reached 0.81 μmol/mg protein in medium containing 4.5% NaCl, whereas the total solute pool in strain VC-16S was only 0.50 μmol/mg protein. Nevertheless, at higher salinities not tolerated by the parental organism, the variant VC-16S accumulated huge amounts of compatible solutes (Table III.3).

Effect of the growth phase on the accumulation of solutes in *A. fulgidus* VC-16S

The profile of solute accumulation was not drastically affected by the growth phase (Fig. III.7). Maximum accumulation of organic solutes occurred at the beginning of the stationary phase and the total pool decreased during the late stationary phase of growth. Diglycerol phosphate was the major solute during all growth phases decreasing towards the stationary phase, while di-*myo*-inositol phosphate and glycero-phospho-*myo*-inositol tended to increase relatively to diglycerol phosphate during the late exponential and stationary phases of growth.

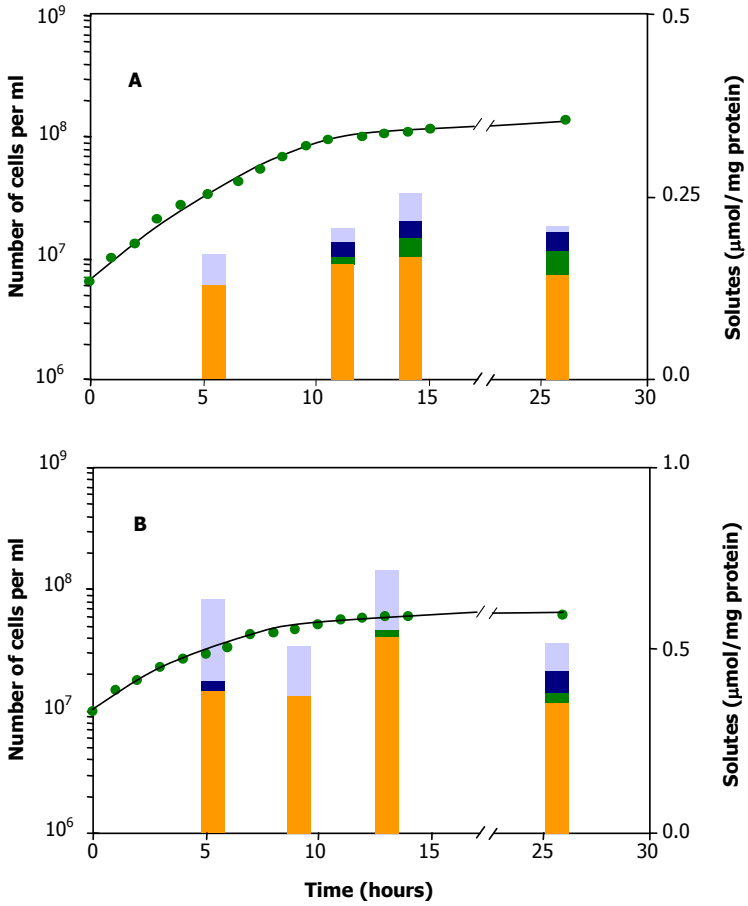

Figure III.7. Correlation between growth phase and accumulation of organic solutes by *A. fulgidus* VC-16S. The culture was grown in medium containing 1.8% (**A**) and 4.5% NaCl (**B**), at 83°C. The intracellular concentrations of the solutes were determined in different phases of growth. Bar code: diglycerol phosphate (■), glycero-phospho-*myo*-inositol (■), di-*myo*-inositol-phosphate (■), and α-glutamate (■).

Effect of salinity on the intracellular levels of K^+ and Cl^- in *A. fulgidus* VC-16S

The intracellular content of K^+ and Cl^- in *A. fulgidus* VC-16S was determined at two salinities of the growth medium: 4.5 and 5.5% NaCl. Contrasting with the 4-fold difference in the total organic solute pool (0.5 and 1.81 μmol/mg protein, respectively), the levels of K^+ and Cl^- were not significantly altered when the two growth conditions were compared. As expected, the K^+ content was higher than the Cl^- content, but surprisingly the excess of K^+ was

insufficient to account for the concentration of anionic organic solutes present in the cells (Fig. III.8).

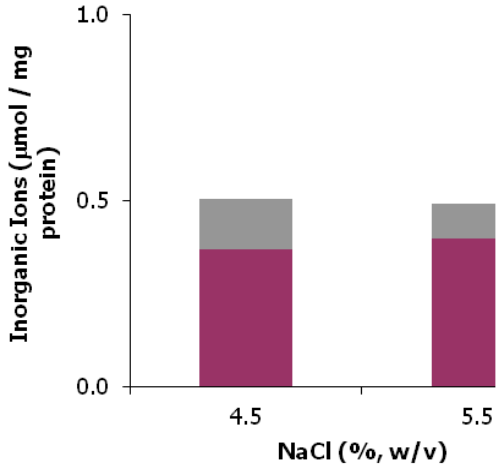

Figure III.8. Effect of salinity on the intracellular contents of K^+ and Cl^- in *A. fulgidus* VC-16S. Samples were collected during the late exponential phase of growth. Bar code: K^+ (■) and Cl^- (■).

Effect of the carbon source and salinity on the accumulation of solutes in *A. fulgidus* 7324

The carbon source used for growth of *A. fulgidus* 7324 affected drastically the solute pool during osmo-adaptation. When lactate was used, the pattern of solute accumulation as a function of salinity was very similar to that observed in *A. fulgidus* VC-16. Diglycerol phosphate was the solute that primarily responded to increased salinity (from 1.8 to 4.5% NaCl), with a 4-fold concentration increase and constituting 92% of the total pool at the highest NaCl concentration examined. The levels of glycero-phospho-*myo*-inositol increased and those of di-*myo*-inositol phosphate decreased. When the organism was grown on starch the pattern of solutes changed substantially. In addition to the usual solutes (diglycerol phosphate, glycero-phospho-*myo*-inositol and di-*myo*-inositol phosphate), mannosylglycerate accumulated as well. At optimum salinity, mannosylglycerate constituted 34% of the total pool and diglycerol phosphate accounted for 57%. At high salinity levels, 4.5% NaCl, mannosylglycerate was the sole solute present in cell-free extracts, with a 5-fold increase relative to conditions of optimum salinity (Fig. III.9).

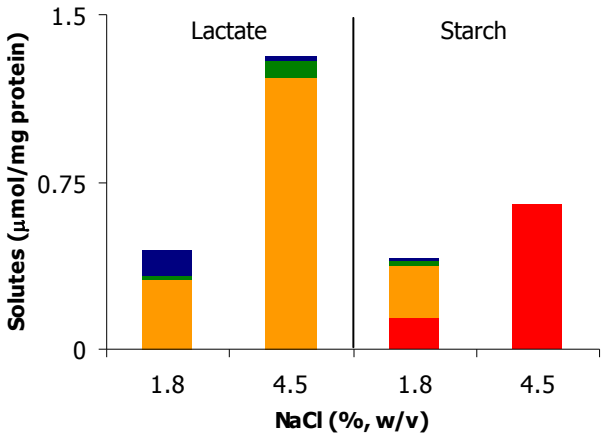

Figure III.9. Effect of increased salinity on the accumulation of solutes by *A. fulgidus* 7324, using lactate (left) or starch (right) as carbon source for growth. Samples were withdrawn during the late exponential phase of growth. Bar code: mannosylglycerate (■), diglycerol phosphate (■), glycero-phospho-*myo*- inositol (■), and di-*myo*-inositol-phosphate (■).

Discussion

Most hyperthermophilic organisms, being isolated from marine hot springs are slightly halophilic and the vast majority of these organisms is unable to grow in media containing more than about 5.0% NaCl. The species of the genus *Archaeoglobus* described to date for example, do not grow in media containing NaCl above 4.5% (Burggraf et al. 1990; Huber et al. 1997). In this work, a new a variant of the type strain of *A. fulgidus* VC-16 was selected, which is clearly better adapted to high salinity than the parental strain, being able to grow in media containing 6.0% NaCl. This feature makes it one of the most halophilic hyperthermophilic archaea known. This variant also has a higher growth rate than the parental strain at high salt concentrations (up to 4.5% NaCl) and it could be argued that a fast growing variant was selected and isolated. However, the fact remains that variant VC-16S also grows at higher salinities than the parental strain and is, therefore, more halotolerant.

Surprisingly, the variant appears to have a discontinuous behaviour for osmotic adaptation; at moderate salinities (up to 4.5% NaCl) the total organic solute pool in *A. fulgidus* VC-16S was considerably lower than in the parental strain, but at high salinities, not tolerated

by the parental strain, there was an enormous accumulation of compatible solutes, clearly reflecting that osmolytes are essential for osmotic adjustment at these extreme salinities.

Therefore, it seems that at moderate salinities this variant relies less on the accumulation of osmolytes for osmoadaptation. The hypothesis that the accumulation of inorganic solutes, such as KCl contributed to the osmotic equilibrium of the cytoplasm was not supported by quantification of these ions in total cell extracts. It is conceivable that the nature of the cell wall and/or membrane has been altered in the salt-adapted variant to endow the cell with a higher resistance to gradients of osmotic pressure; in addition, macromolecules could replace small osmolytes in protecting cell components against dehydration.

The physiological conditions leading to the accumulation of compatible solutes in thermophiles and hyperthermophiles have been studied in some detail only in a few organisms, namely *Pyrococcus furiosus*, *Thermococcus litoralis, Rhodothermus marinus*, *Thermotoga neapolitana* and *Palaeococcus ferrophilus* , and *Aquifex pyrophilus* (Martins and Santos 1995; Martins et al. 1996; Lamosa et al. 1998; Silva et al. 1999; Neves et al. 2005, Lamosa et al 2007). From these studies a general trend is clear: mannosylglycerate generally accumulates in response to salt stress, while the level of di-*myo*-inositol phosphate responds primarily to heat stress (Santos and da Costa 2001).

Archaeoglobus fulgidus VC-16 and its variant, VC-16S, presented a similar behaviour to those organisms, but in this case mannosylglycerate was replaced by a unique solute, diglycerol phosphate, that has been found only in the genus *Archaeoglobus*. Diglycerol phosphate is preferentially accumulated at high salinity, being the major solute at supra-optimal salinities. On the other hand, and corroborating previous results for other hyperthermophiles (Martins et al. 1996; Lamosa et al. 1998; Lamosa et al. 2006), the intracellular levels of di-*myo*-inositol phosphate increased considerably at temperatures above the optimum for growth. Therefore, these results further support the view that compatible solutes in hyperthermophiles have specialised roles: some, such as mannosylglycerate and diglycerol phosphate, have a primary role in osmoadaptation, while others, namely di-*myo*-inositol phosphate, are preferentially involved in thermoadaptation. For now, this hypothesis remains speculative because definite experimental evidence obtained with suitable knockout mutants is still missing. Such experiments would show if mannosylglycerate and diglycerol phosphate could replace di-*myo*-inositol phosphate in the thermal protection of the organisms at supraoptimum growth temperatures.

Di-*myo*-inositol phosphate accumulates in all *Archaeoglobus* strains studied herein, which is in agreement with di-*myo*-inositol phosphate being the most widespread solute among

marine (hyper)thermophiles (Santos and da Costa 2002). Thus far, di-*myo*-inositol phosphate was never found in mesophiles. Besides di-*myo*-inositol phosphate, α-glutamate was also present in all the *Archaeoglobus* strains examined. This amino acid is a common compatible solute during low-level osmotic adjustment in many halotolerant and halophilic organisms independently of their growth temperature (Csonka 1989; Galinski 1995; da Costa et al. 1998). In the case of hyperthermophiles, α-glutamate occurs in many members of almost all lineages in both the domains, *Archaea* and *Bacteria* (Santos and da Costa 2001; 2002), responding mostly to an increase in the salinity of the medium, as seen in *A. fulgidus* VC-16S. In *Palaeococcus ferrophilus*, one of the few marine hyperthermophiles that did not accumulate di-*myo*-inositol phosphate, α-glutamate together with mannosylglycerate replaced the role of di-*myo*-inositol phosphate in thermo-adaptation (Neves et al. 2005).

In contrast with di-*myo*-inositol phosphate and mannosylglycerate, two widespread solutes among hyperthermophiles, diglycerol phosphate is a very unusual solute. It was only found in *A. fulgidus* and *A. veneficus*, not being found in *A. profundus*. This solute is primarily involved in osmo-adaptation, being the major solute in *A. fulgidus* VC-16 and VC-16S at high salinity. Diglycerol phosphate was also the major solute in *A. fulgidus* 7324 when lactate was utilised as carbon source, but the replacement of lactate by starch led to the disappearance of diglycerol phosphate at high salinity, being the solute pool composed exclusively of mannosylglycerate. In contrast with the initial reports on growth of *A. fulgidus* VC-16 (Stetter et al. 1987; Stetter 1988), we failed to cultivate *A. fulgidus* VC-16 on starch. This inability of *A. fulgidus* VC-16 to use starch as carbon source for growth was also experienced by other groups (Labes and Schönheit 2001). Diverse genes and enzymatic activities involved in the utilisation of starch as carbon source were observed in *A. fulgidus* 7324 (Labes and Schönheit 2001; Johnsen et al. 2003; Labes et al. 2003; Hansen and Schönheit 2004), but neither those genes were found nor the enzymatic activities were detected in the strain VC-16 (Klenk et al. 1997; Labes and Schönheit 2001). Probably, the genes that allowed the utilisation of sugars as carbon source for growth were lost during the repeated transfer of *A. fulgidus* VC-16 cultures in lactate medium.

The genes involved in the synthesis of MG in *Pyrococcus horikoshii*, *Thermus thermophilus, Rhodothermus marinus*, *Dehalacoccoides ethenogenes* and *Palaeococcus ferrophilus* have been characterised, but homologues of these genes are absent in the genome sequence of *A. fulgidus* VC-16 (Empadinhas et al. 2001; Empadinhas et al. 2003; Borges et al. 2004; Empadinhas et al. 2004; Neves et al. 2005). Surprisingly, they are present in *A. fulgidus*

7324. It appears as though the genes implied in the synthesis of MG have been lost concomitantly with the genes involved in sugar degradation.

We were also able to unequivocally establish that the "unidentified isomer of di-*myo*-inositol phosphate" (Martins et al. 1997), early found in *A. fulgidus* , is glycero-phospho-*myo*-inositol. This newly identified solute exhibits very appealing features: structurally, it resembles a chimera between diglycerol phosphate and di-*myo*-inositol phosphate. Bearing in mind that the level of di-*myo*-inositol phosphate responds mainly to heat, while that of diglycerol phosphate responds strongly to salinity (Martins et al., 1996; Gonçalves et al., 2003), it is interesting that, from the physiological point of view, glycero-phospho-*myo*-inositol also seems to play a double role. Its level responds slightly to increases in either temperature or salinity, but responds strongly when these stresses are applied concomitantly. This behaviour was observed in *A. fulgidus* VC-16S, in which glycero-phospho-*myo*-inositol accounted for 14% of the total solute pool at supra-optimal temperature and salinity, and was even more patent in *Aq. pyrophilus*. In this hyperthermophilic bacterium, high amounts of glycero-phospho-*myo*-inositol accumulated when the two stresses were combined, reaching 2.27 μmol/mg protein and 50% of the total solute pool (Lamosa et al. 2006). The disparity in the levels of glycero-phospho-*myo*-inositol accumulated in the two organisms could be associated with the large amount of diglycerol phosphate present in *A. fulgidus*, which responds very strongly to salt stress, and probably replaces the role of glycero-phospho-*myo*-inositol during osmoadaptation.

While the properties of di-*myo*-inositol phosphate as an enzyme stabiliser have not been clearly demonstrated, the effect of diglycerol phosphate as protein protector against heat has been thoroughly illustrated in our team (Lamosa et al. 2000; Lamosa et al. 2001; Lamosa et al. 2003; Pais et al. 2005). Since glycero-phospho-*myo*-inositol accumulates in response to increased salt concentration at high temperatures, it is reasonable to speculate that it will display good stabilising properties. In fact, most of the solutes accumulating in (hyper)thermophiles exhibit notable protein stabilising properties. In this context, it would be interesting to ascertain these properties in the newly discovered glycero-phospho-*myo*-inositol; however, the difficulty in obtaining the required amounts of this solute precludes that intent for the time being.

Another interesting feature of glycero-phospho-*myo*-inositol is its distribution in the phylogenetic tree. Thus far this rare solute has been detected only in *Aquifex pyrophilus* and *Aquifex aeolicus*, bacterial members of the order *Aquificales*, and in *Archaeoglobus fulgidus*, an archaeon of the order *Archaeoglobales*. It is hard to explain that glycero-phospho-*myo*-inositol

occurs in two organisms so far apart in phylogenetic terms. Taking into consideration that such organisms are likely to share similar habitats, the occurrence of lateral gene transfer could be a plausible explanation for this peculiar distribution.

Acknowledgements I thank Dr. Pedro Lamosa for help in the identification of glycero-phospho-*myo*-inositol by NMR, Marta Rodrigues for the purification of this compound, and Susana Gonçalves for assistance to cultivate *A. profundus* and *A. veneficus.* The isolation of *Archaeoglobus fulgidus* VC-16S was carried out by Dr. R. Huber, Regensburg University. Dr. Ana Coelho from the mass spectrometry service at ITQB performed the mass spectra. This work was supported with funds from the BIOTECH Program, Biotechnology of Extremophiles (QLK3-CT-2000-00640) and by Fundação para a Ciência e a Tecnologia (FCT), Portugal, Programme Sapiens 99, Project POCTI 35719/BIO/2000 and FEDER.

CHAPTER 4

Mannosylglycerate biosynthesis in *Archaeoglobus* spp.

Chapter | 4 | Contents

Abstract

Mannosylglycerate is the most widely used compatible solute for osmotic adjustment in marine (hyper)thermophiles, whether *Bacteria* or *Archaea*. Within members of the genus *Archaeoglobus*, mannosylglycerate accumulated in *A. profundus*, *A. veneficus* and *A. fulgidus* 7324, but was not detected in *A. fulgidus* VC-16 or VC-16S. Two different pathways for mannosylglycerate synthesis have been identified in (hyper)thermophiles: the single-step pathway and the two-step pathway. In this work, the activity of mannosyl-3-phosphoglycerate synthase (MPGS, the key-enzyme of the two-step pathway) was detected in cell extracts of *A. profundus* and *A. fulgidus* 7324. Therefore, the synthesis of mannosylglycerate in these organisms proceeds via the condensation of GDP-mannose with D-3-phosphoglycerate into mannosyl-3-phosphoglycerate (MPG) in a reaction catalysed by mannosyl-3-phosphoglycerate synthase; subsequently, the phosphorylated intermediate was dephosphorylated by a specific phosphatase (MPGP). The genes encoding these enzymes were identified using degenerate primers and inverse PCR. DNA fragments (around 4-kb) were isolated from *A. profundus* and *A. veneficus* genomes and contained three open reading frames (ORFs). Two contiguous ORFs were annotated to *mpgS* (encoding MPGS) and *mpgP* (encoding MPGP) based on high homologies to known MPGSs and MPGPs. The third ORF was putatively annotated as coding for mannosidase. Thus far, this organisation of the genes involved in the synthesis of mannosylglycerate, comprising a putative mannosidase, has not been observed in any of the other mannosylglycerate producers.

INTRODUCTION

Mannosylglycerate is widely distributed among thermophilic bacteria (*Thermus thermophilus, Rhodothermus marinus* and *Rubrobacter xylanophilus*) and also among hyperthermophilic euryarchaeotes of the genera *Pyrococcus*, *Thermococcus*, *Palaeococcus*, and *Archaeoglobus* (Chapter 3; Martins and Santos 1995; Nunes et al. 1995; Neves et al. 2005; Empadinhas et al. 2007; Santos et al. 2007). The crenarchaeotes *Aeropyrum pernix* and *Stetteria hydrogenophila* also accumulate mannosylglycerate (Santos and da Costa 2001; Neves et al. 2005).

This compatible solute accumulates primarily in response to osmotic stress (Santos et al. 2007); an exception to this behaviour is found in *Rhodothermus marinus*, whose content in mannosylglycerate increases considerably at supraoptimal growth temperatures (Silva et al. 1999). Two distinct pathways have been described for the synthesis of mannosylglycerate. The two-step pathway, present in all hyperthermophiles examined thus far, involves the condensation of GDP-mannose and D-3-phosphoglycerate to form a phosphorylated intermediate, mannosyl-3-phosphoglycerate (MPG), a reaction catalysed by mannosyl-3-phosphoglycerate synthase (MPGS); this intermediate is subsequently dephosphorylated by a specific phosphatase, mannosyl-3-phosphoglycerate phosphatase (MPGP) (Empadinhas et al. 2001; Empadinhas et al. 2003; Borges et al. 2004; Empadinhas et al. 2004; Alarico et al. 2005; Neves et al. 2005). In the single-step pathway, the direct condensation of GDP-mannose and D-glycerate occurs to yield mannosylglycerate through the action of mannosylglycerate synthase (MGS). This pathway was only found in *Rhodothermus marinus* (Martins et al. 1999) and in the red *algae Calogossa leprieurii* (Santos et al. 2007).

The main goal of the present work was to investigate the metabolic pathways involved in the synthesis of mannosylglycerate in *Archaeoglobus* species. We found that the two-step pathway was operative in these organisms. The *mpgS* and *mpgP* genes of *A. profundus* and *A. veneficus* were identified, and the corresponding genes of *A. fulgidus* 7324 were partially sequenced. Moreover, a gene coding for a putative mannosidase was found downstream of the mannosylglycerate biosynthetic genes.

MATERIAL AND METHODS

Archaeoglobus strains and growth conditions

Archaeoglobus strains were grown as previously described in Chapter III. *A. fulgidus* 7324 was cultivated using starch and sulfate as carbon and electron sources, while acetate and thiosulfate were used to cultivate *A. profundus* and *A. veneficus*.

Preparation of cell extracts

A. profundus and *A. fulgidus* 7324 cells were harvested by centrifugation (1,000 × g, 10 min) during the late exponential growth phase (OD_{600}=0.35), and washed twice with MOPS buffer (50 mM, pH 7.6) containing 1.8% NaCl. The cell pellet was suspended in Tris-HCl (50 mM, pH 7.6) with 15 mM $MgCl_2$. Cells were disrupted by passing twice through a French pressure cell at 3.3 MPa, and the cell debris was removed by centrifugation (30,000 × g, 4ºC, 30 min). Low molecular mass compounds were removed in a PD-10 column (Amersham Biosciences) equilibrated with Tris-HCl (50 mM, pH 7.6) containing 15 mM $MgCl_2$. All steps during the preparation of cell extracts were performed under anoxic conditions.

Enzyme assays

The activity of mannosylglycerate synthase (MGS) was determined in a reaction mixture (final volume of 100 µl) containing Tris-HCl (50 mM, pH 7.6), 10 mM $MgCl_2$, 0.2 mM GDP-mannose (Amersham Biosciences, 25 µCi/ml, 200 mCi/mmol) and 4 mM glycerate (hemicalcium salt). The reaction was initiated with addition of cell extract and stopped by cooling on ice; the reaction mixture was incubated at 75°C for 1 hour. Mannosylglycerate production was monitored by Thin Layer Chromatography (TLC) as described below.

Mannosyl-3-phosphoglycerate synthase (MPGS) activity was detected in a reaction mixture containing Tris-HCl (50 mM, pH 7.6), 10 mM $MgCl_2$, 0.2 mM GDP-mannose and 4 mM D-3-phosphoglycerate. After addition of cell extract, the reaction mixture was incubated at 75ºC during 1 hour. The end-product, mannosyl-3-phosphoglycerate, was subsequently dephosphorylated into mannosylglycerate by treatment with 2 U of alkaline phosphatase for 30 minutes at 37ºC. The presence of mannosylglycerate was evaluated by TLC as described below.

Mannosidase activity was investigated in cell extracts of *A. profundus* by TLC and ^{1}H-NMR. A cell-extract was incubated with 0.2 mM of [U-^{14}C]-mannosylglycerate (synthesised as described in Sampaio et al. 2003) for one hour at 75°C in Tris-Hcl buffer (50 mM). The assay was performed at two pH values, 7.6 and 5.8. The reaction products were analysed by TLC as described below. For the NMR assays, cell extracts were incubated with 5 mM mannosylglycerate for 24 hours at 75°C, at pH values of 7.5 and 5.8. ^{1}H-NMR spectra were acquired at the beginning and at the end of the incubation period.

Thin layer chromatography conditions

Thin layer chromatography was performed on Silica Gel 60 plates (Merck) with a solvent system composed of chloroform/methanol/acetic acid (glacial)/water (15:25:4:2, v/v/v/v). Radioactive compounds (GDP-mannose, mannosylglycerate and mannose) were visualised by exposing the TLC plates to Kodak BioMax films for 72 hours. Unlabelled mannosylglycerate or mannose were visualised by spraying with α-naphtol-sulfuric acid solution followed by charring at 120ºC. Pure mannosylglycerate and mannose were used for comparison.

NMR spectroscopy

^{1}H-NMR spectra were acquired in a Bruker AMX300 spectrometer using a 5-mm inverse detection probe head at 30°C, with pre-saturation of the water signal, 60° flip angle and a repetition delay of 40 s. Proton chemical shifts were referenced with respect to 3-(trimethylsilyl)propanesulfonic acid (sodium salt).

Identification of *mpgS* and *mpgP* genes

Chromosomal DNA from *A. profundus*, *A. veneficus*, and *A. fulgidus* was isolated according to Ramakrishnan and Adams (Ramakrishnan and Adams 1995). Degenerate primers, based on two conserved regions of known MPGS proteins, and on two conserved regions of known MPGP proteins, were designed to amplify *mpgS* and *mpgP* genes, respectively (Table IV.1).

Table IV.1. Oligonucleotide primers used in this study.

Name	Nucleotide sequence (5' to 3')	Organism	gene
mpgsdeg6	AGGAGTGGAAA(AGT)GG(AGT)GA(AGT)GG(AGT)ATG(ACT)T(AC)(AG)TAGG	degenerate	*mpg*S
mpgsdeg8	TCC(AT)GC(AG)TT(CT)CC(AC)GT(AG)ACCATTAT(AGC)GT(AGT)GTTTC	degenerate	*mpg*S
mpgPdeg8	(AT)(CT)TTCGC(AGC)GC(CT)TT(CT)CC(CT)TTGTC(AGC)(GC)(AT)ATT(CT)C	degenerate	*mpg*P
mpgPdeg9	AG(T)ATA(GC)C(G)TCTCA(G)CTGTAT(C)TCCCT	degenerate	*mpg*P
impgs_apr_for1	CTGAACTACTTCGGAAGGCGCATAGG	*A. profundus*	*mpg*S
impgs_apr_rev1	ATCCAACAGGTGCAACCTCTCATCC	*A. profundus*	*mpg*S
impgs_apr_for2	CCATATGCAATGGTCAGACTGCATTGG	*A. profundus*	*mpg*S
impgs_apr_rev2	CCGCAAGCTTCATAGTCATCGCATGTTCTCC	*A. profundus*	*mpg*S
impgs_ave_for	ATGCAGGCGAACATGCAATGACCATGAGG	*A. veneficus*	*mpg*S
impgs_ave_rev	ATGTACTCGTTCACCGCACATGGAACG	*A. veneficus*	*mpg*S
impgs_afu_for	GACTATGCTGCTGGCTTCCTGATGAG	*A. fulgidus*	*mpg*S
impgs_afu_rev	CTCATCAGGAAGCCAGCAGCATAGTC	*A. fulgidus*	*mpg*S

A single PCR product of 690-bp (for *mpgS*) was amplified, and cloned into pGEM-T (Promega). This procedure led to the amplification of a *mpgS* fragment from the genome of *A. profundus*. The complete sequence of *mpgS* gene was obtained by inverse PCR. For this, *A. profundus* genomic DNA was partially digested with *Sau3*A (New England Biolabs, Ipswich, MA) for 1 hour at 37°C. The restriction endonuclease was inactivated by heating at 65°C for 20 minutes. After deproteinisation with phenol:chloroform:isoamyl alcohol (25:24:1, v/v/v), the DNA fragments (between 2.0 to 8.0 kb) were re-circularised for 24 hours at 16ºC by T4 DNA ligase (New England Biolabs, Ipswich, MA) in buffer containing 1 mM ATP. Based on the sequence of the 690-bp fragment, primers (Table IV.1) with inverse orientations to the coding region were designed, and used to perform the inverse PCR using the re-circularised DNA as template. A single PCR product of 4-kb was obtained, cloned into pGEM-T, and sequenced (AGOWA, Berlin, Germany). The same strategy was followed for the identification of *mpgS* and *mpgP* genes from the genomes of *A. veneficus and A. fulgidus*.

Cloning and expression of *mpgS, mpgP*, and the mannosidase gene

The genes from *A. profundus* were amplified by PCR using *Pfu* DNA polymerase (Fermentas, Burlington, Canada) (Table IV.2). The resulting products had the expected length and were purified with a Qiagen gel extraction kit, digested with the suitable restriction enzymes and cloned by T4 DNA ligase (New England Biolabs, Ipswich, MA) into the corresponding sites at the polylinker multiple cloning site of different expression vectors: pET15b, pGEX-4T-2 and pKK233-2. Expression using the vectors pET15b or pGEX-4T-2 produce a recombinant protein fused with His-tag or a GST, respectively. The correct nucleotide sequences of the inserts were confirmed (Agowa, Berlin, Germany). Constructions with pET15b and pKK233-2 were propagated in *E. coli* DH-5α, while constructions involving pGEX-4T-2 were propagated in *E. coli* JM107.

E. coli strains, BL-21(DE3) and Rosetta, were used as expression hosts. *E. coli* BL-21(DE) cells, carrying the constructs, were grown at 37°C in LB medium with ampicillin (100 μg/ml) to an OD_{600} of 0.5, induced with 1 mM IPTG, and incubated for 4 hours. *E. coli* Rosetta cells, containing the constructs, were grown at 37°C in LB medium with ampicillin (100 μg/ml) and chloramphenicol (34 μg/ml) to an OD_{600} of 0.6, and induced with 0.5 mM IPTG. In this case, two different procedures were followed: after induction, the cells were further grown for 4 hours at 37°C or for 12 hours at 30ºC. In all cases, the cells were harvested by centrifugation (1,000 $\times$ g, 10 min), suspended in Tris-HCl (20 mM, pH 7.6) containing 10 mM

$MgCl_2$ and disrupted in a French press; cell debris was removed by centrifugation (30,000 × g, 4°C, 1 h).

Table IV.2. Oligonucleotide primers used in the expression studies.

Name	Nucleotide sequence (5' to 3')	gene
Bam_mpgs_apr_f	CGCGGATCCATGCTCATCGAATTACCAAAGC	*mpgS*
Eco_mpgs_apr_r	CGCGAATTCTTAATCATAGCATAGGAATGTTTCGG	*mpgS*
Bam_mpgs_apr_r	CGCGGATCCTTAATCATAGCATAGGAATGTTTCGG	*mpgS*
Eco_mpgs_apr_f	GCGGAATTCATGCTCATCGAATTACCAAAGC	*mpgS*
Pst_mpgs_apr_r	GCGCTGCAGTTAATCATAGCATAGGAATGTTTC	*mpgS*
Bam_ mpgp_apr_f	CGGGATCCATGATTAAAATAATATTTACCGAC	*mpgP*
pKK_Xma_mpgp_apr_f	GCGCCCCGGGCTATGATTAAAATAATATTTACCGAC	*mpgP*
pKK_Pst_mpgp_apr_r	CGCCTGCAGTCAATCACCTCCAACAAACTT	*mpgP*
pET_Ned_mpgp_apr_f	GCGCATATGATTAAAATAATATTTACCGAC	*mpgP*
Xho_mpgp_apr_r	CGCCTCGAGTCAATCACCTCCAACAAACTTC	*mpgP*
pKK_Xma_man_apr_f	GCGCCCCGGGATGGAGGAGAGGGATGTAAT	*man*
pKk_Pst_man_apr_r	CGCCTGCAGTCAATCGAATTTCACTTTCAGCG	*man*
pET_Xho_man_apr_r	GCGCTCGAGTCAATCGAATTTCACTTTCAGCGTAAC	*man*
pET_Nco_man_apr_f	GCGCCATGGAGGAGAGGGATGTAATATACCTCG	*man*

Gene expression was evaluated by SDS-PAGE with 10% (w/v) polyacrylamide after protein purification using a GSTprep FF16/10 column (Promega, Madison, WI) for the proteins produced in pGEX-4T-2, or His-Trap Prep column (Pharmacia, Uppsala, Sweden) for the proteins produced in pET15b. In the case of pKK233-3, no purification step was performed.

RESULTS

Enzyme activities involved in the synthesis of mannosylglycerate

The enzyme activities implicated in the two known pathways for the synthesis of mannosylglycerate were sought in dialysed extracts of *A. profundus* and *A. fulgidus* 7324. In both organisms, mannosylglycerate was only produced when 3-phosphoglycerate and GDP-mannose were provided to a cell extract (Fig. IV.1). No mannosylglycerate synthesis was detected when glycerate and GDP-mannose were supplied as potential substrates. These results definitively showed that the synthesis of mannosylglycerate proceeds via mannosyl-3-phosphoglycerate synthase (the two-step pathway).

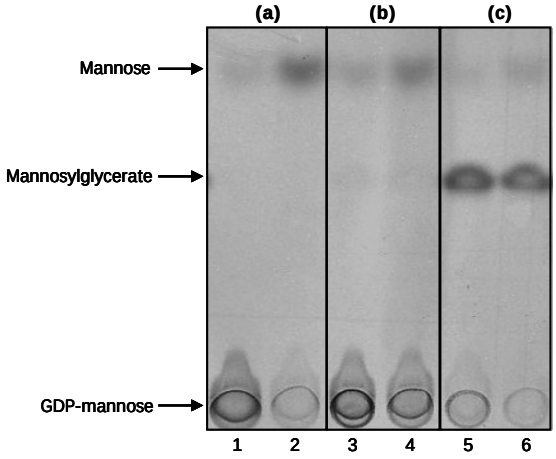

Figure IV.1 Identification of enzymatic activities in cell extracts of *A. profundus* by TLC analysis of reaction products using radioactive labelled GDP-mannose. (a) Cell extract incubated with GDP-[U-^{14}C]-mannose before (lane 1) and after (lane 2) treatment with alkaline phosphatase; (b) cell extract incubated with GDP-[U-^{14}C]-mannose and glycerate before (lane 3) and after (lane 4) alkaline phosphatase treatment; (c) cell extract incubated with GDP-[U-^{14}C]-mannose and 3-phosphoglycerate before (lane 5) and after (lane 6) treatment with alkaline phosphatase.

Mannosyl-3-phosphoglycerate was expected as final product of the reaction catalysed by MPGS, but it was not observed in the TLC of the reaction mixtures; no differences were observed in the level of mannosylglycerate produced in the reaction mixtures before and after treatment with alkaline phosphatase (Fig. IV.2). This result indicates that the second activity involved in the two-step pathway, mannosyl-3-phosphoglycerate phosphatase, is very high. A weak spot of mannose was always detected in the TLC of the reaction mixtures, and it is more evident when the reaction mixtures were treated with alkaline phosphatase. This could be explained by a pyrophosphatase activity as a contaminant of the commercial alkaline phosphatase preparation, which could hydrolyse GDP-mannose into mannose-1-phosphate.

Identification of *mpgS* and *mpgP* genes

A 690-bp PCR fragment of the *mpgS* gene from *A. profundus* was amplified using degenerate primers based on known MPGS sequences. Subsequently, a 4-kb fragment of *A. profundus* genome carrying the entire *mpgS* gene (encoding MPGS) was obtained using inverse PCR. Immediately downstream of the *mpgS* gene, an ORF encoding a protein with 249 amino acids with high identity with known MPGPs was found. Downstream of the *mpgP* gene, a

third ORF was found encoding a 903 amino acid protein with 55% identity to a putative mannosidase from an uncultured archaeon GZfos3D4 (accession number AAU84238), and around 25% identity to other mannosidases from different sources (*Clostridium perfringes*, *Clostridium difficile*, *Halothermothrix orenii*, *Rubrobacter xylanophilus*, *Roseiflexus* sp. and *Listeria monocytogenes*). The deduced amino acid sequence of the MPGS, MPGP, and the putative mannosidase are shown in Figure IV.2. A possible ribosome binding site was identified 8-bp upstream of the start codon of *mpgS* gene, and a putative promoter region was predicted upstream of the *mpgS* gene using a prokaryotic promoter database (www.fruitfly.org/seq_tools/promoter.html).

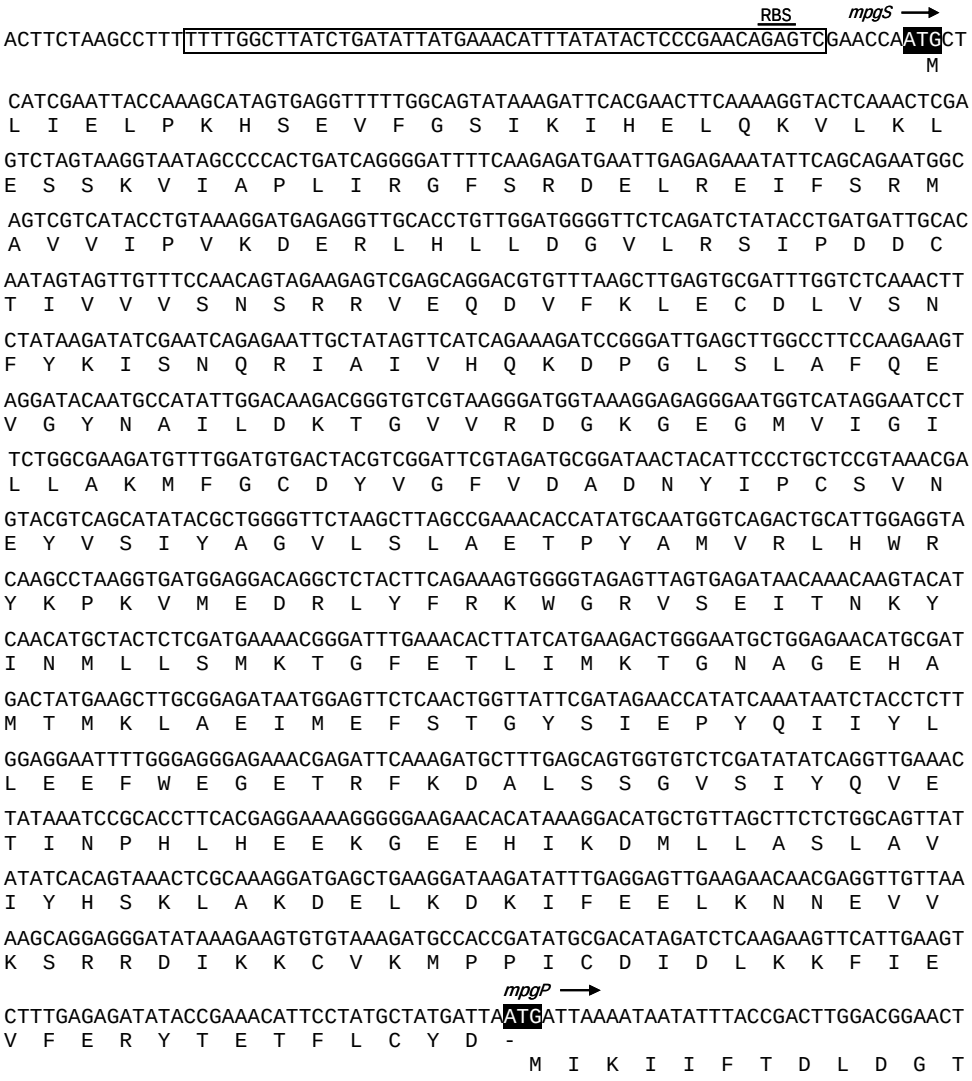

```
TTGCTAGACAAAAATTACAGATGTGACAAAGCCTTGGAGCTGATTAAAAAGCTGGAAGTTCCTATCGTGTTCGTA
  S  A  K  T  I  F  E  Q  E  V  F  R  K  M  L  G  I  S  D  P  F  V  V  E  D

TCTGCGAAGACGATATTTGAACAGGAGGTCTTTAGAAAGATGCTTGGAATAAGCGATCCGTTCGTGGTTGAGGAC
  L  L  D  K  N  Y  R  C  D  K  A  L  E  L  I  K  K  L  E  V  P  I  V  F  V

GGTTCCGCGATATACGCACCTCTGAACTACTTCGGAAGGCGCATAGGGTATAGGAGGCACGGATACGATGCCTTA
  I  L  G  V  E  R  E  V  I  L  Q  H  I  K  S  L  N  V  K  S  Y  A  N  M  S

ATATTGGGTGTTGAAAGGGAAGTGATACTTCAACATATCAAATCCCTGAACGTTAAGAGCTACGCTAATATGAGT
  G  S  A  I  Y  A  P  L  N  Y  F  G  R  R  I  G  Y  R  R  H  G  Y  D  A  L

GTTGAGGAGATTTCTAAATTAACGGGATTGAGCTTGGAAATGTCTGAACTTGCCAAGAGAAGGGAATTCAGCGAA
  V  E  E  I  S  K  L  T  G  L  S  L  E  M  S  E  L  A  K  R  R  E  F  S  E

GTAATAGTTGAAGCAGATGAAAAGGCTTTAAAATACCTCAAAAAGTTCTTCAACGTTCAAATCGGTGGGAGGTTC
  V  I  V  E  A  D  E  K  A  L  K  Y  L  K  K  F  F  N  V  Q  I  G  G  R  F

ATTCACGTATACGGGAAAGGTGCAGATAAGGGTAAAGCTGTAAGAATACTTACGGAACTTTACGAAGATTTGTAC
  I  H  V  Y  G  K  G  A  D  K  G  K  A  V  R  I  L  T  E  L  Y  E  D  L  Y

GGAGAGGTAGTGACGATAGGTATAGGCAACTCCTATACGGACATACCCATGTTAAGGGAGGTGGACATTCCTGCC
  G  E  V  V  T  I  G  I  G  N  S  Y  T  D  I  P  M  L  R  E  V  D  I  P  A

CTTGTTAGGAACGAGGATGGTTGGATCGAGGTAGATTTTGAGGTTTATAGGGCTAATGGGGTTGCAACTGAGGGT
  L  V  R  N  E  D  G  W  I  E  V  D  F  E  V  Y  R  A  N  G  V  A  T  E  G

                                RBS          man ──►
TGGGTTGAAGTTGTTAAGAAGTTTGTTGGAGGTGATTGAATGATGGAGGAGAGGGATGTAATATACCTCGTTCCG
  W  V  E  V  V  K  K  F  V  G  G  D  -  M  M  E  E  R  D  V  I  Y  L  V  P

CACTCACATTACGATGCGATGTGGATTTTCACAAAAGAGGATTATTTCTATATTAACATTGATATAATTTTGAAG
  H  S  H  Y  D  A  M  W  I  F  T  K  E  D  Y  F  Y  I  N  I  D  I  I  L  K

AAAGTAATTGAGATAATGGAGGAATCTAAGGATTACAAATTCCTGATAGAGCAGACACATCTCCTCGAAGAAGTC
  K  V  I  E  I  M  E  E  S  K  D  Y  K  F  L  I  E  Q  T  H  L  L  E  E  V

GAGAGGAGGTATCCTGACCTCTTTAAGAAAATTGGAGAGTACATCAGAGAAGGCAGGATAGAGATAGCTGACGGA
  E  R  R  Y  P  D  L  F  K  K  I  G  E  Y  I  R  E  G  R  I  E  I  A  D  G

GAATACGTGATGGCTGATACAATGCTCCCTCAGGAGGAGACATTGATTAGAGAGATACTCTTTGGAAAGAGGTAT
  E  Y  V  M  A  D  T  M  L  P  Q  E  E  T  L  I  R  E  I  L  F  G  K  R  Y

GTTAGGGAGAAGTTTGGTGCCGATGTCGTTGTGATGTGGGTTGCCGACAGCTTCGGCCTAAACGCTCAACTTCCA
  V  R  E  K  F  G  A  D  V  V  V  M  W  V  A  D  S  F  G  L  N  A  Q  L  P

CAAATTTACAGAAAGTGCGGTTACAAGTACGTTGCCTTCAGGAGAGGCTGTCCCGAAATAAAACCTTCCGAATTC
  Q  I  Y  R  K  C  G  Y  K  Y  V  A  F  R  R  G  C  P  E  I  K  P  S  E  F

CTCTGGGAAGGGCTTGATGGAACTAGGATAATTGCCCACTTCTTCCCCTTGGGTTACAGAGCCGGTCTGTATCTG
  L  W  E  G  L  D  G  T  R  I  I  A  H  F  F  P  L  G  Y  R  A  G  L  Y  L

GACAGGCTTGAGGAAGCTTATGCGAAGCTTAAGAGGGTCGCTTTTTCGAATCATATCCTAATGCCATCTGGAAGT
  D  R  L  E  E  A  Y  A  K  L  K  R  V  A  F  S  N  H  I  L  M  P  S  G  S

GGCTCTATTCCACCGCAGGAAGAGACTCCGAAAGTTGTGGAGGAGTGGAACAAAAAGCACAGGGCATTGATGAAA
  G  S  I  P  P  Q  E  E  T  P  K  V  V  E  E  W  N  K  K  H  R  A  L  M  K

ATTGCAACTCCCTCGGAGTTTTTCAAGGCTATTGAGAAGTTTAAGGATAAGTTACCTGTGAGAAAGGGTGAGATG
  I  A  T  P  S  E  F  F  K  A  I  E  K  F  K  D  K  L  P  V  R  K  G  E  M

TACTCTGGAAAATATTCTCAGGTGTTTCCGGATACTGCTTCAAGCAGAATATGGGTTAAGAAGAATTTGAGAAAG
  Y  S  G  K  Y  S  Q  V  F  P  D  T  A  S  S  R  I  W  V  K  K  N  L  R  K

TTCGAAAACTGGATACTCTTCTTCGAATGCTTCTCGACCATAAACTACCTTTTAGGAGGAGAGTACAGGGTTGAA
  F  E  N  W  I  L  F  F  E  C  F  S  T  I  N  Y  L  L  G  G  E  Y  R  V  E

GAGTTGAAGAACTGCTGGAAGAAGGTTCTCTTTATGGCTTTCCACGATGTTGTTCCGGGGACGAGCATGGACACG
  E  L  K  N  C  W  K  K  V  L  F  M  A  F  H  D  V  V  P  G  T  S  M  D  T

GGTTATCAGGACATAAGGCATGACATCGATTTCCTGAAAACAAAGCTGAGTTACCTTACCCCGAGGGTTTTGAAA
```

```
  G  Y  Q  D  I  R  H  D  I  D  F  L  K  T  K  L  S  Y  L  T  P  R  V  L  K
GAGATAATTGAGAGGGACAGCGATGGAGAGGACTTCGGTGACGTTATAGTCTTCAACCCTCTTAGCTGGGATGTT
  E  I  I  E  R  D  S  D  G  E  D  F  G  D  V  I  V  F  N  P  L  S  W  D  V
ACGAACTGGGTTGAGGTGGATTTGAACTTCGATGAGGGGCAGGTTTACAGGATAGAGGGTTTGAAGTGTGGAGAT
  T  N  W  V  E  V  D  L  N  F  D  E  G  Q  V  Y  R  I  E  G  L  K  C  G  D
GAGGACAGCGATGGAGAGGACTTCGGTGACGTTATAGTCTTCAACCCTCTTAGCTGGGATGTTACGAACTGGGTT
  E  D  S  D  G  E  D  F  G  D  V  I  V  F  N  P  L  S  W  D  V  T  N  W  V
GAGGTGGATTTGAACTTCGATGAGGGGCAGGTTTACAGGATAGAGGGTTTGAAGTGTGGAGATGAGGAGATAGAC
  E  V  D  L  N  F  D  E  G  Q  V  Y  R  I  E  G  L  K  C  G  D  E  E  I  D
GTTGAAGTTATAAGGTTCAGAAGATACGATGATGAATCTCTCAGCTACGCAAGGATAGGATTTGTAGCAAGTGTT
  V  E  V  I  R  F  R  R  Y  D  D  E  S  L  S  Y  A  R  I  G  F  V  A  S  V
CCAGCCTTGGGGTATAAGGTTTACAAGATCGTTGAGGAGAGAAAAAGGAAGAGGAGAGAGAAAAACTTCATAAGG
  P  A  L  G  Y  K  V  Y  K  I  V  E  E  R  K  R  K  R  R  E  K  N  F  I  R
ATCGTTGGAAACACCATAGAGACCAAACACTTCAACGTAACATTTTCGCCAGAGGACGGGCTGATTACGGTAACG
  I  V  G  N  T  I  E  T  K  H  F  N  V  T  F  S  P  E  D  G  L  I  T  V  T
AAGAACGGGAATACCATCTTTAGAGACGGAAACGAGCTTGTGATTGAAAGTGAGATAGGAGACCTCTACTACCAC
  K  N  G  N  T  I  F  R  D  G  N  E  L  V  I  E  S  E  I  G  D  L  Y  Y  H
AGAGAGGACATAGACATTCCCATAAGAACTGAAGGAGGAGAGGGTTTACAGTTCGGCTCTTTCAGAGTCAAGAAC
  R  E  D  I  D  I  P  I  R  T  E  G  G  E  G  L  Q  F  G  S  F  R  V  K  N
TTCTGGATCGAGAAATCACCGCTGAGGAGGGTAATTAACGTTCATACGGACTACTATTCCGTTAGATGGCCCTAC
  F  W  I  E  K  S  P  L  R  R  V  I  N  V  H  T  D  Y  Y  S  V  R  W  P  Y
AGATACATAGAAAGATTTAAACCGCTGATGTGGAGACATAGATTCATCTCTTTCAGGAAGAAAATCATCGTTTAC
  R  Y  I  E  R  F  K  P  L  M  W  R  H  R  F  I  S  F  R  K  K  I  I  V  Y
AGGGATATACCGCGAATAGACTTCGTAACGTATGTGGACAACAAGCATCCGAGAGTAAGGCTGAGAGTTAGATTC
  R  D  I  P  R  I  D  F  V  T  Y  V  D  N  K  H  P  R  V  R  L  R  V  R  F
AAAACTGACATGAACCTTCCAGAATACACGTGCGAGTGCCAGTTTGGTGCTGTGAACAGGAAAACGAACACTTAC
  K  T  D  M  N  L  P  E  Y  T  C  E  C  Q  F  G  A  V  N  R  K  T  N  T  Y
TACTTCAAACCCAAGGATTGGAAGGAAAAACCATCGGGCGTTTATCCCTCTCTGCGATGGATAGATTACAGCGAT
  Y  F  K  P  K  D  W  K  E  K  P  S  G  V  Y  P  S  L  R  W  I  D  Y  S  D
GGAGAAAAGGGTTTAGCCATTTTAAACAGGGGTAATCCAGAGAACGAAGTTAGGGATGGAAACGTTTACATAACA
  G  E  K  G  L  A  I  L  N  R  G  N  P  E  N  E  V  R  D  G  N  V  Y  I  T
CTGCTAAGGTCCGTCGGAATACTTTCAAACGGCTCAGCTGGTCCTGTTATCCCAGTTCCAGATGCGAGGGAGCTT
  L  L  R  S  V  G  I  L  S  N  G  S  A  G  P  V  I  P  V  P  D  A  R  E  L
AAGAGGTATTCGTTTAAATATGCAGTCTATCCACATGAAGGAGACTGGAAGCAAGCTAAAGTTTACAAGATGGGT
  K  R  Y  S  F  K  Y  A  V  Y  P  H  E  G  D  W  K  Q  A  K  V  Y  K  M  G
TACGAGTTCAACTACAATTTGGTGGCTTTACAGGTTCCGAGAAATAGAAGGTATAGACTCAAGAGGAGCTTTTTA
  Y  E  F  N  Y  N  L  V  A  L  Q  V  P  R  N  R  R  Y  R  L  K  R  S  F  L
AGAATAGATCCAGATAACGTAATTCTAACTGCTTTCAAACTGGCTGAAGATGGAGACGGAATAATAGTCAGGTTT
  R  I  D  P  D  N  V  I  L  T  A  F  K  L  A  E  D  G  D  G  I  I  V  R  F
TACGAGGCTGAAGGTAGTGAAGTTAAAGCCAAACTCACGTTCTTCAAGGAGATTAAGGAGGCTAAGGTCGTGAAC
  Y  E  A  E  G  S  E  V  K  A  K  L  T  F  F  K  E  I  K  E  A  K  V  V  N
ATGCTTGAAGAGACAGACGAAGAGTTTGAGAGGGAATTTGGCAAAGATGTTAAGGTCGATGGAAATGTTGTAGAG
  M  L  E  E  T  D  E  E  F  E  R  E  F  G  K  D  V  K  V  D  G  N  V  V  E
GTAGAGATGAAACCTTTCGAAGTTGTTACGCTGAAAGTGAAATTCGATTGA
  V  E  M  K  P  F  E  V  V  T  L  K  V  K  F  D  -
```

Figure IV.2. Nucleotide sequence of the mpgS/mpgP/mannosidase region in *A. profundus* chromosome. The deduced amino acid sequence is shown in one-letter code. The predicted start codons of *mpgS, mpgP*

and *mannosidase* genes are indicated in a black background. Putative promoter regions are inserted in a box, and putative ribosome biding sites are labelled with "RBS".

BLAST searches of the protein data banks with the *A. profundus* and *A. veneficus* MPGS and MPGP amino acid sequences revealed high homologies with several proteins (Table IV.3). The amino acid sequences of MPGS from *A. profundus* and *A. veneficus* showed a 55% identity. The MPGPs from these two species of *Archaeoglobus* have a 57% amino acid identity, and this value decreased significantly when comparing to other organisms, excepting with the uncultured archaeon GZfos3D4, that showed an amino acid identity of 63%.

Table IV.3. Comparison of the *A. profundus* MPGS and MPGP amino acid sequence with their homologous proteins.

Organism	MPGS			MPGP		
	N° a.a.	% identity	% similarity	n° a.a.	% identity	% similarity
A. profundus	389	100	100	249	100	100
A. veneficus	387	55	78	266	57	72
P. horikoshii	394	55	75	243	41	58
P. abyssii	394	54	75	243	41	57
P. furiosus	394	53	76	242	38	50
T. litoralis	394	54	74	243	42	59
P. ferrophilus	393	50	72	243	39	55
GZfos3D4	391	56	75	265	63	76
R. marinus	427	44	67	277	39	55
T. thermophilus	391	43	65	259	35	52

The identity and similarity of the sequences were determined using the BLASTP algorithm (http://www.ncbi.nlm.nih.gov/blast/Blast.cgi). GZfos3D4, uncultured archaeon GZfos3D4.

Mannosidase activity in *A. profundus*

An open reading frame encoding a putative mannosidase was found in the region immediately flanking *mpgS*/*mpgP* in the genome of *A. profundus*, which leads to the hypothesis that this protein could be involved in the degradation of mannosylglycerate. Therefore, this activity was sought in cell extracts of *A. profundus*. In contrast to our expectations, no degradation of mannosylglycerate could be detected when [U-^{14}C]-mannosylglycerate was incubated with a cell extract of *A. profundus*, neither at pH 7.6 nor at 5.8 (Fig. IV.3).

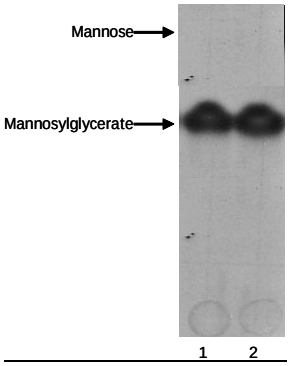

Figure IV.3. Thin layer chromatography of an extract of *A. profundus* after incubation with [U-^{14}C]-mannosylglycerate for 1 hour at 75°C and pH 7.6 (lane 1) or pH 5.8 (lane 2). No reaction product was detected.

These results were also confirmed by ^{1}H-NMR assays: no changes were observed in the resonances of mannosylglycerate after 24 hours incubation at 75°C, both at pH 7.6 and 5.8 (data not shown). Therefore, the presence of a mannosidase activity in *A. profundus* could not be confirmed.

Cloning and expression of the *mpgS*, *mpgP* and *mannosidase* genes

Genes coding for MPGS, MPGP and the putative mannosidase from *A. profundus* were cloned and expressed in *E. coli* with the objective of validating the predicted functions. The genes were cloned separately in different plasmids, namely pGEX-4T-2, pET15b, and pKK233-3. *E. coli* BL-21DE and Rosetta strains were used to express the genes. Cell extracts and pellets of the different *E. coli*, harbouring the different constructions, were analysed by SDS-PAGE. No expression was observed for the constructs in pKK233-3 regardless of the host used. In all the remaining cases, produced proteins were always found in inclusion bodies. MPGS, MPGP, and mannosidase activities were also assayed in cell extracts, but no evidence for these activities was found.

Discussion

Mannosylglycerate is one of the most common compatible solutes of (hyper)thermophilic organisms (Santos et al. 2007). It has been found in the three species of the genus *Archaeoglobus* (*A. profundus*, *A. veneficus* and *A. fulgidus* 7324), but oddly it was not detected in the type strain *A. fulgidus* VC-16 and its variant, VC-16S, (chapter III). Two

distinct pathways leading to the formation of mannosylglycerate have been identified (Martins et al. 1999). While the single-step pathway was only found in the thermophilic bacterium *Rhodothermus marinus* and in the mesophilic red algae *Calogossa leprieurii*, the two-step pathway was encountered in all the (hyper)thermophiles accumulating mannosylglycerate studied thus far (Martins et al. 1999; Empadinhas et al. 2001; Empadinhas et al. 2003; Borges et al. 2004; Empadinhas et al. 2004; Neves et al. 2005).

In the present work, the pathway for the synthesis of mannosylglycerate in the three species of the genus *Archaeoglobus* (*A. profundus, A. veneficus*, and *A. fulgidus* strain 7324) was identified through the detection of the relevant enzymatic activities in cell extracts. These strains used the two-step pathway for the production of mannosylglycerate. Moreover, the *mpgS* and *mpgP* genes, encoding the mannosyl-3-phosphoglycerate synthase and mannosyl-3-phosphoglycerate phosphatase, respectively, were identified in *A. profundus* and *A. veneficus*. Only part of the sequences of the two genes was identified in *A. fulgidus* 7324. Genes *mpgS* and *mpgP* are located consecutively, and organised in an operon-like structure together with another gene (Fig. IV.2). The latter gene codes for a 903 amino acid polypeptide with high sequence homology (around 55%) to a protein of an uncultured archaeon Gsz3D4 (annotated as a putative mannosidase), and low homologies (around 25%) with several known mannosidases. In addition, the product of this gene contains three conserved domains, characteristic of α-mannosidases. Therefore, this gene was putatively annotated as coding for an α-mannosidase; unfortunately our attempts to demonstrate its functionality were unsuccessful.

Archaeoglobus spp. are unique as far as containing this putative mannosidase in the mannosylglycerate gene cluster (Fig IV.4). In members of the order *Thermococcales* (*Palaeococcus ferrophilus*, *Thermococcus litoralis*, *Pyrococcus furiosus*, *Pyrococcus horikoshii* and *Pyrococcus abyssii*) the genes *mpgS* and *mpgP* are organised in an operon-like structure that includes the genes encoding the enzymes that convert fructose 6-phosphate into GDP-mannose (bifunctional phosphomannose isomerase/mannose 1-phosphate guanylyl transferase, M1P-GT/PMI, and phosphomannose mutase, PMM) (Empadinhas et al. 2001; Neves et al. 2005). In *Thermus thermophilus* and *Rhodothermus marinus*, the *mpgS* gene overlaps the *mpgP* gene, while in *Aeropyrum pernix* both genes are separated by 21 base pairs. These three organisms do not have the genes coding for M1P-GT/PMI and PMM in an adjacent location (Empadinhas et al. 2001; Empadinhas et al. 2003; Borges et al. 2004). A peculiar organisation was found in the genome of the mesophilic bacterium *Dehalococcoides ethenogenes*; in this organism the *mpgS* and *mpgP* genes are fused in a single gene (Empadinhas et al. 2004).

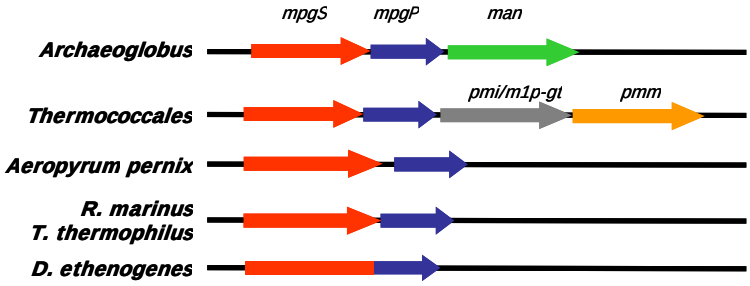

Figure IV.4. Schematic representation of the genomic organisation of the genes encoding mannosyl-3-phosphoglycerate synthase (MPGS) and mannosyl-3-phosphoglycerate phosphatase (MPGP) in the genomes of *Archaeoglobus* spp., *Pyrococcus* spp., *R. marinus*, *T. thermophilus*, *A. pernix* and *D. ethenogenes*. Genes are indicated with arrows: red arrow, mannosyl-3-phosphoglycerate synthase (*mpgS*); blue arrow, mannosyl-3-phosphoglycerate phosphatase (*mpgP*); green arrow, mannosidase (*man*); grey arrow, bifunctional phosphomannose isomerase/mannose 1-phosphate guanylyltransferase (*pmi/m1p gt*); and orange arrow, phosphomannose mutase (*pmm*).

An unrooted phylogenetic tree constructed based on the alignment of the amino acid sequences of known MPGSs is in agreement with the phylogenetic distribution of the organisms based on their 16S rRNA sequences (Fig IV.5). The MPGSs from *Thermococcales* form a tight cluster, as occurs for the bacterial MGPSs (*Thermus thermophilus* and *Rhodothermus marinus*), while MPGS of an uncultured crenarchaeote and *Aeropyrum pernix* form distinct branches from the other homologues. As expected, MPGSs from *A. profundus* and *A. veneficus* are grouped together, forming a new branch. Interestingly, the MPGS from the uncultured archaeon Gsz3D4 falls in this cluster. Gsz3D4 is an environmental genomic sample from methane-oxidizing archaeal populations found in deep-sea methane seeps and it was observed that contains genomic features of both methanogenic and sulfate-reducing *Archaea* (the genus *Archaeoglobus)* (Hallam et al. 2004).

As described above, the putative mannosidase of *A. profundus* contains all the domains associated with mannosidase activity. Moreover, the occurrence of a gene coding for a putative mannosidase in the immediate flanking region of the *mgpS/mpgP* genes in *A. profundus* and *A. veneficus*, leads to the speculation that this gene could be involved in mannosylglycerate degradation. Unfortunately, no experimental evidence for this activity was observed in extracts derived from *A. profundus* cells grown under optimal conditions. Nevertheless, it is possible that under these conditions the putative mannosidase gene was not expressed. Actually, the activity assays were performed with cells that accumulate mannosylglycerate and it is conceivable that the enzymes for the synthesis and degradation of

mannosylglycerate are not produced concomitantly. In fact, it seems more logical that the mannosidase gene would only be translated, or the protein activated, when the osmotic stress was removed in order to reduce the level of mannosylglycerate. The catabolism of mannosylglycerate has not been studied in any of the organisms that accumulate mannosylglycerate. Thus far, degradation of mannosylglycerate has only been observed in a modified strain of *E. coli* K12 (named MC4110), which does not produce mannosylglycerate (Sampaio et al. 2004). In this organism, mannosylglycerate is taken up via a phosphoenolpyruvate transport system (PTS) with concomitant phosphorylation at position 6 of the mannose moiety. Once inside the cell, this compound is hydrolysed to mannose 6-phosphate and glycerate by a mannosidase. The genes encoding the transporter and the mannosidase are found in a gene cluster together with a gene encoding a regulator, which is inducible by mannosylglycerate (Sampaio et al. 2004). No target with homology to these proteins was found in the genome of any mannosylglycerate producing organism. It is worth to note, that the mannosidase activity proposed to be involved in the hydrolysis of 6-phospho-mannosylglycerate could not be confirmed in *E. coli* extracts, despite several attempts.

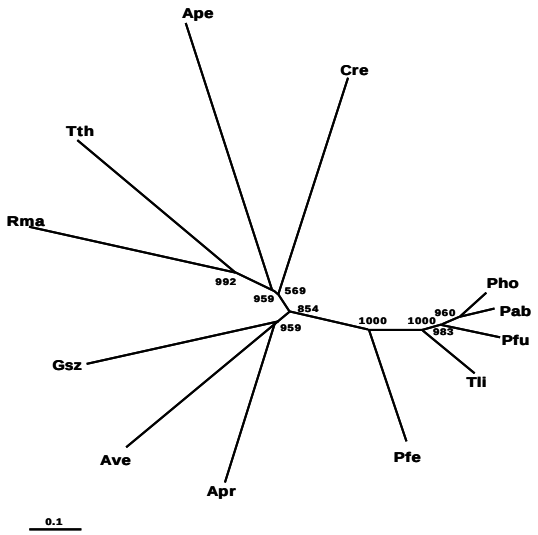

Figure IV.5. Unrooted phylogenetic tree based on mannosyl-3-phosphoglycerate synthase protein sequence. The ClustalX and TreeView programs 5,7 were used for sequence alignment and to generate the phylogenetic tree. The significance of the branching order was evaluated by bootstrap analysis of 1000 computer generated trees. Bar, 0.1 change per site. Abbreviations: Apr, *Archaeoglobus profundus*; Ave, *Archaeoglobus veneficus*, Gsz, uncultured archaeon Gsz4d3; Ape, *Aeropyrum pernix*; Pfe, *Palaeococcus*

ferrophilus; Pfu, *Pyrococcus furiosus*; Pab, *Pyrococcus abyssii*; Pho, *Pyrococcus horikoshii*; Rma, *Rhodothermus marinus*; Tth, *Thermus thermophilus*; Tli, *Thermococcus litoralis*.

In many microorganisms, the rapid efflux of compatible solutes is a common response to a hypo-osmotic shift (Blumwald et al. 1983; Schleyer et al. 1993; Ruffert et al. 1997; Sauer and Galinski 1998; Ciulla and Roberts 1999; Booth et al. 2007). In particular, among (hyper)thermophiles, release of mannosylglycerate has been observed in *Thermus thermophilus* RG-1, with nearly 90% of the mannosylglycerate cell content being excreted to the medium when the salinity was changed from 3 to 0% NaCl (Egorova et al. 2007). Although solute release is the most usual mechanism used for a rapid decrease of the solute pool, an interesting case has been described in *Rhodobacter sphaeroides* (Makihara et al. 2005). In the wild type organism, trehalose decreases sharply after a hypo-osmotic shock, while the level of this sugar remained unaltered in a mutant deficient in trehalose synthase, the activity that converts trehalose into maltose. These results show that trehalose catabolism, and not efflux, is the mechanism used to reduce the intracellular osmotic pressure in this case. The mannosidase, putatively present in *Archaeoglobus profundus*, could have a similar role in regard to adjustment of mannosylglycerate levels. On the other hand, the operon-like structure comprising the gene encoding mannosidase suggests a common regulation of mannosylglycerate biosynthesis and catabolism that seems futile. Alternatively, the putative mannosidase could be involved in the degradation of mannan, or other mannose-containing polymer. Further work needs to be done to clarify this issue.

In conclusion, this work showed that *Archaeoglobus* spp. synthesise mannosylglycerate via the two-step pathway, like all the (hyper)thermophiles known to accumulate this solute. Moreover, the genes encoding MPGS and MPGP have been identified in *A. profundus and A. veneficus* and a unique operon-like organisation, that includes a putative mannosidase gene, has been found. The identification of the mannosylglycerate biosynthetic genes in *Archaeoglobus* spp. is an important contribution to our understanding of the phylogenetic distribution of mannosylglycerate synthesis.

Acknowledgements. I thank Dr. Clélia Neves and Susana Gonçalves for the identification of the genes involved in the synthesis of mannosylglycerate. This work was supported by the BIOTECH Program, Biotechnology of Extremophiles (QLK3-CT-2000-00640) and by Fundação para a Ciência e a Tecnologia (FCT), Portugal, Programme Sapiens 99, Project POCTI 35719/BIO/2000 and FEDER.

CHAPTER 5

Diglycerol phosphate biosynthesis in *Archaeoglobus fulgidus*

Part of this chapter was published in:

Borges N., **Goncalves L.G.**, Rodrigues M.V., Siopa F., Ventura R., Maycock C., Lamosa P. and Santos H. 2006. Biosynthetic pathways of inositol and glycerol phosphodiesters used by the hyperthermophile *Archaeoglobus fulgidus* in stress adaptation. *J Bacteriol* **188:** 8128-8135.

Chapter | 5 | Contents

Abstract

Diglycerol phosphate is a negatively charged compatible solute encountered thus far only in members of the genus *Archaeoglobus*. In this work, the pathway for the biosynthesis of diglycerol phosphate was established in *Archaeoglobus fulgidus* based on the detection of the relevant enzymatic activities in cell extracts and characterisation of the intermediate metabolites by nuclear magnetic resonance (NMR). The synthesis of diglycerol phosphate proceeds from glycerol 3-phosphate via three steps: (1) glycerol 3-phosphate was activated to CDP-glycerol at the expense of CTP; (2) CDP-glycerol was condensed with glycerol-3-phosphate to yield a phosphorylated intermediate, diglycerol phosphate phosphate; (3) finally, diglycerol phosphate phosphate was dephosphorylated into diglycerol phosphate by the action of a phosphatase. The phosphorylated intermediate, diglycerol phosphate phosphate, was purified and structurally characterised by NMR.

Two different approaches were followed to identify the gene encoding the key-enzyme involved in the biosynthesis of diglycerol phosphate, diglycerol phosphate phosphate synthase (DGGPS). In the first approach, the purification of DGPPS activity from *Archaeoglobus fulgidus* biomass was attempted to obtain the N-terminal amino acid sequence of DGPPS. However, after several chromatographic steps, the DGPPS activity was lost. In parallel, the complete genome of *Archaeoglobus fulgidus* was searched for the presence of genes belonging to the family of proteins containing a domain characteristic of CDP-alcohol phosphatidyltransferases. Five genes were found, but only one of them, the open reading frame AF2299, lacked

annotation. This gene was cloned in *E. coli* as a way to validate its hypothetical biochemical function.

INTRODUCTION

Archaeoglobus fulgidus is a hyperthermophilic archaeon first isolated from marine hydrothermal vents (Achenbach-Richter *et al.*, 1987). In addition to the type strain, designated *A. fulgidus* VC-16, a few other strains belonging to the same species were isolated from hot marine sediments (strain Z) (Zellner et al., 1989) and oil field water (strain 7324) (Beeder et al., 1994). The type strain is able to grow between 60°C and 90°C, with an optimum around 83°C. Like other marine hyperthermophiles, *A. fulgidus* is slightly halophilic, displays optimal growth in medium containing 1.9% NaCl (w/v), and is unable to grow above 5.5% NaCl. Osmoregulation in this organism involves accumulation of organic solutes, some of them very unusual (Chapter III, Lamosa et al., 2006). The solute pool comprises diglycerol phosphate, di-*myo*-inositol phosphate, minor amounts of α-glutamate, and the newly discovered glycero-phospho-*myo*-inositol (chapter III, 2006, Martins et al., 1997). Di-*myo*-inositol phosphate was first discovered in members of the genus *Pyrococcus* (Scholz et al., 1992). Since then, accumulation of this phosphodiester compound has been reported in a large proportion of hyperthermophiles, whether from the domain *Archaea* or *Bacteria*, and therefore, it is presently regarded as the canonical solute of life at extremely high temperatures (Roberts, 2005, Santos et al., 2006). Diglycerol phosphate has been found only in *Archaeoglobus* species, accumulating primarily in response to supraoptimal salinity of the growth medium (Chapter III, Martins et al., 1997); glycero-phospho-*myo*-inositol, a structural chimera of di-*myo*-inositol phosphate and diglycerol phosphate, was recently identified in bacteria of the genus *Aquifex* and in the archaeon *A. fulgidus*, strains VC-16 and 7324 (Lamosa et al., 2006).

The most salient feature of the solute pool of *A. fulgidus* is the preponderance of polyol-phosphodiesters, a class of compatible solutes encountered in organisms thriving in hot environments, but totally absent in mesophiles (Santos & da Costa, 2001, Santos et al., 2006). Accordingly, a putative thermo protective function of cell components *in vivo* was ascribed to them; indeed, their action as protein stabilisers *in vitro* has been confirmed at least for di-*myo*-inositol phosphate and diglycerol phosphate (Lamosa et al., 2000, Ramakrishnan et al., 1997, Scholz et al., 1992).

To our knowledge, the biosynthetic pathway of diglycerol phosphate has not yet been investigated, but the synthesis of di-*myo*-inositol phosphate has been studied in *Methanococcus*

igneus and *Pyrococcus woesei* (Chen et al. 1998; Scholz et al. 1998), and two distinct synthetic routes were proposed. In *M. igneus*, Chen and co-workers (Chen et al. 1998) proposed that *myo*-inositol 1-phosphate is synthesised from glucose 6-phosphate by *myo*-inositol 1-phosphate synthase. Part of the *myo*-inositol 1-phosphate is dephosphorylated into *myo*-inositol while another part is presumably activated to CDP-inositol, both molecules then being condensed to yield di-*myo*-inositol phosphate; biosynthesis of CDP-inositol was not observed. In *P. woesei*, it was proposed that two molecules of *myo*-inositol 1-phosphate are condensed to yield di-*myo*-inositol phosphate with consumption of NTP (Scholz et al. 1998).

The curious structural relationships between the three polyol-phosphodiesters accumulating in *A. fulgidus* are also reflected in their pattern of accumulation. While di-*myo*-inositol phosphate and diglycerol phosphate increase consistently in response to elevated temperature and osmotic stress, respectively, the level of glycero-phospho-*myo*-inositol seems to respond to a combination of both stresses (Chapter III, Lamosa et al. 2006). Thus, the synthesis and accumulation of these three solutes seems intertwined by a regulatory mechanism linked to osmotic pressure and heat, which can only be unravelled once the biosynthetic routes of these solutes are clarified. With this goal in mind, the biosynthetic pathway of diglycerol phosphate was established in the present work based on the activities of relevant enzymes detected in cell extracts of *A. fulgidus* and the NMR structural characterisation of intermediate metabolites.

MATERIAL AND METHODS

Materials

L-glycerol 3-phosphate, DL-glycerol 3-phosphate, CTP, ATP, UTP, GTP, and CDP-glycerol were purchased from Sigma-Aldrich (St. Louis, USA). NaF was obtained from Pfizer (New York, USA). Diglycerol phosphate was obtained by chemical synthesis and provided by bitop AG (Witten, Germany).

Strains and culture conditions

Archaeoglobus fulgidus strain VC-16 (DSM 4304^T) was routinely maintained on medium described in chapter III. *Archaeoglobus fulgidus* strain 7324 (DSM 8774) was grown using the medium described by Labes & Schönheit (Labes and Schönheit 2001) with modifications. The basal medium contained (per litre) 0.5 g yeast extract, 10 mmol of L-lactate, 3 g PIPES, 30 g NaCl, 2 mg $(NH_4)_2Fe(SO_4)_2 \cdot 7H_2O$, 100 ml of salt solution (without NaCl) and 10

ml of a modified trace element solution. The salt solution contained (per litre) 74 g $MgSO_4 \cdot 7H_2O$, 3.4 g KCl, 27.5 g $MgCl_2 \cdot 6H_2O$, 2.5 g NH_4Cl, 1.4 g $CaCl_2 \cdot 2H_2O$, and 1.4 g K_2HPO_4. The modified trace element solution contained (per litre) 1.5 g nitriloacetic acid, 0.05 g $CoSO_4 \cdot 6H_2O$, 0.1 g $CaCl_2 \cdot 2H_2O$, 0.1 g $ZnSO_4 \cdot 7H_2O$, 0.01 g $KAl(SO_4)_2 \cdot 12H_2O$, 0.1 g H_3BO_3, 0.01 g $Na_2WO_4 \cdot 2H_2O$, 0.01 g $Na_2MoO_4 \cdot 2H_2O$, 0.3 g Na_2SeO_3, and 0.1 g $NiCl_2 \cdot 6H_2O$. The paramagnetic ions were removed from the trace element solution to improve the quality of NMR spectra. The organisms were grown anaerobically in 2-litre static vessels at 83°C with a gas phase composed of N_2 and CO_2 (80:20, v/v). Cell growth was monitored by optical density (OD) at 600 nm. Biomass for enzyme purification was obtained from large-scale fermentation (300 litres) using the culture medium described above. The identification of the phosphorylated intermediate was done in *A. fulgidus* 7324, instead of *A. fulgidus* VC-16, since that strain displayed greater biomass yield and different growths produced very reproducible results insofar as enzymatic activities were concerned.

Preparation of *A. fulgidus* cell extracts

Cells were harvested by centrifugation (1,000 × g, 10 min) during late exponential growth phase (OD=0.35), and washed twice with MOPS buffer (50 mM, pH 7.6) containing 3% NaCl in anaerobic conditions. The cell pellet was suspended in MOPS (50 mM, pH 7.6) containing 5 mM $MgCl_2$. Cells were disrupted in a French press, and the cell debris was removed by centrifugation (30,000 × g, 4 °C, 30 min). Low molecular mass compounds were removed in a PD-10 column (Amersham Biosciences) equilibrated with MOPS (50 mM, pH 8.1) containing 5 mM $MgCl_2$. Protein content was estimated by the BCA Protein Assay Kit (Pierce).

Purification of diglycerol phosphate phosphate.

Diglycerol phosphate phosphate was partially purified from a reaction mixture of 1 ml, containing 5 mM glycerol-3-phosphate, 5 mM CDP-glycerol, 7.5 mM NaF and 200 mg (total protein) of *A. fulgidus* cell extract. After one hour incubation at 80°C, the reaction mixture was centrifuged, and the presence of diglycerol phosphate phosphate was confirmed by ^{31}P-NMR. The supernatant was applied onto a QAE-Sephadex A-25 column previously equilibrated with 5.0 mM sodium bicarbonate (pH 9.8) and eluted with one bed volume of the same buffer, followed by a linear gradient of 5.0 mM to 1 M $NaHCO_3$. The eluted fractions were analysed by ^{31}P-NMR, and subsequently desalted using an activated Dowex 50W-X8 resin and distilled water for elution. The active fractions were pooled, and the pH adjusted to 6 with KOH. The samples were lyophilised and dissolved in D_2O prior to NMR analysis.

NMR spectroscopy

The identification and characterisation of the phosphorylated intermediate in the synthesis of diglycerol phosphate was accomplished using ^{1}H, ^{13}C and ^{31}P-NMR. One-dimensional and two-dimensional spectra were recorded on a Bruker DRX500 spectrometer using standard Bruker pulse programs (Bruker, Rheinstetten, Germany) following a strategy previously described (chapter II and III). ^{13}C-^{1}H correlation spectra were recorded using a delay of 3.44 ms for the evolution of the scalar couplings, while a delay of 62.5 ms was used for ^{31}P-^{1}H correlation spectra. ^{1}H and ^{13}C-NMR spectra were referenced to 3 (trimethylsilyl)propanesulfonic acid (sodium salt), and ^{31}P NMR spectra were referenced to external 85% H_3PO_4, both designated at 0 ppm. Assignment of resonances to diglycerol phosphate, and CDP-glycerol were confirmed by addition of small amounts of the authentic compounds.

Cloning and expression of putative *dgpps* genes

Five genes (AF0263, AF1143, AF1744, AF2044, and AF2299) whose predicted products belong to the family of proteins containing a domain characteristic of CDP-alcohol phosphatidyltransferases (www.sanger.ac.uk//cgi-bin/Pfam) were found in the *A. fulgidus* genome (www.tigr.org). Three of them (AF1143, AF1744, and AF2044) are annotated as coding for enzymes implicated in the synthesis of phospholipids; members of our team have demonstrated that the gene AF2299 encodes the synthase involved in the synthesis of di-*myo*-inositol phosphate (Borges et al. 2006). Therefore, the gene AF0263 is the only candidate to encode diglycerol phosphate phosphate synthase. This gene was expressed in *E. coli* with the objective of validating the predicted function. Chromosomal DNA of *A. fulgidus* was isolated according to Ramakrishnan and Adams (Ramakrishnan and Adams 1995). Two sets of primers based on the DNA sequence of gene AF0263 were designed to add suitable restriction sites (Table V.1).

Table V.I. Primers used in this study.

Name	Nucleotide sequence (5' to 3')[1]	Restriction enzyme	gene
NdedipF	GCG**CATATG**GTGATTCTGCCCTGTGAGTC	*Nde*I	AF0263
BamHdipR	CGC**GGATCC**TTATTTAGAAACCAAAACAGCA	*Bam*HI	AF0263
BsaDip	GATC**GGTCTC**ACATGATTCTGCCCTGTGAGTCCTTAACGGCG	*Bsa*I	AF0263
xbadip	GC**TCTAGA**TTATTTAGAAACCAAAACAGCAAG	*Xba*I	AF0263

[1] The restriction sites are highlighted.

The AF0263 gene was amplified by using Pfu DNA polymerase (Fermentas) and cloned separately in pTRC99c plasmid between BsaI and XbaI sites, and in pET15b plasmid between NdeI and BamHI sites. Cloning methodology followed standard protocols (Sambrook et al., 1989). The correct nucleotide sequences of the inserts were confirmed by sequencing (Agowa, Berlin, Germany). The plasmids were designated as pET15b_AF0263, and pTRC_AF0263.

Different *E. coli* strains were tested as hosts for these plasmids, namely BL-21(DE3), CD43 (with the plasmid pSJS1240) and Rosetta. *E. coli* BL-21(DE3) cells, harbouring the constructs, were grown at 37°C in LB medium with ampicillin (100 μg/ml) to an OD_{600} of 0.5, and induced with 1 mM IPTG for 4 hours. *E. coli* CD43 cells, carrying the construct, were grown at 37°C in LB medium with ampicillin (100 μg/ml) and spectinomycin (50 μg/ml) to an OD_{600} of 0.8, and induced with 0.5 mM IPTG for 4 hours. *E. coli* Rosetta cells, containing the constructs, were grown at 37°C in LB medium with ampicillin (100 μg/ml) and chloramphenicol (34 μg/ml) to an OD_{600} of 0.6, and induced with 0.5 mM IPTG. Two different procedures were followed: (i) the cells were grown for further 4 hours at 37°C or (ii) the cells were grown for 12 hours at 30°C.

In all the cases, the cells were harvested, suspended in Tris-HCl (20 mM, pH 7.6) containing 10 mM $MgCl_2$ and disrupted in a French press; cell debris was removed by centrifugation (30,000 × g, 4ºC, 1 h). The presence of diglycerol phosphate phosphate synthase activity was tested using the ^{31}P-NMR discontinuous assay described above. Expression of the genes was monitored by SDS-PAGE analysis.

Partial purification of diglycerol phosphate synthase activity

Cells of *A. fulgidus* (approximately 150 grams, wet mass) were harvested during late exponential phase of growth (OD_{600nm} = 0.35), and suspended in Tris-HCl (20 mM, pH 7.6), containing 5 mM $MgCl_2$ and DNase I (10 μg/ml). After cell disruption in a French press and removal of cell debris by centrifugation, the supernatant was ultra-centrifuged at 40,000 × g for 90 min. The supernatant was dialysed against Tris-HCl (50 mM, pH 7.0), containing a cocktail of protease inhibitors (200 μM PMSF, 5 μM leupeptin, 5 μM antipain and 1 mM EDTA) and 1mM $MgCl_2$. The native DGPPS was partially purified by liquid chromatography (Amersham Biosciences) at room temperature.

(i) Ionic-exchange chromatography

The cell extract was applied to a DEAE-Sepharose fast flow column equilibrated with Tris-HCl (10 mM, pH 7.6) and eluted with a linear gradient of NaCl (0.0-1.0 mM) in the same

buffer. DGPPS activity was detected at 0.8 M NaCl. Active samples were combined, dialysed, and loaded to a Q-Sepharose fast flow column equilibrated with Tris-HCl (10 mM, pH 7.6) and eluted with a linear NaCl gradient (0.0-1.0 M) in the same buffer. The DGPP activity was detected at 500 mM of NaCl. After desalting, the sample was applied again on a Q-Sepharose fast flow column equilibrated with Tris-HCl (10 mM, pH 7.6) and eluted with a linear NaCl gradient (0.0-1.0 M) in the same buffer. The activity was eluted with 1 M of NaCl.

(ii) Hydrophobic chromatography

Fractions containing DGPPS activity were pooled and dialysed against Tris-HCl (10 mM, pH 7.6) containing 1.5 M $(NH_4)_2SO_4$. The sample was applied to a phenyl-sepharose HP column equilibrated with the same buffer and elution was carried out using a linear gradient of $(NH_4)_2SO_4$ (1.5-0.0 M) in Tris-HCl (10 mM, pH 7.6). The activity was eluted at 0.0 M of $(NH_4)_2SO_4$.

(iii) Hydroxyapatite chromatography

The active fractions were dialysed against phosphate buffer (10 mM, pH 7.0), and loaded onto a hydroxyapatite column equilibrated with phosphate buffer (10 mM, pH 7.6). Elution was carried out with a linear gradient of phosphate buffer (0.0-1.0 M). The active fractions were eluted at 0.6 M of phosphate buffer.

(iv) Molecular mass exclusion chromatography

The active fractions were pooled, concentrated and dialysed against Tris-HCl (10 mM, pH 7.6), and applied on a Superose G200 column. The elution was carried out with Tris-HCl (10 mM, pH 7.6).

Enzyme assays

Both continuous and discontinuous methods were used to measure the activities of the enzymes involved in the synthesis of diglycerol phosphate in *A. fulgidus*. In the continuous method, a reaction mixture containing 50 mM MOPS (potassium salt) pH 8.1, 5 mM $MgCl_2$, 250 µl of D_2O, and 5 mM of putative substrates were added to a 10-mm NMR tube and the reactions were started by addition of 200 mg (total protein) of *A. fulgidus* cell extract. The time-course of product formation was followed by sequential acquisition of ^{31}P-NMR spectra. The enzymatic assays were performed at 80ºC, in a total volume of 2.5 ml, under anoxic conditions. The substrates tested were CTP, CDP-glycerol, DL-glycerol 3-phopsphate, and glycerol. Control assays lacking the cell extracts or the substrates were also carried out. The reaction was considered over when no changes in the resonances due to end products were observed. At this point, the reaction mixtures were centrifuged, 5 mM EDTA (pH 8.0) was added to the

supernatant, and the pH was adjusted to 7.6; these samples were analysed by ^{31}P-NMR. To favour the detection of a phosphorylated intermediate compound, a general phosphatase inhibitor (NaF) was added to the reaction mixture to a final concentration of 7.5 mM.

In the discontinuous method, the reaction mixtures, containing 50 mM MOPS pH 8.1, 5 mM $MgCl_2$, 250 μl of D_2O, and 5 mM of putative substrates, were incubated at 80°C in a total volume of 0.5 ml. The reaction mixtures were initiated by addition of *A. fulgidus* cell extract (equivalent to 50 mg total protein). After 1 hour incubation, the reaction mixtures were centrifuged; 5 mM EDTA (pH 8.0) and 50 μl of D_2O were added to the supernatant, and the pH was adjusted to 7.6. These samples were analysed by ^{31}P-NMR. The substrates examined were: CTP, CDP-glycerol, DL-glycerol 3-phosphate, L-glycerol 3-phosphate and glycerol. To test the specificity of the enzymes regarding nucleotide usage, all the reactions requiring CTP were also carried out in the presence of ATP, UTP, or GTP. To favour the presence of phosphorylated intermediate compounds a phosphatase inhibitor (NaF) was added to the reaction mixtures at a final concentration of 5 to 20 mM.

During the purification of diglycerol phosphate phosphate synthase activity, fractions eluted were examined for the presence of the enzyme by the discontinuous assay method described above. For this, reaction mixtures containing CDP-glycerol, and L-[U-^{14}C]-glycerol 3-phosphate were incubated for 1 hour at 80ºC. Reaction mixtures were centrifuged, and the supernatant solution applied onto a TLC plate (Silica 60; Merck). The reaction products were separated on a TLC plate with a solvent system composed of *n*-propanol and 25% ammonia (1:1, v/v). After being dried, the TLC plate was autoradiographed for 16 hours to a Kodak BioMax film. Non-labelled standards of diglycerol phosphate, glycerol 3-phosphate and CDP-glycerol were visualised by spraying with 5% ammonium molybdate in ethanol followed by charring at 120°C.

Synthesis of glycerol 3-[^{32}P]phosphate and CDP[^{32}P]-glycerol.

To investigate the presence of a phosphorylated intermediate in the biosynthesis of diglycerol phosphate, an enzymatic assay with radioactive ^{32}P-labelled substrates was used. Since glycerol 3-[^{32}P]phosphate and CDP[^{32}P]-glycerol were not commercially available, it was necessary to produce them in our laboratory.

To synthesise glycerol 3-[^{32}P]phosphate, a reaction mixture (50 μl), containing 50 mM Tris-HCl (pH 7.6), 5 mM $MgCl_2$, 5 U of glycerol kinase from *Bacillus stearothermophilus* (Sigma), 40 μM glycerol and 1 μM [γ-^{32}P]ATP (Amersham Biosciences, 3000 Ci/mmol, 10 mCi/ml), was incubated for 1 hour at 25°C. The enzymatic reaction was stopped by cooling on ice for

2 minutes, and the nucleotides were removed by adding 1 mg of charcoal. This mixture was kept on ice for 30 minutes, and the charcoal was removed by centrifugation. The glycerol 3-[^{32}P]phosphate produced was contaminated with minor amounts of radioactive ATP and inorganic phosphate (Fig. V.1).

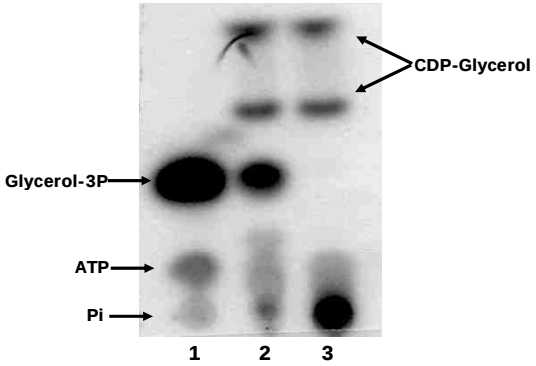

Figure V.1. TLC analysis of the synthesised ^{32}P radiolabelled compounds. The glycerol 3-[^{32}P]phosphate produced from γ-[^{32}P]ATP and glycerol by the action of glycerol kinase (lane 1); CDP[^{32}P]-glycerol phosphate produced using the previous glycerol 3-[^{32}P]phosphate and CTP by action of the glycerol 3-phosphate cytidylyltransferase before (lane 2) and after (lane 3) treatment with alkaline phosphatase.

CDP[^{32}P]-glycerol was produced by using a cell extract of *E. coli* BL21(DE3) bearing the pET11a-GCT (plasmid containing the CTP:glycerol-3-phosphate cytidylyltransferase gene from *Bacillus subtilis* (Park et al. 1993). Cells were grown at 37°C in LB medium containing ampicillin (100 µg/ml) until OD_{600nm} reached 0.8. The cells were induced with IPTG (final concentration of 1 mM) during 4 hours. Cells were harvested by centrifugation at 5,000 × g at 4°C for 10 min and suspended in Tris-HCl (10 mM, pH 8.0), 300 mM NaCl, 10% (v/v) glycerol. After cell disruption in a French press, the lysate was centrifuged at 12,000 × g for 30 min. The supernatant solution was applied onto a HisTrap column (Pharmacia Biotech) equilibrated with phosphate buffer (20 mM, pH 7.4) containing 0.5 M NaCl and 10 mM imidazole. CTP:glycerol-3-phosphate cytidylyltransferase was eluted with 5 ml of phosphate buffer (20 mM, pH 7.4) containing 0.5 M NaCl and 0.5 M imidazole. Imidazole was removed from the protein preparation by using a PD-10 column (Amersham Biosciences) equilibrated with Tris-HCl (20 mM, pH 7.6) containing 6 mM of $MgCl_2$. The pure enzyme was incubated at 37ºC with CTP and glycerol 3-[^{32}P]phosphate (produced in this work). After one hour, residual glycerol 3-[^{32}P]phosphate was hydrolysed using alkaline phosphatase. After the incubation, alkaline

phosphatase was inactivated by boiling for 5 minutes. The final preparation of CDP-[^{32}P]glycerol was contaminated with radiolabelled inorganic phosphate (Fig. V.1).

RESULTS

Biosynthesis of diglycerol phosphate

To investigate diglycerol phosphate biosynthesis, DL-glycerol 3-phosphate and CTP were incubated with cell extracts of *A. fulgidus*, and the consumption of substrates and formation of products were monitored *on line* by ^{31}P-NMR (Fig. V.2). CDP-glycerol and diglycerol phosphate were identified as final products in the reaction mixture, and the NMR assignments were confirmed by spiking with the pure compounds.

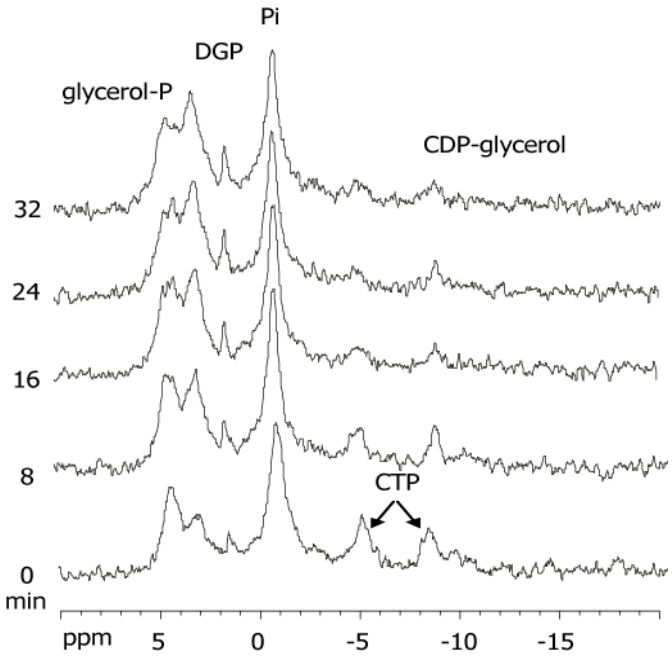

Figure V.2. Time course for the formation of diglycerol phosphate from glycerol 3-phosphate and CTP in a cell extract of *A. fulgidus* VC-16 at 80ºC as monitored by ^{31}P-NMR. Glycerol-P, DL-glycerol 3-phosphate; DGP, diglycerol phosphate; and Pi, inorganic phosphate.

Diglycerol phosphate was also formed when CDP-glycerol and DL-glycerol 3-phosphate were used as substrates (Fig. V.3).

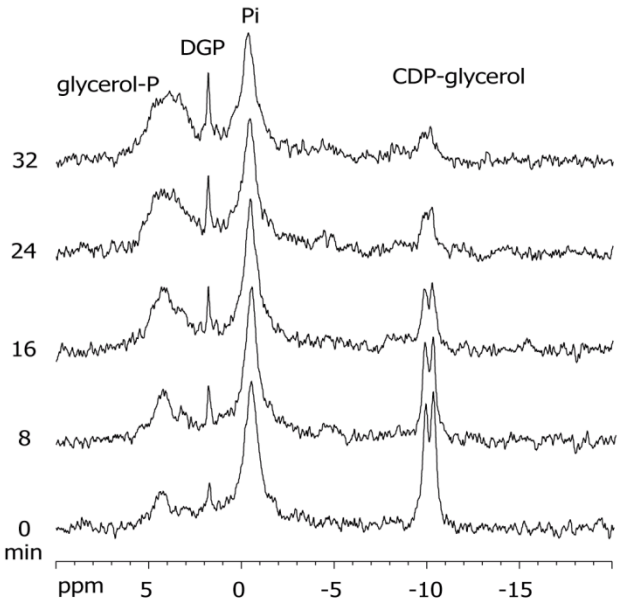

Figure V.3. Time course for the formation of diglycerol phosphate from CDP-glycerol and glycerol 3-phosphate in a cell extract of *A. fulgidus* VC-16 at 80ºC as monitored by ^{31}P-NMR. Glycerol-P, DL-glycerol 3-phosphate; DGP, diglycerol phosphate; Pi, inorganic phosphate.

Diglycerol phosphate synthesis was also studied using CDP-glycerol, DL-glycerol 3-phosphate, and glycerol, as possible substrates. Maximal production of diglycerol phosphate was observed with CDP-glycerol and DL-glycerol 3-phosphate. Production of diglycerol phosphate (around 55% of the maximum) was also detected when CDP-glycerol alone, or in combination with glycerol, was provided. This production was attributed to the presence of glycerol 3-phosphate, resulting from the thermal degradation of CDP-glycerol. No activity was observed when DL-glycerol 3-phosphate and/or glycerol were used as sole substrates (Fig. V.4). Additionally, it was verified that the pure enantiomeric form, L-glycerol 3-phosphate, was a substrate for the enzyme; D-glycerol 3-phosphate was not examined as it is not commercially available.

The synthesis of diglycerol phosphate or CDP-glycerol from DL-glycerol 3-phosphate and each of the following nucleotides ATP, UTP and GTP was also examined. It was observed that ATP, UTP, or GTP did not replace CTP in the synthesis of diglycerol phosphate or CDP-glycerol (Fig. V.4).

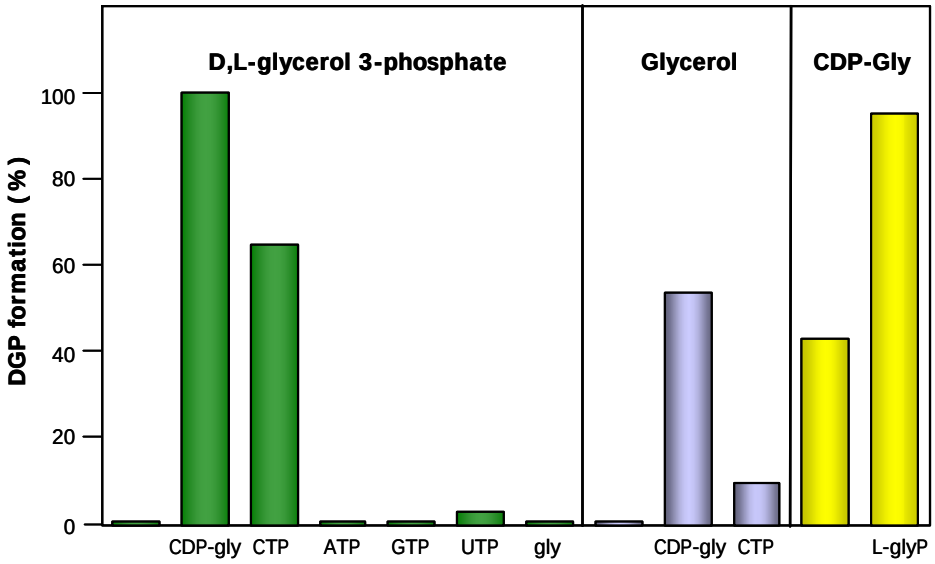

Figure V.4. Different substrate combinations examined for the formation of diglycerol phosphate in *A. fulgidus* VC-16 cell extracts, followed by ^{31}P-NMR. Maximal production of diglycerol phosphate (normalised to 100%) was observed when DL-glycerol 3-phosphate and CDP-glycerol were used as substrates. Gly, glycerol; CDP-gly, CDP-glycerol; L-glyP, L-glycerol 3-phosphate. Unlabelled bars refer to control assays, *i. e.*, only D,L-glycerol 3-phosphate, glycerol, or CDP-gly were added as substrates.

At this stage, two possible pathways for the synthesis of diglycerol phosphate were hypothesised (Fig. V.5): 1) a single-step pathway involving the condensation of glycerol 3-phosphate with the glycerol moiety of CDP-glycerol, forming diglycerol phosphate and CDP; and 2) a two-step pathway, in which the phosphodiester bond of CDP-glycerol is attacked by the hydroxyl group at position 1 of glycerol 3-phosphate, yielding a phosphorylated intermediate (diglycerol phosphate phosphate) and CMP; in this case, the phosphorylated intermediate would be subsequently dephosphorylated into diglycerol phosphate.

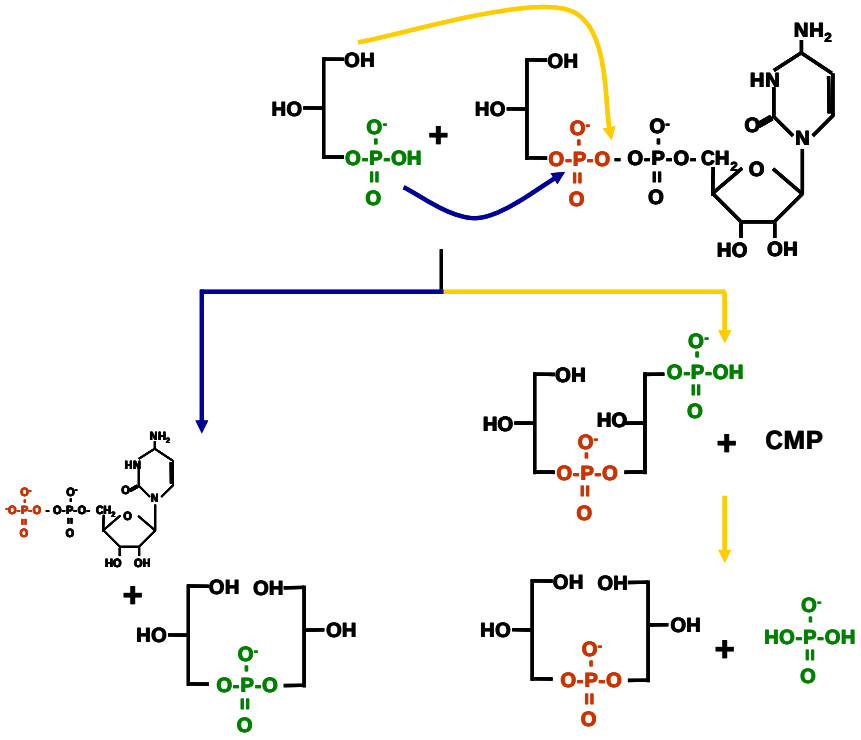

Figure V.5. The two hypothetical schemes proposed for the synthesis of diglycerol phosphate.

Two strategies were devised to determine the correct pathway for the synthesis of diglycerol phosphate. In the first approach, the use of selectively ^{32}P-labelled substrates would allow us to determine the pathway simply by following the fate of the radioactive label in the reaction products by TLC. For example, if labelled glycerol 3-phosphate were used in combination with unlabeled CDP-glycerol, the formation of labelled diglycerol phosphate would prove the operation of the single-step pathway. Conversely, if the reaction were carried out with the radioactive label in CDP-glycerol, the formation of labelled diglycerol phosphate would be possible only if the two step-pathway were functional. (Fig. V.5). Glycerol 3-[^{32}P]phosphate and CDP[^{32}P]-glycerol were produced as described above and the experiments performed as planned. Unfortunately, the two radioactive substrates were extensively metabolised by cell extracts to form products other than diglycerol phosphate and the results were inconclusive.

In a second approach, an attempt was made to detect the presence of the hypothetical phosphorylated intermediate, which would establish the presence of the two-step pathway. For this purpose, NaF (7.5 mM), a general phosphatase inhibitor, was added to the

reaction mixture containing CDP-glycerol and DL-glycerol 3-phosphate as substrates, and the reaction followed by ^{31}P-NMR. Upon NaF addition, a new resonance in the ^{31}P-NMR spectrum of the reaction mixture was detected at 2.14 ppm, near the resonance due to diglycerol phosphate (1.78 ppm), indicating the production of a new phosphodiester compound (Fig. V.6).

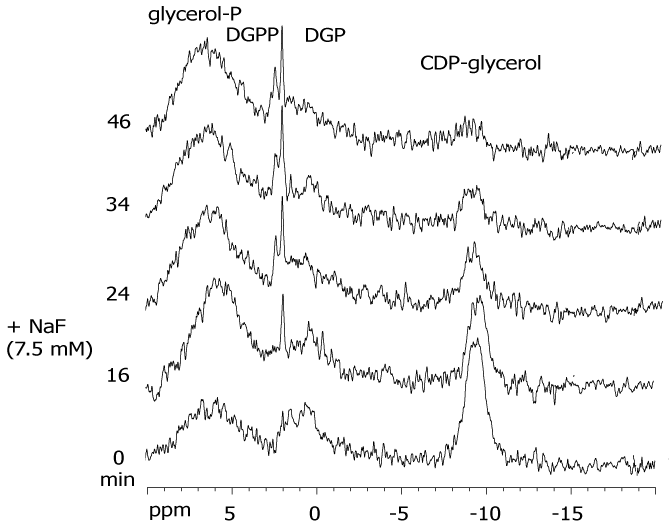

Figure V.6. Time course for the formation of diglycerol phosphate from CDP-glycerol and glycerol 3-phosphate by a cell extract of *A. fulgidus* strain 7324 as monitored by ^{31}P-NMR at 80°C. NaF (7.5 mM) was added to the reaction mixture prior to incubation. Glycerol-P, DL-glycerol 3-phosphate; DGP, diglycerol phosphate; DGPP, diglycerol phosphate phosphate. The chemical shift scale was calibrated using external 80% phosphoric acid at 27 ºC.

To facilitate the NMR analysis of the reaction products, the mixture was placed in a boiling water bath for 10 min, and subsequently centrifuged to remove denatured proteins and other cell debris. As stated above, the ^{31}P-NMR spectrum showed an extra resonance near the signal assigned to diglycerol phosphate. Treatment with alkaline phosphatase led to the disappearance of this resonance; furthermore, the intensity of the signal due to diglycerol phosphate increased by the corresponding amount (Fig. V.7). It is worth pointing out that in this case, spectra of the reaction mixtures were run at 30ºC, and the resonances due to diglycerol phosphate and the phosphorylated intermediate, diglycerol phosphate phosphate were positioned at 1.58 and 1.51 ppm, respectively. The same experiment was performed with extracts of the type strain, *A. fulgidus* VC-16, yielding similar results (data not shown).

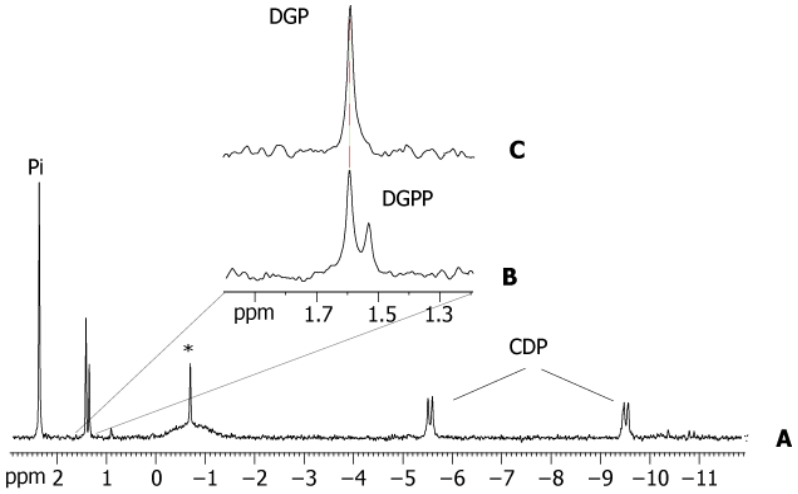

Figure V.7. Section of the ^{31}P-NMR spectrum (3 to -12 ppm region), acquired at 30°C, of the final products resulting from the incubation at 80°C of the reaction mixture containing: *A. fulgidus* 7324 cell free extract, 2 mM of DL-glycerol 3-phosphate, 2 mM CDP-glycerol and 7.5 mM NaF (A). The inset shows an expanded region of the ^{31}P-NMR spectrum before (B), and after (C) treatment with alkaline phosphatase. DGP, diglycerol phosphate; DGPP, diglycerol phosphate phosphate; Pi, inorganic phosphate; and * unknown compound.

This experiment firmly established the formation of a phosphorylated intermediate in the synthesis of diglycerol phosphate. After partial purification of the phosphorylated compound by anion exchange chromatography its structure was established by NMR (see below).

NMR characterisation of the phosphorylated intermediate

The partially purified sample containing the phosphorylated intermediate involved in the synthesis of diglycerol phosphate was contaminated with CMP and other minor compounds. Even so, it was suitable for an NMR characterisation of the compound. The two-dimensional spectra showed the presence of two distinct spin systems, which were assigned to the two glycerol moieties present in the compound. The proton correlation spectrum (COSY) allowed following sequentially all resonances of the two distinct moieties in the compound. The combination of the ^{13}C-^{1}H HMQC spectrum and the COSY spectrum, permitted the assignment of all proton and carbon signals (Table V.2.).

Table V.2. ^{13}C, ^{1}H and ^{31}P chemical shifts of diglycerol phosphate phosphate.

Moiety	Chemical shift (ppm)		
	^{13}C	^{1}H	^{31}P
Glycerol			
C_1	66.8	3.92; 3.85	
C_2	71.0	3.90	
C_3	62.3	3.70; 3.60	
Glycerol-phosphate			
C_1	67.0	3.94; 3.90	
C_2	70.7	3.98	
C_3	63.2	4.02; 3.94	4.88
Diester phosphate			1.51

^{13}C and ^{1}H chemical shifts were referenced to TSPSA. ^{31}P chemical shifts measured at 30 ºC and referenced to external 85% (w/v) H_3PO_4, designated at 0 ppm. The pH of the sample was 9.0.

The proton decoupled ^{31}P-NMR spectrum of the partially purified sample showed two signals, one in the monoester and another in the diester region (at 4.88 and 1.51 ppm, respectively). Upon removal of proton decoupling, the diester signal at 1.51 ppm turned into a complex multiplet, while the signal at 4.88 ppm split into a triplet, meaning that it is coupled to a CH_2 group. Therefore, the additional phosphate group can only be located at position 3 of one of the glycerol moieties. This conclusion was further strengthened by the acquisition of ^{1}H-^{13}C and ^{1}H-^{31}P HMQC spectra. In the ^{1}H-^{13}C correlation spectrum we found a set of signals that mimic those of diglycerol phosphate, and another set shifted towards lower field in the proton dimension (Fig. V.8). In the ^{1}H-^{31}P correlation spectrum the phosphorous signal in the diester region at 1.51 ppm showed correlations to positions 1 of both glycerol moieties, while the monoester signal at 4.88 ppm showed only one correlation to the signal assigned to position 3 of the low-field-shifted set of signals, thus establishing the phosphorylated intermediate as: diglyceryl phosphate 3-phosphate.

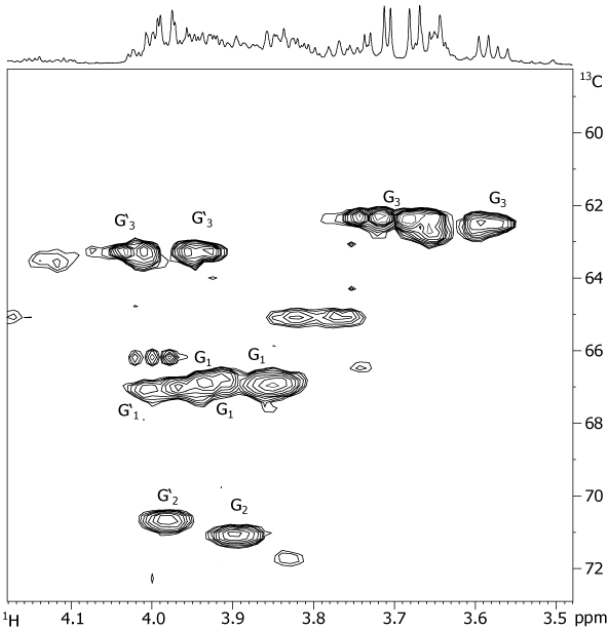

Figure V.8. ^{13}C-^{1}H HMQC of diglycerol phosphate phosphate partially purified from the reaction mixtures. Peaks due to the glycerol and glycerol 3-phosphate moieties are labelled with G and G', respectively. The subscripts represent proton numbering. Cross peaks correspond to connectivities between proton and carbon atoms covalently bonded.

Identification of the genes involved in diglycerol phosphate synthesis

The identification of the gene encoding diglycerol phosphate phosphate synthase in *A. fulgidus* was attempted by reverse genomics, *i. e.*, purification of the respective activity to obtain N-terminal sequence information that would lead to the identification of the encoding gene in the genome sequence of the organism. After five chromatographic steps (DEAE-Sepharose, Q-Sepharose (pH values 7.6 and 8.1), Phenyl-Sepharose, and Superose G200), the purification yield was not satisfactory, and the DGPPS activity was vestigial.

In parallel, the *A. fulgidus* genome (www.tigr.org) was searched for genes encoding proteins possessing domains characteristic of CDP-alcohol phosphatidyltransferases (www.sanger.ac.uk//cgi-bin/Pfam). The members of this protein family catalyse the displacement of CMP from a CDP-alcohol by a second alcohol with the formation of a phosphodiester bond and the concomitant hydrolysis of a phospho-anhydride bond, which is the enzymatic reaction used in the pathway identified for the synthesis of diglycerol phosphate. Five genes belonging to this family (AF0263, AF1143, AF1744, AF2044, and AF2299) were found.

Three of them (AF1143, AF1744, and AF2044) are annotated as coding for enzymes implicated in the synthesis of phospholipids: CDP-diacylglycerol--glycerol-3-phosphate 3-phosphatidyltransferase (pgsA-1), CDP-diacylglycerol--glycerol-3-phosphate 3-phosphatidyltransferase (pgsA-2) and CDP-diacylglycerol--serine *o*-phosphatidyltransferase (pssa), respectively. Meanwhile, our team demonstrated that the gene AF0263 codes for the synthase involved in the synthesis of di-*myo*-inositol phosphate (Borges et al., 2006). Therefore, gene AF2299 appeared specially promising to encode DGPP synthase. To prove this hypothesis, gene AF2299 was cloned into pTRC99a and pET15b under the control of an IPTG-inducible promoter, and introduced in different hosts, namely, *E. coli* BL-21(DE3), CD43 (with the plasmid pSJS1240) and Rosetta CodonPlus. Protein expression of induced and control cells was analysed by SDS-PAGE (data not shown). The pattern of protein expression was not affected by induction with IPTG, indicating that the desired protein was not overproduced. Moreover, the DGPPS activity was not detected in the extracts of induced cells.

DISCUSSION

Diglycerol phosphate has only been encountered in strains belonging to two species of the genus *Archaeoglobus*, namely *A. fulgidus* and *A. veneficus*. In *A. fulgidus*, diglycerol phosphate was the major compatible solute accumulating in response to an increase in the salinity of the medium (Martins et al. 1997). Herein, the biosynthetic pathway of diglycerol phosphate was elucidated based on the detection of the relevant enzymatic activities in cell extracts of *A. fulgidus* and the characterisation of the intermediate and final products by NMR spectroscopy.

The route for the synthesis of diglycerol phosphate proceeded from glycerol 3-phosphate via three steps: (i) glycerol 3-phosphate is activated into CDP-glycerol at the expense of CTP; (ii) CDP-glycerol is coupled with glycerol 3-phosphate to yield a phosphorylated intermediate, diglycerol phosphate 3-phosphate; (iii) finally, diglycerol phosphate phosphate is dephosphorylated into diglycerol phosphate by the action of a phosphatase (Fig V.9).

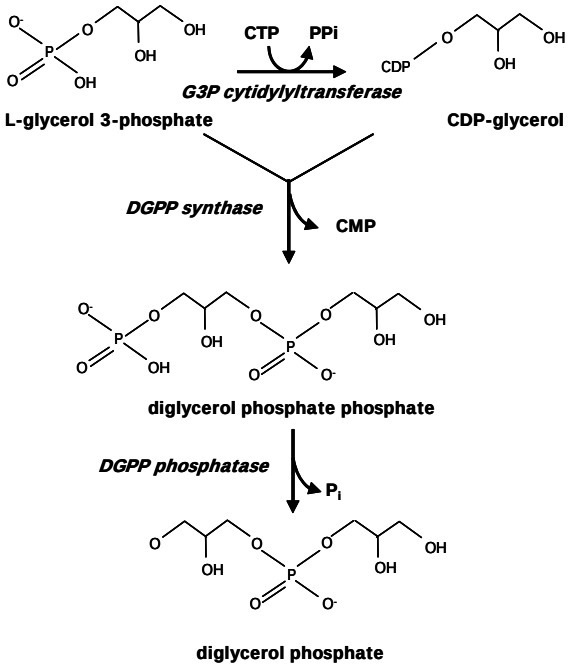

Figure V.9. Proposed pathway for the synthesis of diglycerol phosphate in *A. fulgidus*. Enzymes: G3P cytidylyltransferase, CTP:glycerol 3-phosphate cytidylyltransferase; DGPP synthase, diglycerol phosphate phosphate synthase; DGPP phosphatase, diglycerol phosphate phosphate phosphatase. The stereochemical configuration of the compounds has not been established.

CDP-glycerol is one of the substrates in diglycerol phosphate synthesis, but it is also the principal precursor for the synthesis of the linear polymer 1,3-linked poly(glycerol phosphate), which is a major component of teichoic acids in the walls of gram-positive cells (Pooley et al. 1991; 1992). The synthesis of CDP-glycerol has been studied in detail, particularly in *Bacillus subtilis* (Park et al. 1993; Pattridge et al. 2003). CTP:L-glycerol-3-phosphate cytidylyltransferase (GCT) catalyses the reversible formation of CDP-glycerol and pyrophosphate from CTP and L-glycerol 3-phosphate. A search with the *A. fulgidus* genome revealed an open reading frame (AF1418) with 36% identity with the GCT of *B. subtilis* that most likely encodes the activity responsible for CDP-glycerol synthesis in the archaeon.

Diglycerol phosphate has been found only in strains of the genus *Archaeoglobus*, but if the stereochemistry is ignored, the unit glycero-phospho-glycerol also appears in the lipid phosphatidylglycerol and in a linear 1,3-linked poly(glycerol phosphate) polymer. It is interesting to note the resemblance between the route disclosed here for diglycerol phosphate synthesis in *A. fulgidus* and the biosynthetic pathways reported for those biomolecules in

different organisms (Schertzer and Brown 2003; Daiyasu et al. 2005). For example, phosphatidylglycerol is formed by dephosphorylation of a phosphorylated intermediate (phosphatidylglycerol phosphate), resulting from the condensation of CDP-phosphatidyl and glycerol-3-phosphate (Daiyasu et al. 2005). In the synthesis of 1,3-linked poly(glycerol phosphate), CDP-glycerol is condensed with the poly(glycerol phosphate)$_n$, forming poly(glycerol phosphate)$_{n+1}$, a reaction catalysed by CDP-glycerol:poly(glycerophosphate) glycerophosphotransferase (Burger and Glaser 1964; Pooley et al. 1992).

The logical extension of this work would be the characterisation of the genes and enzymes involved in the synthesis of diglycerol phosphate. In a first approach, the diglycerol phosphate phosphate synthase activity was partially purified from *A. fulgidus* cell extracts in order to obtain protein sequence information, which would lead to the identification of the gene in the genome of this organism. Unfortunately, the purification process was not successful due to significant activity loss during the several purification steps. One of the major drawbacks leading to this failure relates to the difficult and time-consuming radioactive assay needed to detect the activity. Also, the substrates of this enzyme (glycerol 3-phosphate and CDP-glycerol) were highly metabolised by the cell extract, making the detection of the desired product even more difficult. To overcome this problem, an alternative enzymatic assay for DGPP synthase must be developed in the future.

A genomic approach was also followed to identify the gene encoding DGPP synthase. This enzyme catalyses the displacement of CMP from CDP-glycerol by glycerol 3-phosphate with the formation of a phosphodiester bond and concomitant hydrolysis of a pyrophosphate bond. Proteins that catalyse this type of reaction belong to the family of CDP-alcohol phosphatidyltransferases (www.sanger.ac.uk//cgi-bin/Pfam). Five genes (AF0263, AF1143, AF1744, AF2044, and AF2299), whose predicted products belong to this family, were found in the genome of *A. fulgidus*. Three of them (AF1143, AF1744, and AF2044) are annotated as coding for enzymes implicated in the synthesis of phospholipids, leaving only two genes (AF0263 and AF2299) as good candidates to encode DGPPS. Recently, it was unequivocally demonstrated that the gene AF0263 encodes the bifunctional IPCT/DIPPS (DIPP synthase) involved in di-*myo*-inositol phosphate biosynthesis. The DIPP synthase activity was part of a bifunctional enzyme that catalyses the condensation of L-*myo*-inositol 1-phosphate and CTP into CDP-inositol (N-terminal domain), as well as the synthesis of di-*myo*-inositol phosphate phosphate from CDP-inositol and L-*myo*-inositol 1-phosphate (C-terminal domain) (Rodrigues et al. 2007).

The protein encoded by AF2299 shows high homology to the C-terminal domain (CDP-alcohol phosphatidyltransferase) of DIPP synthase, and also contains the conserved motif (D-G-2[X]-A-R-8[X]-G-3[X]-D-3[X]-D) that is characteristic of the CDP-alcohol phosphatidyltransferase family. Therefore, the gene AF2299 was considered as a likely candidate to encode DGPP synthase. However, our attempts to express this gene in *E. coli* were unsuccessful. This failure deserves further comment: (i) it is relatively common to encounter difficulties in the expression of archaeal genes in mesophilic bacterial hosts due to different codon usage and/or incorrect protein folding; however, protein expression was also not detected, nor DGPPS activity observed, when we attempted to express the gene AF2299 in a strain of *E. coli* harbouring a plasmid encoding tRNAs for rare codons. (ii) An alternative reason for this difficulty could derive from in the fact that several transmembrane segments were predicted in the protein sequence (www.ch.embnet.org/software/TMPRED_form.html). Hydropathic profiles predicted the presence of three transmembrane segments in the protein: the stretches comprising residues 177 to 197, 261 to 279 and 305 to 333 have sufficient length and hydrophobicity to span the membrane. In the future, different heterologous hosts, more appropriate for the expression of membrane proteins, must be used to establish the function of this gene.

Two other phosphodiesters, besides diglycerol phosphate, accumulate in *A. fulgidus*: di-*myo*-inositol phosphate and glycerol-phospho-*myo*-inositol. The pattern of compatible solute accumulation in *A. fulgidus* VC-16 was previously reported (chapter 3): the levels of di-*myo*-inositol phosphate and diglycerol phosphate increased in response to heat and osmotic stress, respectively, while glycerol-phospho-*myo*-inositol increased primarily when the two stresses were combined. The biosynthetic routes for the other two phosphodiester compounds were recently elucidated (Borges et al. 2006; Rodrigues et al. 2007). Interestingly, the routes for the synthesis of these three phosphodiester compounds have many features in common. (i) In all cases, CTP is the only nucleoside triphosphate used to activate the polyol, either glycerol or inositol; thus, CDP-glycerol or CDP-inositol are the polyol donors. (ii) The polyol acceptor is always in the phosphorylated form, *i. e.*, L-glycerol 3-phosphate or L-*myo*-inositol-1-phosphate. (iii) The central biosynthetic step involves the condensation of CDP-polyol with the phosphorylated polyol to form a phosphorylated intermediate. (iv) Finally, the dephosphorylation of this intermediate leads to the final product.

It is interesting that the synthesis of diglycerol phosphate (and also of di-*myo*-inositol phosphate and glycerol-phospho-*myo*-inositol) proceeds in two steps with the involvement of a phosphorylated intermediate, as this is the most common strategy for the synthesis of sugars or

sugar derivatives that serve as compatible solutes during osmoprotection or thermoprotection, such as mannosylglycerate, glucosylglycerate, glucosylglycerol, trehalose, and sucrose (Porchia and Salerno 1996; Martins et al. 1999; Empadinhas et al. 2001; Hagemann et al. 2001; Borges 2004; Costa et al. 2006, chapter IV). It seems as though the concerted action of a synthase and a phosphatase, resulting in the irreversible synthesis of the final product, was selected throughout evolution as the most efficient strategy to allow accumulation of compatible solutes to high levels.

In conclusion, the work presented here uncovered the route for the synthesis of a major compatible solute of *A. fulgidus*, diglycerol phosphate. This pathway has many similarities with the biosynthetic pathways of two other compatible solutes of this organism: di-*myo*-inositol phosphate and glycero-phospho-*myo*-inositol. The biosynthetic pathways must be differentially regulated by salt and temperature as the pattern of accumulation of the solutes depends clearly on the type of stress imposed. This study represents an important step towards the elucidation of the role of diglycerol phosphate in the strategies of osmo- and thermoadaptation in hyperthermophiles, a goal that can only be achieved with knowledge on the genes and enzymes implicated in this novel biosynthetic route. Work is in progress in our lab to reach this objective.

Acknowledgements I thank Dr. Paula Fareleira for her contribution to the identification of the diglycerol phosphate biosynthetic pathway by *on line* ^{31}P-NMR. I thank Dr. Nuno Borges for his help in the identification of the diglycerol phosphate phosphate and Dr. Pedro Lamosa for the NMR characterisation. This work was supported by the BIOTECH Program, Biotechnology of Extremophiles (QLK3-CT-2000-00640) and by Fundação para a Ciência e a Tecnologia (FCT), Portugal, Programme Sapiens 99, Project POCTI 35719/BIO/2000 and FEDER.

CHAPTER 6

General discussion

Chapter |6 | Contents

Compatible solutes of *Archaeoglobus* spp.

All microorganisms are subjected to fluctuations in the osmolarity and/or temperature of the environment, and accordingly, suitable adaptation mechanisms had to be developed. A common mechanism found in marine (hyper)thermophiles involves the accumulation of compatible solutes, not only in response to increasing osmolarity, but also at supra-optimal growth temperatures. The occurrence in (hyper)thermophiles of compatible solutes, never or rarely found in mesophiles, suggests a thermoprotective role for these compounds (Santos et al. 2007).

The present work was devoted primarily to investigate the strategies of osmo- and thermo-adaptation in organisms belonging to the genus *Archaeoglobus*: *A. profundus*, *A. veneficus* and three strains of *A. fulgidus* (7324, VC-16 and VC-16S). The compatible solute di-*myo*-inositol phosphate is present in all *Archaeoglobus* species investigated thus far, and actually it is widely distributed among marine (hyper)thermophiles (Santos et al. 2007). In *Bacteria*, di-*myo*-inositol phosphate has been found in members of the two hyperthermophilic genera, *Thermotoga* and *Aquifex* (Martins et al. 1996; Ramakrishnan et al. 1997b; Lamosa et al. 2006), as well as in the thermophiles, *Persephonella marina* and *Rubrobacter xylanophilus* (Empadinhas et al. 2007; Santos et al. 2007). Di-*myo*-inositol phosphate occurs frequently within hyperthermophilic *Archaea*, namely in all the marine species of *Pyroccoccus* and *Thermococcus* examined to date (Scholz et al. 1992; Martins and Santos 1995; Ramakrishnan et al. 1997a; Lamosa et al. 1998; Santos et al. 2007), in the methanogen *Methanotorris igneus* (Ciulla et al. 1994b), and in the crenarchaeotes *Aeropyrum pernix*, *Stetteria hydrogenophila* and

Pyrodictium occultum (Martins et al. 1997; Santos and da Costa 2001; Santos et al. 2007). Additionally, as reported in chapter II, di-*myo*-inositol phosphate is the major compatible solute of the extreme hyperthermophile *Pyrolobus fumarii*, a crenarchaeote that is able to grow at temperatures up to 113°C (Fig. VI.1).

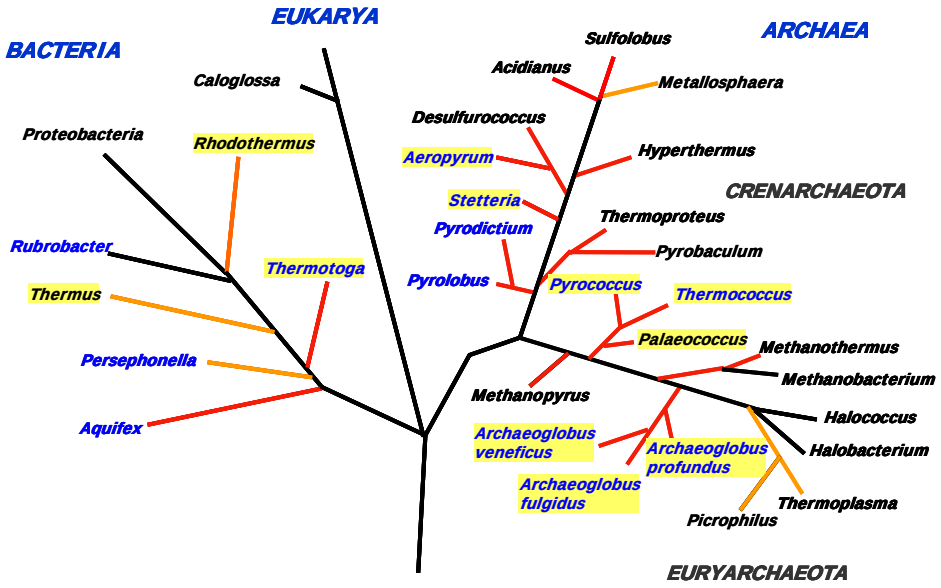

Figure VI.1. Distribution of di-*myo*-inositol phosphate (blue font) and mannosylglycerate (yellow background) in the Tree of Life. Red branches indicate hyperthermophiles and orange branches designate thermophilic organisms.

In *Archaeoglobus fulgidus* VC-16 and VC-16S, di-*myo*-inositol phosphate accumulates preferentially at supra-optimal growth temperatures, behaviour also found in all other organisms that are able to produce this solute. The use of di-*myo*-inositol phosphate as major compatible solute by *Pyrolobus fumarii*, the most hyperthermophilic organism found to date, and the correlation between the intracellular level of this compound and the temperature up-shift above the optimum, strongly supports a role of this solute in thermo-adaptation of marine hyperthermophiles. In accordance with this hypothesis, di-*myo*-inositol phosphate acts as a stabiliser of proteins *in vitro* (Shima et al. 1998, our unpublished results); in addition, di-*myo*-inositol phosphate is able to prevent protein aggregation and fibril formation *in vitro* (Santos et al. 2007).

Mannosylglycerate is the second most widespread solute among (hyper)thermophiles. This solute was found in *A. profundus*, *A. veneficus* and *A. fulgidus* 7324, although it is absent

in the type strain of the genus *Archaeoglobus*, *A. fulgidus* VC-16, and its variant, VC-16S (chapter III). It is also absent in *Pyrolobus fumarii*. Mannosylglycerate was firstly identified in a mesophilic red algae of the order *Ceramiales* (Bouveng et al. 1955). Since then, it has been found in several (hyper)thermophilic organisms: the thermophilic bacteria *Rhodothermus marinus, Thermus thermophilus* and *Rubrobacter xylanophilus* (Nunes et al. 1995; Martins et al. 1996; Silva et al. 1999; Empadinhas et al. 2007), the crenarchaeotes *Aeropyrum pernix* and *Stetteria hydrogenophila*, and the three genera of the order *Thermococcales*, *Thermococcus*, *Pyrococcus*, and *Palaeococcus* (Martins and Santos 1995; Martins et al. 1997; Lamosa et al. 1998; Neves et al. 2005) (Fig. VI.1). Contrarily to di-*myo*-inositol phosphate, mannosylglycerate accumulates preferentially in response to supra-optimal salinities (Martins and Santos 1995; Martins et al. 1996; Lamosa et al. 1998; Silva et al. 1999; Neves et al. 2005; Empadinhas et al. 2007). This trend was also confirmed in *A. fulgidus* 7324, which showed a strong increase in the intracellular content of mannosylglycerate in response to the increased salinity of the growth medium. In fact, when this organism was transferred from a medium containing 1.8% NaCl (the optimum for growth) to 4.5% NaCl, the intracellular level of mannosylglycerate increased 5-fold, and this compound was the sole compatible solute present in the cells (chapter III).

The absence of mannosylglycerate in *A. fulgidus* VC-16 and in its variant VC-16S is intriguing, especially in the view that this solute was found in all the members of the genus *Archaeoglobus* examined thus far. *A. veneficus* and *A. profundus* accumulate mannosylglycerate when growing with acetate as carbon source, while the accumulation of this compound in *A. fulgidus* 7324 was dependent on the use of starch as a substrate for growth. The inability of *A. fulgidus* VC-16 to grow on carbohydrates (despite early reports contradicting this observation) and the absence of mannosylglycerate synthesis could be connected traits (Stetter et al. 1987; Labes and Schönheit 2001). In fact, several genes and enzymatic activities involved in starch catabolism were detected in *A. fulgidus* 7324 (Labes and Schönheit 2001; Johnsen et al. 2003; Labes and Schönheit 2003; Hansen and Schönheit 2004; Labes and Schönheit 2007), but were absent in strain VC-16 (Klenk et al. 1997; Labes and Schönheit 2001). Since *A. fulgidus* VC-16 has been isolated and propagated using lactate as carbon source, the repeated growths under these conditions could have induced the loss of the genes that allowed the utilisation of sugars. Along the same lines, it is reasonable to speculate that the genes involved in the synthesis of mannosylglycerate could have been lost in the same way (Klenk et al. 1997, chapter IV).

In *A. fulgidus* VC-16, diglycerol phosphate appears to replace mannosylglycerate in its role of primary osmolyte. Diglycerol phosphate is a very rare compatible solute, apparently confined to the genus *Archaeoglobus*. It is present in all strains of *A. fulgidus* examined, and also in *A. veneficus*, but it was absent in *A. profundus*. In *A. fulgidus* VC-16S, the level of diglycerol phosphate was 28-fold higher in cells grown at high salinity (6.0% NaCl) than in cells grown at low salinity (0.9% NaCl). The same trend was observed in *A. fulgidus* VC-16 and *A. fulgidus* 7324. Therefore, the results obtained in this work further support the view that compatible solutes of hyperthermophiles have specialised roles; some, such as mannosylglycerate and diglycerol phosphate, have a primary role in osmo-adaptation, while others, like di-*myo*-inositol phosphate, are preferentially involved in thermo-adaptation.

Yet another solute, glycero-phospho-*myo*-inositol, accumulates in *A. fulgidus*. Structurally, this newly identified polyol-phosphodiester is a chimera between diglycerol phosphate and di-*myo*-inositol phosphate (Fig. VI.2). Interestingly, the accumulation profile of glycero-phospho-*myo*-inositol seems to match the structural mixed relations with diglycerol phosphate and di-*myo*-inositol phosphate, accumulating preferentially in response to a combination of heat and salt stresses. This trait is even more evident in the hyperthermophilic bacterium *Aquifex pyrophilus*, where a combination of the two stresses led to a huge intracellular accumulation of glycero-phospho-*myo*-inositol (Lamosa et al. 2006).

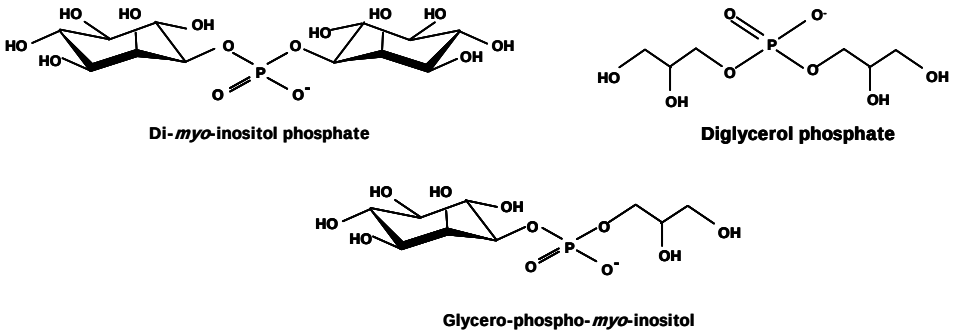

Figure VI.2. Structures of the polyol-phosphodiesters present in *Archaeoglobus* spp.

The distribution of glycero-phospho-*myo*-inositol is rather intriguing. In fact, this solute has been found only in members of two genera (*Archaeoglobus* and *Aquifex*), which are distantly related in phylogenetic terms. Also, di-*myo*-inositol phosphate was never found in mesophiles, although it is widespread among hyperthermophiles, regardless of being *Bacteria* or *Archaea* (Santos et al. 2007). Apparently, the distribution of thermolytes does not carry

much phylogenetic significance, and perhaps is more related with functional and environmental aspects.

Besides the accumulation of specific compatible solutes, there are a few other examples of tentative hyperthermophilic "markers", like the presence of reverse gyrase, an enzyme found in all hyperthermophiles known. Phylogenetic studies indicate that reverse gyrase has an archaeal origin, and that it was subsequently acquired by *Bacteria* through lateral gene transfer (Forterre et al. 2000; Forterre 2002; Brochier-Armanet and Forterre 2007). However, knocking-out the gene encoding reverse gyrase in *Thermococcus kodakaraensis* has shown that the presence of this activity is not a prerequisite for hyperthermophilic life (Atomi et al. 2004). Evidence for lateral gene transfer in hyperthermophiles was found in *Thermotoga* spp., whose genomes contain genes coding for oligopeptide-binding proteins, *myo*-inositol 1-phosphate synthase, and glutamate synthase, all of them appearing to have an hyperthermophilic archaeal origin (Nesbo et al. 2001; Nanavati et al. 2006). Furthermore, the genomes of *Thermotoga maritima* and *Aquifex aeolicus* contain approximately 20% of open reading frames with high homology to archaeal counterparts (Aravind et al. 1998; Nelson et al. 2001). The large number of genes with archaeal hyperthermophilic origin encountered in hyperthermophilic bacteria suggests that a common habitat may have promoted mechanisms of lateral gene transfer, which in turn, were decisive in the successful adaptation of the ancestors of bacterial hyperthermophiles to hot environments (Nesbo et al. 2001).

Despite the close phylogenetic relationship between *Archaeoglobus* and methanogenic *Archaea*, highlighted by the presence of features that were considered exclusive of methanogens, like the presence of coenzyme F_{420}, (Stetter et al. 1987), methanofuran (White 1988), tetrahydromethanopterin (Stetter et al. 1987), and acetyl-CoA decarbonylase/synthase (Dai et al. 1998), *Archaeoglobus* spp. do not accumulate compatible solutes typical of methanogens, such as β-glutamate, N^{ε}-acetyl-β-lysine, and cyclic-2,3-bisphosphoglycerate. β-Glutamate is an uncommon compatible solute, found in the hyperthermophilic bacteria, *Aquifex pyrophilus* and *Thermotoga neapolitana*, as well as in the methanogens *Methanotorris igneus, Methanothermococcus thermolithotrophicus* and *Methanocaldococcus jannaschii* (Robertson et al. 1990; Lai et al. 1991; Ciulla et al. 1994b; Martins et al. 1996; Lamosa et al. 2006). In all these organisms, β-glutamate accumulates preferentially in response to supra-optimal NaCl concentrations. N^{ε}-acetyl-β-lysine is also found in methanogens at supra-optimal salinity, being either halophilic (*Methanohalophilus portucalensis* FDF1 and *Methanohalophilus* Z7302), or halotolerant (*Methanosarcina thermophila*, *Methanothermococcus thermolithotrophicus* and *Methanosarcina mazei* Gö1) in respect to their requisites for NaCl in

the growth medium (Robertson et al. 1990; Sowers et al. 1990; Lai et al. 1991; Sowers and Gunsalus 1995). Cyclic-2,3-bisphosphoglycerate is absolutely restricted to methanogens, but its distribution seems unrelated with the temperature range for growth of the organism. *Methanothermobacter thermoautotrophicus*, *Methanobrevibacter smithii*, *Methanopyrus kandleri* and *Methanothermus fervidus* accumulate cyclic-2,3-bisphosphoglycerate (Lehmacher et al. 1990; Gorkovenko and Roberts 1993; Ciulla et al. 1994a; Martins et al. 1997); the intracellular concentration of this solute does not respond to variations in the salinity of the growth medium, and its role is probably unrelated with stress protection (Gorkovenko and Roberts 1993).

Accumulation of glycine-betaine, a common osmolyte within mesophiles, was not detected in *A. fulgidus*, despite the presence of a transport system for glycine betaine in this organism, and the inclusion of this compound in the growth medium. The glycine-betaine binding protein (ProX) of *A. fulgidus* VC-16 has been characterised structurally, both the complex protein/solute and the free protein. The interaction mechanism of *A. fulgidus* ProX with glycine betaine relies on the spatial arrangement of four tyrosine residues, forming a binding pocket that is capable of interacting effectively with the quaternary amine of the ligand (Schiefner et al. 2004). Interestingly, a similar mechanism operates in the homofunctional protein of *E. coli*, despite the low degree of sequence identity between the two proteins and the large difference of working temperatures.

In general, during osmoadaptation, the uptake of solutes from the external medium is preferred over *de novo* synthesis. Studies on the uptake of thermolytes are very scarce primarily due to the unavailability of radioactive thermolytes needed for the transport assays. In our team, ^{14}C-labelled mannosylglycerate was produced using *E. coli* engineered for this purpose (Sampaio et al. 2003) and a few thermophiles and hyperthermophiles were screened for their ability to take up that compatible solute. Surprisingly, typical producers like *Pyrococcus furiosus, Rhodothermus marinus*, and *Thermus thermophilus* showed none or very poor transport capacity. It may be that the amount of these solutes in (hyper)thermophilic biotopes is very limited and, therefore, hyperthermophiles rely primarily on *de novo* synthesis of these unique compounds. Further work is required in this area before a more reliable hypothesis can be put forward.

Mannosylglycerate biosynthesis

The pathways for the synthesis of mannosylglycerate have been genetically and biochemically characterised in *Rhodothermus marinus*, *Thermus thermophilus*, *Pyrococcus horikoshii*, *Palaeococcus ferrophilus*, and *Thermococcus litoralis* (Martins et al. 1999; Borges et

al. 2004; Empadinhas et al. 2003; Neves et al. 2005). All these (hyper)thermophilic microorganisms use exclusively the two-step pathway, with the exception of *R. marinus*, in which the single-step pathway is also functional. The two alternative pathways are shown in Figure VI.3.

In this work, we showed that the three species of the genus *Archaeoglobus*, *A. profundus*, *A. veneficus* and *A. fulgidus* (strain 7324), produce mannosylglycerate solely via the two-step pathway. The synthesis of mannosylglycerate involves the condensation of GDP-mannose with D-3-phosphoglycerate through the action of mannosyl-3-phosphoglycerate synthase (MPGS), forming a phosphorylated intermediate, mannosyl-3-phosphoglycerate (MPG), which is subsequently dephosphorylated by a specific phosphatase, mannosyl-3-phosphoglycerate phosphatase (MPGP). The activity of mannosylglycerate synthase, the key-enzyme of the single-step pathway, was not detected in cell extracts of these three organisms.

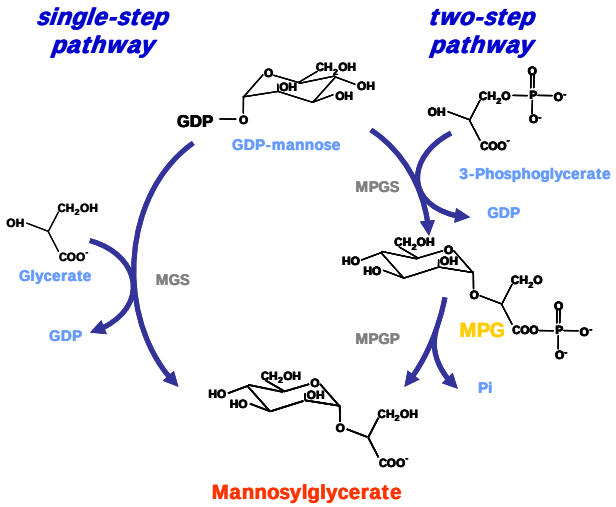

Figure VI.3. The two pathways for the synthesis of mannosylglycerate in (hyper)thermophiles. Single-step pathway uses mannosylglycerate synthase (MGS), while the two-step pathway includes mannosyl-3-phosphoglycerate synthase (MPGS), and mannosyl-3-phosphoglycerate phosphatase (MPGP). MPG, mannosyl-3-phosphoglycerate.

As the genome sequences of *A. profundus* and *A. veneficus* are not available (*A. fulgidus* VC-16 is the only *Archaeoglobus* strain whose genome sequence is known, but it does not produce mannosylglycerate), the genes involved in the two-step pathway were

obtained using degenerate primers and inverse PCR. The genes encoding MPGS and MPGP are contiguous and, immediately downstream of the *mpgP* gene, a putative mannosidase was found. This genomic organisation of the mannosylglycerate gene cluster, comprising a putative mannosidase, has not been observed elsewhere. It differs from the three other genera of the *Thermococcales* (*Pyrococcus*, *Thermococcus*, and *Palaeococcus*), in which the *mpgS* and *mpgP* genes are organised in an operon-like structure that includes the genes encoding the enzymes for the biosynthesis of GDP-mannose (Empadinhas et al. 2001; Neves et al. 2005). In *Rhodothermus marinus* and *Thermus thermophilus*, the *mpgS* gene overlaps the *mpgP* gene by 4-bp (Empadinhas et al. 2003; Borges et al. 2004), while in *Aeropyrum pernix* the genes are adjacent, but separated by 21-bp (Empadinhas et al. 2001). A fragment of the genome of an uncultured crenarchaeote was found to contain a *mpgS* gene, but no *mgpP* gene was detected in its flanking regions. In the mesophilic bacterium *Dehalococcoides ethenogenes*, the *mpgS* and *mpgP* genes are fused in a unique gene (Empadinhas et al. 2004) (Fig. VI.4).

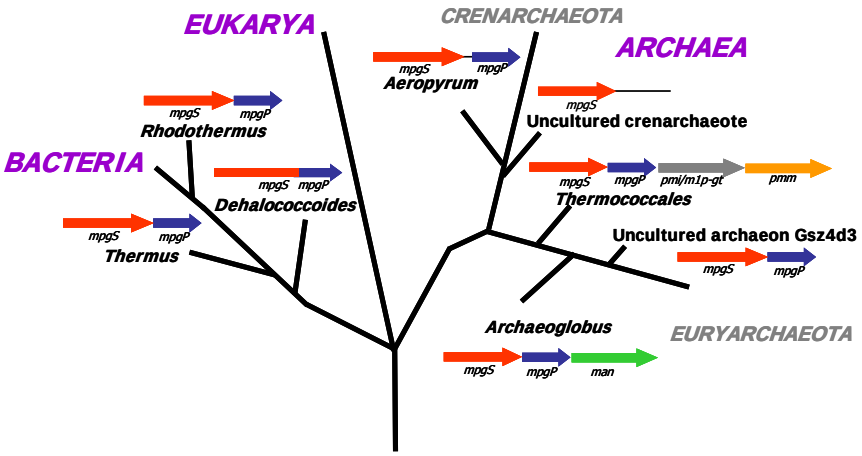

Figure VI.4. The different genomic organisations of the mannosylglycerate cluster. Gene designation: *mpgS* mannosyl-3-phosphoglycerate synthase; *mpgP*, mannosyl 3-phosphoglycerate phosphatase, *man*, mannosidase; *pmi/m1p-gt*, bifunctional phosphomannose isomerase/mannose 1-phosphate guanylyltransferase; *pmm*, phosphomannose mutase (adapted from Borges 2004).

The unrooted phylogenetic tree based on the comparative analysis of the amino acid sequences of known or putative MPGS proteins is in general agreement with the phylogenetic organisation of the organisms based on their 16S rRNA sequences (chapter IV). The bacterial MPGSs (from *Thermus thermophilus* and *Rhodothermus marinus*) are grouped together in a

separate cluster. The crenarchaeotal MPGSs (from an uncultured crenarchaeote and *Aeropyrum pernix*) form a distinct branch from their euryarchaeotal homologues. As expected, the *Thermococcales* (*Palaeococcus ferrophilus*, *Thermococcus litoralis*, *Pyrococcus furiosus*, *P. horikoshii* and *P. abyssii*) form a very tight cluster. The MPGSs of *A. profundus* and *A. veneficus* are grouped together with the MPGS from the uncultured archaeon Gsz3D4. Interestingly, the type strain *A. fulgidus* VC-16 lacks the *mpgS|mpgP|man* gene cluster. We speculate that this gene cluster organisation was a common feature in members of the genus *Archaeoglobus*, but was lost by the type strain during evolution. The same occurs in *Thermococcus kodakaraensis*, as compared with the other members of the *Thermococcales*: the genes encoding M1P-GT/PMI are located immediately upstream the phosphomannomutase gene, but the *mpgS|mpgP* cluster is absent (Rashid et al. 2004).

The presence of a gene encoding a putative mannosidase in the genomes of *A. profundus* and *A. veneficus*, and located immediately downstream of *mpgS|mpgP* genes, is a very interesting feature. It is tempting to speculate that this putative mannosidase may be involved in the hydrolysis of mannosylglycerate when salt-acclimated cells are transferred to medium with low salinity. However, we failed to find experimental evidence for mannosylglycerate hydrolysis in cell extracts of *A. profundus*, despite the fact that this putative mannosidase contains all conserved domains characteristic of α-mannosidases. One could speculate that this enzyme is produced only at a specific growth condition or activated by an unknown post-translational mechanism. So far, no degradation pathway for mannosylglycerate was found in any of the (hyper)thermophilic organisms that synthesise and accumulate this solute. In contrast, several compatible solutes of mesophiles can be hydrolysed and used as carbon sources, such as glycine-betaine, trehalose, ectoine or sucrose (Roberts 2005; Vargas et al. 2006). Surprisingly, a modified *E. coli* K12 strain (designated by MC4110), which can not produce mannosylglycerate, is able to use mannosylglycerate as carbon source for growth (Sampaio et al. 2004). In this organism, mannosylglycerate is transported into the cytoplasm by a PTS transporter that phosphorylates the mannose moiety yielding phosphomannosylglycerate, which is then presumably hydrolysed by a mannosidase into mannose 6-phosphate and glycerate. The expression of the corresponding genes is controlled by a regulator, which is inducible by mannosylglycerate (Sampaio et al. 2004). However, like us, the authors failed to detect mannosidase activity in cell extracts (Sampaio et al. 2004).

In this context, it is important recalling that the release of compatible solutes into the medium is a common strategy used by bacteria, whenever salt-adapted cells are submitted to a hypo-osmotic shock (Blumwald et al. 1983; Schleyer et al. 1993; Ruffert et al. 1997; Sauer and

Galinski 1998; Ciulla and Roberts 1999; Booth et al. 2007). Therefore, it is conceivable that the putative mannosidase of *A. fulgidus* is not involved in the catabolism of mannosylglycerate, but rather in the degradation of large molecules containing mannose, such as mannan. In fact, oligosaccharide transporters are annotated in the genome of *A. fulgidus* (Klenk et al. 1997) and the putative mannosidase could hydrolyse manno-oligosaccharides, eventually providing the precursors for the synthesis of mannosylglycerate. Mannan and other mannose-containing polymers seem to be usual components in hot biotopes. For example, the hyperthermophilic archaeon *Thermococcus litoralis* produces an exopolysaccharide that is exclusively composed of mannose. In natural environments, this exopolysaccharide could be used as carbon source by other hyperthermophilic organisms present in the same community (Rinker and Kelly 1996). It has also been reported that the hyperthermophile *Thermotoga neapolitana* is able to use mannan as sole substrate for growth (Jannasch et al. 1988).

Yet another role for the putative α-mannosidase of *Archaeoglobus* spp. could be the hydrolysis of endogenous glycolipids and/or glycoproteins. This hypothesis is supported by the fact that mannose is frequently found in the composition of *A. fulgidus* glycolipids (Tarui et al. 2007). Moreover, the genes encoding a mannose 1-phosphate guanylyltransferase and dolichol phosphate mannose synthase were found in the genome of *A. fulgidus* VC-16 (Klenk et al. 1997); both these proteins are essential for a glycosylation pathway involving mannose. Although to date no mannose-containing glycoprotein was described in *Archaeoglobus* spp., mannose is present in several glycoproteins of other archaeons, like *Haloferax volcanni*, *Thermoplasma acidophilum*, *Halobacterium salinarum*, *Methanothermus fervidus* and *Sulfolobus solfataricus* (Mescher and Strominger 1976; Yang and Haug 1979; Kärcher et al. 1993; Parolis et al. 1996; Kuntz et al. 1997; Elferink et al. 2001). Therefore, the involvement of mannosidase in the hydrolysis of mannose-containing glycoproteins in *Archaeoglobus* can not be immediately excluded.

Interestingly, α-mannosidases are very rare in *Archaea*; only ten genes encoding putative α-mannosidases were found in this Domain of Life, and so far only the α-mannosidase from *Picrophilus torridus* has been biochemically characterised. This enzyme presents a broad substrate spectrum, hydrolysing all possible types of α-glycosidic bonds between mannose disaccharides and α3, α6-mannopentaose; however, it is not able to hydrolyse mannosyl-3-phosphoglycerate (Angelov et al. 2006). In eukaryotes, several α-mannosidases have been studied, which are mainly involved in the synthesis and catabolism of glycoproteins (Daniel et al. 1994). In bacteria only a few α-mannosidases have been investigated, which are implicated

in the synthesis of glycolipids and in the degradation of xanthan and other mannose polymers (Maruyama et al. 1994; Parker et al. 2001; Rivera-Marrero et al. 2001; Nakajima et al. 2003).

Diglycerol phosphate biosynthesis

Diglycerol phosphate has been found only in two species of the genus *Archaeoglobus*, *i., e.*, *A. fulgidus* and *A. veneficus*. The synthesis of diglycerol phosphate proceeds from glycerol 3-phosphate via three steps (Fig. VI.5): (i) glycerol 3-phosphate is activated to CDP-glycerol via the activity of CTP:glycerol 3-phosphate cytidylyltransferase; (ii) CDP-glycerol is condensed with glycerol 3-phosphate to yield a phosphorylated intermediate, diglycerol phosphate 3-phosphate; (iii) that is, finally, dephosphorylated into diglycerol phosphate by the action of a phosphatase.

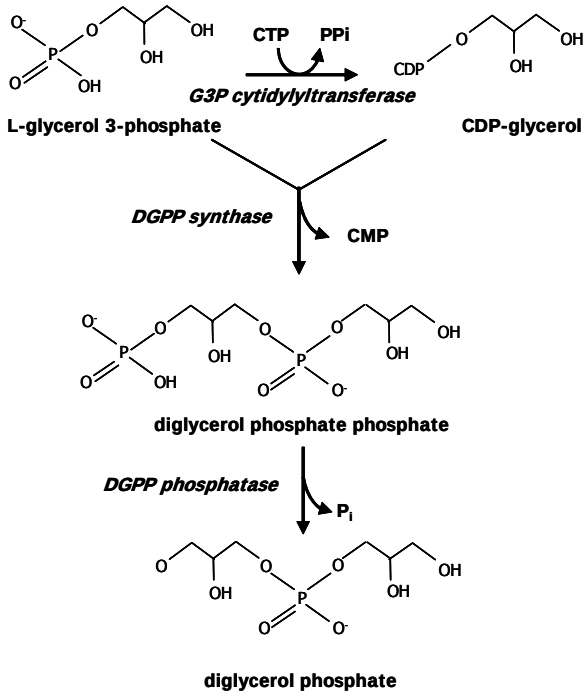

Figure VI.5. Proposed pathway for the synthesis of diglycerol phosphate in *A. fulgidus*. Enzymes: G3P cytidylyltransferase, CTP:glycerol 3-phosphate cytidylyltransferase; DGPP synthase, diglycerol phosphate phosphate synthase; DGPP phosphatase, diglycerol phosphate phosphate phosphatase.

In living systems, CDP-glycerol is synthesised from the condensation of CTP and L-glycerol 3-phosphate in a reaction catalysed by CTP:L-glycerol-3-phosphate cytidylyltransferase (GCT). GCT has been identified in a variety of organisms and extensively

studied in *Bacillus subtilis*: the encoding gene was identified, the recombinant protein characterised, the three-dimensional structure solved, and the catalytic mechanism clarified (Park et al. 1993; Badurina et al. 2003; Pattridge et al. 2003; Fong et al. 2006). Many homologous genes were found in *Bacteria* and *Archaea*, but no archaeal GCT has been characterised thus far. The GCT gene found in the *A. fulgidus* genome (AF1418) has 36% identity with the *B. subtilis* GCT, and most likely encodes the activity responsible for the synthesis of CDP-glycerol, one of the two precursors of diglycerol phosphate. Careful searches of the literature revealed that CDP-glycerol is not used in any metabolic pathway other than the synthesis of the polymer 1,3-linked poly(glycerol phosphate), the major component of teichoic acids found in Gram-positive bacterial cell walls (Pooley et al. 1991; 1992). It is therefore utterly intriguing that genes involved in the synthesis of a precursor of teichoic acid, a compound that does not occur in *Archaea*, are present in so many archaeal genomes. In *A. fulgidus*, it is clear that the putative GCT is involved in the production of CDP-glycerol for the synthesis of diglycerol phosphate; the function of GCTs in other *Archaea*, however, remains a mystery since *A. fulgidus* is the only archaeon that accumulates diglycerol phosphate.

Disregarding stereochemistry, the unit glycerol-phospho-glycerol is also present in the head group of phosphatidylglycerol (named archaetidylglycerol, in the case of archaeons), and in 1,3-linked poly(glycerol phosphate) (Fig. VI.6).

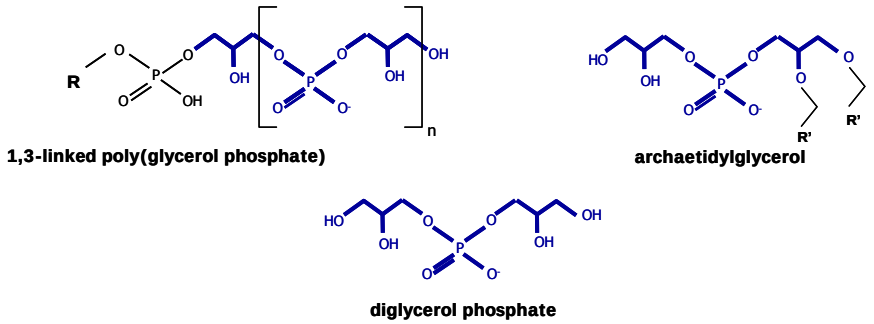

Figure VI.6. Molecular representation of compounds containing the unit of glycerol-phospho-glycerol (represented in blue), ignoring stereochemistry. R- peptydoglycan, R', acyl chain.

It is interesting the resemblance between the route disclosed here for the synthesis of diglycerol phosphate in *A. fulgidus* and the biosynthetic pathway reported for those biomolecules in different organisms (Schertzer and Brown 2003; Daiyasu et al. 2005). The synthesis of phosphatidylglycerol proceeds from the activation of diacylglycerol into CDP-diacylglycerol at the expense of CTP; subsequently, CDP-diacylglycerol is condensed with glycerol 3-phosphate, yielding a phosphorylated intermediate, phosphatidylglycerol phosphate.

Finally, this phosphorylated intermediate is dephosphorylated into phosphatidylglycerol (Ohta et al. 1981; Gilfillan et al. 1986; Nishihara et al. 1999; Daiyasu et al. 2005; Murakami et al. 2007). Therefore, this pathway also involves a phosphorylated intermediate, which is dephosphorylated into the final product. In contrast, the biosynthesis of teichoic acids does not involve the action of a phosphatase. CDP-glycerol is formed by CTP:L-glycerol 3-phosphate cytidylyltransferase, and the glycerol phosphate moiety is subsequently used for the extension of the teichoic acid chain; this step involves the transference of glycerol phosphate from CDP-glycerol to a yet unknown membrane acceptor, resulting in the formation of poly(glycerol phosphate)$_{n+1}$ (Burger and Glaser 1964; Pooley et al. 1992, Schertzer and Brown, 2003).

DGPP synthase catalyses the displacement of CMP from CDP-glycerol by glycerol 3-phosphate with the formation of a phosphodiester bond and concomitant hydrolysis of a pyrophosphate bond. Enzymes with such activity are classified in the family of CDP-alcohol phosphatidyltransferases. A search in the genome of *A. fulgidus* led us to propose gene AF2299 as the best candidate to encode the DGPP synthase, a key enzyme in the synthesis of diglycerol phosphate. Unfortunately, this hypothesis could not be confirmed because we failed to express AF2299, despite investing considerable effort.

A. fulgidus also accumulates two other polyol-phosphodiester compounds, di-*myo*-inositol phosphate and glycero-phospho-*myo*-inositol, and their biosynthetic pathways were recently established (Borges et al., 2006). Furthermore, the route for the synthesis of di-*myo*-inositol phosphate has been also demonstrated in cell extracts of *Thermotoga maritima*, *Thermococcus kodakaraensis* and *Pyrococcus furiosus* (Borges et al., 2006, Rodrigues et al., 2007, unpublished results of our group). In all these organisms, L-*myo*-inositol 1-phosphate is activated to CDP-inositol via CTP:L-*myo*-inositol-1-P cytidylyltransferase; then CDP-inositol is condensed with L-*myo*-inositol 1-phosphate, producing a phosphorylated form of di-*myo*-inositol-phosphate, designated di-*myo*-inositol phosphate phosphate. Finally, di-*myo*-inositol phosphate phosphate is dephosphorylated into di-*myo*-inositol phosphate. More recently, Rodrigues and co-workers (2007) demonstrated that the two activities (L-*myo*-inositol-1-P cytidylyltransferase and DIPP synthase) involved in the synthesis of di-*myo*-inositol phosphate were fused in a single gene product in *A. fulgidus*. Fused genes were also found in *Pyrococcus furiosus*, *Thermococcus kodakaraensis*, *Aquifex aeolicus* and *Rubrobacter xylanophilus*, while separate genes were predicted in *Aeropyrum pernix*, *Thermotoga maritima*, and *Hyperthermus butylicus* (Rodrigues et al., 2007). The bifunctional enzyme catalyses the condensation of CTP and L-*myo*-inositol 1-phosphate into CDP-L-*myo*-inositol (cytidylyltransferase domain), and also the synthesis of di-*myo*-inositol phosphate phosphate from CDP-L-*myo*-inositol and L-*myo*-

inositol 1-phosphate (synthase domain). The cytidylyltransferase domain (N-terminal domain) is absolutely specific for CTP and L-*myo*-inositol 1-phosphate, while the DIPP synthase domain (C-terminal domain) uses L-*myo*-inositol 1-phosphate in combination with either CDP-inositol or CDP-glycerol (Rodrigues et al. 2007b). Therefore, either di-*myo*-inositol phosphate phosphate or glycero-phospho-*myo*-inositol phosphate are the end-products of this activity, depending on the specific CDP-alcohol provided (CDP-inositol or CDP-glycerol, respectively). This plasticity for the alcohol activated donor indicates that this enzyme is also involved in the synthesis of glycero-phospho-*myo*-inositol (Rodrigues et al., 2007).

The ability of using CDP-glycerol for the synthesis of glycero-phospho-*myo*-inositol was found in all DIPPS examined to date, although this compatible solute has been found only in species of the genera *Archaeoglobus* and *Aquifex* (Lamosa et al., 2006). Therefore, the observation that glycero-phospho-*myo*-inositol does not occur in members of other hyperthermophilic genera, namely *Pyrococcus* or *Thermococcus*, is intriguing. A possible explanation could be related with the low availability of CDP-glycerol, the substrate besides L-*myo*-inositol-1-P, which is needed for the synthesis of glycero-phospho-*myo*-inositol (Rodrigues et al. 2007). In the bacterium *Aquifex aeolicus* the genes encoding the glycerol-3-phosphate cytidylyltransferase and DIPPS are organised in the same operon-like structure, and probably under the control of the same promoter (Rodrigues et al. 2007).

Interestingly, the routes for the synthesis of the three phosphodiester compounds (diglycerol phosphate, glycero-phospho-*myo*-inositol and di-*myo*-inositol phosphate) in *A. fulgidus* have several features in common: i) In all cases, CTP is the only nucleoside triphosphate used to activate the polyol, either glycerol or inositol; thus, CDP-glycerol or CDP-inositol are the polyol donors. ii) The polyol acceptor is always in the phosphorylated form, *i. e.,* L-glycerol 3-phosphate or L-*myo*-inositol-1-phosphate. iii) The central step involves the condensation of CDP-polyol with the phosphorylated polyol to form a phosphorylated intermediate. iv) Finally, the dephosphorylation of this intermediate leads to the final product, *i. e.,* diglycerol phosphate, glycero-phospho-*myo*-inositol or di-*myo*-inositol phosphate (Fig VI.7).

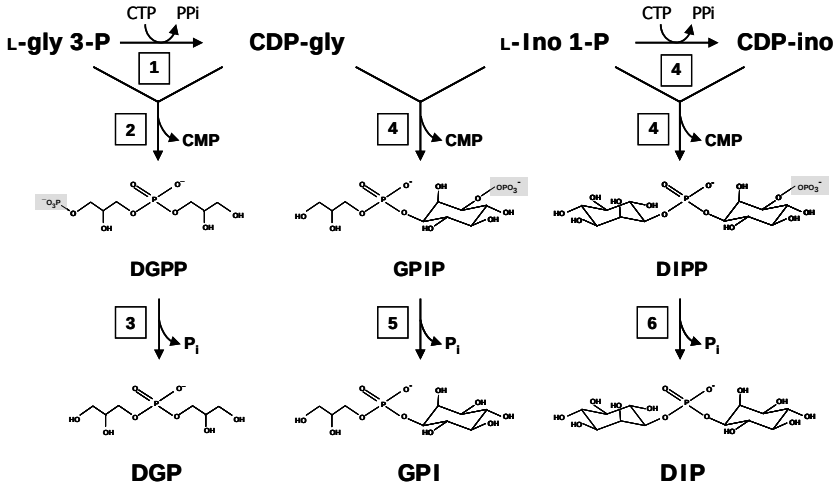

Figure VI.7. Proposed pathways for the synthesis of di-*myo*-inositol phosphate (DIP), diglycerol phosphate (DGP) and glycero-phospho-*myo*-inositol (GPI) in *A. fulgidus*. Enzymes: (1) CTP:glycerol-3-P cytidylyltransferase, (2) DGPP synthase, (3) DGPP phosphatase, (4) Bifunctional enzyme with CTP:L-*myo*-inositol-1-P cytidylyltransferase and DGPP synthase activities (this enzyme also synthesises GPIP), (5) GPIP phosphatase, (6) DIPP phosphatase. DGPP, diglycerol phosphate phosphate; DIPP, di-*myo*-inositol phosphate phosphate; GPIP, glycero-phospho-*myo*-inositol phosphate; L-Ino-1-P, L-*myo*-inositol 1-phosphate; and L-gly-3-P, L-glycerol 3-phosphate. The stereochemical configuration of the DGP and DGPP has not been established.

Surprisingly, the synthesis of these unusual polyol-phosphodiesters uses a two-step pathway involving a phosphorylated intermediate, like the synthesis of sugar or sugar-derivatives that serve as compatible solutes in mesophilic organisms, namely glucosylglycerol, galactosylglycerol, trehalose, sucrose, and glucosylglycerate (Thomson 1983; Giaever et al. 1988; Porchia and Salerno 1996; Curatti et al. 1998; Hagemann et al. 2001; Costa et al. 2006). Two plausible explanations for this preference can be put forward: i) the phosphorylated substrates, 3-phosphoglycerate, glycerol 3-phosphate, and glucose 6-phosphate, are relatively available in the cell as intermediates in central metabolism, and this could act as an evolutionary constraint; and ii) the concerted action of a synthase and a phosphatase, resulting in the irreversible synthesis of the final product, was selected throughout evolution as the most efficient strategy for enabling accumulation of compatible solutes to high level, which can easily reach the molar range in the cytoplasm.

Overview of stress response in *Archaeoglobus fulgidus*

Our knowledge about the regulation of stress responses in (hyper)thermophilic archaeons in general, and in *Archaeoglobus fulgidus* in particularly, is still poor. The heat shock

response of *A. fulgidus* was recently investigated at the transcriptomic level using a whole-genome microarray approach (Rohlin et al. 2005). It was shown that approximately 14% of the open reading frames exhibited changes in the transcript levels, displaying either increased or reduced mRNA abundance; these ORFs comprise a diversity of cell functions, such as energy production, amino acid and lipid metabolism, and signal transduction, the majority of which are still uncharacterised (Rohlin et al. 2005). As expected, the ORFs encoding the two chaperonins (*thsB* and *thsA*), which accumulate in response to an up-shift of the growth temperature (Emmerhoff et al. 1998), were among the most up-regulated genes. Also, two genes encoding small heat shock proteins (*hsp20-1* and *hsp20-2*) were significantly induced. Interestingly, the *hsp20-1* gene is part of an operon that also contains two other genes, encoding an AAA^+ ATPase and a heat shock regulatory protein (HSR1). The operon is self regulated by HSR1, which binds to the promoter region of its own gene, blocking its transcription starting site. Although the recognition sequence associated with HSR1 binding to DNA was not yet determined, it was further observed that it also regulates the expression of the *hsp20-2* gene (Rohlin et al. 2005).

Surprisingly, upon heat shock, no significant changes were detected in the transcript levels of the genes involved in the synthesis of di-*myo*-inositol phosphate (encoding *myo*-inositol synthase and IPCT/DIPPS) and diglycerol phosphate (encoding GCT and the putative DGP synthase) (Rohlin et al. 2005). However, a 1.4-fold increase was observed in the mRNA levels of the gene encoding the phosphatase probably involved in the dephosphorylation of di-*myo*-inositol phosphate phosphate (Rohlin et al. 2005). This protein presents interesting features: it is a bifunctional enzyme, showing both inositol-1-phosphate phosphatase (di-*myo*-inositol phosphate phosphate is also a probable substrate) and fructose bisphosphatase activities. The K_m for inositol-1-phosphate decreases 8 times with a temperature up-shift from 75 to 85°C, which correlates with the accumulation of di-*myo*-inositol phosphate by the organism. The K_m for fructose 1,6-bisphosphate does not change with temperature, suggesting that the temperature dependence of the K_m is specific for inositol-1-phosphate (Wang et al. 2006). Moreover, this temperature dependence was not observed in the homologous enzyme from *Methanococcus jannaschii*, an organism that does not accumulate di-*myo*-inositol phosphate (Chen and Roberts 1998).

The effect of heat stress in the membrane core lipids of *A. fulgidus* was recently investigated (Lai et al. 2008). It was observed that the tetraether to diether lipid ratio increased at supra-optimal temperatures (89 ºC), as well as the number of pentacyclic groups in

tetraether lipids. Similar results had been described in *Methanococcus jannaschii*, another hyperthermophilic archaeon (Sprott et al. 1991).

Despite being a strict anaerobe, *A. fulgidus* is able to cope with oxygen toxicity (Beeder et al. 1994; Lapaglia and Hartzell 1997) and possesses several enzymes related with protection against oxygen: (i) NADH oxidases, that convert O_2 to H_2O_2 and H_2O; (ii) a catalase-peroxidase that reduces H_2O_2 and (iii) neelaredoxin and superoxide reductase, replacing superoxide dismutase activity in the reduction and dismutation of $O_2^{\cdot -}$ (Abreu et al. 2000; Abreu et al. 2001; Kengen et al. 2001; Abreu et al. 2002; Pagala et al. 2002; Rodrigues et al. 2007a).

Like many other microorganisms, *A. fulgidus* can form biofilms in response to diverse environmental stresses, such as extremes of pH and temperature, low nutrient concentrations, and exposure to metals, antibiotics, xenobiotics, or oxygen (Lapaglia and Hartzell 1997). The formation of biofilms increases the tolerance to toxic conditions, by providing a protective barrier against the aggressive environmental conditions. The biofilms formed by *A. fulgidus* are composed by polysaccharides, metals and proteins (Lapaglia and Hartzell 1997).

FINAL REMARKS

The results disclosed in this thesis represent an important contribution for the ambitious goal of understanding the complex mechanisms of osmo- and thermo-adaptation in the hyperthermophylic archaeon *Archaeoglobus fulgidus*. This organism responds to heat stress and osmotic stress by accumulating three polyol-phosphodiester solutes, di-*myo*-inositol phosphate (DIP), diglycerol phosphate (DGP) and glycero-phospho-*myo*-inositol (GPI) that apparently play different roles during the process of stress adaptation. These three solutes show a curious structural relationship, which is also reflected in their pattern of accumulation. While di-*myo*-inositol phosphate increases consistently in response to elevated temperature and diglycerol phosphate to osmotic stress, the level of glycero-phospho-*myo*-inositol seems to respond to a combination of both stresses. The elucidation of the biosynthetic pathways leading to the formation of these solutes was achieved during this thesis, and it is a crucial step towards the full understanding of the regulatory mechanism that determines their accumulation profiles. However, to obtain a global description of the heat (and osmotic) stress response in this organism, it is also important to elucidate the chain of events starting with sensing stress, proceeding to the pathways of signal transduction and finally the activation of the biosynthetic genes.

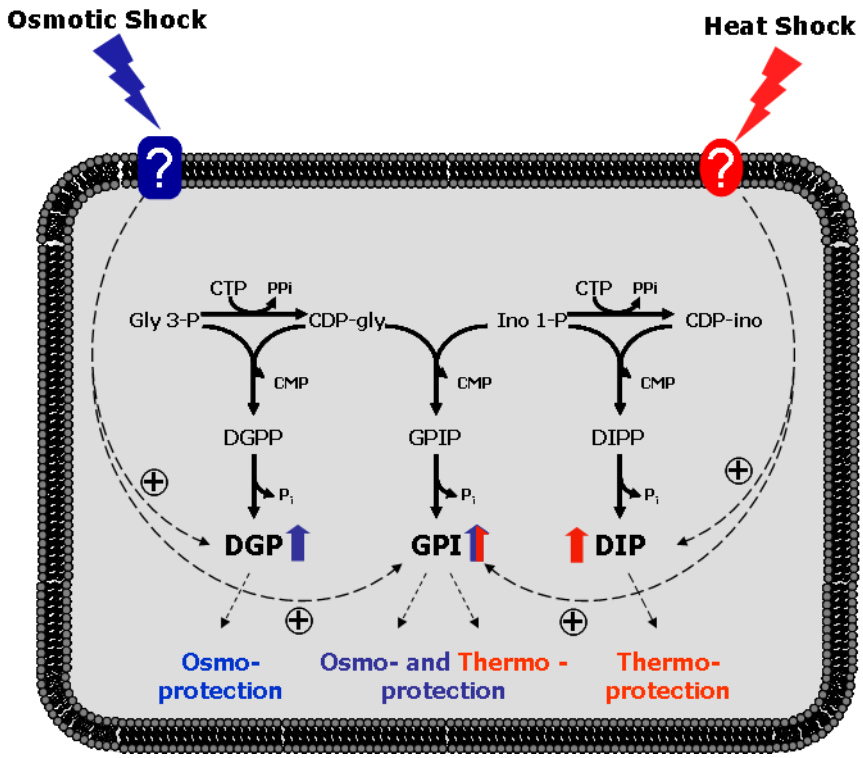

Figure VI 8. Schematic overview of our current knowledge on osmotic and heat-stress responses in *A. fulgidus*, which comprises the differential accumulation pattern of DIP/DGP/GPI in response to osmotic, heat or combination of both stresses, the biosynthetic pathways of these three polyol-phosphodiester solutes, the gene encoding the bifunctional enzyme involved in the synthesis of DIP and GPI, and the protein-stabilising role of DGP and DIP, *in vitro*. The genes involved in DGP synthesis, the protein-stabilising properties of GPI, the differential regulation of the three biosynthetic pathways at the level of expression, the stress sensors and respective signal transduction remain elusive.

In order to accomplish this ambitious goal, it is essential: 1) to characterise the genes and the enzymes involved in diglycerol phosphate synthesis (good candidates are already available); 2) to characterise the enzymes committed to the synthesis of polyol-phosphodiesters (PPDs); 3) to study the physiological roles of di-*myo*-inositol phosphate and diglycerol phosphate under heat (and/or osmotic) stress conditions; 4) to investigate the regulation of compatible solute synthesis in response to heat and/or osmotic stress at transcriptional and translational levels; and finally 4) to identify stress-sensors and response regulators in the transduction cascade leading to PPDs. The majority of these goals can only be achieved with the development of genetic tools for manipulation of *A. fulgidus*, a task that should be pursued.

REFERENCES

REFERENCES

Abreu, I.A., Saraiva, L.M., Carita, J., Huber, H., Stetter, K.O., Cabelli, D., and Teixeira, M. 2000. Oxygen detoxification in the strict anaerobic archaeon *Archaeoglobus fulgidus*: superoxide scavenging by neelaredoxin. *Mol Microbiol* **38:** 322-334.

Abreu, I.A., Saraiva, L.M., Soares, C.M., Teixeira, M., and Cabelli, D.E. 2001. The mechanism of superoxide scavenging by *Archaeoglobus fulgidus* neelaredoxin. *J Biol Chem* **276:** 38995-39001.

Abreu, I.A., Xavier, A.V., LeGall, J., Cabelli, D.E., and Teixeira, M. 2002. Superoxide scavenging by neelaredoxin: dismutation and reduction activities in anaerobes. *J Biol Inorg Chem* **7:** 668-674.

Achenbach-Richter, L., Stetter, K.O., and Woese, C.R. 1987. A possible biochemical missing link among *archaebacteria*. *Nature* **327:** 348-349.

Alarico, S., Empadinhas, N., Simoes, C., Silva, Z., Henne, A., Mingote, A., Santos, H., and da Costa, M.S. 2005. Distribution of genes for synthesis of trehalose and Mannosylglycerate in *Thermus* spp. and direct correlation of these genes with halotolerance. *Appl Environ Microbiol* **71:** 2460-2466.

Angelov, A., Putyrski, M., and Liebl, W. 2006. Molecular and biochemical characterization of α-glucosidase and alpha-mannosidase and their clustered genes from the thermoacidophilic archaeon *Picrophilus torridus*. *J Bacteriol* **188:** 7123-7131.

Anton, J., Oren, A., Benlloch, S., Rodriguez-Valera, F., Amann, R., and Rossello-Mora, R. 2002. *Salinibacter ruber* gen. nov., sp. nov., a novel, extremely halophilic member of the *Bacteria* from saltern crystallizer ponds. *Int J Syst Evol Microbiol* **52:** 485-491.

Aravind, L., Tatusov, R.L., Wolf, Y.I., Walker, D.R., and Koonin, E.V. 1998. Evidence for massive gene exchange between archaeal and bacterial hyperthermophiles. *Trends Genet* **14:** 442–444.

Atomi, H., Matsumi, R., and Imanaka, T. 2004. Reverse gyrase is not a prerequisite for hyperthermophilic life. *J Bacteriol* **186:** 4829-4833.

Badurina, D.S., Zolli-Juran, M., and Brown, E.D. 2003. CTP:glycerol 3-phosphate cytidylyltransferase (TarD) from *Staphylococcus aureus* catalyzes the cytidylyl transfer via an ordered Bi-Bi reaction mechanism with micromolar K_M values. *Biochim Biophys Acta* **1646:** 196-206.

Barns, S.M., Delwiche, C.F., Palmer, J.D., and Pace, N.R. 1996. Perspectives on archaeal diversity, thermophily and monophyly from environmental rRNA sequences. *Proc Natl Acad Sci U S A* **93:** 9188-9193.

Beeder, J., Nilsen, R.K., Rosnes, J.T., Torsvik, T., and Lien, T. 1994. *Archaeoglobus fulgidus* isolated from hot north sea oil field waters. *Appl Environ Microbiol* **60:** 1227-1231.

Blöchl, E., Rachel, R., Burggraf, S., Hafenbradl, D., Jannasch, H.W., and Stetter, K.O. 1997. *Pyrolobus fumarii,* gen. and sp. nov., represents a novel group of *Archaea*, extending the upper temperature limit for life to 113ºC. *Extremophiles* **1:** 14-21.

Blumwald, E., Mehlhorn, R.J., and Packer, L. 1983. Ionic osmoregulation during salt adaptation of the cyanobacterium *Synechococcus* 6311. *Plant Physiol* **73:** 377-380.

Booth, I.R., Edwards, M.D., Black, S., Schumann, U., Bartlett, W., Rasmussen, T., Rasmussen, A., and Miller, S. 2007. Physiological analysis of bacterial mechanosensitive channels. *Methods Enzymol* **428:** 47-61.

Borges, N. 2004. The role of mannosylglycerate in thermo- and osmo-adaptation of *Rhodothermus marinus*: biosynthesis, regulation and applications. In *Instituto de Tecnologia Química e Biológica*. Universidade Nova de Lisboa, Oeiras. PhD thesis.

Borges, N., Gonçalves, L.G., Rodrigues, M.V., Siopa, F., Ventura, R., Maycock, C., Lamosa, P., and Santos, H. 2006. Biosynthetic pathways of inositol and glycerol phosphodiesters used by the hyperthermophile *Archaeoglobus fulgidus* in stress adaptation. *J Bacteriol* **188:** 8128-8135.

Borges, N., Marugg, J.D., Empadinhas, N., da Costa, M.S., and Santos, H. 2004. Specialized roles of the two pathways for the synthesis of mannosylglycerate in osmoadaptation and thermoadaptation of *Rhodothermus marinus*. *J Biol Chem* **279:** 9892-9898.

Borges, N., Ramos, A., Raven, N.D., Sharp, R.J., and Santos, H. 2002. Comparative study of the thermostabilizing properties of mannosylglycerate and other compatible solutes on model enzymes. *Extremophiles* **6:** 209-216.

Bouthier de la Tour, C., Portemer, C., Nadal, M., Stetter, K.O., Forterre, P., and Duguet, M. 1990. Reverse gyrase, a hallmark of the hyperthermophilic archaebacteria. *J Bacteriol* **172:** 6803-6808.

Bouveng, H., Lindberg, B., and Wickberg, B. 1955. Low-molecular carbohydrates in *algae*. Structure of the glyceric acid mannoside from red *algae*. *Acta Chem Scand* **9:** 807-809.

Bradford, M.M. 1976. A rapid and sensitive method for the quantitation of microgram quantities of protein utilizing the principle of protein-dye binding. *Anal Biochem* **72:** 248-254.

Brochier, C., Gribaldo, S., Zivanovic, Y., Confalonieri, F., and Forterre, P. 2005. Nanoarchaea: representatives of a novel archaeal phylum or a fast-evolving euryarchaeal lineage related to Thermococcales? *Genome Biol* **6:** R42.

Brochier-Armanet, C., and Forterre, P. 2007. Widespread distribution of archaeal reverse gyrase in thermophilic bacteria suggests a complex history of vertical inheritance and lateral gene transfers. *Archaea* **2:** 83-93.

Brown, A.D. 1976. Microbial water stress. *Bacteriol. Rev.* **40:** 803-846.

Burger, M.M., and Glaser, L. 1964. The synthesis of teichoic acids. I. Polyglycerophosphate. *J Biol Chem* **239:** 3168-3177.

Burggraf, S., Jannasch, H.W., B., N., and Stetter, K.O. 1990. *Archaeoglobus profundus*, sp. nov., represents a new species within the sulfate-reducing archaebacteria. *Syst Appl Microbiol* **13:** 24-28.

Cary, C.S., Skank, T.M., and Stein, J.L. 1998. Worms bask in extreme temperatures. *Nature* **391:** 545-546.

Chen, L., and Roberts, M.F. 1998. Cloning and expression of the inositol monophosphatase gene from *Methanococcus jannaschii* and characterization of the enzyme. *Appl Environ Microbiol* **64:** 2609-2615.

Chen, L., and Roberts, M.F. 2000. Overexpression, purification, and analysis of complementation behavior of *E. coli* SuhB protein: comparison with bacterial and archaeal inositol monophosphatases. *Biochemistry* **39:** 4145-4153.

Chen, L., Spiliotis, E.T., and Roberts, M.F. 1998. Biosynthesis of di-*myo*-inositol-1,1'-phosphate, a novel osmolyte in hyperthermophilic *Archaea*. *J Bacteriol* **180:** 3785-3792.

Ciulla, R., Clougherty, C., Belay, N., Krishnan, S., Zhou, C., Byrd, D., and Roberts, M.F. 1994a. Halotolerance of *Methanobacterium thermoautotrophicum* delta H and Marburg. *J Bacteriol* **176:** 3177-3187.

Ciulla, R.A., Burggraf, S., Stetter, K.O., and Roberts, M.F. 1994b. Occurrence and role of di-*myo*-inositol-1,1'-phosphate in *Methanococcus igneus*. *Appl Environ Microbiol* **60:** 3660-3664.

Ciulla, R.A., and Roberts, M.F. 1999. Effects of osmotic stress on *Methanococcus thermolithotrophicus*: ^{13}C-edited ^{1}H-NMR studies of osmolyte turnover. *Biochim Biophys Acta* **1427:** 193-204.

Claus, H., Akca, E., Debaerdemaeker, T., Evrard, C., Declercq, J.P., Harris, J.R., Schlott, B., and Konig, H. 2005. Molecular organization of selected prokaryotic S-layer proteins. *Can J Microbiol* **51:** 731-743.

Claus, H., Akca, E., Debaerdemaeker, T., Evrard, C., Declercq, J.P., and Konig, H. 2002. Primary structure of selected archaeal mesophilic and extremely thermophilic outer surface layer proteins. *Syst Appl Microbiol* **25:** 3-12.

Cory, Q.W., Daniels, G., Keates, R.A.B., Brewer, D., and Lam, J.S. 2005. Evidence that WbpD is an N-acetyltransferase belonging to the hexapeptide acyltransferase superfamily and an important protein for O-antigen biosynthesis in *Pseudomonas aeruginosa* PAO1. *Molr Microbiol* **57:** 1288-1303.

Costa, J., Empadinhas, N., Gonçalves, L., Lamosa, P., Santos, H., and da Costa, M.S. 2006. Characterization of the biosynthetic pathway of glucosylglycerate in the archaeon *Methanococcoides burtonii*. *J Bacteriol* **188:** 1022-1030.

Csonka, L.N. 1989. Physiological and genetic responses of bacteria to osmotic stress. *Microbiol Rev* **53:** 121-147.

Curatti, L., Folco, E., Desplats, P., Abratti, G., Limones, V., Herrera-Estrella, L., and Salerno, G. 1998. Sucrose-phosphate synthase from *Synechocystis* sp. strain PCC 6803: identification of the *spsA* gene and characterization of the enzyme expressed in *Escherichia coli*. *J Bacteriol* **180:** 6776-6779.

da Costa, M.S., Santos, H., and Galinski, E.A. 1998. An overview of the role and diversity of compatible solutes in *Bacteria* and *Archaea*. *Adv Biochem Eng Biotechnol* **61:** 117-153.

Dahl, C., Speich, N., and Truper, H.G. 1994. Enzymology and molecular biology of sulfate reduction in extremely thermophilic archaeon *Archaeoglobus fulgidus*. *Methods Enzymol* **243:** 331-349.

Dai, Y.R., Reed, D.W., Millstein, J.H., Hartzell, P.L., Grahame, D.A., and DeMoll, E. 1998. Acetyl-CoA decarbonylase/synthase complex from *Archaeoglobus fulgidus*. *Arch Microbiol* **169:** 525-529.

Daiyasu, H., Kuma, K., Yokoi, T., Morii, H., Koga, Y., and Toh, H. 2005. A study of archaeal enzymes involved in polar lipid synthesis linking amino acid sequence information, genomic contexts and lipid composition. *Archaea* **1:** 399-410.

Daniel, P.F., Winchester, B., and Warren, C.D. 1994. Mammalian α-mannosidases-multiple forms but a common purpose? *Glycobiology* **4:** 551-566.

Daniel, R.M., and Cowan, D.A. 2000. Biomolecular stability and life at high temperatures. *Cell Mol Life Sci* **57:** 250-264.

De Farias, S.T., and Bonato, M.C. 2002. Preferred codons and amino acid couples in hyperthermophiles. *Genome Biology* **3:** preprint0006.

Dorr, C., Zaparty, M., Tjaden, B., Brinkmann, H., and Siebers, B. 2003. The hexokinase of the hyperthermophile *Thermoproteus tenax*. ATP-dependent hexokinases and ADP-dependent glucokinases, two alternatives for glucose phosphorylation in *Archaea*. *J Biol Chem* **278:** 18744-18753.

Drlica, K., and Rouviere-Yaniv, J. 1987. Histone-like proteins of bacteria. *Microbiol Rev* **51:** 301-319.

Egorova, K., Grudieva, T., Morinez, C., Kube, J., Santos, H., da Costa, M.S., and Antranikian, G. 2007. High yield of mannosylglycerate production by upshock fermentation and bacterial milking of trehalose-deficient mutant *Thermus thermophilus* RQ-1. *Appl Microbiol Biotechnol* **75:** 1039-1045.

Eichler, J., and Adams, M.W. 2005. Posttranslational protein modification in *Archaea*. *Microbiol Mol Biol Rev* **69:** 393-425.

Elferink, M.G., Albers, S.V., Konings, W.N., and Driessen, A.J. 2001. Sugar transport in *Sulfolobus solfataricus* is mediated by two families of binding protein-dependent ABC transporters. *Mol Microbiol* **39:** 1494-1503.

Emmerhoff, O.J., Klenk, H.P., and Birkeland, N.K. 1998. Characterization and sequence comparison of temperature-regulated chaperonins from the hyperthermophilic archaeon *Archaeoglobus fulgidus*. *Gene* **215:** 431-438.

Empadinhas, N., Albuquerque, L., Costa, J., Zinder, S.H., Santos, M.A., Santos, H., and da Costa, M.S. 2004. A gene from the mesophilic bacterium *Dehalococcoides ethenogenes* encodes a novel mannosylglycerate synthase. *J Bacteriol* **186:** 4075-4084.

Empadinhas, N., Albuquerque, L., Henne, A., Santos, H., and da Costa, M.S. 2003. The bacterium *Thermus thermophilus*, like hyperthermophilic *Archaea*, uses a two-step pathway for the synthesis of mannosylglycerate. *Appl Environ Microbiol* **69:** 3272-3279.

Empadinhas, N., Marugg, J.D., Borges, N., Santos, H., and da Costa, M.S. 2001. Pathway for the synthesis of mannosylglycerate in the hyperthermophilic archaeon *Pyrococcus horikoshii*. Biochemical and genetic characterization of key enzymes. *J Biol Chem* **276:** 43580-43588.

Empadinhas, N., Mendes, V., Simoes, C., Santos, M.S., Mingote, A., Lamosa, P., Santos, H., and Costa, M.S. 2007. Organic solutes in *Rubrobacter xylanophilus*: the first example of di-*myo*-inositol-phosphate in a thermophile. *Extremophiles* **11:** 667-673.

Farias, S.T., and Bonato, M.C. 2003. Preferred amino acids and thermostability. *Genet Mol Res* **2:** 383-393.

Flint, J., Taylor, E., Yang, M., Bolam, D.N., Tailford, L.E., Martinez-Fleites, C., Dodson, E.J., Davis, B.G., Gilbert, H.J., and Davies, G.J. 2005. Structural dissection and high-throughput screening of mannosylglycerate synthase. *Nat Struct Mol Biol* **12:** 606-614.

Fong, D.H., Yim, V.C., D'Elia, M.A., Brown, E.D., and Berghuis, A.M. 2006. Crystal structure of CTP:glycerol-3-phosphate cytidylyltransferase from *Staphylococcus aureus*: examination of structural basis for kinetic mechanism. *Biochim Biophys Acta* **1764:** 63-69.

Forterre, P. 2002. A hot story from comparative genomics: reverse gyrase is the only hyperthermophile-specific protein. *Trends Genet* **18:** 236-237.

Forterre, P., Bouthier De La Tour, C., Philippe, H., and Duguet, M. 2000. Reverse gyrase from hyperthermophiles: probable transfer of a thermoadaptation trait from *Archaea* to *Bacteria*. *Trends Genet* **16:** 152-154.

Galinski, E.A. 1995. Osmoadaptation in bacteria. *Adv Microb Physiol* **37:** 272-328.

Giaever, H.M., Styrvold, O.B., Kaasen, I., and Strom, A.R. 1988. Biochemical and genetic characterization of osmoregulatory trehalose synthesis in *Escherichia coli*. *J Bacteriol* **170:** 2841-2849.

Gilfillan, A.M., Smart, D.A., and Rooney, S.A. 1986. Comparison of the enzyme activities of phosphatidylcholine, phosphatidylglycerol and phosphatidylinositol synthesis in freshly isolated type II pneumocytes and whole lung from the adult rat. *Biochim Biophys Acta* **877:** 151-157.

Gonçalves, L.G., Huber, R., da Costa, M.S., and Santos, H. 2003. A variant of the hyperthermophile *Archaeoglobus fulgidus* adapted to grow at high salinity. *FEMS Microbiol Lett* **218:** 239-244.

Gonzalez, J.M., Shecklells, D., Viebahn, M., Krupatkina, D., Borges, K.M., and Robb, F.T. 1999. *Thermococcus waiotapuensis* sp. nov., an extremely thermophilic archaeon isolated from freshwater hot spring. *Arch Microbiol* **172:** 95-101.

Gorkovenko, A., and Roberts, M.F. 1993. Cyclic 2,3-diphosphoglycerate as a component of a new branch in gluconeogenesis in *Methanobacterium thermoautotrophicum* delta H. *J Bacteriol* **175:** 4087-4095.

Goude, R., Renaud, S., Bonnassie, S., Bernard, T., and Blanco, C. 2004. Glutamine, glutamate, and α-glucosylglycerate are the major osmotic solutes accumulated by *Erwinia chrysanthemi* strain 3937. *Appl Environ Microbiol* **70:** 6535-6541.

Grammann, K., Volke, A., and Kunte, H.J. 2002. New type of osmoregulated solute transporter identified in halophilic members of the bacteria domain: TRAP transporter TeaABC mediates uptake of ectoine and hydroxyectoine in *Halomonas elongata* DSM 2581(T). *J Bacteriol* **184:** 3078-3085.

Gribaldo, S., and Brochier-Armanet, C. 2006. The origin and evolution of *Archaea*: a state of the art. *Philos Trans R Soc Lond B Biol Sci* **361:** 1007-1022.

Habicht, K.S., Salling, L., Thamdrup, B., and Canfield, D.E. 2005. Effect of low sulfate concentrations on lactate oxidation and isotope fractionation during sulfate reduction by *Archaeoglobus fulgidus* strain Z. *Appl Environ Microbiol* **71:** 3770-3777.

Hagemann, M., Effmert, U., Kerstan, T., Schoor, A., and Erdmann, N. 2001. Biochemical characterization of glucosylglycerol-phosphate synthase of *Synechocystis sp.* strain PCC 6803: comparison of crude, purified, and recombinant enzymes. *Curr Microbiol* **43:** 278-283.

Hallam, S.J., Putnam, N., Preston, C.M., Detter, J.C., Rokhsar, D., Richardson, P.M., and DeLong, E.F. 2004. Reverse methanogenesis: testing the hypothesis with environmental genomics. *Science* **305:** 1457-1462.

Hansen, T., and Schönheit, P. 2004. ADP-dependent 6-phosphofructokinase, an extremely thermophilic, non-allosteric enzyme from the hyperthermophilic, sulfate-reducing archaeon *Archaeoglobus fulgidus* strain 7324. *Extremophiles* **8:** 29-35.

Hartmann, E., and Konig, H. 1989. Uridine and dolichyl diphosphate activated oligosaccharides are intermediates in the biosynthesis of the S-layer glycoprotein of *Methanothermus fervidus*. *Arch Microbiol* **151:** 274-281.

Hartmann, E., and König, H. 1990. Comparison of the biosynthesis of the methanobacterial pseudomurein and the eubacterial murein. *Naturwissenschaften* **77:** 472-475.

Hartmann, E., Konig, H., Kandler, O., and Hammes, W. 1990. Isolation of nucleotide activated amino acid and peptide precursors of the pseudomurein of *Methanobacterium thermoautotrophicum*. *FEMS Microbiol Lett* **57:** 271-275.

Hartzell, P., and Reed, D. 2006. The genus *Archaeoglobus*. In *The Prokaryotes Volume 3: Archaea. Bacteria: Firmicutes, Actinomycetes*. (ed. E. Stackebrandt), pp. 82-100. Springer, New York, USA.

Hensel, R. 1993. Proteins of extreme thermophiles. *New Comp Biochem* **26:** 209–221.

Hensel, R., and König, H. 1988. Thermoadaptation of methanogenic bacteria by intracellular ion concentration. *FEMS Microbiol Lett* **49:** 75-79.

Horlacher, R., Xavier, K.B., Santos, H., DiRuggiero, J., Kossmann, M., and Boos, W. 1998. Archaeal binding protein-dependent ABC transporter: molecular and biochemical analysis of the trehalose/maltose transport system of the hyperthermophilic archaeon *Thermococcus litoralis*. *J Bacteriol* **180:** 680-689.

Huber, H., Hohn, M.J., Rachel, R., Fuchs, T., Wimmer, V.C., and Stetter, K.O. 2002. A new phylum of *Archaea* represented by a nanosized hyperthermophilic symbiont. *Nature* **417:** 63-67.

Huber, H., Hohn, M.J., Stetter, K.O., and Rachel, R. 2003. The phylum *Nanoarchaeota*: present knowledge and future perspectives of a unique form of life. *Res Microbiol* **154:** 165-171.

Huber, H., Jannasch, H., Rachel, R., Fuchs, T., and Stetter, K.O. 1997. *Archaeoglobus veneficus* sp. nov., a novel facultative chemolithoautotrophic hyperthermophilic sulfite reducer, isolated from abyssal black smokers. *Syst Appl Microbiol* **20:** 374-380.

Huber, R., Burggraf, S., Mayer, T., Barns, S.M., Rossnagel, P., and Stetter, K.O. 1995. Isolation of a hyperthermophilic archaeum predicted by in situ RNA analysis. *Nature* **376:** 57-58.

Huber, R., Huber, H., and Stetter, K.O. 2000. Towards the ecology of hyperthermophiles: biotopes, new isolation strategies and novel metabolic properties. *FEMS Microbiol Rev* **24:** 615-623.

Huber, R., Langworthy, T.A., König, H., Thomm, M., Woese, C.R., Sleytr, U.B., and Stetter, K.O. 1986. *Thermotoga maritima* sp. nov. represents a new genus of unique extremely thermophilic eubacteria growing up to 90°C. *Arch Microbiol* **144:** 324-333.

Jaenicke, R. 1991. Protein stability and molecular adaptation to extreme conditions. *Eur J Biochem* **202:** 715-728.

Jaenicke, R. 1996. Glyceraldehyde-3-phosphate dehydrogenase from *Thermotoga maritima*: strategies of protein stabilization. *FEMS Microbiol Rev* **18:** 215-224.

Jannasch, H.W., Huber, R., Belkin, S., and Stetter, K.O. 1988. *Thermotoga neapolitana* sp. nov. of the extremely thermophilic, eubacterial genus *Thermotoga*. *Arch Microbiol* **150:** 103-104.

Johnsen, U., Hansen, T., and Schönheit, P. 2003. Comparative analysis of pyruvate kinases from the hyperthermophilic archaea *Archaeoglobus fulgidus*, *Aeropyrum pernix*, *Pyrobaculum aerophilum* and the hyperthermophilic bacterium *Thermotoga maritima*: unusual regulatory properties in hyperthermophilic archaea. *J Biol Chem* **278:** 25417-27.

Jolivet, E., Corre, E., L'Haridon, S., Forterre, P., and Prieur, D. 2004. *Thermococcus marinus* sp. nov. and *Thermococcus radiotolerans* sp. nov., two hyperthermophilic archaea from deep-sea hydrothermal vents that resist ionizing radiation. *Extremophiles* **8:** 219-227.

Jorge, C.D., Lamosa, P., and Santos, H. 2007a. α–D-Mannopyranosyl-(1,2)-α-d-glucopyranosyl-(->2)-glycerate in the thermophilic bacterium *Petrotoga miotherma* - structure, cellular content and function. *FEBS J* **274:** 3120-3127.

Kamekura, M. 1998. Diversity of extremely halophilic bacteria. *Extremophiles* **2:** 289-295.

Kärcher, U., Schroder, H., Haslinger, E., Allmaier, G., Schreiner, R., Wieland, F., Haselbeck, A., and Konig, H. 1993. Primary structure of the heterosaccharide of the surface glycoprotein of *Methanothermus fervidus*. *J Biol Chem* **268:** 26821-26826.

Kashefi, K., and Lovley, D.R. 2003. Extending the upper temperature limit for life. *Science* **301:** 934.

Kates, M. 1993. Membrane lipids of *archaea*. In *The Biochemistry of Archaea (Archaebacteria)*. (ed. A.T. Matheson), pp. 261–296. Elsevier, Amsterdam.

Keeling, P.J., and Doolittle, W.F. 1995. *Archaea*: narrowing the gap between prokaryotes and eukaryotes. *Proc Natl Acad Sci U S A* **92:** 5761-5764.

Kengen, S.W., Bikker, F.J., Hagen, W.R., de Vos, W.M., and van der Oost, J. 2001. Characterization of a catalase-peroxidase from the hyperthermophilic archaeon *Archaeoglobus fulgidus*. *Extremophiles* **5:** 323-332.

Kengen, S.W., de Bok, F.A., van Loo, N.D., Dijkema, C., Stams, A.J., and de Vos, W.M. 1994. Evidence for the operation of a novel Embden-Meyerhof pathway that involves ADP-dependent kinases during sugar fermentation by *Pyrococcus furiosus*. *J Biol Chem* **269:** 17537-17541.

Kessel, M., Volker, S., Santarius, U., Huber, R., and Baumeister, W. 1990. Three-dimensional reconstruction of the surface protein of the extremely thermophilic archaebacterium *Archaeoglobus fulgidus*. *Syst Appl Microbiol* **13:** 207–213.

Kikuchi, A., and Asai, K. 1984. Reverse gyrase- a topoisomerase which introduces positive superhelical turns DNA. *Nature* **309:** 677-681.

Klenk, H.P., Clayton, R.A., Tomb, J.F., White, O., Nelson, K.E., Ketchum, K.A., Dodson, R.J., Gwinn, M., Hickey, E.K., Peterson, J.D., et al. 1997. The complete genome sequence of the hyperthermophilic, sulphate-reducing archaeon *Archaeoglobus fulgidus*. *Nature* **390:** 364-370.

Kobayashi, T. 2001. Genus I. *Thermococcus*. In *Bergey's manual for systematic bacteriology*, 2 ed. (ed. G.M. Garrity), pp. 234-245. Springer, Berlin Heidelberg New York.

Koga, S., Yoshioka, I., Sakuraba, H., Takahashi, M., Sakasegawa, S., Shimizu, S., and Ohshima, T. 2000. Biochemical characterization, cloning, and sequencing of ADP-dependent (AMP-forming) glucokinase from two hyperthermophilic archaea, *Pyrococcus furiosus* and *Thermococcus litoralis*. *J Biochem (Tokyo)* **128:** 1079-1085.

Köhle, D., and Kauss, H. 1984. Purification of a membrane-derived proteinase capable of activating a galactosyltransferase involved in volume regulation. *Biochim et Bioph Acta* **799:** 59-67.

König, K., Hartmann, E., and Kärcher, U. 1994. Pathways and principles of the biosynthesis of methanobacterial cell wall polymers. *Syst Appl Microbiol* **16:** 510-517.

Kristjánsson, J.K., and Hreggvidsson, G.O. 1995. Ecology and habitats of extremophiles. *WJMB* **11:** 17-25.

Kunow, J., Linder, D., and Thauer, R.K. 1995. Pyruvate: ferredoxin oxidoreductase from the sulfate-reducing *Archaeoglobus fulgidus*: molecular composition, catalytic properties, and sequence alignments. *Arch Microbiol* **163:** 21-28.

Kuntz, C., Sonnenbichler, J., Sonnenbichler, I., Sumper, M., and Zeitler, R. 1997. Isolation and characterization of dolichol-linked oligosaccharides from *Haloferax volcanii*. *Glycobiology* **7:** 897-904.

Labes, A., and Schönheit, P. 2001. Sugar utilization in the hyperthermophilic, sulfate-reducing archaeon *Archaeoglobus fulgidus* strain 7324: starch degradation to acetate and CO_2 via a modified Embden-Meyerhof pathway and acetyl-CoA synthetase (ADP-forming). *Arch Microbiol* **176:** 329-338.

Labes, A., and Schönheit, P. 2003. ADP-dependent glucokinase from the hyperthermophilic sulfate-reducing archaeon *Archaeoglobus fulgidus* strain 7324. *Arch Microbiol* **7:** 69-75.

Labes, A., and Schönheit, P. 2007. Unusual starch degradation pathway via cyclodextrins in the hyperthermophilic sulfate-reducing archaeon *Archaeoglobus fulgidus* strain 7324. *J Bacteriol***:** 8901-8913.

Labes, A., Schönheit, P., Arguello Jm Fau - Mandal, A.K., -, M.A.F., and Mana-Capelli, S. 2003. ADP-dependent glucokinase from the hyperthermophilic sulfate-reducing archaeon *Archaeoglobus fulgidus* strain 7324. *Arch Microbiol* **7:** 7.

Ladenstein, R., and Antranikian, G. 1998. Proteins from hyperthermophiles: stability and enzymatic catalysis close to the boiling point of water. *Adv Biochem Eng Biotechnol* **61:** 37-85.

Lai, D., Springstead, J., and Monbouquette, H. 2008. Effect of growth temperature on ether lipid biochemistry in *Archaeoglobus fulgidus*. *Extremophiles***:** DOI.10.1007/s00792-00007-00126-00796.

Lai, M.C., Hong, T.Y., and Gunsalus, R.P. 2000. Glycine betaine transport in the obligate halophilic archaeon *Methanohalophilus portucalensis*. *J Bacteriol* **182:** 5020-5024.

Lai, M.C., Sowers, K.R., Robertson, D.E., Roberts, M.F., and Gunsalus, R.P. 1991. Distribution of compatible solutes in the halophilic methanogenic archaebacteria. *J Bacteriol* **173:** 5352-5358.

Lamosa, P., Brennan, L., Vis, H., Turner, D.L., and Santos, H. 2001. NMR structure of *Desulfovibrio gigas* rubredoxin: a model for studying protein stabilization by compatible solutes. *Extremophiles* **5:** 303-311.

Lamosa, P., Burke, A., Peist, R., Huber, R., Liu, M.Y., Silva, G., Rodrigues-Pousada, C., LeGall, J., Maycock, C., and Santos, H. 2000. Thermostabilization of proteins by diglycerol phosphate, a

new compatible solute from the hyperthermophile *Archaeoglobus fulgidus*. *Appl Environ Microbiol* **66:** 1974-1979.

Lamosa, P., Gonçalves, L.G., Rodrigues, M.V., Martins, L.O., Raven, N.D., and Santos, H. 2006. Occurrence of 1-glyceryl-1-*myo*-Inosityl phosphate in hyperthermophiles. *Appl Environ Microbiol* **72:** 6169-6173.

Lamosa, P., Martins, L.O., Da Costa, M.S., and Santos, H. 1998. Effects of temperature, salinity, and medium composition on compatible solute accumulation by *Thermococcus* spp. *Appl Environ Microbiol* **64:** 3591-3598.

Lamosa, P., Turner, D.L., Ventura, R., Maycock, C., and Santos, H. 2003. Protein stabilization by compatible solutes. Effect of diglycerol phosphate on the dynamics of *Desulfovibrio gigas* rubredoxin studied by NMR. *Eur J Biochem* **270:** 4606-4614.

Langelandsvik, A.S., Steen, I.H., Birkeland, N.K., and Lien, T. 1997. Properties and primary structure of a thermostable L-malate dehydrogenase from *Archaeoglobus fulgidus*. *Arch Microbiol* **168:** 59-67.

Langer, D., Hain, J., Thuriaux, P., and Zillig, W. 1995. Transcription in archaea: similarity to that in eucarya. *Proc Natl Acad Sci U S A* **92:** 5768-5772.

Lapaglia, C., and Hartzell, P.L. 1997. Stress-induced production of biofilm in the hyperthermophile *Archaeoglobus fulgidus*. *Appl Environ Microbiol* **63:** 3158-3163.

Larsen, O., Lien, T., and Birkeland, N.K. 1999. Dissimilatory sulfite reductase from *Archaeoglobus profundus* and *Desulfotomaculum thermocisternum*: phylogenetic and structural implications from gene sequences. *Extremophiles* **3:** 63-70.

Lazcano, A., and Miller, S.L. 1996. The origin and early evolution of life: prebiotic chemistry, the pre-RNA world, and time. *Cell* **85:** 793–798.

Lehmacher, A., Vogt, A.B., and Hensel, R. 1990. Biosynthesis of cyclic 2,3-diphosphoglycerate. Isolation and characterization of 2-phosphoglycerate kinase and cyclic 2,3-diphosphoglycerate synthetase from *Methanothermus fervidus*. *FEBS Lett* **272:** 94-98.

Leiros, I., Nabong, M.P., Grosvik, K., Ringvoll, J., Haugland, G.T., Uldal, L., Reite, K., Olsbu, I.K., Knaevelsrud, I., Moe, E., et al. 2007. Structural basis for enzymatic excision of N1-methyladenine and N3-methylcytosine from DNA. *EMBO J* **26:** 2206-2217.

Lentzen, G., and Schwarz, T. 2006. Extremolytes: natural compounds from extremophiles for versatile applications. *Appl Microbiol Biotechnol* **72:** 623-34.

Li, W.F., Zhou, X.X., and Lu, P. 2005. Structural features of thermozymes. *Biotechnol Adv* **23:** 271-281.

Littlechild, J.A., Guy, J.E., and Isupv, M.N. 2004. Hyperthermophilic dehydrogenase enzymes. *Biochem Soc Trans* **32:** 255-258.

Londesborough, J., and Vuorio, O. 1991. Trehalose-6-phosphate synthase/phosphatase complex from bakers' yeast: purification of a proteolytically activated form. *J Gen Microbiol* **137:** 323-330.

Lopez-Garcia, P., Forterre, P., van der Oost, J., and Erauso, G. 2000. Plasmid pGS5 from the hyperthermophilic archaeon *Archaeoglobus profundus* is negatively supercoiled. *J Bacteriol* **182:** 4998-5000.

Lund, P. 1987. *UV method with glutaminase and glutamate dehydrogenase.* VCH, Weinheim, Germany, pp. 357-363.

Martins, L.O., Carreto, L.S., Da Costa, M.S., and Santos, H. 1996. New compatible solutes related to di-myo-inositol-phosphate in members of the order *Thermotogales*. *J Bacteriol* **178:** 5644-5651.

Martins, L.O., Empadinhas, N., Marugg, J.D., Miguel, C., Ferreira, C., da Costa, M.S., and Santos, H. 1999. Biosynthesis of mannosylglycerate in the thermophilic bacterium *Rhodothermus*

marinus. Biochemical and genetic characterization of a mannosylglycerate synthase. *J Biol Chem* **274:** 35407-35414.

Martins, L.O., Huber, R., Huber, H., Stetter, K.O., Da Costa, M.S., and Santos, H. 1997. Organic solutes in hyperthermophilic *Archaea*. *Appl Environ Microbiol* **63:** 896-902.

Martins, L.O., and Santos, H. 1995. Accumulation of mannosylglycerate and di-*myo*-inositol-phosphate by *Pyrococcus furiosus* in response to salinity and temperature. *Appl Environ Microbiol* **61:** 3299-3303.

Maruyama, Y., Nakajima, T., and Ichishima, E. 1994. A 1,2-α-D-mannosidase from a *Bacillus* sp.: purification, characterization, and mode of action. *Carbohydr Res* **251:** 89-98.

Mescher, M.F., Hansen, U., and Strominger, J.L. 1976. Formation of lipid-linked sugar compounds in *Halobacterium salinarium*. Presumed intermediates in glycoprotein synthesis. *J Biol Chem* **251:** 7289-7294.

Mescher, M.F., and Strominger, J.L. 1976. Purification and characterization of a prokaryotic glucoprotein from the cell envelope of *Halobacterium salinarium*. *J Biol Chem* **251:** 2005-2014.

Möller-Zinkhan, D., Börner, G., and Thauer, R.K. 1989. Function of methanofuran, tetrahydromethanopterin, and coenzyme F_{420} in *Archaeoglobus fulgidus*. *Arch Microbiol* **152:** 362-368.

Murakami, M., Shibuya, K., Nakayama, T., Nishino, T., Yoshimura, T., and Hemmi, H. 2007. Geranylgeranyl reductase involved in the biosynthesis of archaeal membrane lipids in the hyperthermophilic archaeon *Archaeoglobus fulgidus*. *FEBS J* **274:** 805-814.

Nakajima, M., Imamura, H., Shoun, H., and Wakagi, T. 2003. Unique metal dependency of cytosolic α-mannosidase from *Thermotoga maritima*, a hyperthermophilic bacterium. *Arch Biochem Biophys* **415:** 87-93.

Nanavati, D.M., Thirangoon, K., and Noll, K.M. 2006. Several archaeal homologs of putative oligopeptide-binding proteins encoded by *Thermotoga maritima* bind sugars. *Appl Environ Microbiol* **72:** 1336-1345.

Nelson, K.E., Eisen, J.A., and Fraser, C.M. 2001. Genome of *Thermotoga maritima* MSB8. *Methods Enzymol* **330:** 169-180.

Nesbo, C.L., L'Haridon, S., Stetter, K.O., and Doolittle, W.F. 2001. Phylogenetic analyses of two "archaeal" genes in *Thermotoga maritima* reveal multiple transfers between *Archaea* and *Bacteria*. *Mol Biol Evol* **18:** 362-375.

Neves, C., da Costa, M.S., and Santos, H. 2005. Compatible solutes of the hyperthermophile *Palaeococcus ferrophilus*: osmoadaptation and thermoadaptation in the order *Thermococcales*. *Appl Environ Microbiol* **71:** 8091-8098.

Nies, D.H. 2003. Efflux-mediated heavy metal resistance in prokaryotes. *FEMS Microbiol Rev* **27:** 313-339.

Nishihara, M., Yamazaki, T., Oshima, T., and Koga, Y. 1999. sn-glycerol-1-phosphate-forming activities in *Archaea*: separation of archaeal phospholipid biosynthesis and glycerol catabolism by glycerophosphate enantiomers. *J Bacteriol* **181:** 1330-1333.

Nunes, O.C., Manaia, C.M., Da Costa, M.S., and Santos, H. 1995. Compatible solutes in the thermophilic bacteria *Rhodothermus marinus* and "*Thermus thermophilus*". *Appl Environ Microbiol* **61:** 2351-2357.

Ohta, A., Waggoner, K., Radominska-Pyrek, A., and Dowhan, W. 1981. Cloning of genes involved in membrane lipid synthesis: effects of amplification of phosphatidylglycerophosphate synthase in *Escherichia coli*. *J Bacteriol* **147:** 552-562.

Olsen, G.J., and Woese, C.R. 1996. Lessons from an Archaeal genome: what are we learning from *Methanococcus jannaschii*? *Trends Genet* **12:** 377-379.

Pagala, V.R., Park, J., Reed, D.W., and Hartzell, P.L. 2002. Cellular localization of D-lactate dehydrogenase and NADH oxidase from *Archaeoglobus fulgidus*. *Archaea* **1:** 95-104.

Pais, T.M., Lamosa, P., dos Santos, W., Legall, J., Turner, D.L., and Santos, H. 2005. Structural determinants of protein stabilization by solutes. The important of the hairpin loop in rubredoxins. *FEBS J* **272:** 999-1011.

Park, Y.S., Sweitzer, T.D., Dixon, J.E., and Kent, C. 1993. Expression, purification, and characterization of CTP:glycerol-3-phosphate cytidylyltransferase from *Bacillus subtilis*. *J Biol Chem* **268:** 16648-16654.

Parker, K.N., Chhabra, S.R., Lam, D., Callen, W., Duffaud, G.D., Snead, M.A., Short, J.M., Mathur, E.J., and Kelly, R.M. 2001. Galactomannanases Man2 and Man5 from *Thermotoga* species: growth physiology on galactomannans, gene sequence analysis, and biochemical properties of recombinant enzymes. *Biotechnol Bioeng* **75:** 322-333.

Parolis, H., Parolis, L.A., Boan, I.F., Rodriguez-Valera, F., Widmalm, G., Manca, M.C., Jansson, P.E., and Sutherland, I.W. 1996. The structure of the exopolysaccharide produced by the halophilic archaeon *Haloferax mediterranei* strain R4 (ATCC 33500). *Carbohydr Res* **295:** 147-156.

Parolis, L.A., Parolis, H., Paramonov, N.A., Boan, I.F., Anton, J., and Rodriguez-Valera, F. 1999. Structural studies on the acidic exopolysaccharide from *Haloferax denitrificans* ATCC 35960. *Carbohydr Res* **319:** 133-140.

Pattridge, K.A., Weber, C.H., Friesen, J.A., Sanker, S., Kent, C., and Ludwig, M.L. 2003. Glycerol-3-phosphate cytidylyltransferase. Structural changes induced by binding of CDP-glycerol and the role of lysine residues in catalysis. *J Biol Chem* **278:** 51863-51871.

Perutz, M.F., and Raidt, H. 1975. Stereochemical basis of heat stability in bacterial ferredoxins and in haemoglobin A2. *Nature* **255:** 256-259.

Pettijohn, D.E. 1988. Histone-like proteins and bacterial chromosome structure. *J Biol Chem* **263:** 12793-12796.

Pfluger, K., and Muller, V. 2004. Transport of compatible solutes in extremophiles. *J Bioenerg Biomembr* **36:** 17-24.

Phipps, B.M., Hoffmann, A., Stetter, K.O., and Baumeister, W. 1991. A novel ATPase complex selectively accumulated upon heat shock is a major cellular component of thermophilic archaebacteria. *EMBO J* **10:** 1711-1722.

Pick, U. 1999. *Dunaliella acidophila*-a most extreme acidophilic alga. In *Enigmatic microorganisms and life in extreme environments*. (ed. J. Seckbach), pp. 467-478. Kluwer, Dordrecht.

Plotz, B.M., Lindner, B., Stetter, K.O., and Holst, O. 2000. Characterization of a novel Lipid A containing D-galacturonic acid that replaces phosphate residues. *J Biol Chem* **275:** 11222-11228.

Pooley, H.M., Abellan, F.-X., and Karamata, D. 1991. A conditional-lethal mutant of *Bacillus subtilis* 168 with a thermsensitive glycerol-3-phosphate cytidylyltransferase, an enzyme specific for synthesis of the major teichoid acid. *J Gen Microbiol* **137:** 921-928.

Pooley, H.M., Abellan, F.-X., and Karamata, D. 1992. CDP-glycerol:poly(glycerophosphate) glycerophosphotransferase, wich is involved in the synthesis of the major wall teichoid acid in *Bacillus subtilis* 168, is encoded by *TagF* (*rodC*). *J Bacteriol* **174:** 646-649.

Porchia, A.C., and Salerno, G.L. 1996. Sucrose biosynthesis in a prokaryotic organism: Presence of two sucrose-phosphate synthases in Anabaena with remarkable differences compared with the plant enzymes. *Proc Natl Acad Sci USA* **93:** 13600-13604.

Rainey, F.A., Zhilina, T.N., Boulygina, E.S., Stackebrandt, E., Tourova, T.P., and Zavarzin, G.A. 1995. The taxonomic status of the fermentative halophilic anaerobic bacteria: description of

Haloanaerobiales ord. nov., *Halobacteroidaceae* fam. nov., *Orenia* gen. nov. and further taxonomic rearrangements at the genus and species level. *Anaerobe* **1:** 185-199.

Ramakrishnan, V., and Adams, M. 1995. Preparation of genomic DNA from sulfur-dependent hyperthermophilic *Archaea*. In *In Archaea: a Laboratory Manual - Thermophiles.*, pp. 95-96. Cold Spring Harbor Press, Cold Spring Harbor, NY.

Ramakrishnan, V., Teng, Q., and Adams, M.W. 1997a. Characterization of UDP amino sugars as major phosphocompounds in the hyperthermophilic archaeon *Pyrococcus furiosus*. *J Bacteriol* **179:** 1505-1512.

Ramakrishnan, V., Verhagen, M., and Adams, M. 1997b. Characterization of di-*myo*-inositol-1,1-phosphate in the hyperthermophilic bacterium *Thermotoga maritima*. *Appl Environ Microbiol* **63:** 347-350.

Ramos, A., Raven, N., Sharp, R.J., Bartolucci, S., Rossi, M., Cannio, R., Lebbink, J., Van Der Oost, J., De Vos, W.M., and Santos, H. 1997. Stabilization of enzymes against thermal stress and freeze-drying by mannosylglycerate. *Appl Environ Microbiol* **63:** 4020-4025.

Reed, D.W., and Hartzell, P.L. 1999. The *Archaeoglobus fulgidus* D-lactate dehydrogenase is a Zn^{2+} flavoprotein. *J Bacteriol* **181:** 7580-7587.

Reed, R.H., Richardson, D.L., Warr, S.R.C., and Stewart, W.D.P. 1984. Carbohydrate accumulation and osmotic stress in cyanobacteria. *J Gen Microbiol* **130:** 1-4.

Rinker, K.D., and Kelly, R.M. 1996. Growth physiology of the hyperthermophilic archaeon *Thermococcus litoralis*: development of a sulfur-free defined medium, characterization of an exopolysaccharide, and evidence of biofilm formation. *Appl Environ Microbiol* **62:** 4478-4485.

Rivera-Marrero, C.A., Ritzenthaler, J.D., Roman, J., and Moremen, K.W. 2001. Molecular cloning and expression of an α-mannosidase gene in *Mycobacterium tuberculosis*. *Microb Pathog* **30:** 9-18.

Robert, H., Le Marrec, C., Blanco, C., and Jebbar, M. 2000. Glycine betaine, carnitine, and choline enhance salinity tolerance and prevent the accumulation of sodium to a level inhibiting growth of *Tetragenococcus halophila*. *Appl Environ Microbiol* **66:** 509-517.

Roberts, M.F. 2005. Organic compatible solutes of halotolerant and halophilic microorganisms. *Saline Systems* **1:** 1:30.

Robertson, D.E., Lai, M.C., Gunsalus, R.P., and Roberts, M.F. 1992. Composition, variation, and dynamics of major osmotic solutes in *Methanohalophilus* Strain FDF1. *Appl Environ Microbiol* **58:** 2438-2443.

Robertson, D.E., Roberts, M.F., Belay, N., Stetter, K.O., and Boone, D.R. 1990. Occurrence of β-glutamate, a novel osmolyte, in marine methanogenic bacteria. *Appl Environ Microbiol* **56:** 1504-1508.

Rodrigues, J.V., Saraiva, L.M., Abreu, I.A., Teixeira, M., and Cabelli, D.E. 2007a. Superoxide reduction by *Archaeoglobus fulgidus* desulfoferrodoxin: comparison with neelaredoxin. *JBIC* **12:** 248-256.

Rodrigues, M.V., Borges, N., Henriques, M., Lamosa, P., Ventura, R., Fernandes, C., Empadinhas, N., Maycock, C., da Costa, M.S., and Santos, H. 2007. Bifunctional CTP:inositol-1-phosphate cytidylyltransferase/CDP-inositol:inositol-1-phosphate transferase, the key enzyme for di-*myo*-inositol-phosphate synthesis in several (hyper)thermophiles. *J Bacteriol* **189:** 5405-5412.

Rohlin, L., Trent, J.D., Salmon, K., Kim, U., Gunsalus, R.P., and Liao, J.C. 2005. Heat shock response of *Archaeoglobus fulgidus*. *J Bacteriol* **187:** 6046-6057.

Roitel, O., Ivinova, O., Muronetz, V., Nagradova, N., and Branlant, G. 2002. Thermal unfolding used as a probe to characterize the intra- and intersubunit stabilizing interactions in phosphorylating D-

glyceraldehyde-3-phosphate dehydrogenase from *Bacillus stearothermophilus*. *Biochemistry* **41:** 7556-7564.

Rothschild, L.J., and Mancinelli, R.L. 2001. Life in extreme environments. *Nature* **409:** 1092-1101.

Ruffert, S., Lambert, C., Peter, H., Wendisch, V.F., and Kramer, R. 1997. Efflux of compatible solutes in *Corynebacterium glutamicum* mediated by osmoregulated channel activity. *Eur J Biochem* **247:** 572-580.

Sakuraba, H., Goda, S., and Ohshima, T. 2004. Unique sugar metabolism and novel enzymes of hyperthermophilic archaea. *Chem Rec* **3:** 281-287.

Sakuraba, H., Yoshioka, I., Koga, S., Takahashi, M., Kitahama, Y., Satomura, T., Kawakami, R., and Ohshima, T. 2002. ADP-dependent glucokinase/phosphofructokinase, a novel bifunctional enzyme from the hyperthermophilic archaeon *Methanococcus jannaschii*. *J Biol Chem* **277:** 12495-12498.

Sampaio, M.M., Santos, H., and Boos, W. 2003. Synthesis of GDP-mannose and mannosylglycerate from labeled mannose by genetically engineered *Escherichia coli* without loss of specific isotopic enrichment. *Appl Environ Microbiol* **69:** 233-240.

Sampaio, M.M., Chevance, F., Dippel, R., Eppler, T., Schlegel, A., Boos, W., Lu, Y.J., and Rock, C.O. 2004. Phosphotransferase-mediated transport of the osmolyte 2-O-α-mannosyl-D-glycerate in *Escherichia coli* occurs by the product of the *mngA* (*hrsA*) gene and is regulated by the *mngR* (*farR*) gene product acting as repressor. *J Biol Chem* **279:** 5537-5548.

Sandigursky, M., and Franklin, W.A. 2000. Uracil-DNA glycosylase in the extreme thermophile *Archaeoglobus fulgidus*. *J Biol Chem* **275:** 19146-19149.

Sandman, K., Krzycki, J.A., Dobrinski, B., Lurz, R., and Reeve, J.N. 1990. HMf, a DNA-binding protein isolated from the hyperthermophilic archaeon *Methanothermus fervidus,* is most closely related to histones. *Proc Natl Acad Sci USA* **87:** 5788-5791.

Santos, H., and da Costa, M.S. 2001. Organic solutes from thermophiles and hyperthermophiles. *Methods Enzymol* **334:** 302-315.

Santos, H., and da Costa, M.S. 2002. Compatible solutes of organisms that live in hot saline environments. *Environ Microbiol* **4:** 501-509.

Santos, H., Lamosa, P., Borges, N., Faria, T., and Neves, C. 2007. The physiological role, biosynthesis and mode of action of compatible solutes from (hyper)thermophiles. In *Physiology and biochemistry of extremophiles*. (ed. C. Gerday and N. Glandorf), pp. 86-104. ASM Press, Washington, D.C.

Santos, H., Lamosa, P., Faria, T.Q., Pais, T.M., de la Paz, M.L., and Serrano, L. Compatible solutes of (hyper)thermophiles and their role in protein stabilization. In *Thermophiles*. (ed. F. Robb). CRC Taylor and Francis, USA.

Sauer, T., and Galinski, E.A. 1998. Bacterial milking: A novel bioprocess for production of compatible solutes. *Biotechnol Bioeng* **57:** 306-313.

Schertzer, J.W., and Brown, E.D. 2003. Purified, recombinant TagF protein from *Bacillus subtilis* 168 catalyzes the polymerization of glycerol phosphate onto a membrane acceptor in vitro. *J Biol Chem* **278:** 18002-18007.

Schleper, C., Jurgens, G., and Jonuscheit, M. 2005. Genomic studies of uncultivated *archaea*. *Nat Rev Microbiol* **3:** 479-488.

Schleyer, M., Schmid, R., and Bakker, E.P. 1993. Transient, specific and extremely rapid release of osmolytes from growing cells of *Escherichia coli* K-12 exposed to hypoosmotic shock. *Arch Microbiol* **160:** 424-431.

Scholz, S., Sonnenbichler, J., Schafer, W., and Hensel, R. 1992. Di-*myo*-inositol-1,1'-phosphate: a new inositol phosphate isolated from *Pyrococcus woesei*. *FEBS Lett* **306:** 239-242.

Scholz, S., Wolff, S., and Hensel, R. 1998. The biosynthesis pathway of di-*myo*-inositol-1, 1'-phosphate in *Pyrococcus woesei*. *FEMS Microbiol Lett* **168:** 37-42.

Sekler, I., Gläser, H.-U., and Pick, U. 1991. Characterization of a plasma membrane H^+-ATPase from the extremely acidophilic alga *Dunaliella acidophila*. *J Membr Biol* **121:** 51-57.

Selig, M., Xavier, K.B., Santos, H., and Schönheit, P. 1997. Comparative analysis of Embden-Meyerhof and Entner-Doudoroff glycolytic pathways in hyperthermophilic *Archaea* and the bacterium *Thermotoga*. *Arch Microbiol* **167:** 217-232.

Shashkov, A.S., Campos-Portuguez, S., Kochanowski, H., Yokota, A., and Mayer, H. 1995. The structure of the O-specific polysaccharide from *Thiobacillus* sp. IFO 14570, with three different diaminopyranoses forming the repeating unit. *Carbohydr Res* **269:** 157-166.

Shekhtman, A., McNaughton, L., Cunningham, R.P., and Baxter, S.M. 1999. Identification of the *Archaeoglobus fulgidus* endonuclease III DNA interaction surface using heteronuclear NMR methods. *Structure Fold Des* **7:** 919-930.

Shima, S., Herault, D., Berkessel, A., and RK., T. 1998. Activation and thermostabilization effects of cyclic 2, 3-diphosphoglycerate on enzymes from the hyperthermophilic *Methanopyrus kandleri*. *Arch Microbiol.* **170:** 469-472.

Siebers, B., Klenk, H.P., and Hensel, R. 1998. PPi-dependent phosphofructokinase from *Thermoproteus tenax*, an archaeal descendant of an ancient line in phosphofructokinase evolution. *J Bacteriol* **180:** 2137-2143.

Silva, Z., Borges, N., Martins, L.O., Wait, R., da Costa, M.S., and Santos, H. 1999. Combined effect of the growth temperature and salinity of the medium on the accumulation of compatible solutes by *Rhodothermus marinus* and *Rhodothermus obamensis*. *Extremophiles* **3:** 163-172.

Silva, Z., Sampaio, M.M., Henne, A., Bohm, A., Gutzat, R., Boos, W., da Costa, M.S., and Santos, H. 2005. The high-affinity maltose/trehalose ABC transporter in the extremely thermophilic bacterium *Thermus thermophilus* HB27 also recognizes sucrose and palatinose. *J Bacteriol* **187:** 1210-1218.

Sowers, K.R., and Gunsalus, R.P. 1995. Halotolerance in *Methanosarcina* spp.: Role of N^{ε}-acetyl-β-lysine, α-glutamate, glycine betaine, and K^+ as compatible solutes for osmotic adaptation. *Appl Environ Microbiol* **61:** 4382-4388.

Sowers, K.R., Robertson, D.E., Noll, D., Gunsalus, R.P., and Roberts, M.F. 1990. N^{ε}-acetyl-β-lysine: an osmolyte synthesized by methanogenic archaebacteria. *Proc Natl Acad Sci U S A* **87:** 9083-9087.

Speich, N., Dahl, C., Heisig, P., Klein, A., Lottspeich, F., Stetter, K.O., and Truper, H.G. 1994. Adenylylsulphate reductase from the sulphate-reducing archaeon *Archaeoglobus fulgidus*: cloning and characterization of the genes and comparison of the enzyme with other iron-sulphur flavoproteins. *Microbiology* **140:** 1273-1284.

Sperling, D., Kappler, U., Truper, H.G., and Dahl, C. 2001. Dissimilatory ATP sulfurylase from *Archaeoglobus fulgidus*. *Methods Enzymol* **331:** 419-427.

Sperling, D., Kappler, U., Wynen, A., Dahl, C., and Truper, H.G. 1998. Dissimilatory ATP sulfurylase from the hyperthermophilic sulfate reducer *Archaeoglobus fulgidus* belongs to the group of homo-oligomeric ATP sulfurylases. *FEMS Microbiol Lett* **162:** 257-264.

Sprott, G.D., Meloche, M., and Richards, J.C. 1991. Proportions of diether, macrocyclic diether, and tetraether lipids in *Methanococcus jannaschii* grown at different temperatures. *J Bacteriol* **173:** 3907-3910.

Steen, I.H., Hvoslef, H., Lien, T., and Birkeland, N.K. 2001. Isocitrate dehydrogenase, malate dehydrogenase, and glutamate dehydrogenase from *Archaeoglobus fulgidus*. *Methods Enzymol* **331:** 13-26.

Steen, I.H., Lien, T., and Birkeland, N.K. 1997. Biochemical and phylogenetic characterization of isocitrate dehydrogenase from a hyperthermophilic archaeon, *Archaeoglobus fulgidus*. *Arch Microbiol* **168:** 412-420.

Stetter, K., Lauerer, G., Thomm, M., and Neuner, A. 1987. Isolation of extremely thermophilic sulfate reducers: evidence for a novel branch of *Archaebacteria. Science* **236:** 822-824.

Stetter, K.O. 1988. *Archaeoglobus fulgidus* gen. nov., sp. nov.: new taxon of extremely thermophilic *Archaebacteria*. *Syst Appl Microbiol* **10:** 172-173.

Stetter, K.O. 1998. Hyperthermophiles: isolation, classification, and properties. In *Extremophiles:microbial life in extreme environments*. (ed. W.D. Grant), pp. 1-24. John Wiley & Sons, New York.

Stetter, K.O. 2006. Hyperthermophiles in the history of life. *Philos Trans R Soc Lond B* **361:** 1837-1843.

Stetter, K.O., Fiala, G., Huber, G., Huber, R., and Segerer, A. 1990. Hyperthermophilic microorganisms. *FEMS Microbiology Letters* **75:** 117-124.

Stetter, K.O., Huber, R., Blochl, E., Kurr, M., Eden, R.D., Fielder, M., Cash, H., and Vance, L. 1993. Hyperthermophilic *Archaea* are thriving in deep North Sea and Alaskan oil reservoirs. *Nature* **365:** 743-745.

Sundaran, T.K. 1986. Physiology and growth of thermophilic bacteria. In *Thermophiles: General Molecular and Applied Mycrobiology*. (ed. T.D. Brock), pp. 75-106. John Wiley & Sons, New York.

Takai, K., and Horikoshi, K. 1999. Genetic diversity of archaea in deep-sea hydrothermal vent environments. *Genetics* **152:** 1285-1297.

Takai, K., Sako, Y., Uchida, A., and Ishida, Y. 1997. Extremely thermostable phosphoenolpyruvate carboxylase from an extreme thermophile, *Rhodothermus obamensis*. *J Biochem* **122:** 32-40.

Tarui, M., Tanaka, N., Tomura, K., Ohga, M., Morii, H., and Koga, Y. 2007. Lipid component parts analysis of the hyperthermophilic sulfate-reducing archaeon *Archaeoglobus fulgidus*. *J Uoeh* **29:** 131-139.

Tetsch, L., and Kunte, H.J. 2002. The substrate-binding protein TeaA of the osmoregulated ectoine transporter TeaABC from *Halomonas elongata*: purification and characterization of recombinant TeaA. *FEMS Microbiol Lett* **211:** 213-218.

Thoma, R., Hennig, M., Sterner, R., and Kirschner, K. 2000. Structure and function of mutationally generated monomers of dimeric phosphoribosylanthranilate isomerase from *Thermotoga maritima*. *Structure* **8:** 265-276.

Thomson, K.-S. 1983. Purification of UDP galactose:sn-glycerol-3-phosphate-D-galactosyltransferase from *Poterioochromas mathamensis. Biochim Biophys Acta* **759:** 156-159.

Tindall, B.J., Stetter, K.O., and Collins, M.D. 1989. A novel, fully saturated menaquinone from the thermophilic, sulphate-reducing archaebacterium *Archaeoglobus fulgidus*. *Microbiology* **135:** 693-696.

Tolner, B., Poolman, B., and Konings, W. 1998. Adaptation of micro-oganisms and their transport systems to high temperatures. *Comp Biochem Physiol* **118A:** 423-428.

Tuininga, J.E., Verhees, C.H., van der Oost, J., Kengen, S.W., Stams, A.J., and de Vos, W.M. 1999. Molecular and biochemical characterization of the ADP-dependent phosphofructokinase from the hyperthermophilic archaeon *Pyrococcus furiosus*. *J Biol Chem* **274:** 21023-21028.

van der Linden, M.G., and Farias, S.T. 2006. Correlation between codon usage and thermostability. *Extremophiles* **10:** 479-481.

Vargas, C., Jebbar, M., Carrasco, R., Blanco, C., Calderon, M.I., Iglesias-Guerra, F., and Nieto, J.J. 2006. Ectoines as compatible solutes and carbon and energy sources for the halophilic bacterium *Chromohalobacter salexigens*. *J Appl Microbiol* **100:** 98-107.

Vermeulen, V., and Kunte, H.J. 2004. *Marinococcus halophilus* DSM 20408T encodes two transporters for compatible solutes belonging to the betaine-carnitine-choline transporter family: identification and characterization of ectoine transporter EctM and glycine betaine transporter BetM. *Extremophiles* **8:** 175-184.

Vicente-Soler, J., Arguelles, J.C., and Gacto, M. 1991. Proteolytic activation of alpha,alpha-trehalose 6-phosphate synthase in *Candida utilis*. *FEMS Microbiol Lett* **66:** 157-161.

Vieille, C., Burdette, D.S., and Zeikus, J.G. 1996. Thermoenzymes. *Biotechnol Annu Rev* **2:** 1-83.

Vieille, C., and Zeikus, J.G. 2001. Hyperthermophilic enzymes: sources, uses, and molecular mechanisms for thermostability. *Microbiol Mol Biol Rev* **65:** 1-43.

Voisin, S., Houliston, R.S., Kelly, J., Brisson, J.R., Watson, D., Bardy, S.L., Jarrell, K.F., and Logan, S.M. 2005. Identification and characterization of the unique N-linked glycan common to the flagellins and S-layer glycoprotein of *Methanococcus voltae*. *J Biol Chem* **280:** 16586-16593.

Walker, J.E., Wonacott, A.J., and Harris, J.I. 1980. Heat stability of a tetrameric enzyme, D-glyceraldehyde-3-phosphate dehydrogenase. *Eur J Biochem* **108:** 581-586.

Wang, Y.K., Morgan, A., Stieglitz, K., Stec, B., Thompson, B., Miller, S.J., and Roberts, M.F. 2006. The temperature dependence of the inositol monophosphatase Km correlates with accumulation of di-*myo*-inositol 1,1'-phosphate in *Archaeoglobus fulgidus*. *Biochemistry* **45:** 3307-3314.

Waters, E., Hohn, M.J., Ahel, I., Graham, D.E., Adams, M.D., Barnstead, M., Beeson, K.Y., Bibbs, L., Bolanos, R., Keller, M., et al. 2003. The genome of *Nanoarchaeum equitans*: insights into early archaeal evolution and derived parasitism. *Proc Natl Acad Sci U S A* **100:** 12984-12988.

Weiss, M., and Pick, U. 1996. Primary structure and effect of pH on the expression of the plasma membrane H^+-ATPase from *Dunaliella acidophila* and *Dunaliella salina*. *Plant Physiol* **112:** 1693 - 1702.

White, R.H. 1988. Structural diversity among methanofurans from different methanogenic bacteria. *J Bacteriol* **170:** 4594-4597.

Woese, C.R., Achenbach, L., Rouviere, P., and Mandelco, L. 1991. Archaeal phylogeny: reexamination of the phylogenetic position of *Archaeoglobus fulgidus* in light of certain composition-induced artifacts. *Syst Appl Microbiol* **14:** 364-371.

Woese, C.R., and Fox, G.E. 1977. Phylogenetic structure of the prokaryotic domain: The primary kingdoms. *Proc Natl Acad Sci USA* **74:** 5088-5090.

Woese, C.R., Kandler, O., and Wheelis, M.L. 1990. Towards a natural system of organisms: Proposal for the domains *Archaea*, *Bacteria*, and *Eucarya*. *Proc Natl Acad Sci USA* **87:** 4576-4579.

Xavier, K.B., da Costa, M.S., and Santos, H. 2000. Demonstration of a novel glycolytic pathway in the hyperthermophilic archaeon *Thermococcus zilligii* by ^{13}C-labeling experiments and nuclear magnetic resonance analysis. *J Bacteriol* **182:** 4632-4636.

Xavier, K.B., Martins, L.O., Peist, R., Kossmann, M., Boos, W., and Santos, H. 1996. High-affinity maltose/trehalose transport system in the hyperthermophilic archaeon *Thermococcus litoralis*. *J Bacteriol* **178:** 4773-4777.

Yamagata, Y., Ogasahara, K., Hioki, Y., Lee, S.J., Nakagawa, A., Nakamura, H., Ishida, M., Kuramitsu, S., and Yutani, K. 2001. Entropic stabilization of the tryptophan syntahse α-subunit from a hyperthermophile, *Pyrococcus furiosus*. X-ray analysis and calorimetry. *J Biol Chem* **276:** 11062-11071.

Yan, Z., Fujiwara, S., Kohda, K., Takagi, M., and Imanaka, T. 1997. In vitro stabilization and in vivo solubilization of foreign proteins by the beta subunit of a chaperonin from the hyperthermophilic archaeon *Pyrococcus* sp. strain KOD1. *Appl Environ Microbiol* **63:** 785-789.

Yang, L.L., and Haug, A. 1979. Purification and partial characterization of a procaryotic glycoprotein from the plasma membrane of *Thermoplasma acidophilum*. *Biochim Biophys Acta* **556:** 265-277.

Zellner, G., Stackebrant, E., Kneifel, H., Messner, P., Sleytr, U.B., Macario, E.C., Zabel, H.-P., Stetter, K.O., and Winter, J. 1989. Isolation and caracterization of a thermophilic, sulfate-reducing Archaebacterium, *Archaeoglobus fulgidus* strain Z. *Syst Appl Microbiol* **11:** 151-160.

ITQB-UNL | Av. da República, 2780-157 Oeiras, Portugal
Tel (+351) 214 469 100 | Fax (+351) 214 411 277

www.itqb.unl.pt